# Petrogenesis of the Ambohiby Complex, Madagascar and the Role of Marion Hotspot plume

by

**Ndivhuwo Cecilia Mukosi**

*Dissertation presented for the degree*
of *Masters of Science in the Faculty of Science at Stellenbosch University*

Promoter: Dr Jodie Miller and Dr Paul Macey

December 2012

**PLAGIARISM DECLARATION**

I, Ndivhuwo Cecilia Mukosi declare that this work submitted for the degree of MSc at the University of Stellenbosch is the result of my own work and has not been previously submitted by me at another University for any degree. An effort to the best of my abilities is made to cite the contribution of others with due reference to the literature.

Signature: ……………………………………….

Date: ………………………………………….

## Abstract

The Cretaceous Ambohiby Complex is an alkaline ring complex located in the central part of Madagascar and covers a mountainous area of approximately 225km$^2$. The complex intrudes into Precambrian basement gneisses and consists of the following rock types in a chronological order; gabbros, monzonite, alkali-syenite, micro-granite and granites. Both mafic and felsic rocks are dominated by sodic mineralogies. Pyroxenes are generally aegirine, aegirine-augite, and hedenbergite and commonly occur in granites, micro-granites, syenites and monzonite. In gabbros and mafic dykes, augite is the more common composition. Amphiboles are represented by bluish to brownish-green varieties with arfvedsonite to eckermannite compositions in granites, and magnesia-arfvedsonite compositions in micro-granites. Ferro-edenite is present in some alkali-syenites and monzonite. Feldspars are usually single phase and are therefore hypersolvus. In granites, micro-granites and alkali-syenites, path and string perthite is very common. Graphic intergrowth of quartz and alkali feldspars is also common in granites and some alkali-syenites.

Major elements variation diagrams plotted against $SiO_2$ indicate that the mafic and felsic rocks of the Ambohiby Complex were formed by processes similar to those of Fractional crystallization. Chondrite normalised mafic rocks have slightly positive Eu anomalies while the felsic rocks have negative Eu anomalies, indicating fractionation of plagioclase feldspars. The Chondrite normalised gabbroic rocks shared similar trends of heavy rare earth with Chondrite normalised Marion Hotspot data. This suggests that the basaltic parent magma for the Ambohiby Complex, possibly related to the Marion hotspot plume. The Fractional crystallization model with an inclusion of olivine in the mineral assemblage seems to fit very well with the actual Ambohiby felsic end member rocks (i.e. granites). It is therefore clear that differentiation mainly occurred by fractional crystallization but variable initial Sr and Nd values indicate the magmas assimilated crustal material during emplacement. The Rb-Sr geochronology gave an age of 90±2.4 Ma for the intrusion of the Ambohiby Complex, which confirms that the Ambohiby Complex is associated with the Gondwana break-up. In addition the Marion Hotspot plume is believed to have been located in the southern tip of the island at around 90 Ma ago.

**Acknowledgement**

I'd like to thank my supervisors, Jodie miller and Paul Macey who offered me the opportunity to undertake this work under their supervision. I thank them for their patience and their advices which have been of great help. I thank my field assistance Santa for his support and guidance during my fieldwork in Madagascar. I thank the Council For Geoscience for their support during the writing up of the thesis. I thank all the following people John Clemens, Martin Klaussen, Madelaine Frazenburg, and Dave Raid for their assistance with mineral chemistry and geochemical data. I also thank Natalie Fish, Cynthia Sanchez-Garrido, Loxie Conradie, Arnaud Villaros, Rob Ward, Mafusi Rapopo and Risa Matsumura for their kind support. I thank my family and friends for their unconditional love and support throughout my studies. Finally I thank God for his grace and faithfulness.

**Table of Contents**

## <u>APPENDIX</u>

**Appendix1.1.** List of the geographic positions of all the collected Ambohiby Complex samples

**Appendix 1.2** Thin sections petrographic descriptions of the Ambohiby Complex

**Appendix 1.3** Mineral Chemistry Analysis

**Appendix 1.4** Major and trace element data of the selected samples of the Ambohiby Complex

**Appendix 1.5** Radiogenic isotope data for Sm-Nd and Rb-Sr geochronology

## LIST OF FIGURES

## List of Tables

## **List of Abbreviations and Acronyms**

**AFC**- Assimilation and Fractional Crystallization

**FC**-Fractional crystallization

**F**-fractional value

**JNdi-1-** The Nd is the isotope standard from the Geological Survey of Japan

**LA-ICP-MS -** Laser Ablation Inductively Coupled Plasma Mass Spectrometry

**NIST**- National Institute of Standards and Technology

**SEM** –Scanning Electron Microscope.

**XRF-** X-ray fluorescence

**EDS-** Energy Dispersive Spectrometry

## List of Mineral Abbreviations

- **Amph**– Amphibole

- **CPX**– Clinopyroxene

- **Chl**–Chlorite

- **OPX**–Orthopyroxene

- **Phl**– Phlogopite

- **Plag**– Plagioclase

# CHAPTER 1: INTRODUCTION

## 1.1. Introduction

A major focus of Gondwana research is the nature of tectonic processes that led to Gondwana breakup and their relationship to magmatic events. In particular, research has focussed on identifying the driving forces for the generation of magmas associated with Gondwana breakup, the compositional variation in the magmas and the source region(s) of these magmas as well as the identification of distinct magmatic events (e.g. Windley *et al.,* 1994; Storey *et al.,* 1995 & 1997; Meert & Van De Voo, 1997; Paquette & Nedelec 1997; Acharyya, 2000; Dalziel *et al.,* 2000; Collins, 2000 & 2006; Collins & Windley, 2002; Melluso *et al.,* 2003; Collins & Pisarevsky, 2005). One of the core aspects of this ongoing debate is the relationship between Gondwana break up, hotspot plumes and Cretaceous alkaline ring complexes (e.g. Bailey, 1964; Morgan, 1972; Gass *et al.,* 1978; Skyes, 1978; Lameyre & Bonin, 1985; Mahoney *et al.,* 1991 & 1992; Storey *et al.,* 1995 &1997; Pique, 1999; Harris *et al.,* 1999). Hotspot plumes, although controversial (Melluso *et al.,* 2003 & 2005), are thought to be one of the driving mechanisms for crustal thinning and rifting, leading to the breakup of the African components of Gondwana (Storey *et al.,* 1995 & 1997). Cretaceous alkaline ring complexes, which are numerous on the African plate and broadly co-eval with Gondwana rifting, are spatially associated with the locations of these hotspot plumes. This link has been further strengthened by geochemical studies, which have supported a petrogenetic link between the two (e.g. Milner & le Roex 1996; Storey *et al.,* 1995 & 1997; Mingram *et al.,* 2000, Melluso *et al.,* 2001; Ewart *et al.,* 2002; Trumbull *et al.,* 2003a).

Madagascar is one of the key areas to look at the relationship between Gondwana breakup, hotspot plumes and Cretaceous alkaline ring complexes (e.g. Janardhan, 1999; Yoshida *et al.,* 1999; Storey *et al.,* 1997; Melluso *et al.,* 2001 & 2005; de Wit, 2003; Chand & Subrahmanyam, 2003). The island is the product of two rifting events. The first rifting event occurred during the Jurassic and separated Madagascar and India from the African plate. The second rifting event occurred during the Late Cretaceous and separated Madagascar from India (Storey *et al.,* 1995 & 1997; Ashwal & Tucker, 1999; Torsvik *et al.,* 2000). This second rifting event is thought to have been influenced by the Marion Hotspot plume, which was underneath the Madagascan-Indian plate at the time, and is thought to have caused crustal thinning accompanied by widespread voluminous magmatism in both Madagascar and India (Storey *et al.,* 1995; Meert and Tamrat, 2006).

Currently, the Marion Hotspot plume is located over 2000km south east of the island close to the Southwest Indian Ridge (SWIR). It has remained fixed in this location for the past 90 Ma (Storey *et al.,* 1995; Pique, 1999; Meert and Tamrat, 2006). Whether the Marion Hotspot plume was instrumental in generating the late Cretaceous alkaline magmatism on Madagascar is still a subject of ongoing debate (e.g. Melluso *et al.,* 1997 Kumar *et al.,* 2001). However, during the Late Cretaceous, plate tectonic reconstructions have placed the southern tip of Madagascar over the location of the Marion Hotspot plume at this time (Storey *et al.,* 1997). In addition, while some of the Late Cretaceous rocks in Madagascar do not record any geochemical link with the Marion Hotspot plume (e.g. Melluso *et al.,* 1997; Melluso *et al.,* 2003), other Late Cretaceous alkaline rocks have shown a strong geochemical link (e.g. Kumar *et al.,* 2001; Mahoney *et al.,* 2008; Storey *et al.,* 1995, 1997). This variation indicates that the Late Cretaceous alkaline rocks of Madagascar have a heterogeneous mantle source (Melluso *et al.,* 1997).

The Volcan de l'Androy Complex, which is located in the southern part of Madagascar (Fig.1.1), contains the thickest sequence of Cretaceous volcanic rocks exposed on the island and is thought to record a geochemical link with the Marion Hotspot plume (Storey *et al.,* 1997). Petrologically the Volcan de l'Androy Complex is comprised of a bimodal basalt-rhyolite association with minor hybrid magmas (Battistini, 1959; Storey *et al.,* 1997; Mahoney *et al.,* 2008). The basalt-rhyolite association forms two compositional groups. Group I basalts and rhyolites are characterized by low total iron, $TiO_2$, pronounced negative Nb, Ta and Sr anomalies, LREE enrichment, low $\varepsilon_{Nd}$ and very high

initial $^{87}Sr/^{86}Sr$ (>0.71) (Storey *et. al.,* 1997). Group II basalts and rhyolites have in contrast higher Nb and Ta concentrations and lower Nd and Sr isotope ratios although the rhyolites still have pronounced negative Sr anomalies (Storey *et. al.,* 1997). While the high Sr isotope ratios and low $\varepsilon_{Nd}$ values of the Group I basalts have been used to infer crustal contamination of
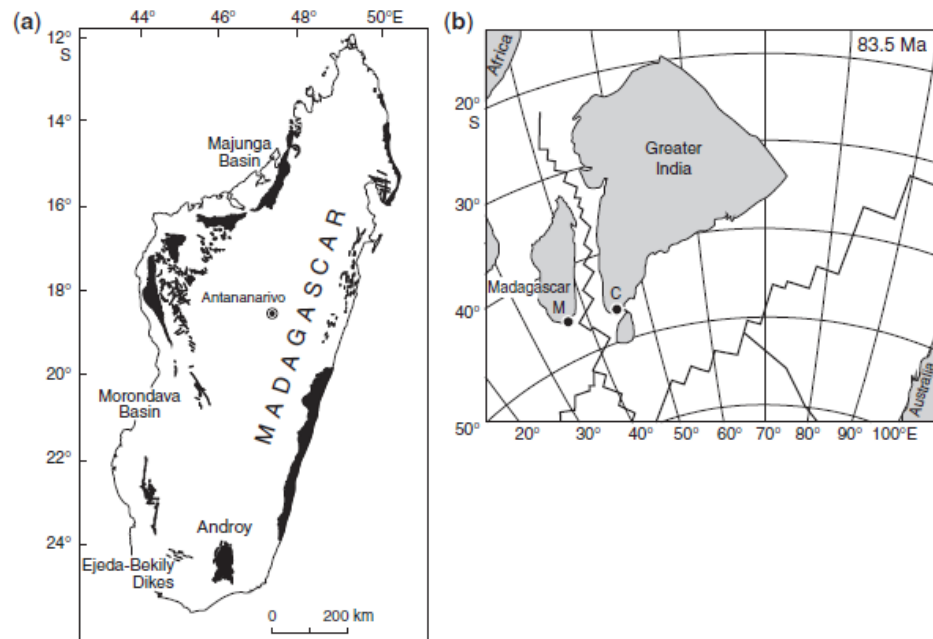


**Figure 1.1:** *(a) Main outcrops of middle Cretaceous Volcanic rocks on Madagascar after Besairie (1964), Mahoney et al., 2008. (b) Plate reconstruction at 83.5 Ma, shortly after the Androy eruptions. The locations of the Marion Hotspot Plume (M) and the Crozet (C) hotspots assume these hotspots have remained stationary relative to the earth's spin axis. (Kent et al., 2002, Mahoney et al., 2008)*

the magmas, other elements of the geochemistry (notably high Nb, Ta and total Fe) are thought to be indicative of a contribution from sub-lithospheric mantle and hence derived from the Marion Hotspot plume (Mahoney, *et al.,* 1991; Storey *et al.,* 1997).

The evidence for a contribution of the Marion Hotspot plume appears to decrease northwards through Madagascar. The basalts of the Volcan de l'Androy Complex, along with the basalt dykes around Mananjary, along with basalt dykes in India such as the Karnataka Dykes all show evidence for a contribution from the Marion Hotspot plume. However, all these rock are or were located near the southern end of Madagascar during the Late Cretaceous and hence were in close proximity to the Marion Hotspot plume. In

contrast, basalts in the northern part of Madagascar show almost no link to the Marion Hotspot plume (Melluso, *et al.,* 1997; Kumar *et al.,* 2001; Melluso *et al.* 2003). These basalts, which occur on the Antanimena, Bongolava and Manasamody Plateaux, have variable geochemical compositions and have been divided into four geochemical groups based on Ti concentrations, incompatible element ratios and Sr-isotope ratios (Melluso *et al.,* 1997). This variation in geochemistry has been used to infer heterogeneous magma sources with variable degrees of contamination and are consistent with a decrease in plume signature and an increase in the contribution of lithospheric and/or MORB mantle signatures. The Ambohiby Complex, which is the subject of this study, is situated in the central part of the island and as such it is not clear what influence the Marion Hot Spot plume has had on its formation. Understanding this contribution though could be central to understanding how the Ambohiby Complex was formed.

There are two major petrogenetic models for the formation of alkaline ring complexes. These are: (1) a fractional crystallization (FC) model where alkaline rocks are produced directly via differentiation of mantle derived magmas; (Bowen, 1928; DePaolo, 1981) and (2) an assimilation and fractional crystallization (AFC) model (Bowen, 1928; DePaolo, 1981) where alkaline rocks are produced via differentiation of mantle derived magmas that are then contaminated with the wallrocks that the magma is in contact with. However, alkaline ring complexes are not often the result of direct fractional crystallisation. Normally, if this were the case, the geochemical composition of the alkaline rocks would be very close to a near-primary mantle melt composition. This has been documented in the basanite and tephrite intrusions of the Erongo Complex in Namibia, which have Sr-Nd-Pb isotope values as well as incompatible trace element ratios consistent with the composition of the Tristan Plume (e.g. Trumbull *et al.,* 2003).

However, many alkaline complexes do not have radiogenic and stable isotope values that are indicative of near-primary mantle melt compositions and are thus inferred to have formed by an AFC process. This is due to the fact that both the radiogenic and stable isotope values are significantly elevated above mantle values, indicating that they must have a crustal component. Among many examples, the ring complexes of the Eastern Desert of Egypt (El Ramly & Hussein, 1984), the Sudanese alkaline ring complexes (Vail, 1984 & O'Halloran, 1985), and the Messum Igneous Ring Complex of Namibia (Harris *et al.,* 1999) have all been shown to be the result of AFC processes. Therefore, the critical question then becomes what is the crustal component and how

much crustal material is incorporated. Determining these two variables is vital to identifying the nature of the mantle component and thus the tectonic setting for alkaline ring complexes.

A schematic fractional crystallisation model developed by Bonin (1998) indicates how this differentiation process might work via a network of magma chambers that are emplaced at various depths to produce all types of melts (Fig. 2; Bonin, 1998). In order for this model to work for these alkaline rocks, very low degrees of partial melting of the mantle source are necessary in order to produce felsic magmas (Yoder, 1973; McKenzie, 1989; Bonin, 1998). Magma ascent occurred when pre-existing fractures are reactivated by tectonic events (Lameyre & Bonin, 1985; Bonin, 1998). Contrasting magmas and rock composition are then later exposed from different structural levels (Bonin, 1998) (Fig.1.2)
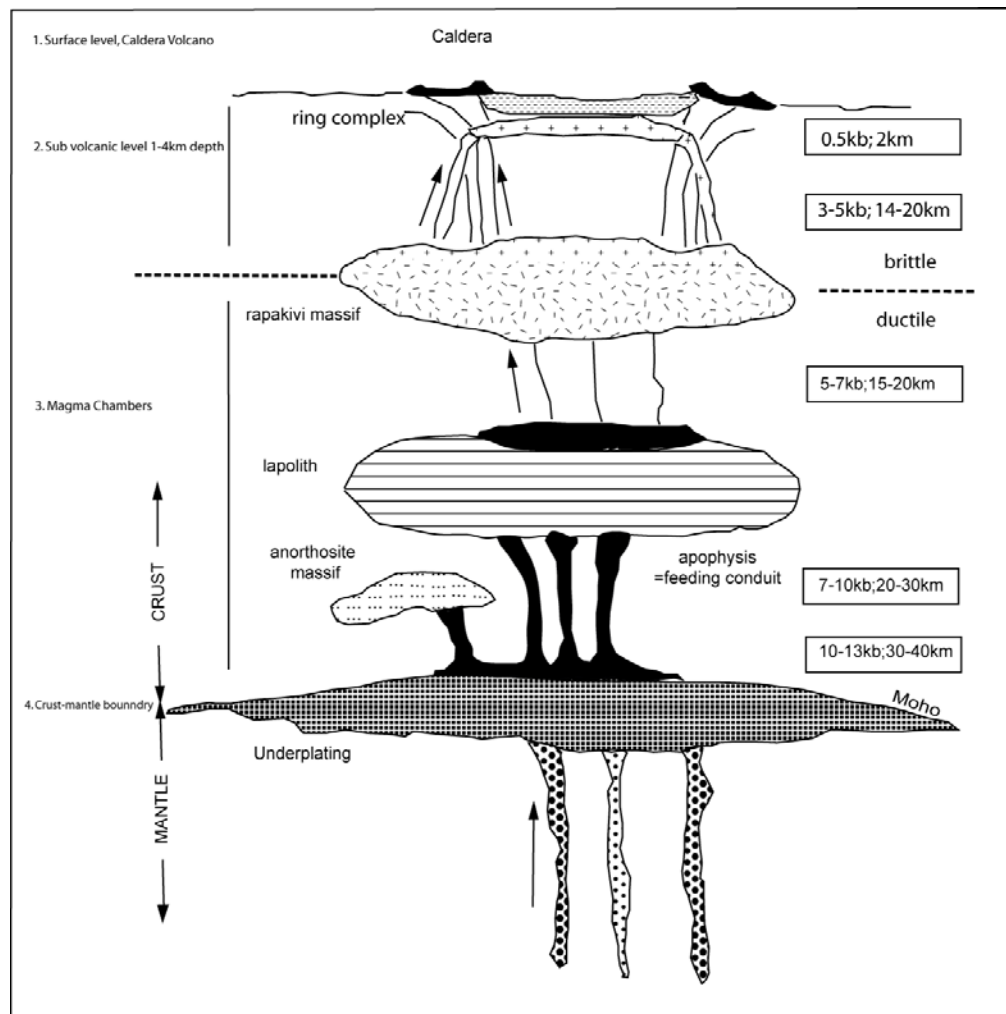


**Figure 1.2:** *Bonin (1998) demonstrates structural levels of alkaline magmatism: 1. Surface level; Caldera volcano; 2. Sub volcanic level (1 to 4km depth): ring complex, cone sheets and dyke*

*swarms; 3. Magma chamber levels (14 to 30 km depth), from bottom to top: apophyeses (black), anorthosite massif, mafic layered lopolith, rapakivi granite massif with alkali feldspar cumulates (dashes) and granitic residual liquids (crosses). 4. Crust-mantle boundary: storage of primary magmas formed within deeper asthenosphere.*

AFC processes can be modelled by assuming a mantle component and a crustal component and further assuming the relative proportions of each. However, the assumed mantle component might represent an evolved version of the mantle that existed at the time of the formation of the alkaline complexes and the mantle over which the alkaline complexes are currently situated is clearly not the same mantle from which they were derived given the change in the geographical position due to plate motions. Another problem is the fact that crustal contamination may have occurred at deep crustal levels, where the chemistry of the contaminant may differ significantly from rocks exposed at the Earth's surface (Lassen *et al.,* 2004).

This project formed part of a larger World Bank and South African government funded mapping programme in Madagascar to produce a revised, and digital geological map of the island. The mapping and allied research was completed by teams from the Council for Geoscience (South Africa), a British and USA Geological Survey consortium, a German consortium (BGR-GAF) and the French Geological Survey (BGRM). The island was last mapped by French colonial and Malagasy geologists during the period 1940-1960 (Ashwal & Tucker, 1999). The whole project was administered in Madagascar by the project de Gouvernance des Resources Minerales under the auspices of the Ministere de l'Energie et des Mines (MEM) of Madagascar. The Council for Geoscience (CGS) of South Africa was given a contract to map the Miandrivazo-Antsirabe-Tsiroanomandidy region (Zone E) in the central Madagascar and the Bekodoka-Ambohipaky-Mahabe region of the north western Madagascar (Zone F; Fig.1.3). This study is located on the north eastern boundary of Zone E near the town of Tsiroanomandidy and focuses on the $225km^2$ Cretaceous Ambohiby alkaline ring complex located in west central Madagascar (Fig. 1.3). The complex, which intrudes into Precambrian basement gneisses, is made up of various mafic and felsic intrusive phases, later cross-cut by a series of mafic and felsic dykes. The study aims to identify and classify the rock types that make up the Ambohiby Complex, to map their distribution, to use major, trace and REE geochemistry as well as radiogenic isotopes to define the petrogenesis of the complex and finally to evaluate its relationship with Gondwana break-up and the Marion hotspot plume.
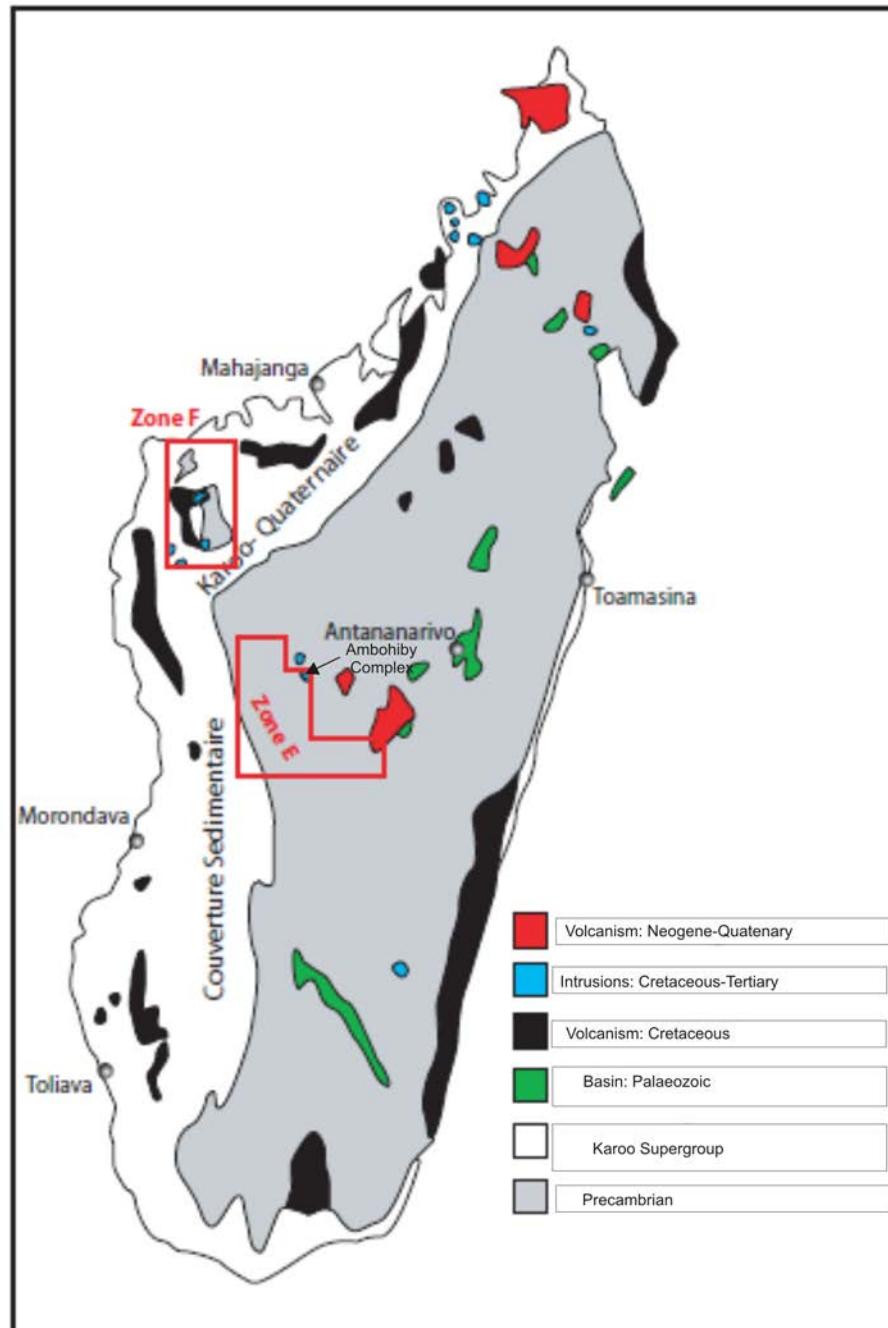
***Figure 1.3:*** *A simplified map of Madagascar showing the distribution of Cretaceous volcanic rocks (black) and ring complexes (blue), Neogene volcanic fields (red) and fault-controlled Plio-Pleistocene lacustrine basins (green) (Macey, 2009).*

## 1.2 Aims of this study

Since the Ambohiby Complex has never been mapped before, the first goal of this project was to map the distribution of rock types within the Ambohiby Complex. Once this had been done the different rock types were investigated to understand the petrogenesis of the plutonic rocks using major and trace elements as well as radiogenic isotopes. In order to achieve this, the following aims and objectives have been outlined.

1. What are the rock types that make up the Ambohiby Complex and what is their spatial distribution within the complex?

   - Based on field and petrographic relationships, what range of rock types make up the Ambohiby Complex?

   - What is the spatial distribution of the different rock types defined above and does the distribution relate to any evolutionary trend?

   - Do the rock types identified above define coherent geochemical groups and if not, how can this be explained?

2. What is the petrogenetic relationship between the different rock types within the Ambohiby Complex and can this be used to define a unique magmatic source region?

   - What petrogenetic processes can be used to explain the geochemical relationships between the different rock types of the Ambohiby Complex?

   - What are the geochemical characteristics of the magmatic source for the Ambohiby Complex defined by the petrogenetic process identified above?

   - How does the modelled source(s) of the Ambohiby Complex compare to that defined for other alkaline ring complexes on Madagascar?

3. How does the composition of Madagascan alkaline ring complexes compare geochemically and temporally to the Marion Hotspot Plume?

   - What is the geochemical relationship between the Madagascan alkaline ring complexes and the Marion Hotspot Plume?

   - If the Madagascan alkaline ring complexes and Marion Hotspot Plume are geochemically related, can they also be temporally related?

   - What does the petrogenesis and timing of the Madagascan alkaline ring complexes in comparison to the Marion Hotspot Plume tell us about Gondwana breakup?

## 1.3 Geological mapping and Sampling Methodology

Geological mapping and rock sampling of the Ambohiby complex was undertaken during May 2007. The fieldwork was completed on foot and motorcycle using a 1:25 000 scale topographic sheet as the base map. Sixty five samples were collected for geochemical and petrographic studies (see Appendix 1.1 and 3.3), representing all the different rock types within the complex. Care was taken to sample the freshest material possible and each sample location was given an individual waypoint. The locations of all samples and waypoints are shown on Figure 3.3. All samples were sent to the University of Stellenbosch for crushing, milling and thin-section preparation. Prior to processing all rock samples were carefully washed to remove dirt and rock dust. For all samples, any weathered portions were removed using a rock saw. The remaining rock was assessed and the freshest and most representative parts were cut up into blocks for thin-section preparation. Thin-section blocks were sent to the Pretoria office of the Council for Geoscience for thin-section making. The remaining portion was used for geochemical purposes. This portion was split into small pieces using a splitter, and then these pieces were put through a jaw crusher. A portion of the crushed rock was then milled in a Tungsten Sieb Swing Mill in the Central Analytical Facility of the University of Stellenbosch. The mill was cleaned with quartz and acetone between each sample. The resultant powder was used for major, trace and rare earth element analysis as well as radiogenic analyses.

## 1.4 Analytical Methodology

### 1.4.1 Major and Trace Element Analysis

The major elements were analysed in the XRF laboratory of the Department of Geological Sciences at the University of Cape Town. The Rb-Sr and Sm- Nd trace elements concentrations were measured by solution LA-ICP-MS at the Department of Geological Sciences of the University of Cape Town. The rest of the trace and rare earth elements were analysed in the LA-ICP-MS laboratory in the Central Analytical Facility at the University of Stellenbosch.

*Major elements*

Eleven major elements, Fe, Mn, Ti, Ca, K, S, P, Si, Al, Mg and Na (with Ni and Cr when Ni and Cr concentrations exceed -2000 ppm or 0.2 %) are determined using fusion disks prepared with LiT-LiM flux in the proportion 57:43 (Sigma Chemicals) and LiBr as releasing agent, according to the method of Fernand Claisse (1999). The disks were

analysed on a Philips PW1480 wavelength dispersive XRF spectrometer with a dual target Mo/Sc x-ray tube. All measurements were made with the tube at 50 kV, 50 mA. Analytical conditions are given in Table 1.1. Fusion disks made up with 100% Johnson Matthey Specpure $SiO_2$ were used as blanks for all elements except Si. Fusion disks made up from mixtures of Johnson Matthey Specpure $Fe_2O_3$ and $CaCO_3$ were used as blanks for Si. Intensity data were collected using the Philips X40 software. All peaks were corrected for background. Spectral overlap corrections were made for Br on Al, Cr on Mn, Al and Ca on Mg, and Mg and Ca on Na. Matrix corrections were made on all elements using the de Jongh model in the X40 software. Theoretical alpha coefficients, calculated using the Philips on-line ALPHAS programme, were used in the de Jongh model. Calculated uncertainties (twice the measured deviations for the standard expressed in wt%) are: 0.35 for $SiO_2$, 0.02 for $TiO_2$, 0.12 for $Al_2O_3$, 0.15 for $FeO^T$, 0.01 for MnO, 0.02 for MgO, 0.07 for CaO, 0.10 for $Na_2O$, 0.02 for $K_2O$ and 0.01 for $P_2O_5$.

*Trace and Rare earth elements*

For all trace and rare earth elements analyzed in the LA-ICP-MS laboratory in the Central Analytical Facility at the University of Stellenbosch the following procedure was taken: 0.28 g of the sample was combined with 1.5g of Spectroflux105 to prepare fused glass beads for the analysis of trace and REE compositions. Loss on ignition was determined at 1000°C. The trace and rare earth element (REE) analyses were performed by laser ablation inductively coupled plasma-mass spectrometry (LA-ICP-MS) using a New Wave 213 nm laser ablation system connected to an Agilent 7500ce ICP-MS. The analysis was performed on fused discs that were mounted in epoxy and polished to ensure a smooth, flat surface for analysis. The laser ablation operated under the specification display in table 1.2 while the ICP-MS operated under the conditions shown in table 1.3. Analytical uncertainties are less than 5%.

Si values (determined by the XRF analysis) were used as the internal standard and the instrument was calibrated using certified NIST 614 and 612 standards. Standard reference material BHVO-2G was used as certified reference standard to establish the level of accuracy of the data set. The following elements were analysed: Sc, Ti, V, Cr, Co, Ni, Cu, Ga, Rb,Sr, Zr, Nb, Y, Cs, Ba, Hf, Ta,Pb, Th, U, La, Ce, Pr, Nd, Sm, Eu, Gd, Tb, Dy, Ho, Er, Tm, Yb and Lu. In addition some of the elements such as Rb, Sr, Sm, Nd were reanalyzed at the department of Geological Sciences, University of Cape town using solution analysis. Analytical uncertainties are better than 5%.

**Table 1.1**: *Analytical conditions for determination of major elements using a Philips PW 1480 WDXRF spectrometer*

| Element /line | Collimator | Crystal | Detector | PHS LWL | UPL | Counting time (s) | Concentration range ** | RMS | Lower limits of determination* | No. of standards |
|---|---|---|---|---|---|---|---|---|---|---|
| NiK | F | LiF(220) | FS | 22 | 70 | 100 | 0 - 0.48 | 0.003 | 0.004 | 11 |
| FeK | F | LiF(220) | FL | 16 | 68 | 100 | 0 - 17 | 0.069 | 0.019 | 20 |
| MnK | F | LiF(220) | FL | 15 | 66 | 100 | 0 - 0.27 | 0.004 | 0.014 | 22 |
| CrK | F | LiF(220) | FL | 14 | 70 | 100 | 0 - 3.5 | 0.011 | 0.008 | 11 |
| TiK | F | LiF(200) | FL | 32 | 68 | 100 | 0 - 3.9 | 0.022 | 0.023 | 22 |
| CaK | F | LiF(200) | FL | 30 | 76 | 50 | 0 - 77 | 0.102 | 0.004 | 21 |
| K K | F | LiF(200) | FL | 32 | 74 | 100 | 0 - 15.5 | 0.037 | 0.003 | 21 |
| S K | C | GE(111) | FL | 32 | 74 | 100 | 0 - 53.5 | 0.112 | 0.100 | 11 |
| P K | C | GE(111) | FL | 34 | 74 | 100 | 0 - 3.4 | 0.011 | 0.008 | 16 |
| SiK | C | PE(002) | FL | 26 | 80 | 100 | 0 - 100 | 0.215 | 0.052 | 20 |
| AlK | C | PE(002) | FL | 26 | 80 | 100 | 0 - 100 | 0.084 | 0.074 | 21 |
| MgK | F | PX-1 | FL | 36 | 68 | 100 | 0 - 85 | 0.141 | 0.102 | 20 |
| NaK | F | PX-1 | FL | 30 | 78 | 100 | 0 - 9.1 | 0.065 | 0.17 | 12 |

** all concentrations expressed as wt% oxide; S as $SO_3$
\* = 10 × lower limit of detection, expressed as wt% oxide

$$RMS = \sqrt{\frac{1}{n-k} \sum \left( Conc_{given} - Conc_{calc} \right)}$$

where
n = no. of standards
k = no. of calibration coefficients, *i.e.* 2, the slope and intercept of the calibration line.
$Conc_{given}$ = recommended concentration for an element in a standard
$Conc_{calc}$ = concentration of an element calculated from the best-fit calibration line

**Table 1.2:** *Laser Ablation specifications*

| Laser output | 213nm flat-top beam |
|---|---|
| Energy | ~ 5 J/cm$^3$ |
| Pulse width | 4ns nominal |
| Pulse rate | 15Hz |
| Spot size | 100 µm |
| Scan pattern | 3 lines of 450 µm per sample |
| Background counting time | 17sec |
| Data acquisition time | 40 sec |

**Table 1.3:** *The ICP-MS specifications*

| | |
|---|---|
| RF Power | 1350 kW |
| Plasma gas flow | 15L/min |
| Auxiliary gas flow | 0.9L/min |
| Carrier gas flow | 0.9L/min Ar, 0.6L/min He |
| Acquisition mode | Time Resolved Analysis |
| Integration time | 0.01 sec / isotope |
| Optimized for oxide levels | < 0.6% |

## 1.4.2. Mineral Compositions

Mineral compositions were determined on a LEO 1430VP Scanning Electronic Microprobe (SEM) utilising Energy Dispersive Spectrometry (EDS) at the University of Stellenbosch. The analysis was performed on polished thin sections that had been coated with a 15 micrometer thick carbon layer. The operating conditions were set at an accelerating voltage of 20 kV with a specimen beam current of 3.97µA and a probe current of 1.50µA with a working distance of 13mm. Minerals were identified with backscattered electron (BSE) and secondary electron images. The mineral compositions were quantified by EDX analysis using an Oxford Instruments® 133KeV detector and Oxford INCA software. Acquisition time was set at 50 seconds and pure Co was used periodically to correct for detector drift. Mineral compositions were recalculated to mineral stoichiometries and the stoichiometric results were used to evaluate the quality of the analytical data. Internal Astimex Scientific mineral standards were used for standardization and verification of the analyses (See Table 1.4). Uncertainites on this method of analysis have been discussed and reported by Moyen et al. (2006).

**Table 1.4:** *Internal Astimex Scientific mineral standards as well as the elements used for different minerals for standardization and verification during mineral chemistry analysis.*

| Astimex Scientific mineral Standards | Amphiboles | Aegirine | Diopside & Augite | Na-feldspar | K-feldspars |
|---|---|---|---|---|---|
| Albite | Na & K | Si & Ca | Si & Ca | Na | Na |
| Almandine garnet | Fe | Fe | Fe | | |
| Biotite | Ti | Ti | Ti & K | Ti | Ti |
| Diopside | Al | Al | Al | | |
| Plagioclase An90 | | | | Ca, Si & Al | Ca, Si & Al |
| Plagioclase An65 | Si & Ca | Mg & Na | Ca & Na | Mg | Mg & K |
| Sanidine | | | | Fe & K | Fe |
| Pyrope | Mg & Mn | Mn | Al, Mg & Na | Mn | Mn |

### 1.4.3 Radiogenic Isotopes

The Sr- and Nd-isotope data were obtained using a NuPlasma High Resolution Multi-Collector ICPMS at the University of Cape Town following standard chemical separation procedures described by le Roex and Lanyon (1998). The standard NIST987 (NIST, 2000) gave 0.710286 ±34 during the Sr-isotope runs and the JNdi-1 Nd-isotope standard (Tanaka *et al.,* 2002) gave a value of 0.5120688 ±16 during the Nd-isotope runs. The radiogenic isotope data were normalized to values of 0.71026 (NIST987) for Sr-isotopes and JNdi-1 standard (Tanaka *et al.,* 2000) 0.512094 ± 0.000014 (VG 54–30, 2σ, n = 11) and 0.512116 ± 0.000010 (IsoProbe-T, 2σ, n = 14).

## CHAPTER TWO: TECTONOSTRATIGRAPHY

### 2.1 Introduction

Madagascar is the fifth largest island in the world after Greenland, New Guinea, Australia and Borneo and covers an area of about 627,000 km$^2$ (Ashwal & Tucker, 1999; de Wit, 2003). The island is situated in the Indian Ocean and is ~1580 km long and 570 km wide and separated from the east coast of Africa by the Mozambique Channel and to the north by the Western Somali and Comores Basin (Storey *et al.,* 1997). Before the formation of Gondwana, the eastern part of Madagascar was part of the Dharwar Craton (Agrawal *et al.,* 1992), while other parts of Madagascar have African origins and date back to 2.5 Ga (de Wit, 2003). Generally, Madagascar is made up of fragments of different continents (Fig. 1.1), some of which comprise very old continental crust that can be dated as far back as 3.2 Ga (de Wit, 2003).

The island of Madagascar was formed due to two major rifting events, which were associated with the progressive breakup of the Gondwana supercontinent. The first rifting event was the separation of Madagascar and India from Africa during the Jurassic (~180 Ma) and began with seafloor spreading in the Western Somali and Comores Basin (Coffin and Rabinowitz 1988; Storey *et al.,* 1995; Meert & Van Der Voo, 1997; Tucker *et al.,* 1999; Kroner, 1999; Kroner *et al.,* 2000; Collins & Windley 2002). The original location of the island before this rifting event has been the subject of extensive debate. Seafloor magnetic anomalies and fracture patterns indicate that prior to the Middle Jurassic, Madagascar either bordered the coast of Somalia, Kenya and Tanzania (Smith and Hallam, 1970; McElhinny *et al.,* 1976; Scrutton *et al.,* 1981; Coffin *et al.,* 1986; Coffin and Robinowitz 1988; de Wit *et al.,* 1988 & 2003, Yishida *et al.,* 1999) rather than

against the Mozambique coast (Green, 1972; Flores, 1984) or was a stationary island in a fixed location relative to Africa (Dixey, 1960, Storey *et al.,* 1997). The southward motion of Madagascar relative to Africa during the Jurassic and Early Cretaceous was influenced by a large transform fault (Davie Ridge) (Coffin and Rabinowitz, 1987; Bassias and Leclaire, 1990). The Davie Ridge led to sedimentation in the western part of the island and formed a basin that was then faulted adjacent to the older ocean crust to form the Mozambique Channel (Storey *et al.,* 1997).

The second rifting event was the separation of India from Madagascar during the Late Cretaceous at ~90 Ma in response to seafloor spreading in the Mascarene Basin (Storey *et al.,* 1997). Madagascar was left behind as a micro-continental plate while the Indian lithospheric plate moved northward at a velocity of 10-19cm/yr (Raval & Veeraswamy, 2003). In addition, evidence suggests that India and Madagascar were once attached to each other as a continental plate. This positioning is supported by the work of Crawford (1978), who traced the Proterozoic Narmada-Son lineament of central-west India into northern Madagascar, and Agrawal *et al.* (1992) who suggest that Madagascar was part of the Dharwar Craton of India before the second rifting event. The Marion Hotspot track that was calculated using the plate motion model of Muller *et al.,* (1993) placed the Marion Hotspot plume 100km south of Madagascar during second rifting event (Storey *et al.,* 1995; 1997). According to this model, the 88-120 Ma Marion hotspot tracks are observed parallel to the rifted margin of Madagascar (Fig. 1, Storey *et al.,* 1997). Subsequent to Gondwana fragmentation that started in the Carboniferous, deposition of Phanerozoic and sedimentary volcanic successions and intrusion of ring complexes occurred.
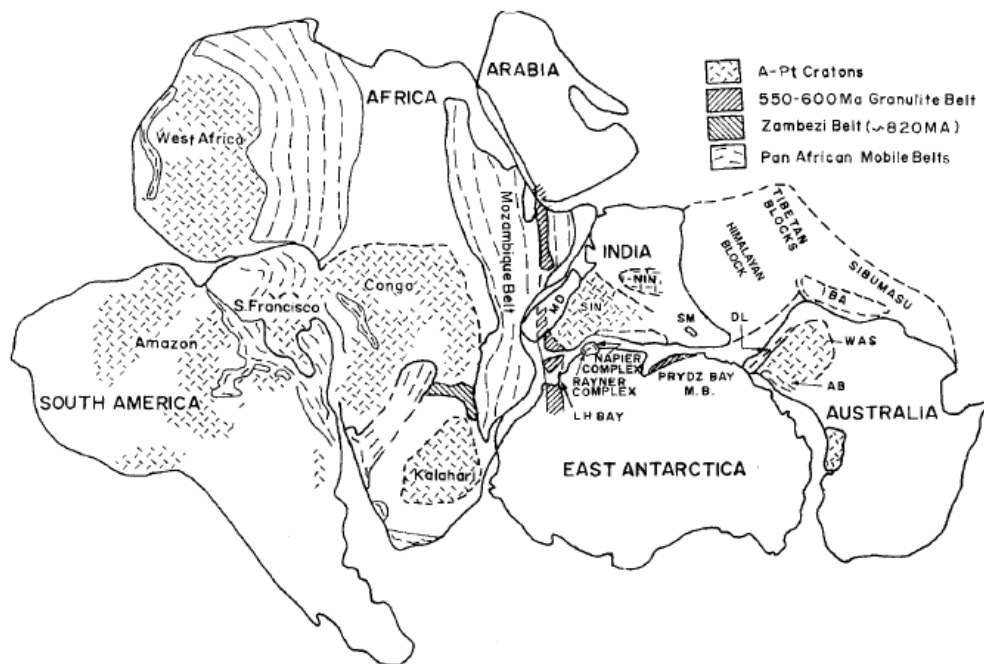
**Figure 2.1:** *Sketch map of Gondwanaland showing the distribution of Archaean-Proterozoic cratons and other older mobile belts. SIN-South Indian craton, NIN-North Indian craton, SM-Precambrian rocks of north east India, WAS-West Australian craton, DL-Darling mobile belt, AB-Albany mobile belt and Stirling basin (these are located in the Australian continent), LH Bay-Lutzow-Holm Bay (in the East Antarctican continent), MD-Madagascar, Disposition of the Himalayan block, the Tibetan blocks, the Sibumasu and Indo Burma Andaman (IBA) in the Greate Indo-Australian Continent are shown in this sketch (Acharyya, 2000)*

## 2.2 Tectonostratigraphic Units

Madagascar is composed of plutonic and metamorphic rocks ranging from Archean to Phanerozoic in age that form a basement to the post Carboniferous sedimentary and volcanic successions. The Precambrian basement of the island consists of tectonic blocks or terranes of Archaean to Phanerozoic age separated by major shear zones. These tectonic blocks have been reworked during repeated continental collisions and fragmentation during the Mesoarchaean and into the early Phanerozoic. The East African Orogeny dominates the tectonometamorphic character of the island and overprints earlier structures and mineral assemblages. Precambrian basement makes up almost two thirds of Madagascar (Macey, *et al.,* 2009).

Madagascar is divided into five tectonic units and each unit is separated from each other by a regionally major unconformity or a shear zone (Collins *et al.,* 2000 and 2006; Kroner *et al.,* 2000; Collins and Windley, 2002). The Precambrian tectonic units are: (1) the

Antongil Block, (2) the Antananarivo Block, (3) the Tsaratanana Thrust Sheet, (4) the Bemarivo Orogenic Belt and (5) Neoproterozoic metasedimentary belts (Fig.2.2 and Table 2.1).
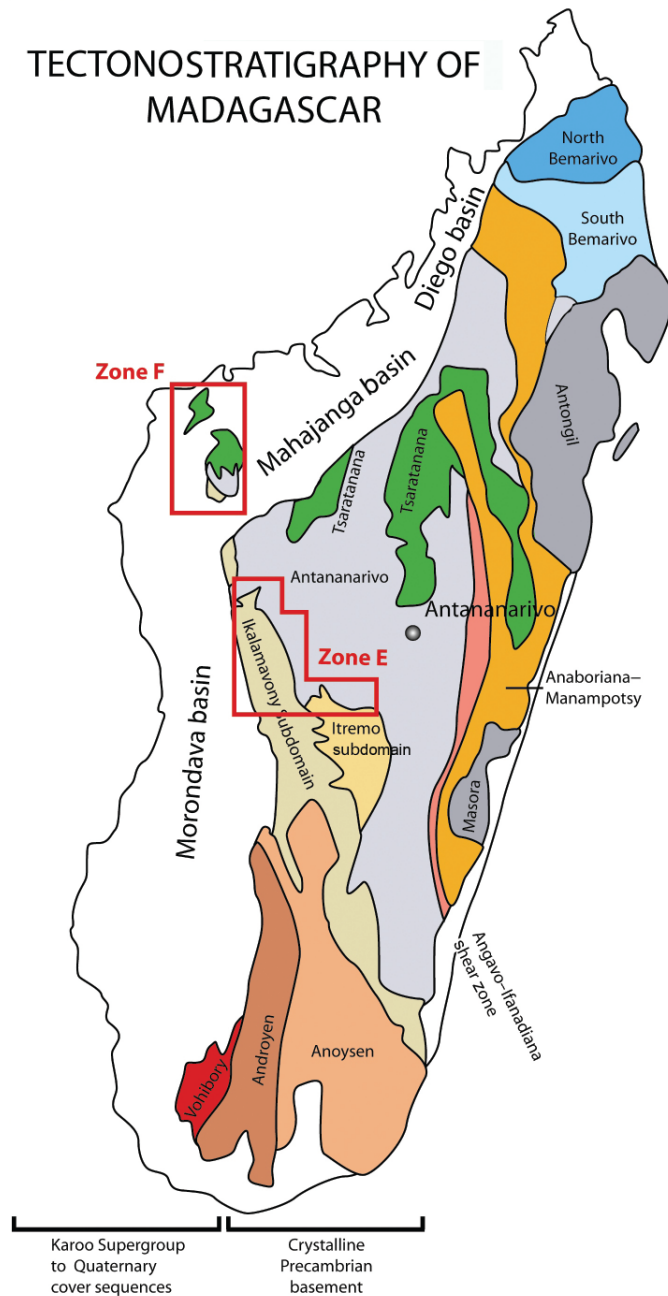


*Figure 2.2: New tectonostratigraphic subdivision for the Precambrian geology of Madagascar proposed by the geological survey teams employed for mapping Madagascar (Macey et al., 2009).*
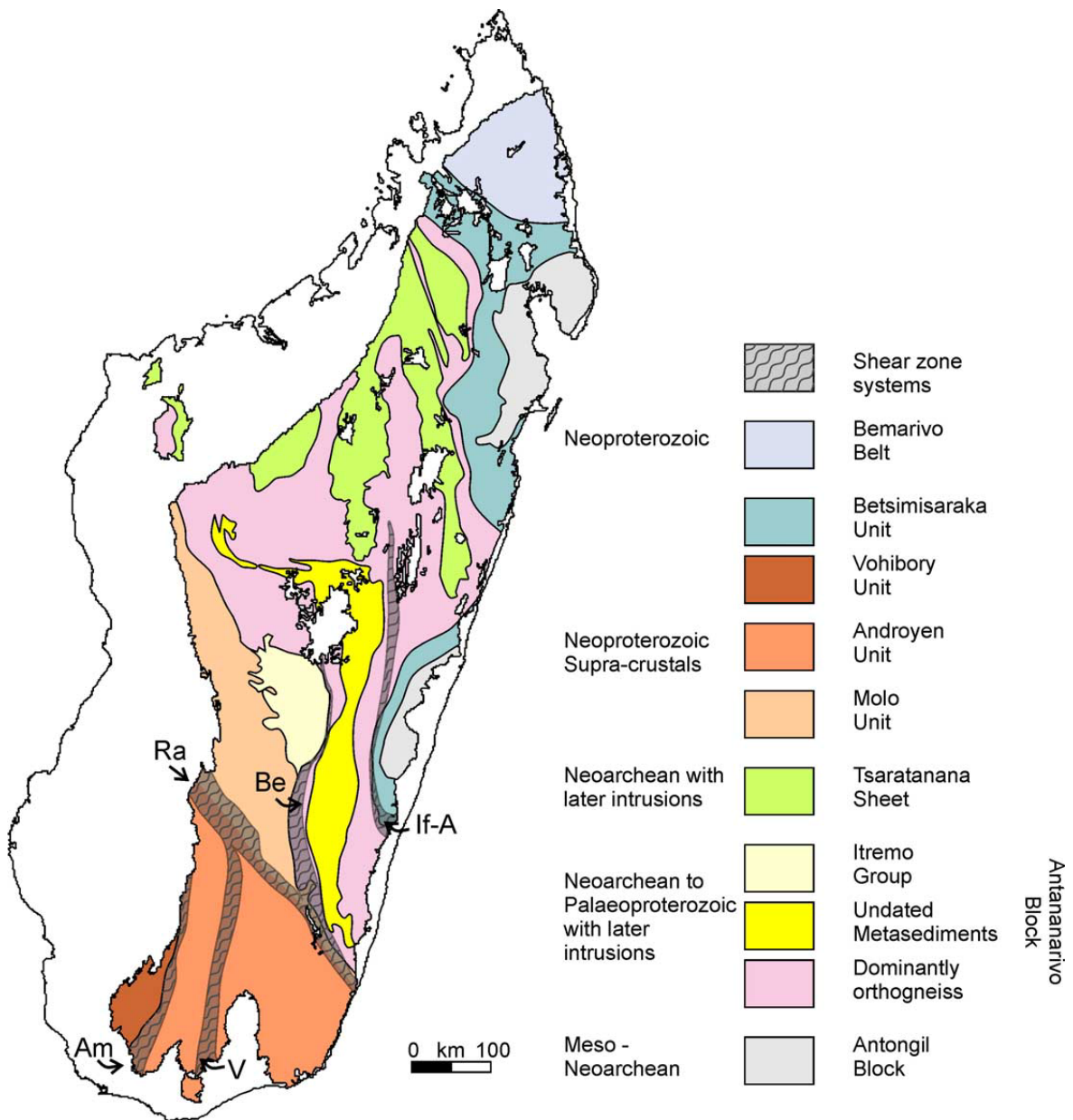
***Figure 2.3:*** *Tectonostratigraphic subdivision for the Precambrian geology of Madagascar proposed by Collins (2006) Am = Ampanihy shear zone; Be = Betsileo shear zone; If-A = Ifanadiana–*
*Angavo; Ra = Ranotsara; V = Vorokafotra*

### 2.2.1 Precambrian Basement

#### 2.2.1.1 *Antongil Block*

The Antongil Block is situated in the north-western part of the island (Fig. 2.1) and consists of gneisses and granitoids surrounded by a sequence of metasediments (Collins, 2000; 2006). This block is characterized by lower temperature metamorphic assemblages compared to the rocks from the Antananarivo Block (Collins, 2006 and references cited therein). The Antongil Block also contains the earliest crustal material in Madagascar, dating back to 3200 Ma with deformation occurring between 3.2-2.5 Ga (Raval & Veeraswamy, 2003) and intrusion of granitic bodies at ~2520 Ma (Tucker *et al.,* 1999b; Collins *et al.,* 2001; Paquette *et al.,* 2003)

#### 2.2.1.2 *Antananarivo Block*

The Antananarivo Block is situated in the central part of the island and is the largest pre-Palaeozoic tectonic unit in Madagascar (Collins *et al.,* 2001). This block underwent three main periods of magmatism. The first period occurred between 2600-2500 Ma and was associated with granitoid intrusions (Table 2.1). The second magmatic episode occurred between 820-740 Ma and was associated with tectonically inter-layered voluminous magmatism of granites, syenites and gabbros. Between 700- 532 Ma the Antananarivo block was thermally and structurally reworked (Kroner *et al.,* 2000) resulting in a granulate facies overprint. The third period of magmatism occurred between 630-530 Ma, during which time the Antananarivo block was intruded by granitoid sills. This last magmatic episode occurred synchronously with extensional deformation that was associated with the crustal-scale extensional of the Betsileo shear zone (Nedelec *et al.,* 1995; Collins, 2000 & 2006).

The Itremo and Ikalamavony Groups non-conformably overlie the amphibolites and gneisses of the Antananarivo Block. These Groups where deposited around ~1800 Ma and consists of quartzites, and carbonates (Tucker *et al.,* 1999b; Collins 2006). The metamorphic grade of the Itremo group generally increases from greenschist facies in the east to amphibolite facies in the west (Tucker *et al.,* 2006). The Itremo group rocks were deformed into large recumbent isoclinal folds that were later intruded by a set of gabbros and syenites between 804 and 779 Ma. These intrusions record chemical affinities of supra-subduction zone and are much less deformed than coeval intrusions in the Antananarivo Block (Handke *et al.,* 1999).

### 2.2.1.3 *Tsaratanana Thrust Sheet,*

The Tsaratanana Sheet is located in the north central part of the island and contains mafic gneisses, tonalities, chromite-bearing ultramafic rocks and meta-pelites (Collin 2006). This unit is a sheet because it comprises rocks that are metamorphosed to ultra high temperatures, contained within three main belts, the Maevatanaa, Andriamena and Beforona belts. These three belts have similar lithologic, geochronologic and structure. Early intrusion in this unit took place between 2.76 and 2.49 Ga, however later intrusion of gabbro between 800-770 Ma over print deformation of older rocks (Tucker *et al.,* 1999b; Paquette *et al.,* 2004).

### 2.2.1.4 *Bemarivo Orogenic Belt*

The Bemarivo Orogenic Belt is located in the northern part of the island and crosscuts the Antananarivo Block, the Antongil Block and the Betsimisaraka suture (Collins, 2006). The Bemarivo Belt consists of two discrete regions: (1) a southern region dominated by upper amphibolite and granulite-grade metasedimentary gneisses; and (2) a northern region consisting of granitic dome-like massifs that intrude through migmatites and orthogneisses (Jourde *et al.,* 1974). There are three major meta-volcano sedimentary regions that occur in the northern region namely, the Daraina, Milanoa and Betsiaka series, and together they form the Daraina Group. The southern region was deformed by top-to the south thrusting, coeval with granulite-grade metamorphism at ~519.2±0.7 Ma (Buchwaldt *et al.,* 2003)

### 2.2.1.5 *Neoproterozoic metasedimentary belts*

Neoproterozoic metasedimentary regions or belts divide the Antongil and Antananarivo Blocks and occur south and west of the Antananarivo Block (Fig. 2.3) (Collins, 2006). The Neoproterozoic metasedimentary regions consist of four regions, namely: Betsimisaraka, Molo, Androyen as well as the Vohibory region.

The **Betsimisaraka region** is the large metasediments region and it divides the Antongil and Antananarivo Blocks (Fig.2.3). This region has been interpreted to have marked the remains of an oceanic suture zone (Collins*,* 2006)

The **Molo metasediments** occur in the west of the Itremo Group and north of the Ranotsara shear zone (also known as Amborompotsy Group) (Cox *et al.,* 2004). The protoliths (e.g. mudrocks) to these rocks were deposited between ~620 and 650 Ma in

an Ediacaran basin that separated central Madagascar from East Africa (Cox *et al.,* 2004; Collins and Pisarevksy, 2005; Fitzsimons and Hulscher, 2005).

The ***Androyen region*** occurs in the south of the Rantosara shear zone and is a high grade metasedimentary terrain that has been metamorphosed (Nicollect, 1990; Ackermand *et al.,* 1991; Martelat *et al.,* 1997; Markl *et al.,* 2000). Neoproterozoic zircons from this region were analyzed from metasedimentary gneisses indicating that some of the sedimentary protoliths were deposited during Neoproterozoic times (Kroner *et al.,* 1996 & 1999; de Wit *et al.,* 2001). Several authors have suggested that the metasediments south of the Rantosara shear zone correlate with the Molo metasediments, north of the crustal-scale shear (e.g. de Wit, 2003), whereas detrital zircons suggest a similar provenance as the Itremo Group (Collins *et al.,* 2005). There is no precise geochronological data but at least some of the Androyen metasediments predate 620-560 Ma deposition of the Molo metasediments (Cox *et al.,* 2004) as ~630 Ma anorthosite intrusions cut metasedimentary rocks in the south of this region (Ashwal *et al.,* 1998).

The ***Vohibory region*** is located in the southwest of the island and consists of pelites, marbles, extensive amphibolites and granitoids (Collins, 2006) (Fg.2.1 and Table 2.1). Nicollect (1990) and Martelat *et al.* (1997) reported that this region underwent high-pressure metamorphic conditions (>10 kbar) compared to the rest of the island. U-Th-Pb ages of detrital zircon from the pelites of this region have an age of ~850 Ma suggesting that they were sourced from an age-restricted Neoproterozoic source. Jons *et al.* (2005) suggested that the amphibolites from this region were sourced from a depleted mantle and represent a slice of ocean crust and interleaved arc that today forms a complex tectonic melangé. The meta-igneous bodies in this region represent the extrusive flows, or sill-like bodies, intruded into a coeval package of Neoproterozoic metasedimentary rocks. Collins (2006) therefore suggested that this region represents an early Neoproterozoic volcanic rift succession.

*Table 2.1:* *Summary of tectonic events recorded in the various tectonic units (Collins, 2006)*

| Tectonic unit | Metasediments | Major Tectonic events |
|---|---|---|
| Bemarvo Belt | | • 717-754 Ma granite magmatism<br><br>• 715 Ma Rhyolite extrusion coeval with deposition of sandstone and conglomerates<br><br>• 510-520 Ma granulite-gade metamorphism, coeval with south-west directed thrusting<br><br>• Extensional deformation |
| Neproterozoic metasediments | Betsimasaraka | • Post-720 Ma deposition of protolith mudrocks<br><br>• Metamorphism at ~ 520 Ma |
| | Molo | • Post 620 Ma deposition of protolith qaurtzites and mudrocks<br><br>• Metamorphism and deformation at ~ 560 Ma |
| | Andriyen | • 750-630 Ma deposition of protolith mudstones, sandstones and limestones<br><br>• Intrusion by 630 Ma anorthosites<br><br>• Metamorphism between 645-545 Ma |
| | Vohibory | • Post 850 Ma deposition of protolith mudrocks, carbonates and possible coeval basic volcanism. No ealier detritus |
| Tsaratanana Sheet | | • 2747-2494 Ma granitoid intrusion through crust dating to 3260 Ma<br><br>• Deformaton and emplacement over Antananarivo Block<br><br>• 787-779 Ma gabbro magmatism coeval with high temperature metamorphism in the country rocks<br><br>• 637-627 Ma granitoid intrusion<br><br>• Intense deformation transporting earlier rocks into gneissic tectonites<br><br>• 549 Ma late diorite magmatism<br><br>• Deformation |
| Antananarivo Block (Inluding Intremo Group) | | • ~ 2500 Ma crust formation<br><br>• 2189-1007 Ma zircon xenocrysts in later granites, whose signifance is unknown<br><br>• Post 1850 Ma deposition of Itremo Group-quartzites, mudrocks and carbonates<br><br>• Pre-820 Ma deformation into large recumbent isoclinal folds<br><br>• 824-719 Ma  Supra-subduction zones: gabbro and granitoid intrusion<br><br>• 633-561Ma granitoid magmatism<br><br>• Pre-550 Ma granulite grade metamorphism and contractional deformation<br><br>• Intrusion of post-tectonic granitoids 573-530 Ma possibly coeval with: Extensional deformation along the Betsileo shear zone |
| Antongil Block | | • 3200-2500 Ma continental crust formation and deformation<br><br>• 2500 Ma Granite intrusion<br><br>• Palaeozoic sediments deposited on erosion surface |

### 2.2.2. Late Neoproterozoic-Cambrian magmatism in Madagascar

Three Neoproterozoic-Cambrian magmatic events occurred in Madagascar, namely;

The ~640–630 Ma magmatic event that resulted in the intrusion of concordant sheet-like bodies of alkaline granitoids of the Kiangara Suite into the Antananarivo domain of central Madagascar (Nédélec *et al.,* 1995; Paquette and Nédélec, 1998; Meert *et al.,* 2001). The second magmatic event was far more widespread, and occurred in the late Neoproterozoic–Cambrian, and led to the formation of the Ambalavao Suite (Macey *et al.,* 2009). The Ambalavao Suite is late-tectonic alkali feldspar- rich granites that dated at between 570 and 530 Ma (Tucker *et al.* 1997, 1999a; Kröner *et al.* 2000; Macey *et al.,* 2009). The third magmatic event is represented by the post-tectonic early Cambrian (530–510 Ma) Maevarano Suite (including the Carion granite) and is particularly common in northern Madagascar where it intrudes the Bemarivo and Antananarivo domains (Macey *et al.,* 2009).

### 2.2.3 Karoo Supergroup

The Late Neoproterozoic–Early Cambrian marked the Gondwana assembly with Madagascar located in the interior of the supercontinent (Reeves *et al.*, 2002; Macy 2009). The intercontinental rifting of Gondwana began during Late carboniferous and Jurassic, and these led to the deposition of the Karoo Supergroup of Madagascar which is equivalent to the Karoo and other Gondwana sequences India and Africa (De Wit, 2003). Three sedimentary basins developed along the western Madagascar during late Jurassic, namely; the Morondava, Mahajanga, and Diego Basin (De Wit, 2003). These basins covers one third of Madagascar. Each basin consisted of identical three-part Karoo stratigraphic division, which are Sakoa, Sakamena, and Isalo Groups (Wescott and Diggens, 1998, De Wit, 2003). The Andafia Formation has been added as an upper unit of the Karoo Supergroup (Geiger *et al.*, 2004; Schandelmeier *et al.*, 2004).

### 2.2.4 Cretaceous Magmatism

Late Cretaceous continental breakup of Madagascar from greater India resulted in widespread volcanism throughout the island, and intrusion of dyke swarms and to a lesser extent ring complexes across large parts of the island (Storey *et al.,* 1995, 1997, Bardintzeff *et al.,* 2001; Melluso *et al.,* 2001, 2003). Cretaceous lava flows are well exposed and mainly occur along the coastal areas that include the Morondava and Mahajanga basins, and also in the rifted margin of the eastern coast (Storey *et al.,* 1997; Melluso *et al.,* 2003). The flood basalts of the late Cretaceous are well exposed in the

Northern part of the island (Fig 1.1 and Fig 1.5) on the Antanimena, Bongolava and Manasomody plateaux that is located south and east of Majunga (Melluso *et al.,* 1997).

Mellluso *et al.,* (2003) grouped the Cretaceous rocks from the northern part of the island into sub provinces (i.e. Eastern subprovince and Western subprovince) in order to study their petrogenesis. The Eastern subprovince comprises (1) the Eastern Mahanga basin and Tampoketsa Kamoreen; (2) Tamatave –Sambava-Sainte Marie Island and (3) The Antampombato –Ambatovy Complex. The Western subprovince comprises of (1) Mailaka-Bemaraha area and (2) Antanimena (western Majanga basin).

In the southern part of the island, the Androy Complex contains the thickest sequence of Cretaceous volcanic rocks exposed on the island (Storey *et al.,* 1997). The complex forms an oval-shaped outcrop of some 50 km wide by 90 km long and consists of interbedded flows of basalt and rhyolite with microgranite intrusions at the northern and western margin of the complex (Battistini, 1959; Storey *et al.,* 1997). Geochemically the Androy Complex is comprised of a bimodal basalt rhyolite association with minor hybrid magmas (Storey *et al.,* 1997). The Androy basalts form two compositional groups. Group I is the most abundant rock type in the complex and generally has low total iron, $TiO_2$ and Nb than Group II basalts. Group I on mantle normalized diagrams shows pronounced negative Nb, Ta, and Sr anomalies and enrichment in the light REE elements. The negative Sr anomalies may be due to plagioclase fractionation during crystallization. Group I also has low initial Nd and very high initial $^{87}Sr/^{86}Sr$ (>0.71) indicating these basalts have assimilated continental crust (Storey et al., 19997).

The Karnataka late Cretaceous dykes that are located in the west coast of India are co-eval and compositionally similar to the Fe-Ti enriched theoleiitic lavas and dykes around Manajary, which is the major phase of late Cretaceous magmatism along the eastern rifted margin of Madagascar. These two areas (i.e. The Karnataka late Cretaceous dykes and Fe-Ti Enriched theoleiitic lavas around Manajary eastern rifted margin of Madagascar) are believed to have been facilitated by Marion Hotspot plume that resulted in the breakup of Madagascar from India (Kumar *et al.,* 2001). Furthermore geochemical and geochronological data shows that the Karnataka Late Cretaceous dykes and the rocks from the Mananjary and Tamatave of the eastern rifted margin of Madagascar were formed as result of the breakup of Madagascar and India that was initiated by Marion Hotspot plume (Kumar *et al.,* 2001).

In the northwest part of the island, there are six late Cretaceous sub-volcanic ring complexes namely, Ambereny Complex, Fonjay Complex, Berevo Complex, Ankibobozaka Complex, Maningoza Complex and Ambohitrosy Complex (Macey *et al.,* 2009). These complexes intrude into two inliers of the Neoarchean-Proterozoic gneiss, the Bekodoka and the Ambohipaky inliers, unconformably overlain by and locally faulted against phanerozoic (Triassic-Cretaceous) sedimentary and volcanic rocks (Besarie, 1969).

The Fonjay and Ambereny Complexes were first mapped in the 1898 by Gautier followed by Boulanger (1959) and recently mapped by Macey *et al.* (2009). These complexes consist of gabbro, gabbronorite, olivine norite, dolerite, syenite/syeno-granite and anorthosite. The circular Fonjay Complex is ~15km in diameter and situated about 25km to the northwest of Morafenobe Town. The topography is dominated by the 450-800m high circular rim of the structure that rises steeply from surrounding plains.

The Ambereny Complex has the same size and shape as the Fonjay Complex but is situated a further 25km northwest of Morafenobe. The Berevo Complex intrudes into the unconformity between the Bekodoka inlier (amphibolite facies gneisses) and the Isalo Group sandstones. The Berevo complex occupies an arid sub-circular area of 12 to 13 km in diameter and situated north of the Ranobe (Macey *et al.,* 2009). It consists of gabbro and dolerite as well as granitic rocks that occur as arcuate ring dykes (Macey *et al.,* 2009).

The Maningoza Complex is the largest ring complex among the six ring complexes in the northwest of the island (Macey *et al.,* 2009). It consists of three major components: (1) a succession of interlayered fine-grained basaltic and rhyolitic lavas (about five cycles) in the north overlain by (2) trachytic and basaltic lavas and intruded by dykes, including a major dyke swarm and (3) two micro-syenite/trachyte and gabbro plugs. The Ankibobozaka Complex is a sub-complex situated in the southern parts of the Maningoza volcanic field and consists of micro-syenite/micro-granite and fine-grained micro-gabbro (Macey *et al.,* 2009). The Ambohitrosy complex is the sixth sub-volcanic complex in the northwest of Madagascar and is mainly dominated by gabbro, basalt, rhyolite, syenite and ambohibengy granite (Macey *et al.,* 2009).

The central part of the island contains the Ambohiby Complex, which is the subject of this thesis as well as the Bevato Complex. The Ambohiby Complex has a diameter of

15km and rises over 1500m above the Belobaka peneplains and consists of several intrusive mafic and felsic rocks cross-cut by younger mafic and felsic dykes. The smaller 5km wide Bevato ring complex (Fig. 2.2), which also intrude into the Antananarivo Archean basement is about 7 km north-west of the Ambohiby Complex and consists of intrusive mafic and felsic rocks. These complexes intrude migmatitic gneisses (Betsiboka Suite) and granitic orthogneisses (Imorona-Itsidro Suite). The Betsiboka and Imorona-Itsidro are part of the Antananarivo block that date back to 3.2 Ga. The Betsiboka suite mainly observed around river section and is very migmatitic. It displays stromatic metamorphic banding that consists of mesocratic grey palaeosomes that constitutes 80-85% of the rock with the remaining 12-15% composed of leucosomes.

### 2.3.3 Younger deposits

Recent Neogene Quaternary volcanic activities are recorded throughout the island, with alkaline dykes and volcanic centres crosscutting the Precambrian basement. These areas include the Ankaratra highland (2300-2700 m) and the Itasy in the central part of Madagascar and with scattered outcrops in the southwestern region of the island (Besairie, 1964; Melluso and Morra, 2000). In the Northern part of the island the Nosy Be archipelago (7-10 Ma) form part of the Ambohitra igneous province. The Nosy Be has an Archean to late Proterozoic basement age, with the late being more dominant and is composed of lava flows, spatter cones and tuff rings from sodic basinites to phonotephrite (Melluso and Morra, 2000). The geochemical and isotopic compositions of the Nosy Be rocks are similar but not identical to those observed on the Comore Islands.

**CHAPTER 3: LITHOLOGY AND PETROGRAPHY**

## 3.1. Introduction and Overview

Field observations in conjunction with petrographic studies indicate that the main rock types making up the Ambohiby Complex are gabbros, monzonites, alkali-syenites, and granites. Both gabbros and granites can be further subdivided into fine-grained and coarse-grained varieties. Most of these rock types are cross-cut by later mafic and felsic dykes. In general all the rocks are weathered to various degrees and occur mostly as loose boulders in tall grass. Fresh outcrops are mainly restricted to river sections. The positions of all the samples taken for this study are presented in Figure 3.1 and listed in Appendix 1.1.

Field relations established in this study indicate that the complex is underlain by a basement of Precambrian gneisses belonging to the Antananarivo Neoproterozoic Block. Intrusive relationships observed in the field indicate the following chronology: (1) the gabbros and monzonites are the oldest rocks of the Ambohiby Complex followed by (2) intrusion of alkali-syenites in the central eastern part of the complex as a ring structure followed by (3) massive intrusion of micro-granites in the central part of the complex as well as in the north-western and southeastern margin of the complex and (4) intrusion of the youngest rocks in the complex, medium-grained to coarse-grained granites, that form a prominent mountainous region in the southern part of the complex.
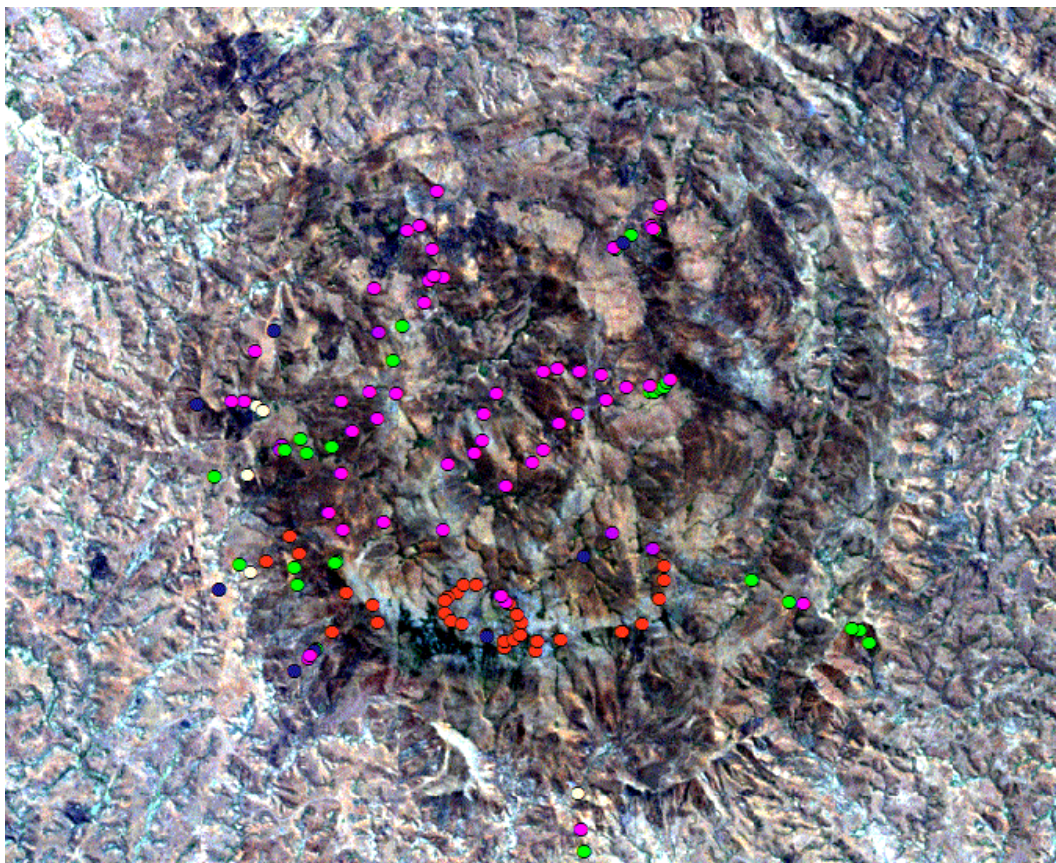
**Figure 3.1:** *Landsat image showing the location of outcrops that were sampled during this study. Green circle=gabbro samples, blue circle=monzonite, pink circle=microgranite, red circle=granite, light brown circle=alkali syenite*
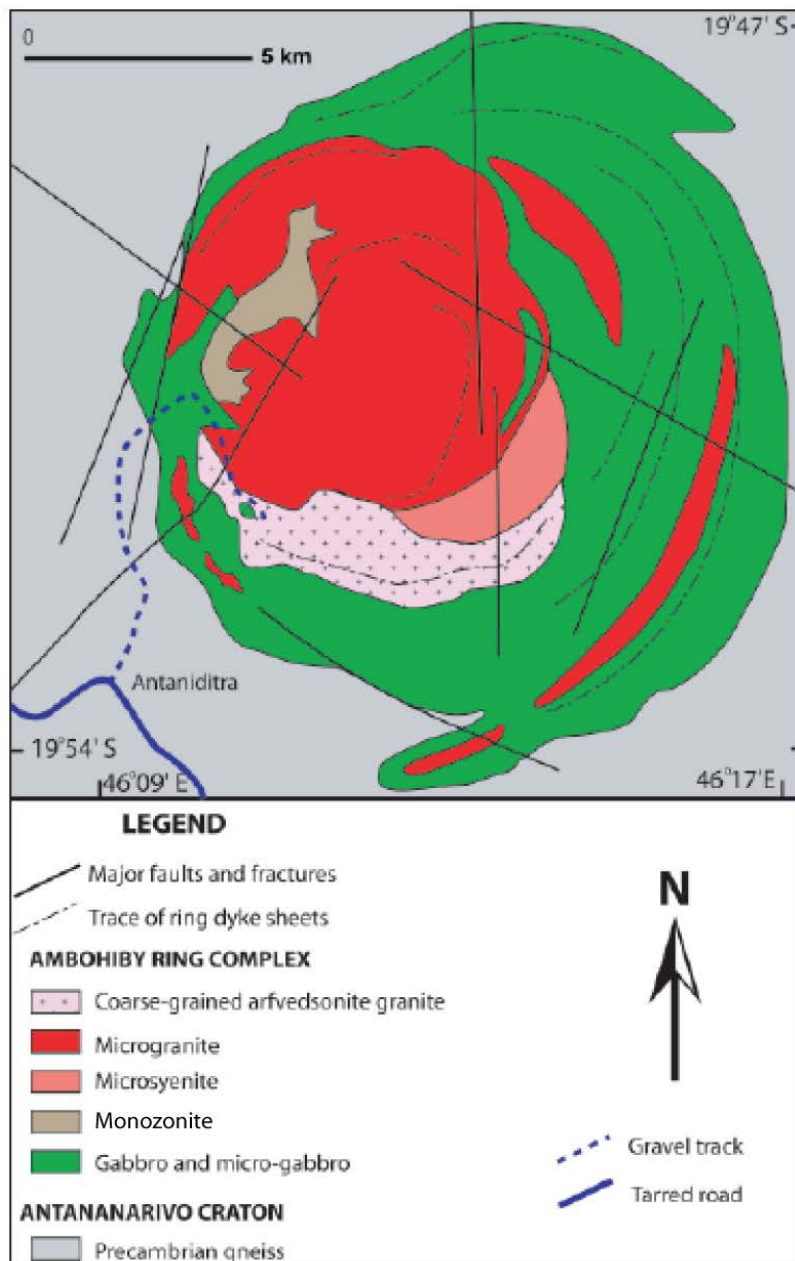
**Figure 3.2:** *Geological sketch map of the Ambohiby Igneous Ring Complex. Precambrian rocks make up the basement of the complex. Gabbroic outcrops dominate the complex, the central part consists of micro-granitic outcrops and there are several micro-granitic arc intrusion bodies at the margin of the complex. alkali-syenites occur in the southeastern part of the complex and form a ring structure. Coarse-grained granite occurs only in the southern part of the complex and display a cylindrical or arc shape*

Mineralogically the rocks of the Ambohiby Complex tend towards sodic-end-members. The classification of the pyroxenes was based on mineral chemistry following the nomenclature of Morimoto *et al.* (1988). The mineral chemistry data was recalculated based on stoichiometric constraints with $Fe^{3+}$ being recalculated following the method of Droop (1987). The primary classification of the pyroxenes was done using the Q-J diagram of Morimoto *et al.* (1988) which divide the pyroxenes into four groups: (1) Ca-Mg-Fe pyroxenes; (2) Na-Ca pyroxenes; (3) Na pyroxenes; and (4) other pyroxenes. The pyroxenes were classified using the total number of specified cations at the M (M1 and M2) sites on the basis of six oxygen. The M1 and M2 sites were considered together without site preference of atoms between the two sites, The number of Ca, Mg, $Fe^{2+}$ and Na cations in the M sites were plotted as $Q=Ca+Mg+Fe^{2+}$ and J=2Na plus any 3+ cations present. Using this nomenclature and classification methodology, the Ambohiby pyroxenes are generally sodic (Na<0.25) with only a few calcic (Ca<0.25) compositions. They vary in composition from aegirine, aegirine-augite, to ferro-hedenbergite and commonly occur in the granites, micro-granites, alkali syenites and monzonites. In the gabbros and mafic dykes, augite is the more common composition.

Amphiboles were recalculated on the basis of 23 oxygen and a total of 8 tetrahedral cation sites. $Fe^{3+}$ was recalculated using equation [6] of Droop (1987) for calcic amphiboles which assumes a total of 13 cations exclusive of Ca, Na and K. For these amphiboles, the standard formula for an amphibole may be written as:

$$(A_{0-1} \, B_2 \, C_5 T_8)_{22} \, (OH, F, Cl)_2$$
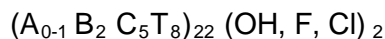
where the preferred site occupancy is as follows:

- A = Na, K
- B = Na, Li, Ca, Mn, $Fe^{+2}$, Mg
- C = Mg, $Fe^{+2}$, Mn, Al, $Fe^{+3}$, Ti
- T = Si, Al

Amphiboles from the Ambohiby Complex are represented by bluish to brownish-green varieties and using the above criteria their compositions range from arfvedsonite to eckermannite in granites, and magnesio-arfvedsonite in micro-granites. For amphiboles to be classified as arfvedsonite the following criteria had to be met: $Fe^{3+} / (Fe^{3+}+Al^{VI})>0.5$;

Na cations >2; A, B, and C sites =7.8±0.2. Ferro-edenite is present in monzonites and alkali-syenites (Deer *et al.,* 1992)

Feldspars are usually single phase (mesoperthite with Carlsbad and Baveno twins) and are therefore hypersolvus. In the granites, micro-granites and alkali-syenites, path and string perthite is very common. Graphic intergrowth of quartz and alkali feldspars is also common in granites and some alkali-syenites. The classification and nomenclature of the feldspars was based on the petrographic studies as well as the mineral chemistry of the grains. The mineral chemistry data was recalculated using stoichiometric constraints.

Other minerals present, particularly in the plutonic members of the complex, include biotite, ubiquitous opaque Fe-Ti oxides (titanium oxide), aenigmatite ($Na_2Fe_5^{2+}TiO_2$ $[Si_6O_{18}]$ as well as accessory minerals such as zircon, sphene and monazite. Detailed petrographic descriptions of all thin sections examined as part of this study are given in Appendix 1.2 and mineral chemistry data is given in Appendix 1.3. In the following sections, detailed petrographic descriptions are given for each of the different rock types making up the Ambohiby Complex.

*Note: All thin sections petrographic images of this chapter were on the microscopic scale of 297µm*

## 3.2  Precambrian gneiss

Precambrian gneisses make up the basement to the complex and are part of the Antananarivo Block (Paquette & Nedelec, 1998). These gneisses form part of the broad band of pre-1000Ma continental crust that stretches from the Yemen, through Somalia and eastern Ethiopia into Madagascar (Collins & Windley, 2002). Two types of gneisses were recorded in the field during this study, namely: (1) migmatitic orthogneiss; and (2) granitic augen gneiss (Fig.3.2 & 3.3)

### 3.2.1 Migmatitic orthogneiss

In outcrop, the migmatitic orthogneisses display stromatic metamorphic banding that consists of mesocratic grey palaeosomes that constitutes 80-85% of the rock with the remaining 12-15% composed of leucosomes (Fig.3.3 a & b). The mesocratic grey palaeosomes are medium-grained (0.7-0.9mm) and consist of K-feldspar (63-65%), quartz

(18-20%) and biotite (13-15%), whereas medium-grained equigranular leucosomes consist of 60-65% K-feldspars, quartz (25-30%) and minor amount of biotite (<5%).

In thin section the migmatitic orthogneiss is comprised of much altered K-feldspars (<40%), elongated muscovite (<4%), and minor amounts of plagioclase (<2%). The K-feldspars are much altered to sericite and there is no any particular pattern of orientation (Fig. 3.4 a & b). The elongated muscovite is replaced by secondary pleochroic light green chlorite (25-30%) and strongly pleochroic brown biotite (10-14%) (Fig. 3.4 c & d). Locally interstitial biotite is observed in K-feldspar and quartz matrix (Fig. 3.3e). Furthermore, some of the biotites exhibit pleochroic haloes that reflect the presence zircon inclusions. The quartz grains (<10%) are often strained and display undulose extinction. The subhedral-euhedral oxides are observed in K-feldspar matrix and seem to be a primary phase, since most of the grains are euhedral and show no reaction pattern with other minerals in this rock type.

### 3.2.2 Granitic augen orthogneiss

These rocks are weakly migmatitic (5-15%, leucosome) and display well-developed stromatic layering and most minerals display an equigranular texture (Fig.3.3 c & d). The mineralogy of the granitic orthogneiss consist of 40-45% K-feldspar augen (3x8mm-4x10mm) with ~ 10% aligned amphiboles (1-3mm), waxy grey quartz (13-15%) and K-feldspars (27-30%). A localised (less than a meter) discrete shear band perpendicular to the gneissic foliation was also observed in this rock unit. Its formation may be due to compression during Ambohiby Complex magmatism. No thin section was made for the granitic augen orthogneiss.
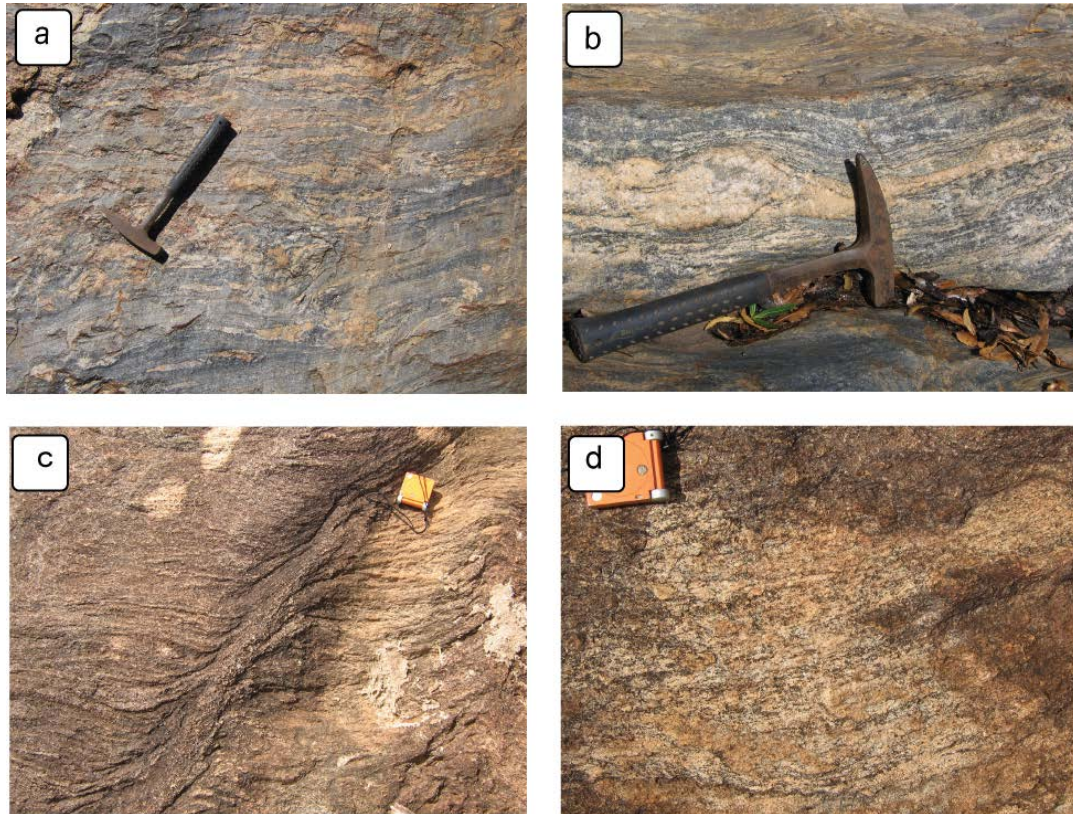
**Figure 3.3:** *Field photographs of Precambrian gneiss. (a). Stromatic migmatitic orthogneiss, with well preserved paleosomes and leucosomes. (b) Illustrates well-preserved foliation bands of leucosomes in stromatic migmatitic orthogneiss. (c) Shows a discrete shear band perpendicular to the gneissic foliation and axial planar to gentle folds. (d) A granitic augen orthogneiss with a well preserved planar foliation.*
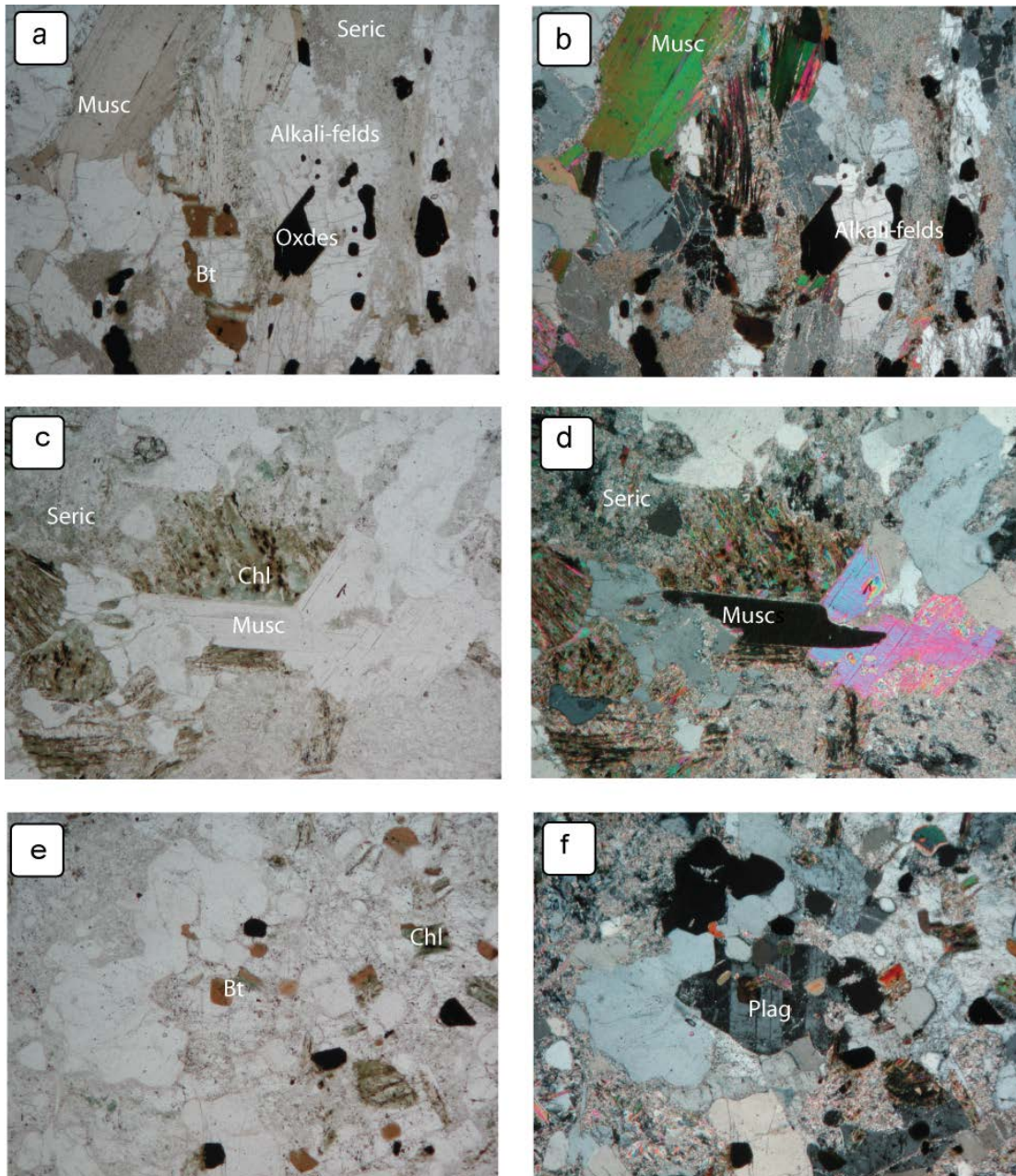
**Figure 3.4:** *Photomicrographs of stromatic migmatitic orthogneiss (T/S MC7001). (a) Elongated muscovite, fine subhedral oxides, secondary biotite set in a fine grained alkali feldspar and quartz matrix (T/S MC7001). (b) Same as (a) under cross polar light (XPL) (c) Showing elongated muscovite, sericitization of the alkali feldspars and secondary chlorite. (d) Same as (c) under XPL. (e) Minor amount of secondary biotite and chlorite, subhedral oxides set in alkali feldspar matrix. (f) Same as (e) under XPL, showing much altered alkali feldspar to sericite, as well as plagioclase grain altered.*

## 3.3. Ambohiby Complex

### 3.3.1 Gabbro

Individual gabbros are generally equigranular, and range from micro-gabbro (grainsize 0.15-0.20mm) to coarse-grained gabbro (grainsize 1.0-5.0mm). The micro-gabbro were observed on the margin of the complex, and along the river section and the coarse-grained gabbro observed as weathered loose boulders and common along the southwestern and eastern part of the complex (Fig.3.5 a ,b ,c , & d).

Both gabbros have similar mineralogies, comprising elongated plagioclase (49-64%), as well as altered weakly pleochroic augite (20-40%) as the main primary phase (Fig.3.6 a & b). The augite is locally skeletal and usually at least partially replaced by secondary pleochroic brown biotite (<5%) and weakly pleochroic light green chlorite (<4%) (Fig.3.6 c). In sample PD06004 most of the augites are replaced by strongly pleochroic brown to green aegirine (up to 35%), whereas in sample MC7049 and MC7050 most of the augites are replaced by strongly pleochroic brown to greenish-blue arfvedsonite (up to 35%). The arfvedsonite is partially replaced by secondary pleochroic light green chlorite (Fig.3.6 c & d). Trace amount of oxides occur as both subhedral to euhedral grains that show a spongy texture, and which therefore seem to be a secondary product formed through breakdown of augites. Hydrothermal alteration has affected the plagioclase grains variably as evidenced by the development of sericite (Fig. 3.6 f). Mineral chemistry was not obtained for the gabbros as part of this study.
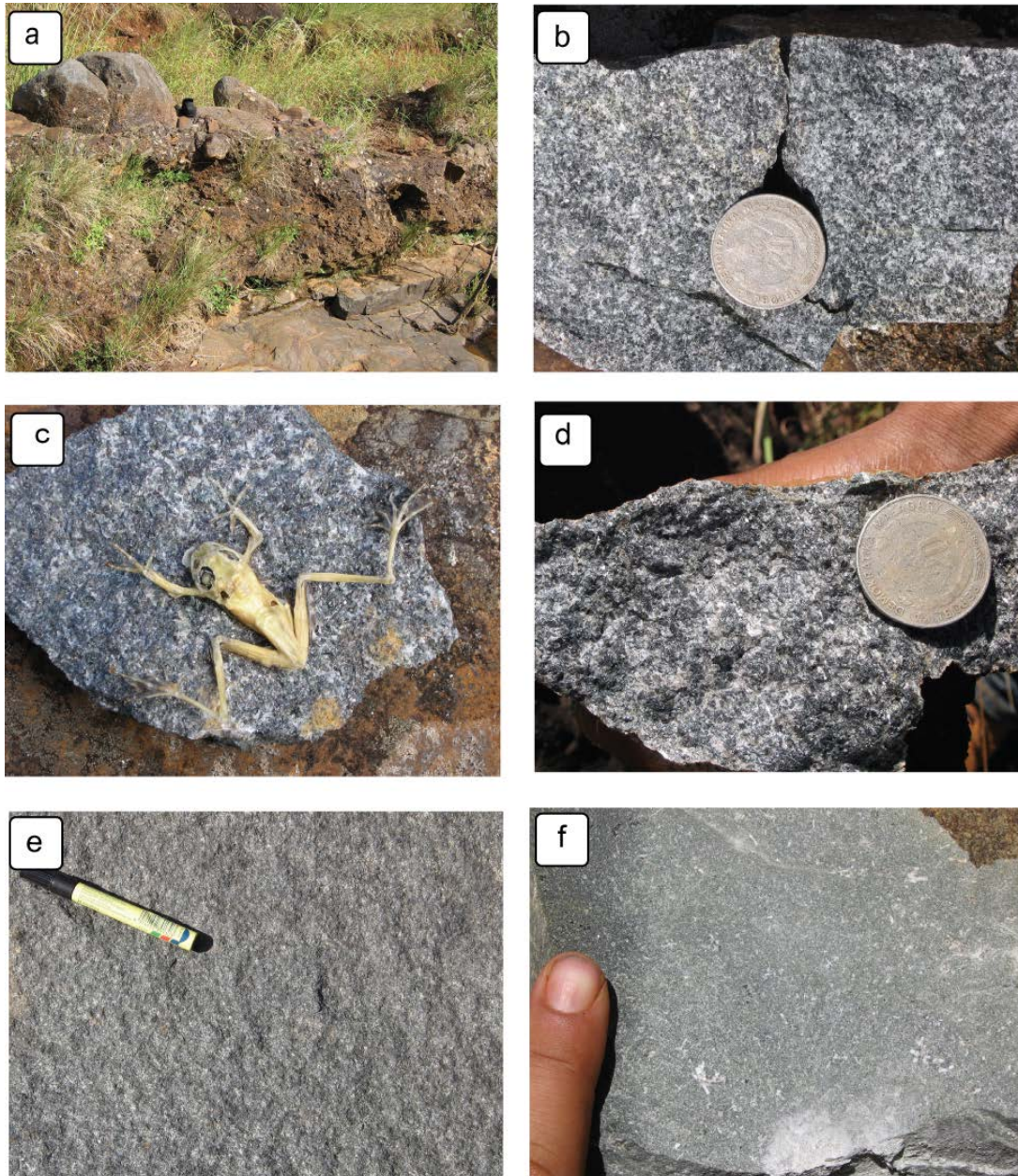
**Figure 3.5:** *Field photographs of gabbros.(a) Shows a medium grained grabboic boulders and insitu outcrop, (b), (c) and (d) shows massive, medium-coarse grained equigranular gabbro's. (e) and (f) shows equigranular micro-gabbro found along the river section and margin of the complex*
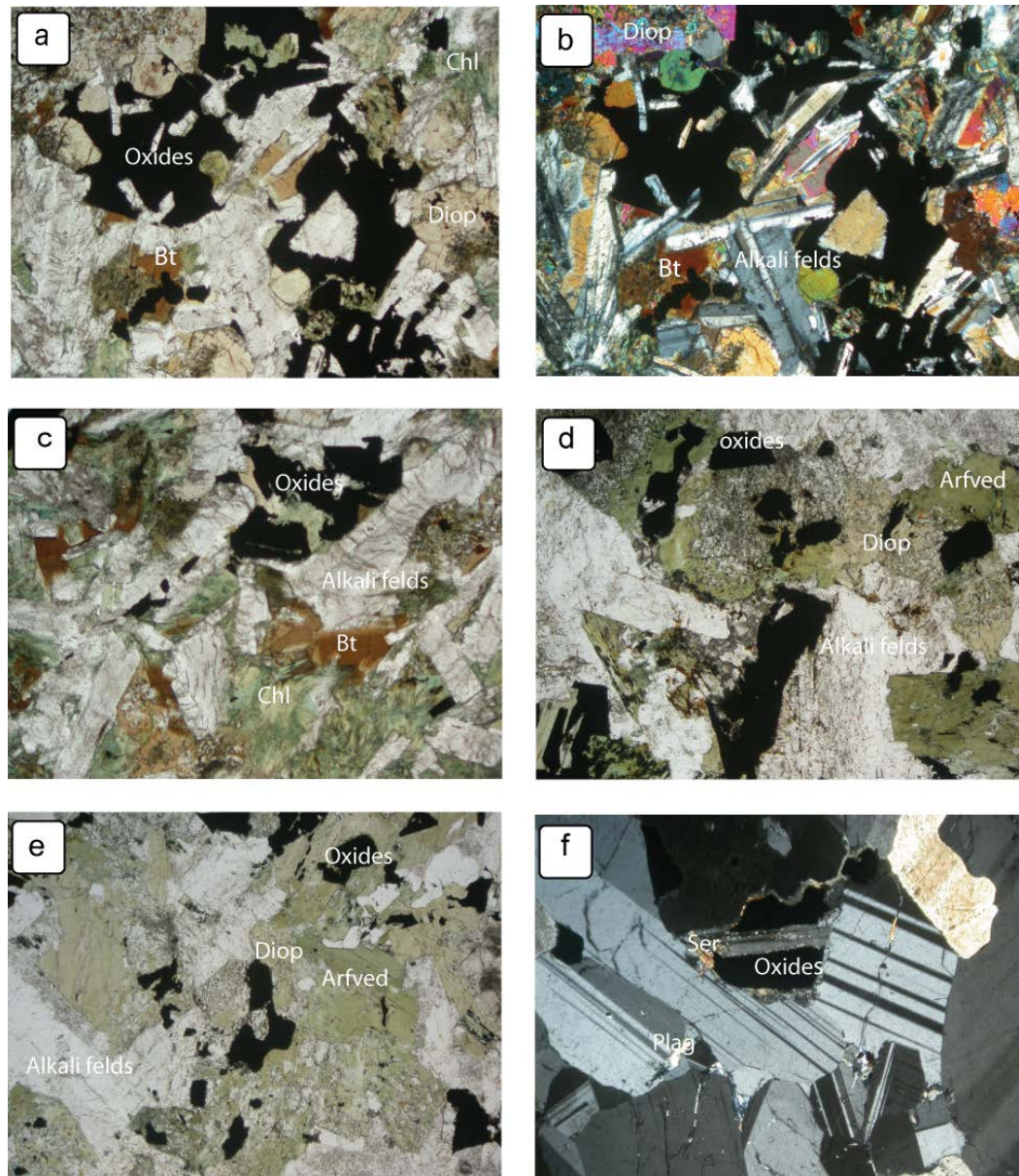
**Figure 3.6**: *Petrographic photographs of gabbros (a) Shows elongated plagioclase, skeletal diopside, secondary chlorite replacing diopside, and secondary biotite (T/S MC7045 (b) Same as (a) under XPL. (c) Showing elongated alkali feldspar, colourless diopside replaced by secondary pleochroic brown biotite and weakly pleochroic light green chlorite (T.S MC7045). (d) Showing alkali feldspar and diopside as primary phases, some of the diopside is replaced by arfvedsonite (T/S MC7049). (e). Shows diopsides being partially replaced by arfvedsonite. Oxides are seen in diopside grains (T/S MC7050). (f) Showing an elongated plagioclase altered by sericite and subhedral oxides randomly distributed (under XPL)*

### 3.3.2 Monzonite

Monzonites are the least common rock type of the Ambohiby Complex and intrude between the marginal gabbros in the west and the microgranite core. The monzonites are generally medium grained (mostly 0.5-1.5mm) and equigranular (Fig.3.7a & b). They generally consist of elongated perthitic alkali feldspar (55-59%), ferro-edenite (10-15%), plagioclase (10-13%), quartz (2-5%), and minor skeletal ferro-augite (2-6%), ferro-hedenbergite (< 2%) as well as chlorite (<2%) (Fig.3.7 c & d). In sample MC7039, ferro-augite and ferro-hedenbergite are replaced by strongly pleochroic brown to greenish-blue ferro-edenite. Weakly pleochroic chlorite occurs as a common retrograde mineral replacing ferro-augite, ferro-hedenbergite and/or ferro-edenite. Minor amounts of quartz are observed in several samples. Trace amounts of secondary biotite and aenigmatite are more rarely present. Trace amount of oxides occur as both subhedral to euhedral primary grains and as spongy secondary products. Sericite is commonly observed as the breakdown product of plagioclase due to hydrothermal alteration. Trace amounts of accessory minerals zircon and monazite are randomly distributed.

Mineral compositions from the monzonites are given in Appendix 1.3. Ferro-augites have Ca contents of up to 0.50 cations pfu and ferro-hedenbergite contains $Fe^{2+}$ contents of up to 1.39 cations pfu and Ca up to 0.47 cations pfu. The ferro-edenite contains $Fe^{3+}$ contents of up to 1.23 cations, $Fe^{2+}$ of 2.1 cations and Ca contents of up to 1.55 cations pfu. Figure 3.8 shows a Q-J diagram of Morimoto *et al.* (1988) indicating that the pyroxenes in this rock type have two sets of compositions. Both sets have low J components (i.e. little Na) but variable Q components, with one set having total Ca+Mg+Fe2+ of around 2 and corresponding to ferro-hedenbergite compositions whereas the second set has a Q total of around 1 corresponding to the ferro-augite composition. Zoning in ferro-edenite observed in thin-section is not supported by variations in the mineral composition between the core and rim of the mineral (Fig. 3.8).
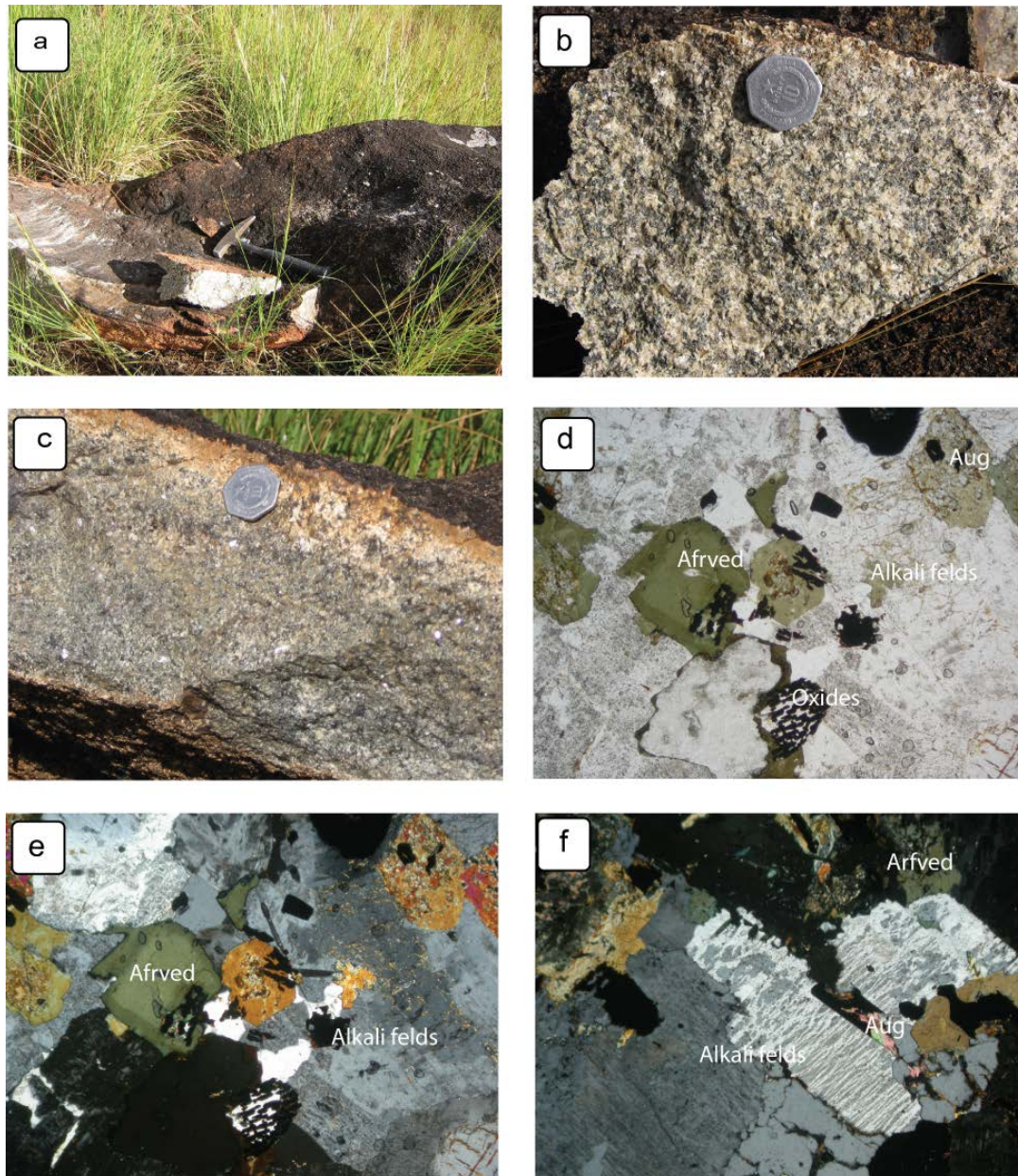
**Figure 3.7:** *(a) field photograph of weathered greyish black monzonite boulder tall grasses; (b) field photograph of fresh sample of medium-grained equigranular monzonite; (c) field photograph of medium-grained weathered monzonite, showing some Fe-leaching. (d)Thin section photograph showing coarse-grained alkali feldspar and colourless skeletal augite as primary phases, zoned ferro-edenites as a retrograde mineral replacing ferro-augite. Blocky and spongy oxides mostly observed ferro-edenite grains and rarely in ferro-augite(T/S MC7039). (e) Same as (d) under XPL. (F). Thin section photograph showing skeletal diopside, retrograde ferro-edenite and perthitic alkali feldspar (T/S MC7040)*
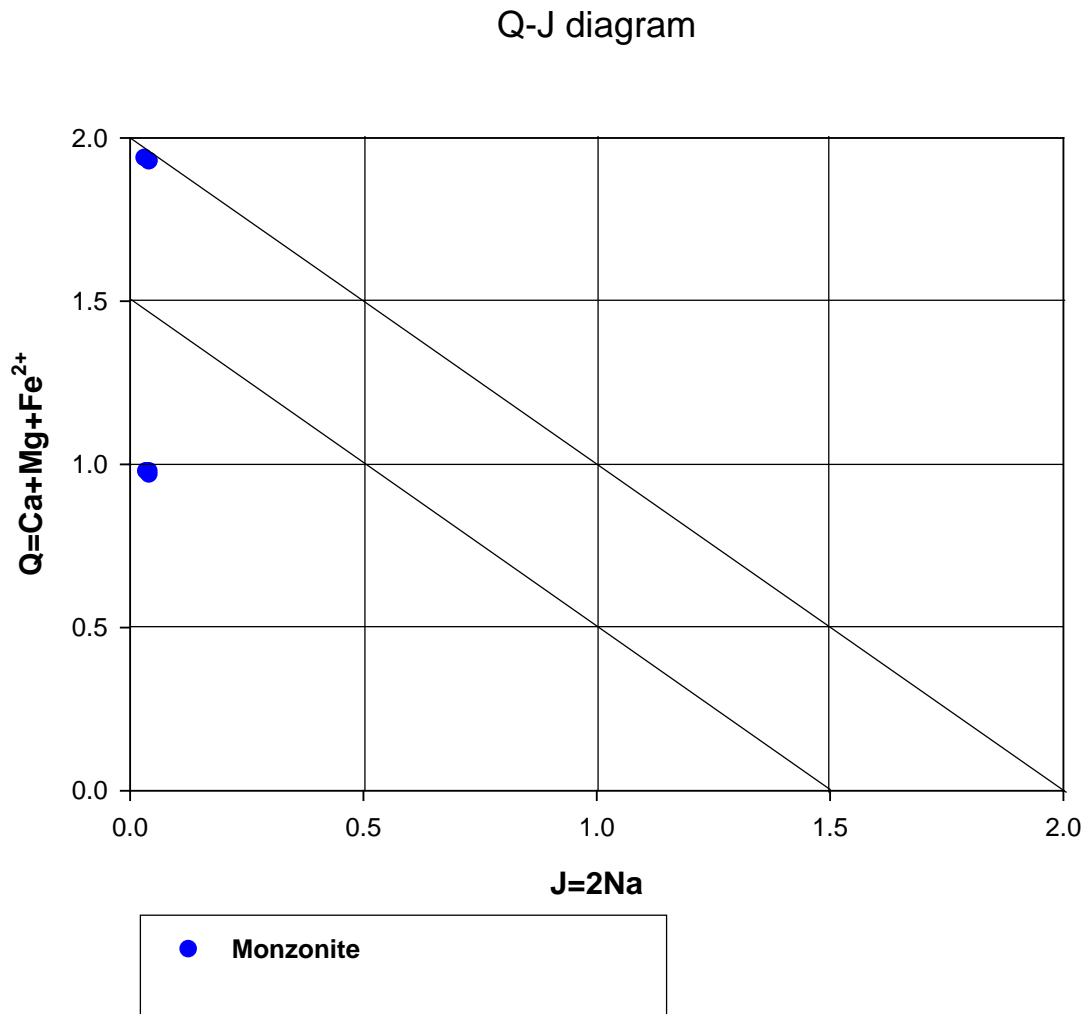
**Figure 3.8:** *Microprobe analysis of pyroxenes from the monzonite samples plotted on the Q-J diagram (after Morimoto et al., 1988). This plot show that the monzonite has two sets of pyroxene, the first with high total of Q that correspond to ferro-hedenbergite and the second with an average Q of 1.0 that is correspond to augite.*

### 3.3.3 Alkali Syenite

This rock generally lacks plagioclase and quartz hence called alkali syenite. Only four samples were collected for this study. The alkali syenites are the second least abundant rock type in the Ambohiby Complex after monzonite and are limited to the southeast centre of the complex (Fig.3.9 a). These rocks are mesocratic, equigranular (Fig.3.9 b & c) and are composed of orthoclase feldspars (70-73%, grainsize 0.5-1.5 mm), set in a slightly finer-grained matrix (<1mm) of anhedral ferro-edenite (12-15%), minor quartz (2-6%) and interstitial augite (2-6%), together with or without plagioclase (<2%), biotite (<3%), and aegirine (<6%) as well as trace amounts of aenigmatite and oxides . This rock exhibits a bimodal grain size distribution of orthoclase and quartz. The feldspars are prismatic and rarely  zoned (i.e. MC7060). Ferro-edenite occurs as a retrograde mineral replacing augite and aegirine (Fig.3.10 a, b, c & d). Aegirine occurs as secondary mineral replacing augite while biotite occurs as a retrograde mineral replacing aegirine. Aenigmatite occurs in reaction with augite as well as with the retrograde ferro-edenite grains in some of the samples (i.e. MC7027 and MC7060, Fig. 3.10 e, f, g & h) The oxides consist of two different morphologies. The first type is characterized by blocky grains. The second type is a skeletal (spongy) texture and occurs mostly in ferro-edenite grains. Zircons occur as accessory minerals and are evenly distributed throughout the rock. Chlorite occurs as a retrograde mineral after ferro-edenite (Fig.3.10 i & j).

Mineral compositions for the alkali-syenites are shown in Appendix 1.3. Augite contains Ca contents up to 0.78 cations pfu, Mg contents up to 0.52 cations pfu, and $Fe^{2+}$ of up to 0.84 cations pfu. Ferro-edenite contains Ca contents of up to 1.70 cations, $Fe^{2+}$ of up to 3.30 cations pfu, Mg contents up to 0.52 cations and $Fe^{3+}$ contents of up to 1.15 cations pfu (Fig.3.11). These alkali-syenites contain orthoclase feldspars with an average composition of $An_0Ab_{06}Or_{94}$ as well as a few sodium-rich plagioclase feldspars with an average composition of $An_0Ab_{99}Or_{01}$. Zoning in orthoclase feldspars observed in thin-section is not supported by variations in the mineral composition between the core and rim of the mineral.
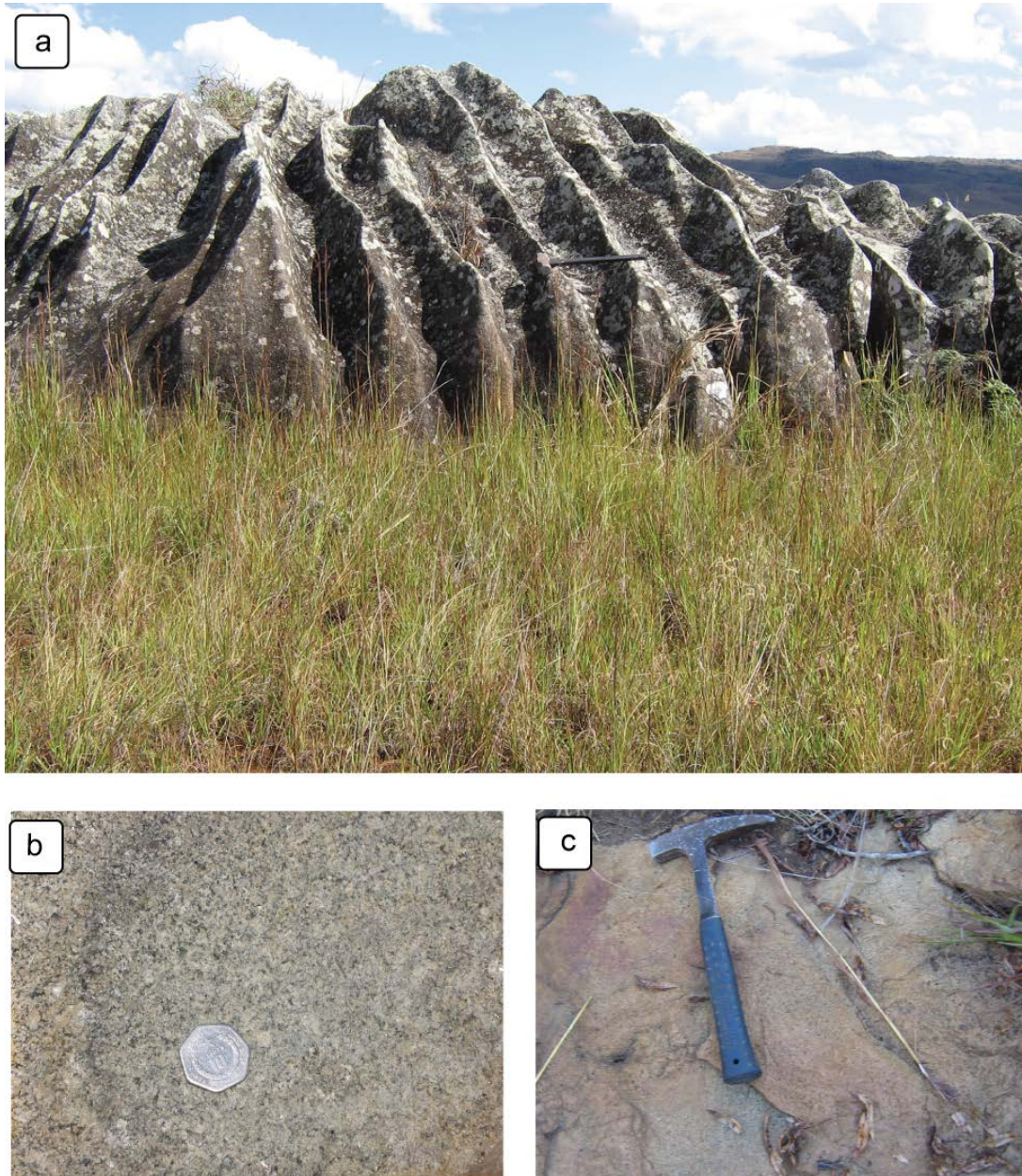
**Figure 3.9**: *Field photographs of alkali syenite (a) Field photograph showing microsyenite in the field with "unique" weathering pattern. (b) Field photograph showing equigranular medium grained micro-syenite, (c) showings a microsyenite outcrop in the field, which is weathered with brownish red in colour.*
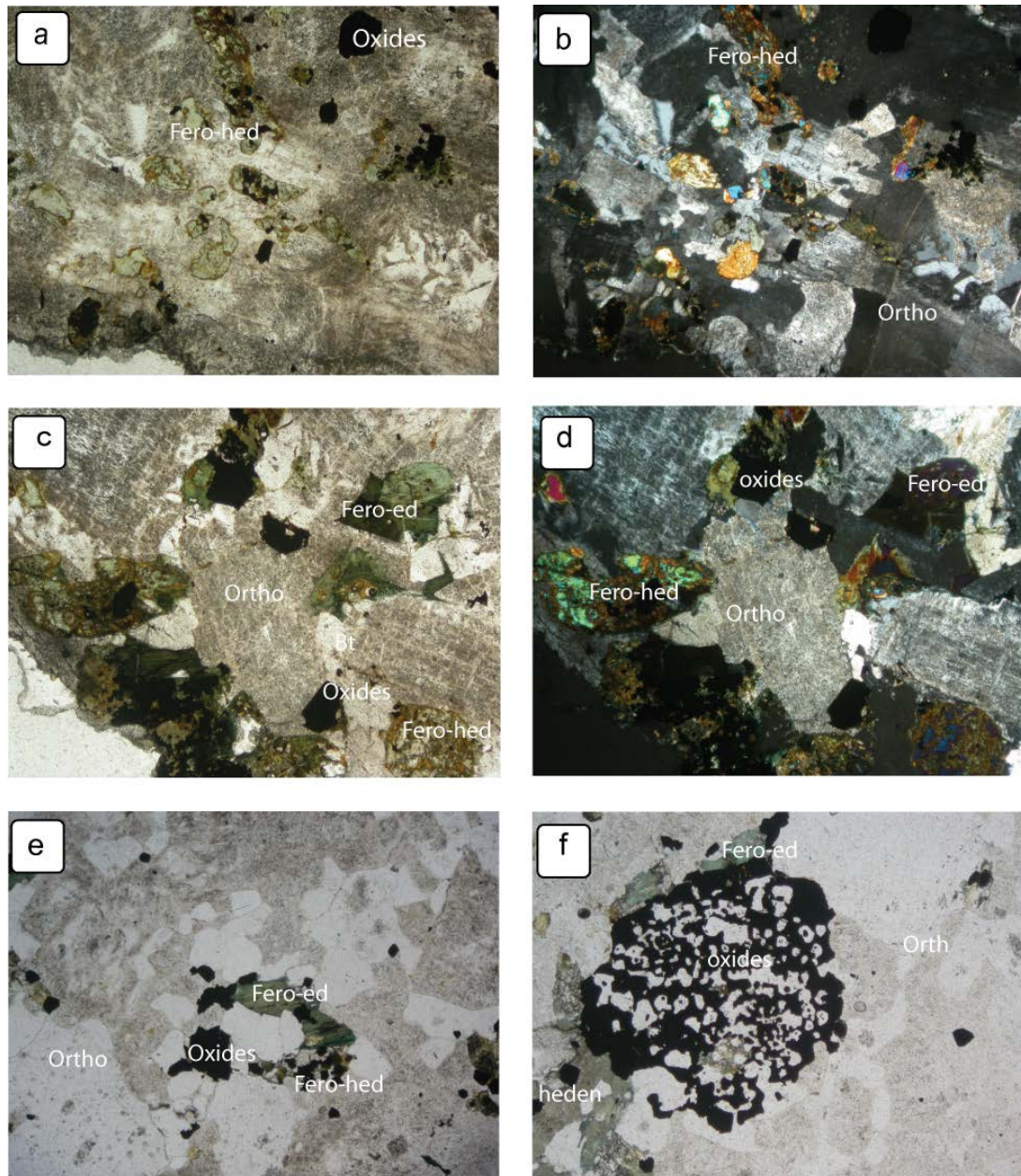
**Figure 3.10:** *Thin section photographs of alkali syenite e samples (a) showing a much altered interstitial augite in alkali feldspar matrix (T/S MC7027). (b) Same as (a) under XPL. (c) Shows fero-edenite replacing augite, as well as blocky oxides in both augite and fero-edenite (T/S MC7026). (d) Same as (c) under XPL. (e) Colourless augite replaced by fero-edenite (T/S MC7029). Oxides display a spongy texture (T/S MC7029). (g) Showing the breakdown of augite to fero-edenite, as well as aenigmatite as a secondary product (reddish-brown in colour) (T/S MC7029). (h) Same as the (g) under XPL. (i) Shows fero-edenite replaced by chlorite in alkali feldspar matrix (T/S MC7026)*
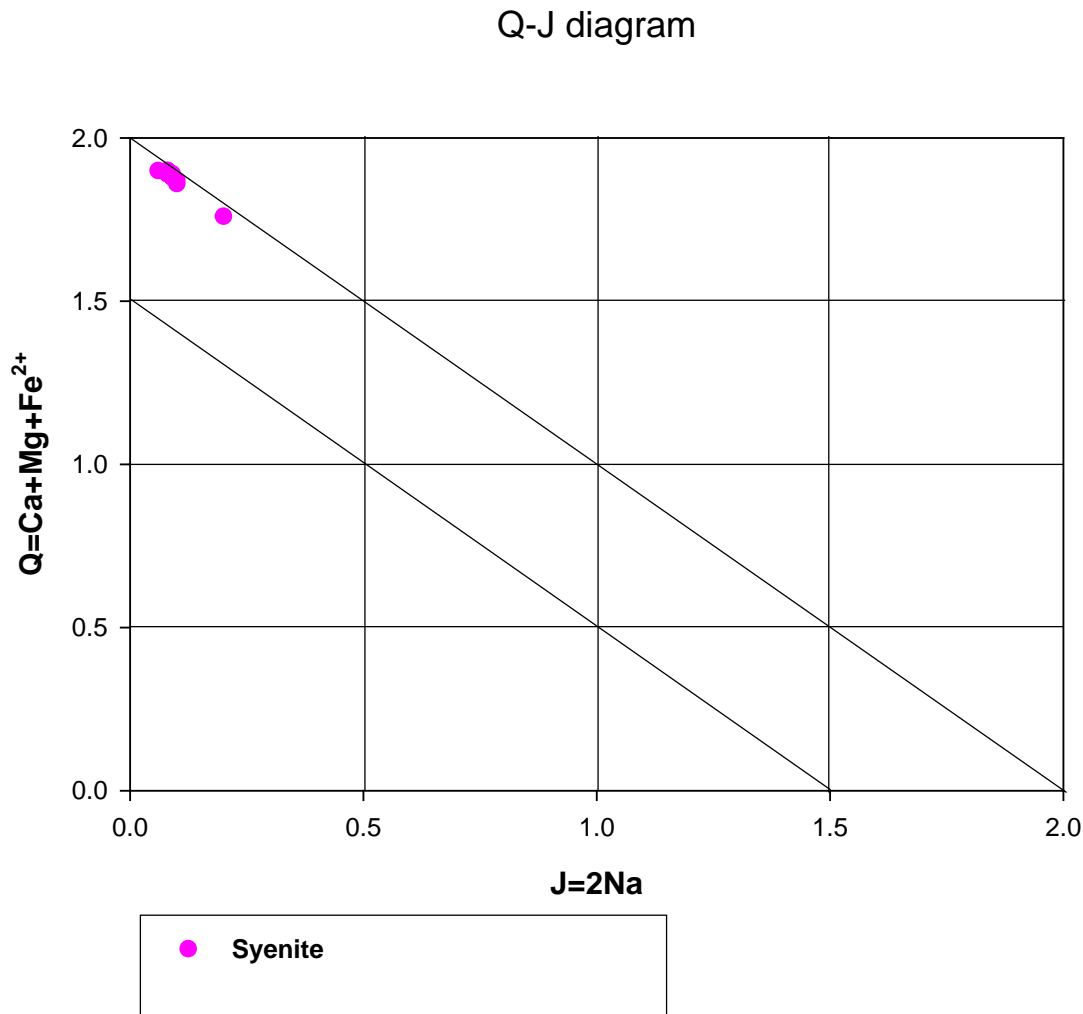
## Q-J diagram



**Figure 3.11:** *Microprobe analysis of pyroxenes from alkali syenite samples plotted on the Q-J diagram (after Morimoto et al., 1988). This plot shows that the alkali syenite has one set of pyroxene, which has high total of Q that is correspond to Augite*

### *3.3.*4 **Granite**

Two types of granite were identified in the field, namely micro-granite and coarse-grained granite. Micro-granites dominate the central and northwestern part of the complex and form outer ring bodies in the northeastern and southeastern margin of the complex (Fig. 3.2). The coarse-grained granite occurs as a prominent mountainous region in the southern part of the complex, and intrudes between gabbro, alkali-syenite and micro-granite outcrops. The coarse-grained texture and the visibility of quartz in-hand specimens make it easy to differentiate the granite from the central micro-granites. The leucocratic coarse-grained granite is quite weathered and generally equigranular (1.5-3.0mm).

*3.3.4.1 Micro-granite*

Micro-granites are equigranular (0.8-1mm) pale-pink to cream-white and are not very weathered as compared to other rock types in the complex. The micro-granites are composed of alkali feldspars (50-60%), quartz (30-37%), and subhedral, strongly pleochroic blue to green arfvedsonite (4-10%). Minor amounts of interstitial augite (<5%) are observed in roughly two thirds of the samples, locally partially replaced by brown to green aegirine (2-6%) (Fig.3.13 a & b).. Elongated plagioclase (<2%) display a carlsbad twins and elsewhere show a reaction texture with orthoclase. The quartz grains are often strained and display undulose extinction. Arfvedsonite occurs as retrograde mineral replacing aegirine and rarely augite, and elsewhere occurs as a reaction rim around aegirine (Fig.3.13 c). The red-brown pleochroic aenigmatite replaces the arfvedsonite (Fig.3.13 e & f).

Mineral compositions for the micro-granites are given are shown in Appendix 1.3. Aegirine contains Na contents up to 0.90 cations pfu, $Fe^{2+}$ 0.37 cations pfu (Fig.3.14). Arfvedsonite contains Na contents of up to 2.47 cations pfu, $Fe^{3+}$ of up to 1.15, $Fe^{2+}$ of up to 3.19 cations pfu, and Mg contents up to 1.18 cations pfu. The mineral chemistry of the amphiboles shows that the amphiboles are magnesium-rich (Mg content up to 1.18 cations pfu) and therefore are magesio-arfevedsonite in composition (Fig.3.15). These micro-granites contain orthoclase feldspars with an average $An_0Ab_{06}Or_{94}$ and also sodium rich plagioclase feldspars with average $An_0Ab_{99}Or_{01}$
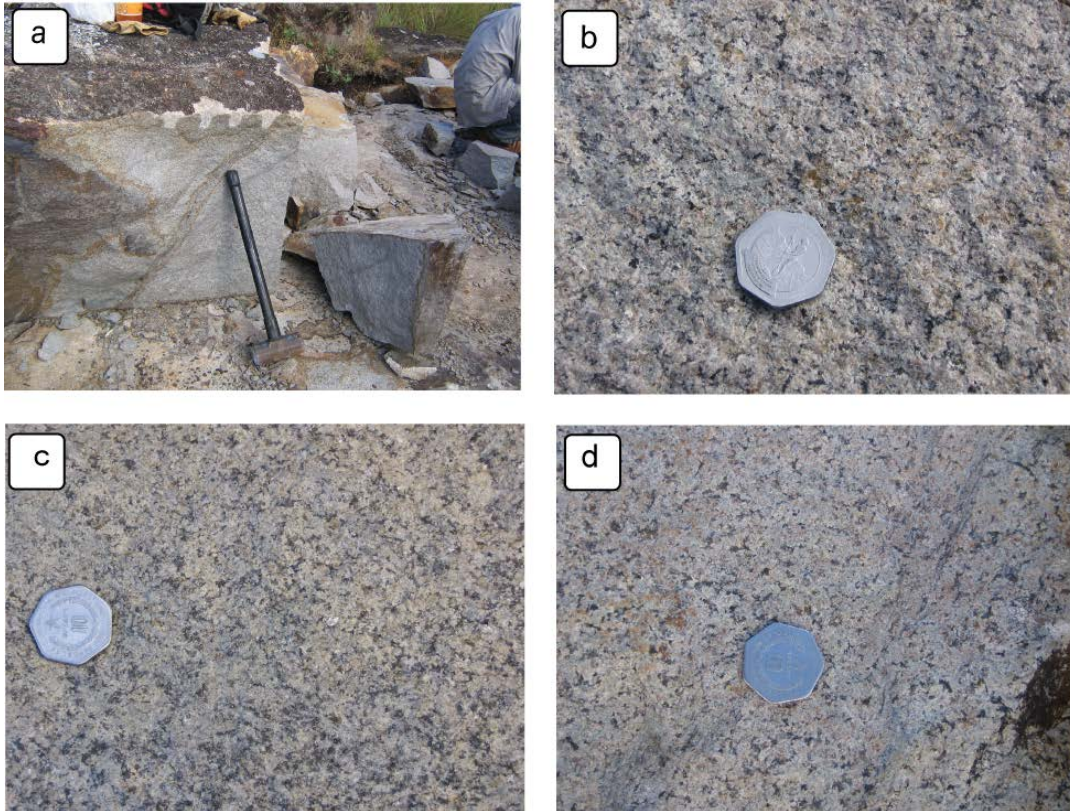
**Figure 3.12:** *Field photographs of microgranite (a) Showing a sliced microgranite outcrop block in the field. (b). Showing equigranular microgranite rock. (c) Same as (b). (d) Showing a post minor intrusion shear zone that is defined by dark mafic minerals defining a sense of shearing in microgranite sample.*
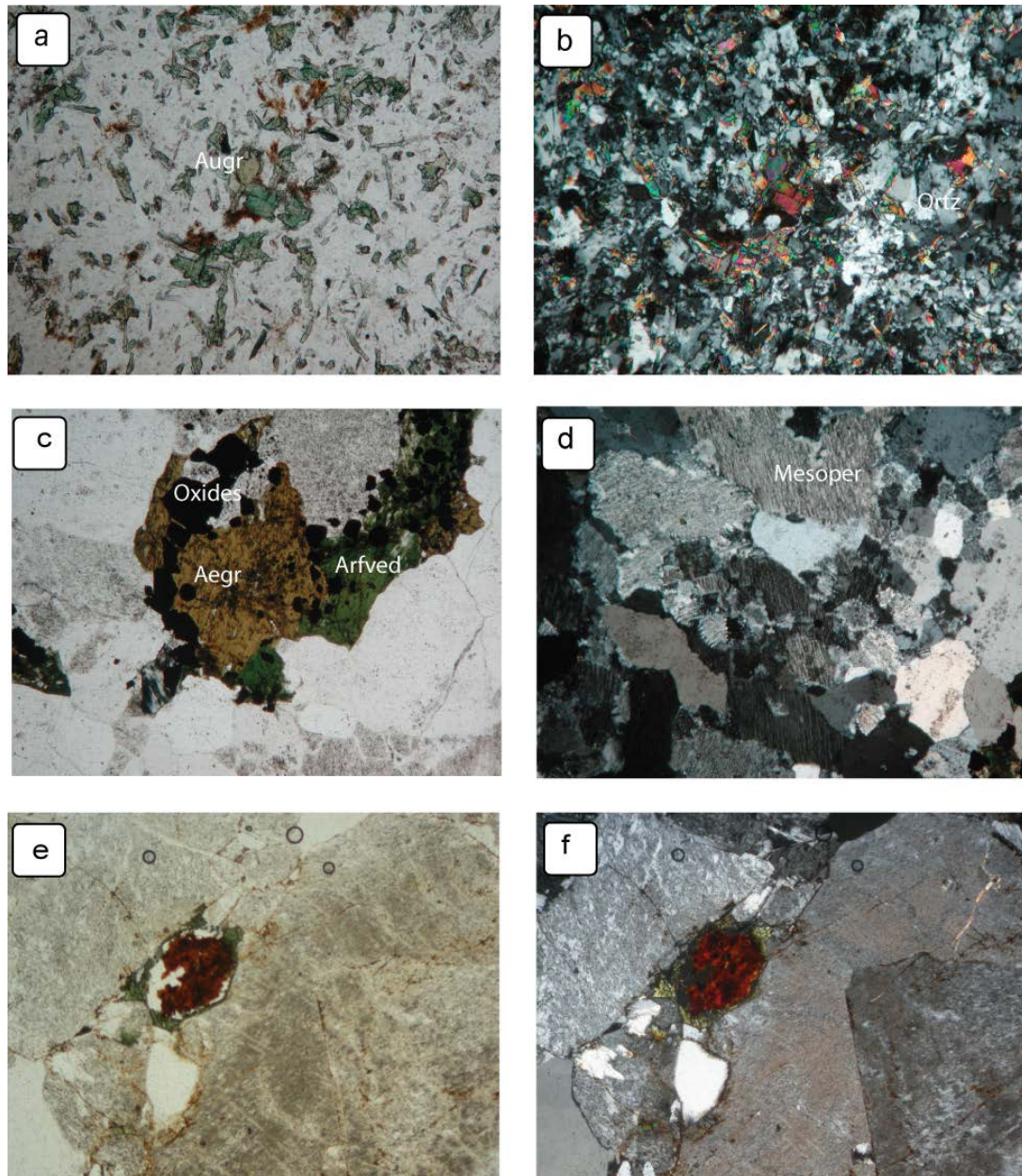
**Figure 3.13:** *Thin section photographs of microgranite (a) & (b) Showing strongly pleochroic brown to green anhedral aegirine, secondary epidote, and quartz that display undulose extinction (see Figure 8.10b) (T/S MC7004). (c) Showing strongly pleochroic brown aegirine replaced by strongly pleochroic green arfvedsonite and presence of blocky oxides in both aegirine and arfvedsonite matrix (T/S MC7006). (d) Showing mesoperthitic texture of the feldspar as well as the fine-grained quartz that displays undulose extinction. (T/S MC7006). (e) Aenigmatite inside the skeletal arfvedsonite indicating that it is a retrograde mineral after arfvedsonite (T/S MC7025). (f) Same as (e) under XPL.*
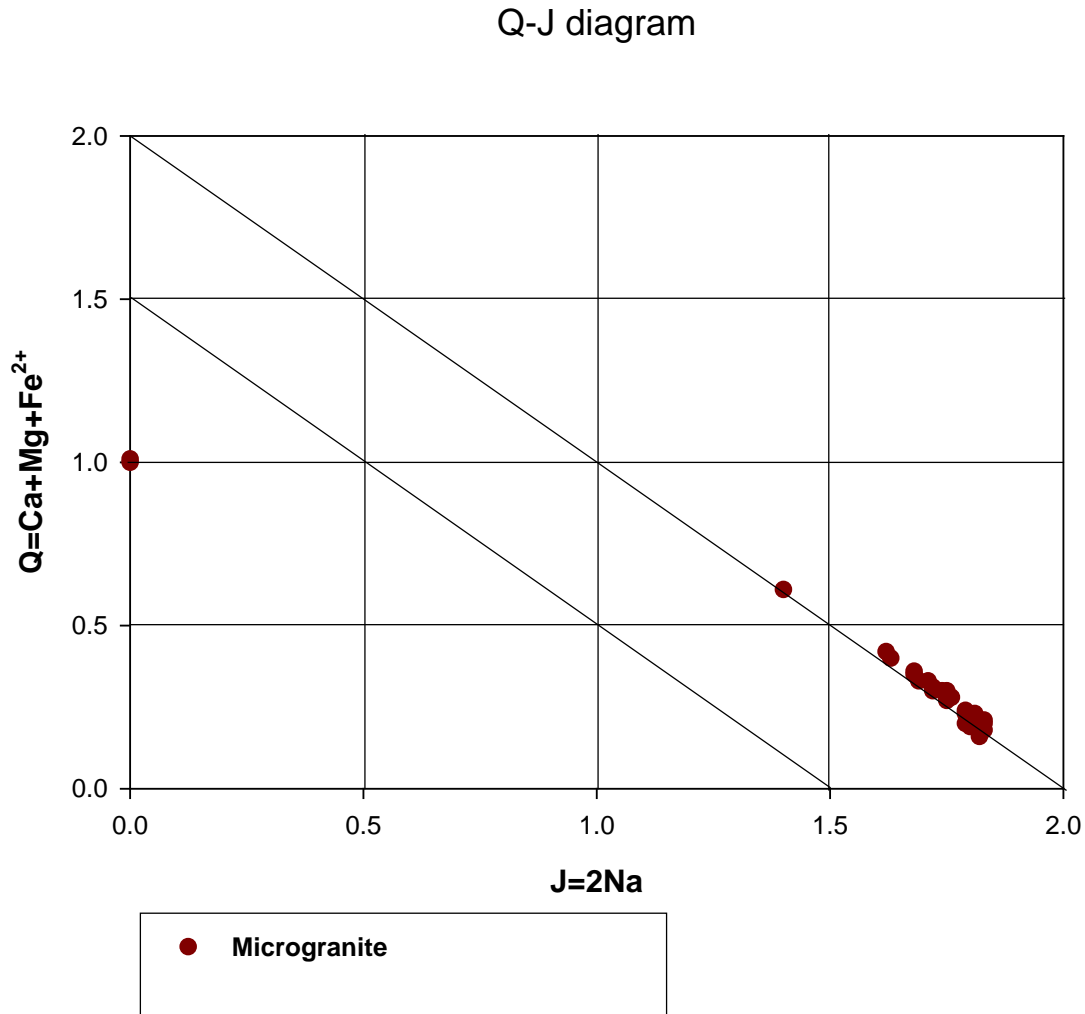
## Q-J diagram



**Figure 3.14:** *Microprobe analysis of pyroxenes from the micro-granite samples plotted on the Q-J diagram (after Morimoto et al., 1988). This plot shows that the micro-granite has two sets of pyroxene, the first with J total ranging from 1.6-1.9 that correspond to aegerine and the second with an average Q of 1.0.*

**Alkali amphiboles with (Na+K)$_A$> or =0.50**
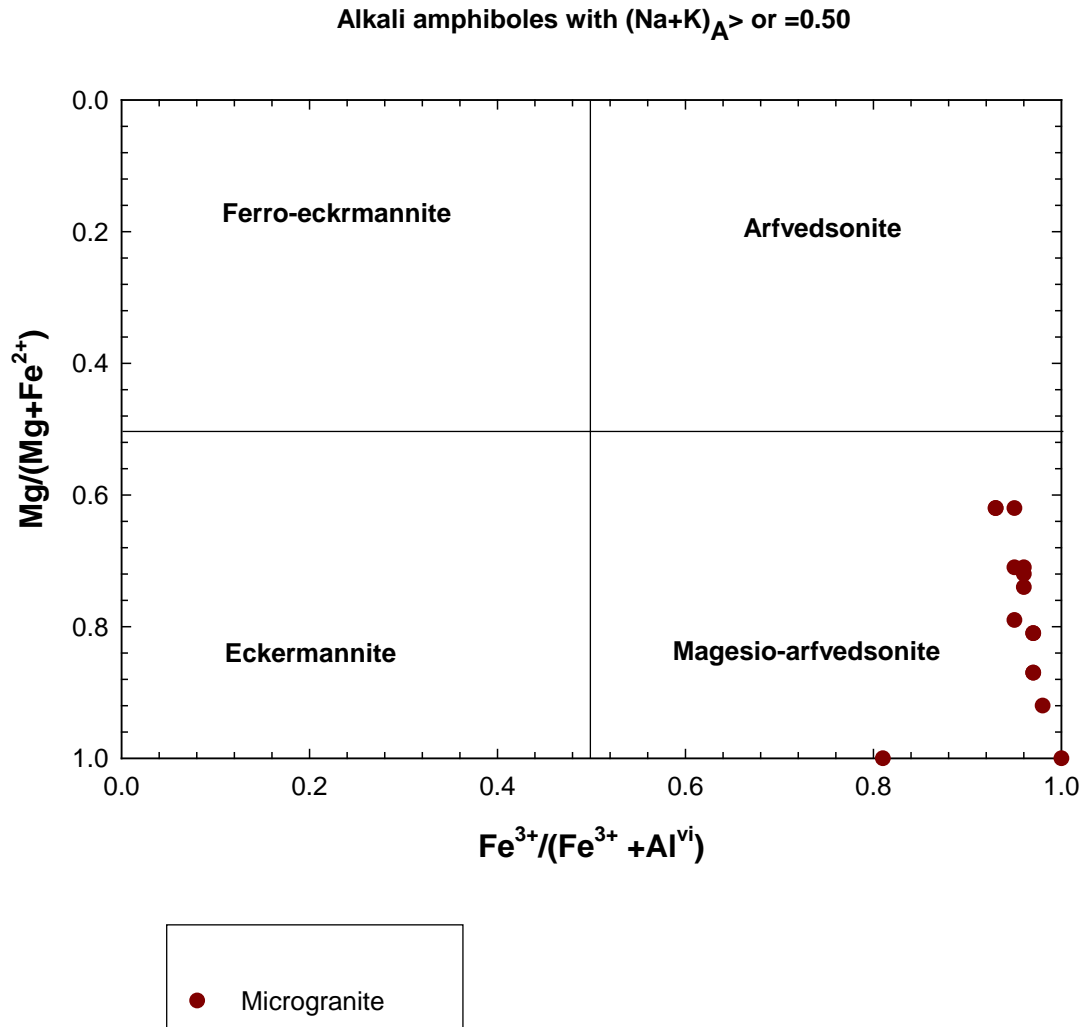


**Figure 3.15:** *Nomenclature for the sodic amphiboles (after Deer et al., 1997). This figure shows that sampled microgranites have amphiboles that are Magesio-arfvedsonite in compositions.*

*3.3.4.2 Granite*

The coarse-grained granite is comprised of alkali feldspars (58-60%), quartz 25-35%), arfvedsonite (5-7%), aegirine (1-3%), augite (2-3%), subhedral microcline feldspars (<2%), and trace amounts of aenigmatite. Other less common minor phases in the coarse-grained granite include eckermannite, plagioclase, sanidine and biotite. The accessory minerals such as apatite, titanite and zircons were only rarely observed. The alkali feldspars show Carlsbad and Baveno twinning. The coarse-grained granite is undeformed and contains no fabric, but the quartz grains are often strained and display undulose extinction. The colourless augite is replaced by strongly pleochroic brown to green aegirine, which is in turn replaced by strongly pleochroic brown to greenish-blue Arfvedsonite. Two thirds of the arfvedsonites have finely zoned rims. (Fig.3.17a & b).

Eckermannite occurs as a retrograde mineral replacing aegirine in some of the samples (MC7013, MC7018). Plagioclase is rarely observed and is only seen in the alkali feldspar matrix (MC7007, see Fig.3.17 c). In sample MC7010, biotite occurs along the cleavage planes of arfvedsonite grains. The red-brown pleochroic aenigmatite is observed in the core of the arfvedsonite grains and seems to indicate that it is forming as a result of arfvedsonite breakdown (Fig.3.17 e & f,).

Mineral compositions for the coarse-grained granites are shown in Appendix 1.3. Aegirine contains Na contents of up to 0.88 cations pfu, $Fe^{2+}$ contents of up to 0.57, and $Fe^{3+}$ contents of up to 0.89 cations pfu. Arfvedsonite grains contain Na contents of up to 2.50 cations pfu, $Fe^{3+}$ contents of up to 1.15, and $Fe^{2+}$ contents of up to 3.27 cations pfu (Fig.3.18). The rim-core arfvedsonite mineral chemistry data do not show any consistent pattern variation of any element between the core and the rim ( see Appendix 1.3). Ekermannite contains Na contents up to 3.02 cations pfu, Ca content up to 1.11 cations pfu, $Fe^{2+}$ contents up to 2.44 and $Fe^{3+}$ up to 1.82 cations pfu (Figure 3.18). Nomenclature for the sodic amphiboles by Deer et al., (1997) showed that majority of sampled granites have amphiboles that are arfvedsonite in compositions and rarely contain fero-eckermannite (Fig.3.19). Granites contain orthoclase feldspars with an average $An_0Ab_{06}Or_{94}$ and sodium-rich plagioclase feldspars with an average $An_0Ab_{100}Or_0$
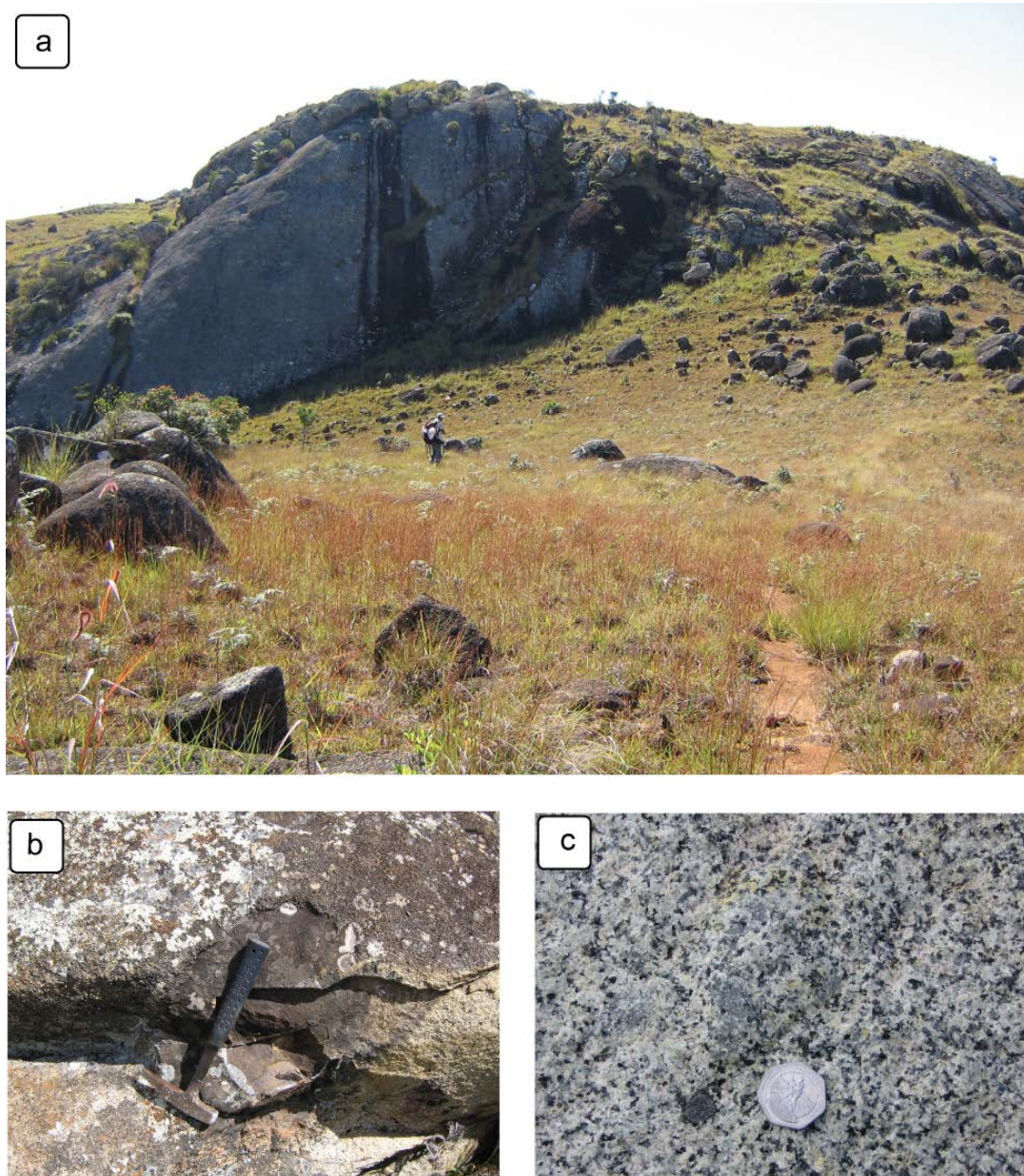
**Figure 3.16:** *Field photographs of coarse-grained granite (a) Showing a prominant arcuate ridge of the granite outcrop in the south of the Ambohiby Complex. (b) showing a large microgabbro xenolith in coarse-grained granitic outcrop. (c) showing a fresh sample of equigranular coarse-grained granite with some minor micrograbbro xenolith.*
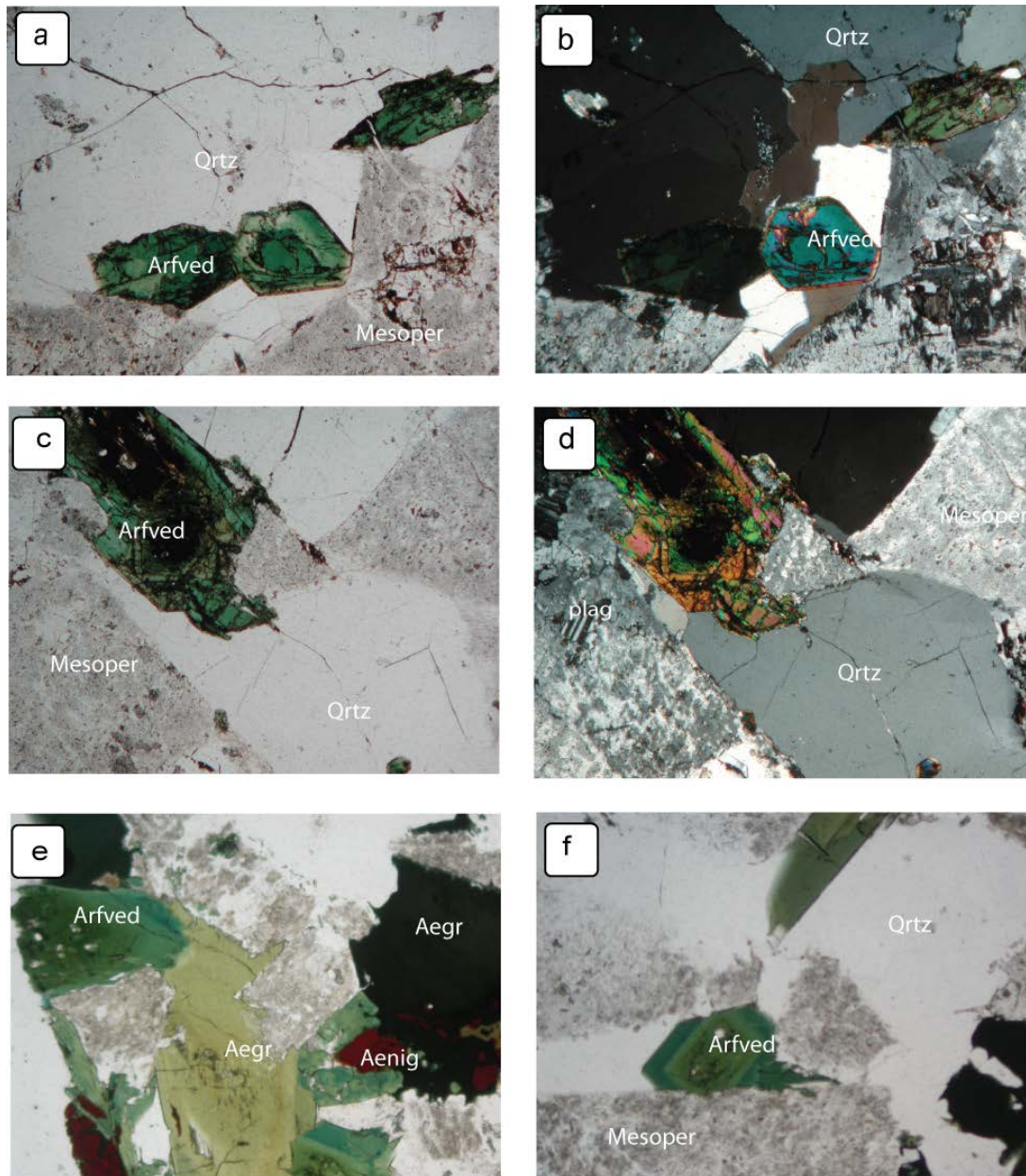
**Figure 3.17**: *Thin section photographs of coarse-grained granite (a) Showing subhedral pleochroic blue to greeen arfvedsonite in quartz and mesoperthite matrix (T/S MC7007). (b) same as (a) under XPL. (c) showing much altered arfvedsonite in mesoprthite and qaurtz matrix. (d) same as (c) under XPL. Showing plagioclase in mesoperthite grains, and fine grained quartz displying undulose extinction. (e) shows replacement reaction texture between arfvedsonite and pale brown aegirine as well as red-brown peleochroic aenigmatitie in arfvedsonite grains (T/S MC7018). (f) Showing zoned subhedral pleochroic blue to green arfvedsonite in mesoperthite and quartz matrix*
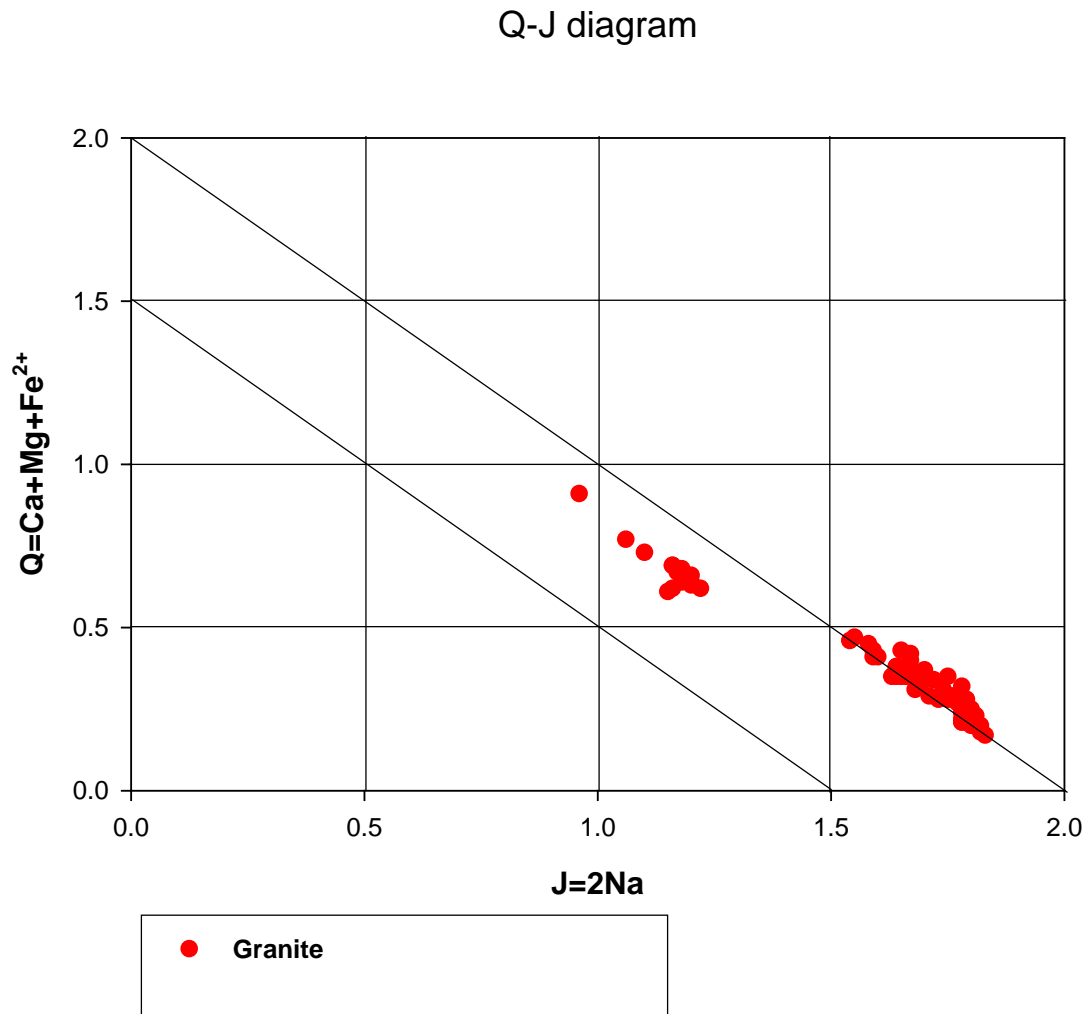
## Q-J diagram



**Figure 3.18:** *Microprobe analysis of pyroxenes from the granite samples plotted on the Q-J diagram (after Morimoto et al., 1988). This plot shows that the granite has two sets of pyroxene, the first set enriched in Na (i.e. aegerine) with high total of J ranges between 1.5-1.8 and the second set both enriched in Ca- Na with an average J of 1.3*

**Alkali amphiboles with (Na+K)$_A$> or =0.50**
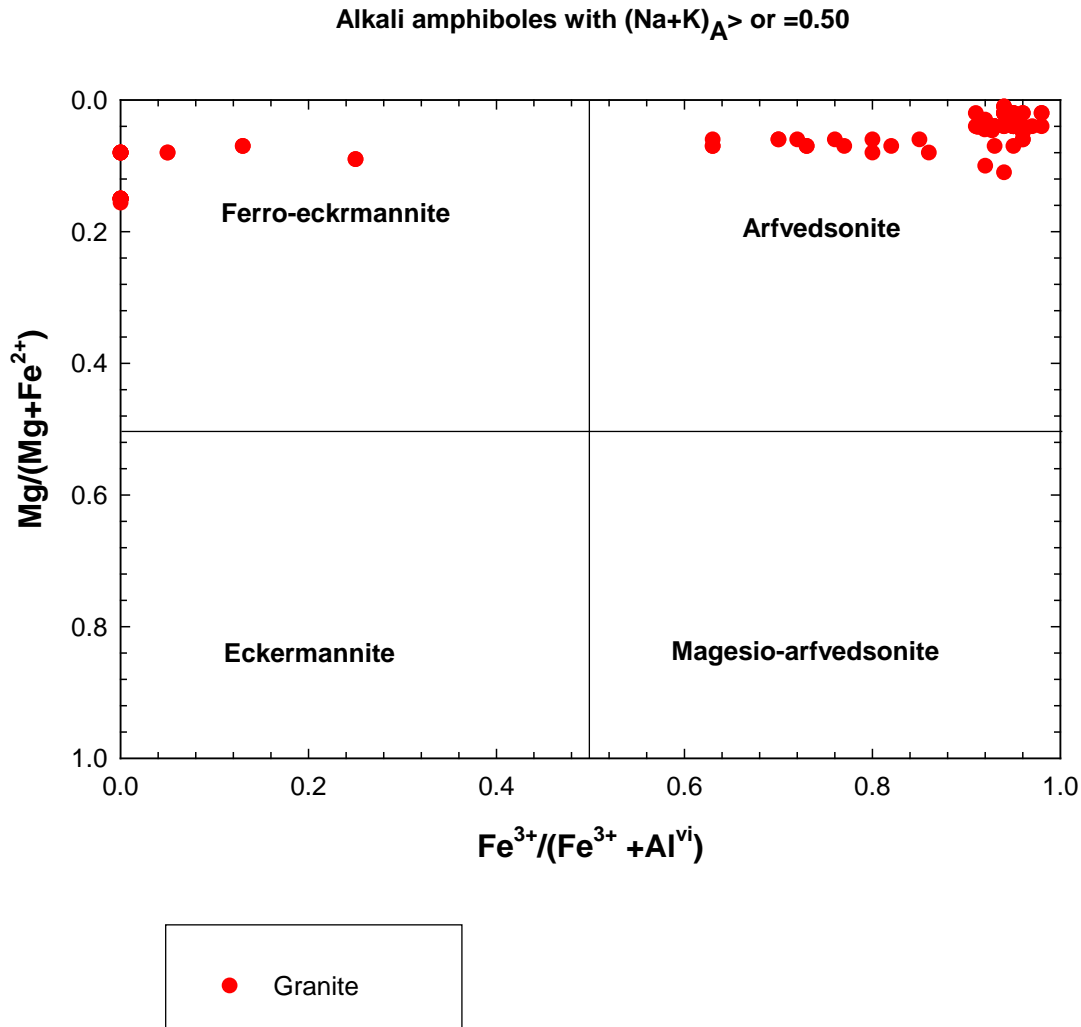


**Figure 3.19:** *Nomenclature for the sodic amphiboles (Deer et al., 1997). This figure shows that majority of sampled granites have amphiboles that are arfvedsonite in compositions and rarely contain fero-eckermannite.*

### 3.3.5 Dykes

*3.3.5.1 Mafic dykes*

Mafic dykes are comprised mainly of elongated plagioclase feldspars (66-68%) anhedral Augite (13-15%), chlorite (8-10%), subhedral magnetite (3-5%), epidote (<2%) and trace amounts of subhedral pyrite (1%). Minor quartz (<2 %) is sometimes

observed. The plagioclase display polysythetic twins. Chlorite and epidote occurs as retrograde minerals replacing anhedral augite, biotite replaces hornblende (Fig.3.20 c, d & e). Blocky magnetite and sulphides are randomly distributed.

Most of the mafic dykes are weakly porphyritic (<3%) with tabular to acicular plagioclase phenocrysts (0.5x1-0.2x1.2mm) and trace amounts of euhedral pyrite cubes (0.8mm) set

in a fine-grained to glassy, melanocratic to mesocratic grey black matrix. Sometimes the plagioclase phenocrysts can be much coarser grained (up to 10mm), and glomeroporphyritic textures were also observed.

Mineral compositions for the mafic dykes are shown in Appendix 1.3. Augite contains Na contents of up to 0.05 cations pfu, Ca contents up to 0.78 cations pfu, Mg contents up to 1.51 cations, pfu, $Fe^{2+}$ contents of up to 0.44 cations pfu (Fig.3.21).
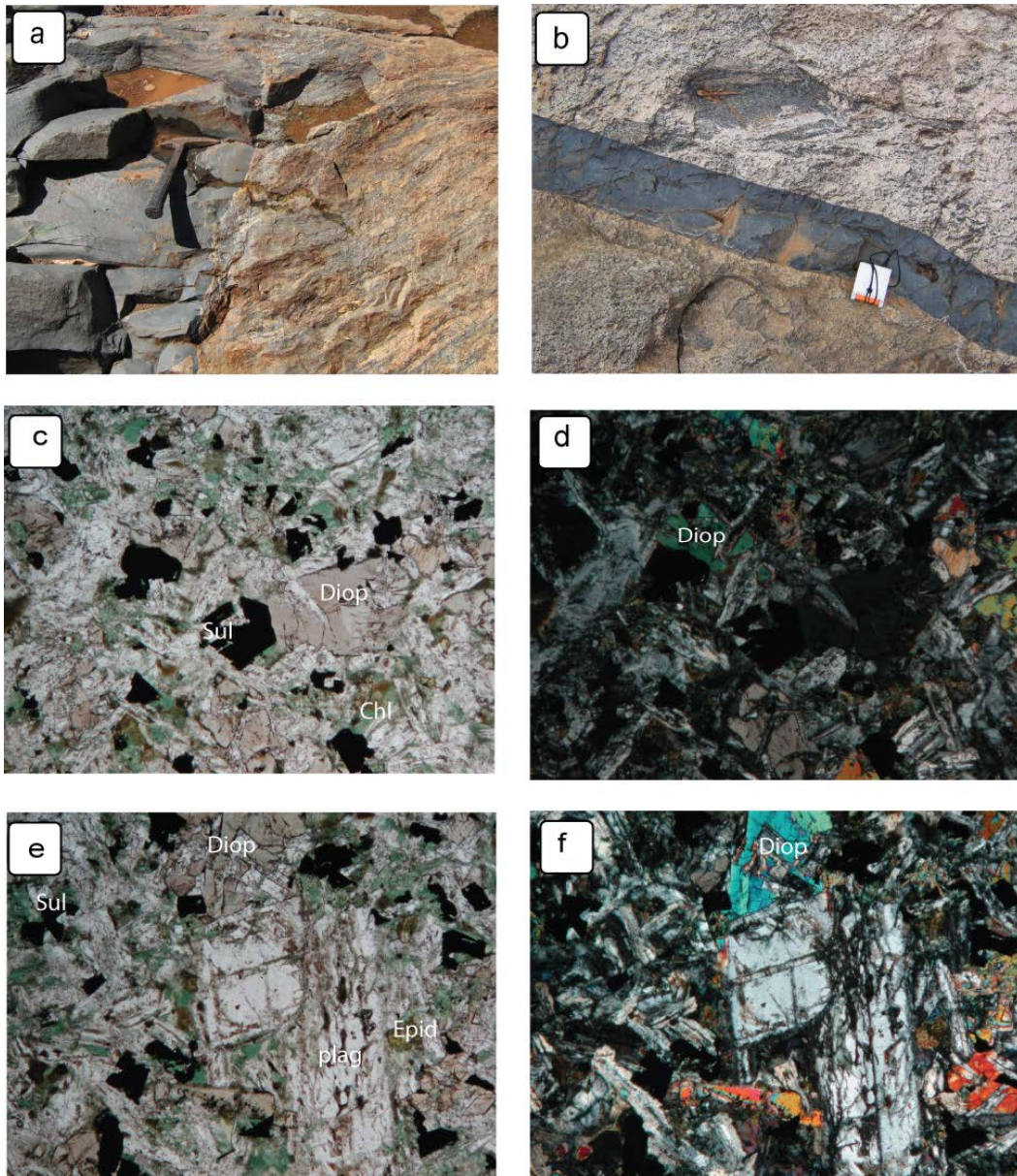
**Figure 3.20:** *(a) Field photograph showing a ~1.8 meters wide melanocratic basaltic dyke cross-cutting the Precambrian orthogneiss basement. (b) Field photograph showing a ~200 mm wide basaltic dyke cross-cutting the Precambrian orthogneiss. (c) Thin section photograph of the basalt dyke showing anhedral diopside as well as plagioclase as primary phases. Diopside is replaced by chlorite. Presence of trace amounts of blocky sulphides, and randomly distributed. (d) Same as (c) under XPL. (e).Thin section photograph of the basalt dyke showing chlorite replaces anhedral colourless diopside. Presence of trace amounts of epidote as well as blocky sulphides. (f) Same as (e) under XPL.*
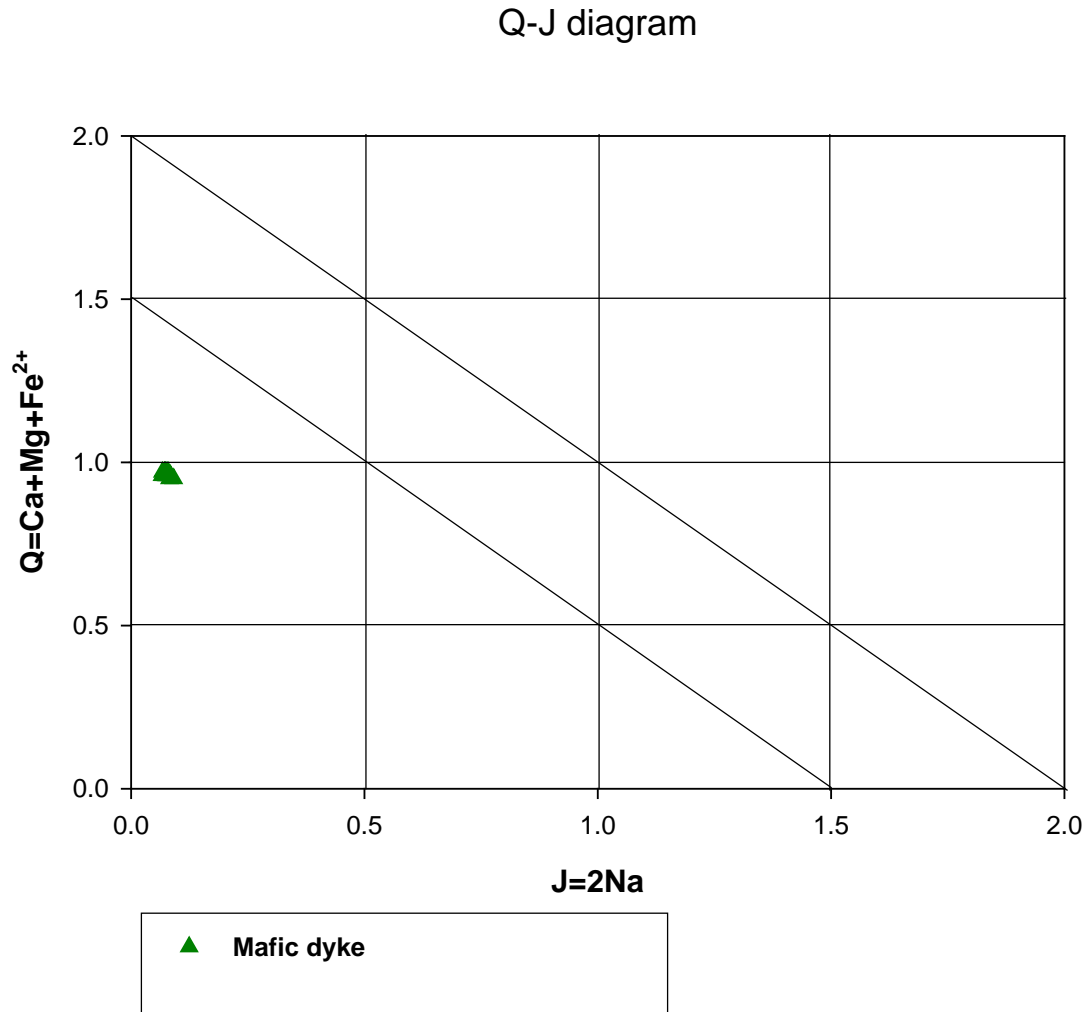
## Q-J diagram



**Figure 3.21:** *Microprobe analysis of pyroxenes from the mafic dyke samples plotted on the Q-J diagram, (after Morimoto et al., 1988). This plot shows that the mafic dyke has one set of pyroxene that is Ca enriched (Augite), and has a total J component of around 1.0*

*3.3.5.2 Felsic dykes*

The felsic dykes are divided into two types, namely: The leucocratic cream to mesocratic blue-grey felsic dykes that intrude mainly into gabbro, monzonite, micro-syenite and microgranite (Fig.3.22 a, b, c & d); while the green-grey rhyolite dykes intrude mainly into granites (Fig. 3.22 e & f). These dykes display two main mesoscopic textures. Many are weakly porphyritic to glomeroporphyritic with tabular feldspar and quartz (0.2-0.75mm) phenocrysts set in a fine-grained matrix. Others have viscous magmatic flow band textures with ~2mm laminations parallel to the edges of the dykes (Fig.3.22 c & d). Locally, the laminations are associated with centimetre-scale spherical nodular structures with concentric rings that give the rock a peculiar appearance (Fig.3.22 e & f). The local

Malagasy people call the rock "Jasper Kambamba" (Kambamba means "something strange"). The local Malagasy people mine the "Jasper Kambamba" for use as an ornamental stone. In thin section the "Jasper Kambamba" comprises mostly of fine-grained spherulites with radiating acicular crystals (Fig.3.22 e & f) and represents a devitrification texture.

In thin section, most of the felsic dykes have mineral compositions similar to the granites. Alkali feldspars are the dominant minerals (>70%) and occur together with primary augite and sometimes skeletal aegirine, orthoclase, quartz, and oxides (Fig.3.23 a & b). Needle like arfvedsonite (<4%) may also be present. Granophyric textures result from the intergrowth between alkali feldspar phenocrysts and quartz. The secondary pleochroic light green chlorite, pleochroic brown biotite and red-brown aenigmatite replace the colourless augite. The alkali feldspars are altered to sericite.

Mineral chemistry was not collected for this rock types
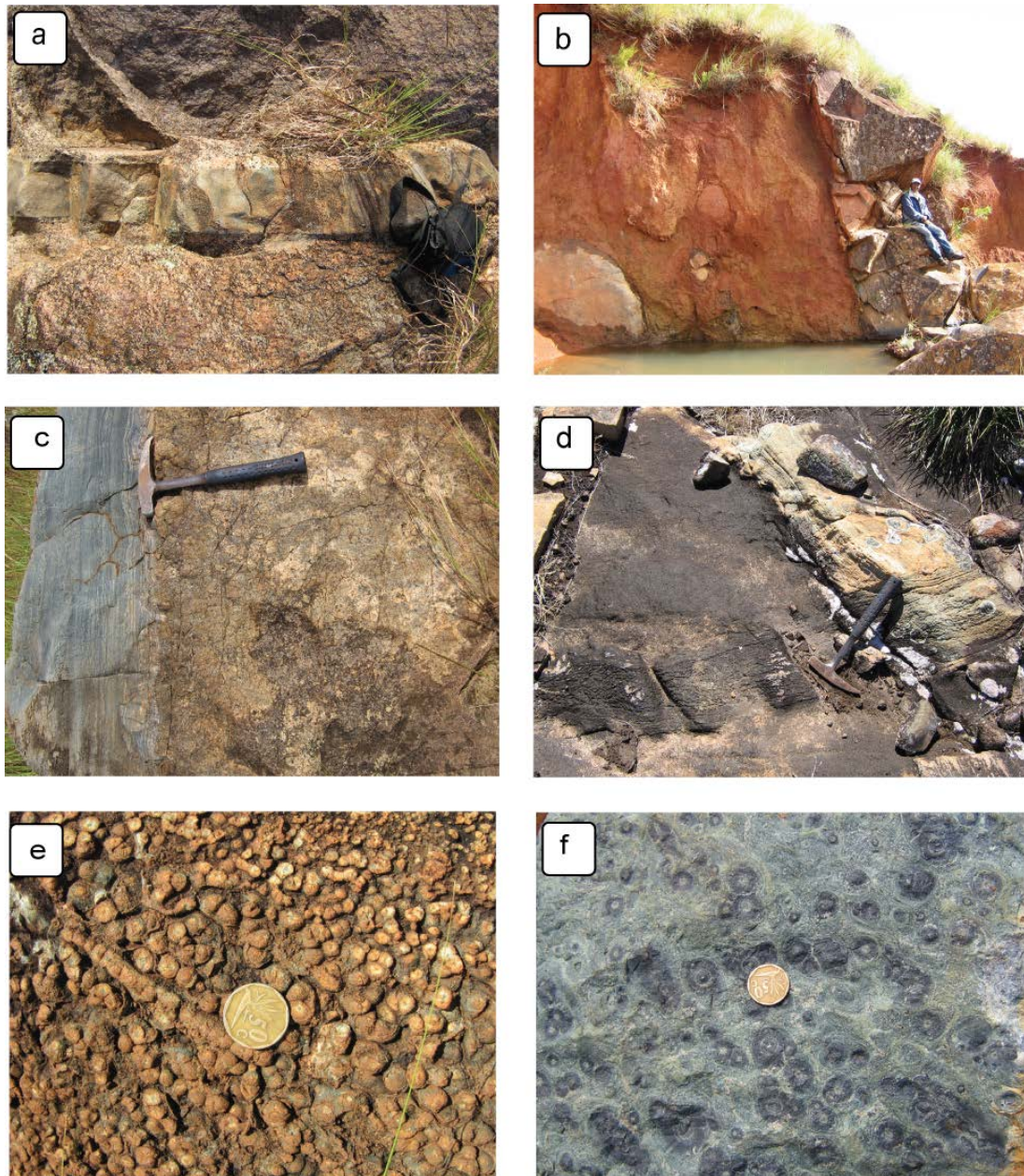
**Figure 3.22***: Field photographs of the felsic dykes (a) Fine-grained leucocratic felsic dyke cross cutting the gabbros. (b) About 1.5 meters wide fine-grained leucocratic felsic dyke. (c) Laminated magma flow structures develop mainly parallel to the dyke walls of the fine-grained leucocratic felsic dykes. (d) Laminated leucocratic fine-grained felsic cross-cut by laminated leucocratic fine-grained felsic dyke. (e) Showing the spherical nodular "Jasper Kambamba" texture. The texture makes these rocks desirable for mining as ornamental stone. (f) Same as (e) except that this sample is a fresh sample.*
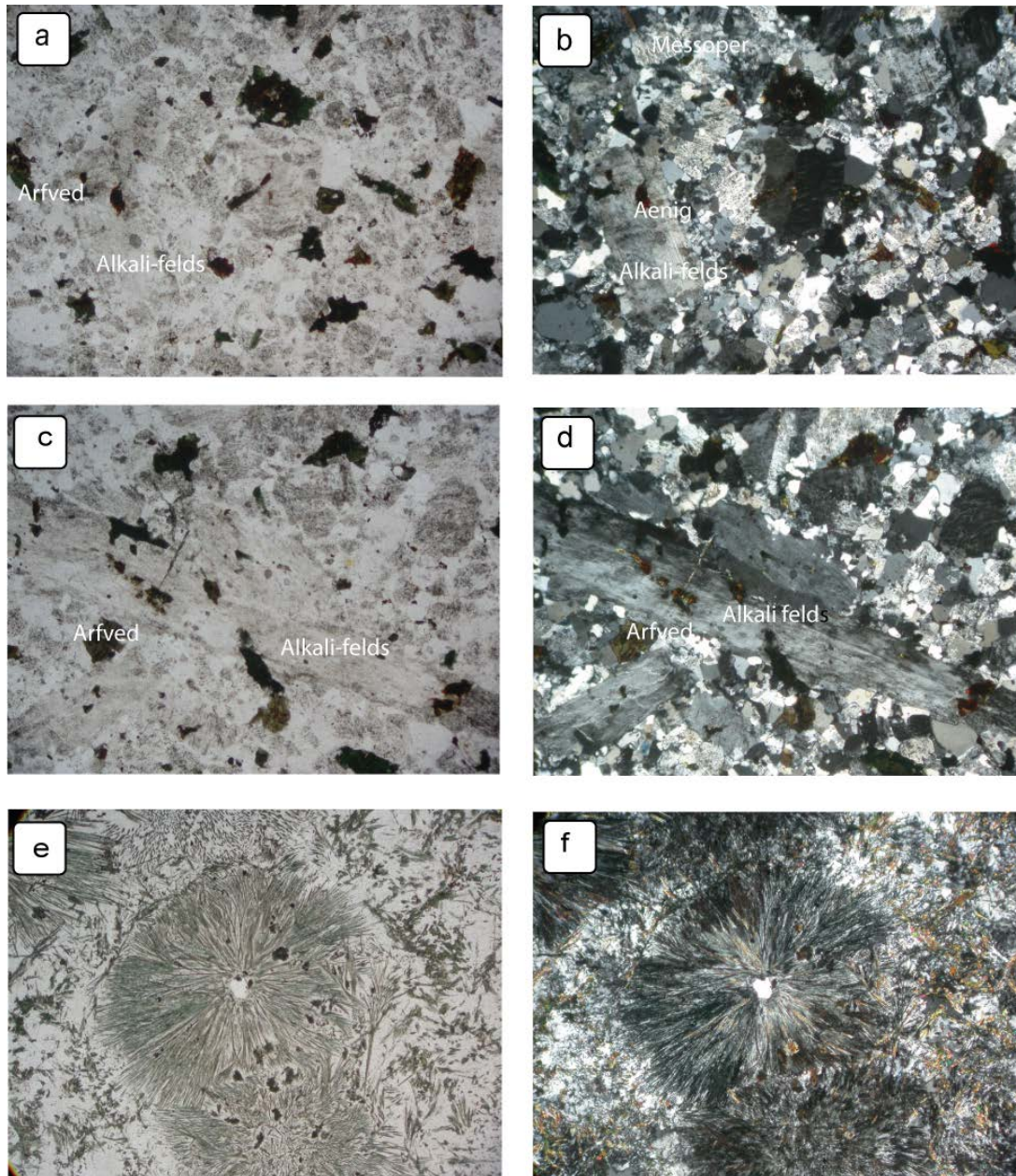
**Figure 3.23:** *Thin section photograph of the felsic dykes (a) Showing a felsic dyke consisting of elongated alkali feldspar, mesoperthite, anhedral reddish-brown aenigmatite and interstitial arfvedsonite. (b) Same as (a) under XPL. (c) Elongated alkali feldspar (PPL). (d) Same as (c) under XPL (T/S MC7047) (e) Displays spherical texture consisting of radiating arrays of crystal fibres. (f) Same as (e) under XPL (T/S MC7023)*

## CHAPTER 4: WHOLE-ROCK GEOCHEMISTRY

### 4.1 Introduction

The main objective of this chapter is to describe the geochemical characteristics of different rock types within the Ambohiby Complex. Sixty-five samples from the Ambohiby Complex were targeted for detailed geochemical analysis to establish their whole rock composition. With the variation in lithologies within the study area a variety of geochemical plots have been used for classification purposes. The whole rock compositions of all sixty five samples were plotted on standard classification diagrams to confirm rock types identified via modal mineralogy in Chapter 3.

### 4.2. Classification of Rock types

The plutonic TAS classification diagram of Cox *et al.* (1979) has been used to determine the rock types in the Ambohiby Complex according to major element geochemistry. The results indicate that all the plutonic rocks classify as gabbros, monzonites, alkali syenites and granites (Fig. 4.1) consistent with the field observations as well as the petrographic studies. The TAS classification diagram for volcanic rocks after Le Bas *et al.,* (1986) indicates that the extrusive mafic dyke samples plot as basalt to trachy-basalts with one sample plotting in the trachy-andesite field (Fig.4.2). The felsic dyke samples all plot in the rhyolite field (Fig.4.2).
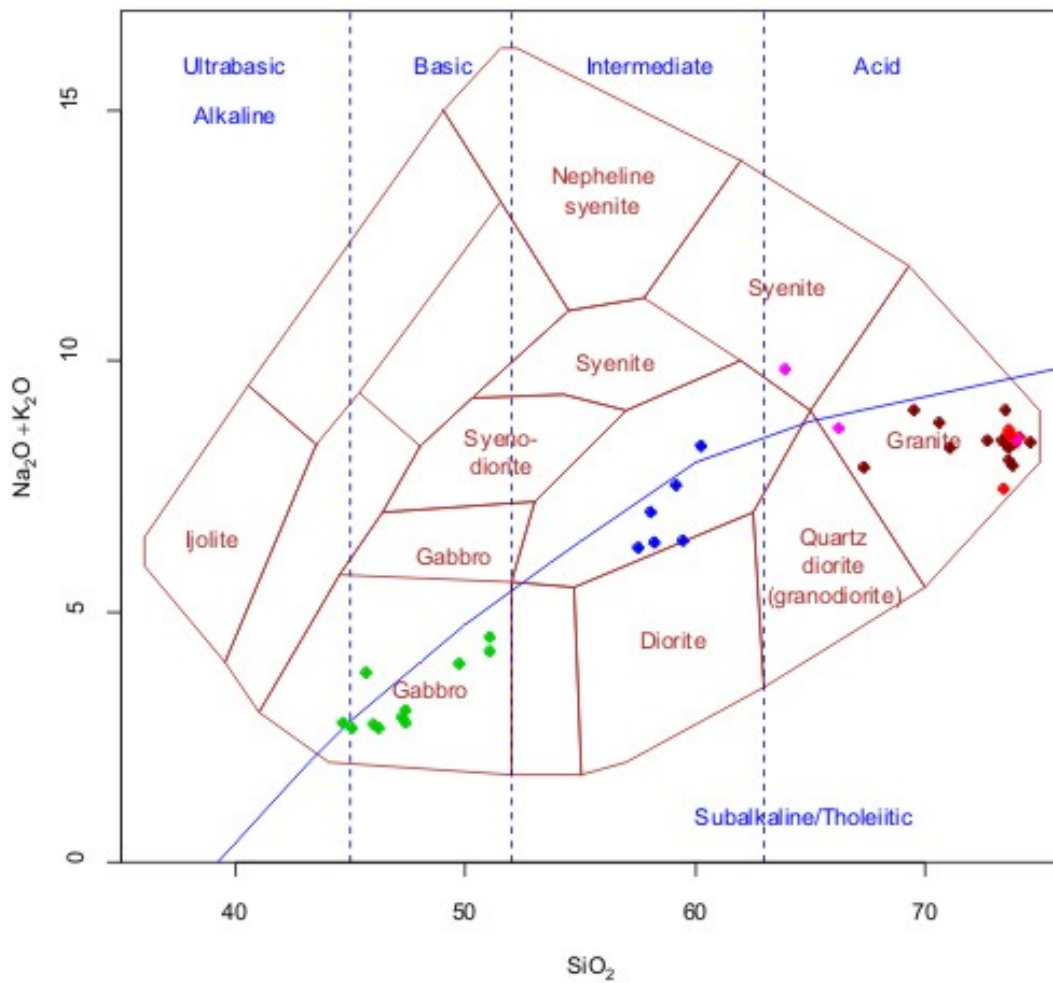
**Figure 4.1:** TAS *classification diagram of Cox et al, (1979) classifying plutonic rocks of the Ambohiby complex. Green diamonds= Gabbro, Blue diamonds=Monzonite, Pink diamonds=Syenite, Brown diamonds=microgranite, Red diamonds=medium to coarsed grained Granite*
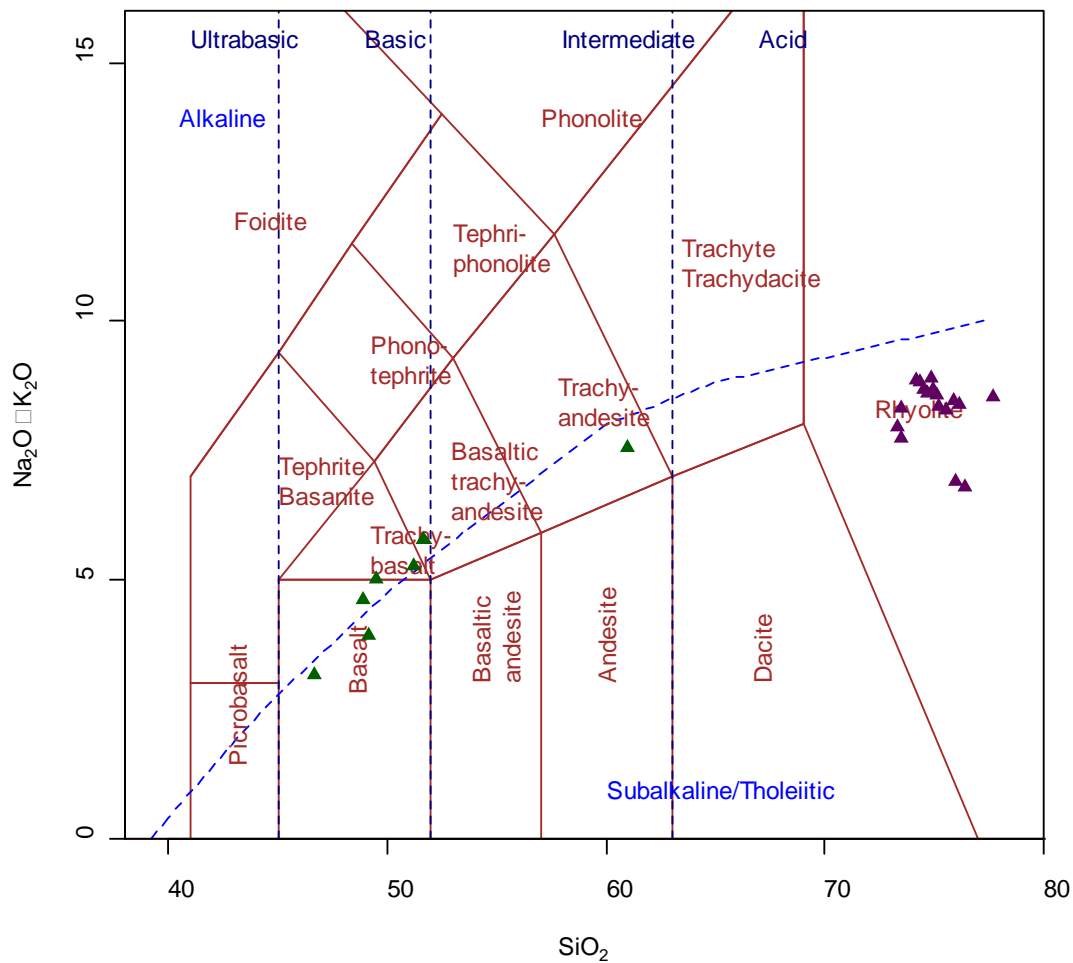
**Figure 4.2:** *TAS classification diagram after Le Bas et al., (1986) is used for the classification of volcanic rocks. Mafic dyke samples plot on the basalt as well as trachyte basalt field. Felsic dyke samples plot under rhyolite field. Green triangles= mafic dykes, Purple triangles=felsic dykes*

## 4.3 Mafic rocks

### 4.3.1 Major elements

Bivariate diagrams for gabbros and basaltic dykes are shown in Figure 4.3 and 4.4.

Gabbroic and basaltic dyke samples have concentrations of MgO (4-8% wt %), FeOt (8-16% wt %), $TiO_2$ (1.4-4.6% wt %), $Al_2O_3$ (12.1-19.8% wt %), and CaO (6.2-13.8% wt %) and depleted in $P_2O_5$ (0.0-0.4%), $K_2O$ (0.0-2.0%) and $Na_2O$ (2.1-3.5%) (Fig.4.3, Table 4.1). In the bivariate plots of wt% $SiO_2$ versus wt % MgO, CaO and $TiO_2$ weak negative correlations are recorded. $K_2O$ and $Na_2O$ show strong positive correlations, while the rest are scattered (Fig.4.3). In the bivariate plots versus wt% MgO, CaO show positive correlations whereas $Na_2O$ and $K_2O$ wt% shows negative correlations (Fig.4.4).
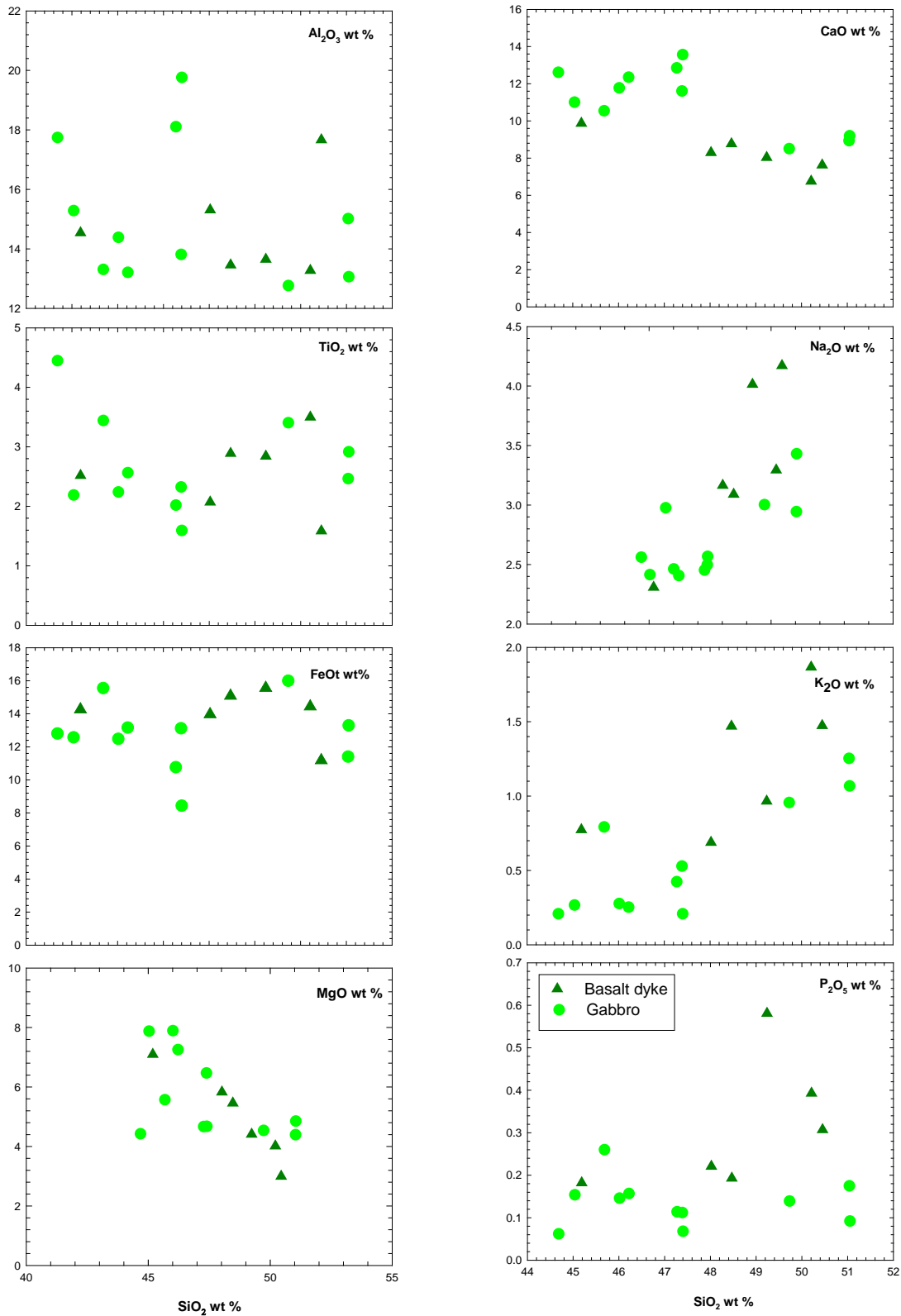
**Figure 4.3 :** *Major element variation diagrams for the Ambohiby Complex mafic rocks: (a) $Al_2O_3$, (b) $TiO_2$, (c) $Fe_2Ot$, (d) MgO,(e) CaO, (f) $Na_2O$ , (g) $K_2O$ and (h) $P_2O_5$ Vs $SiO_2$ (wt%)*
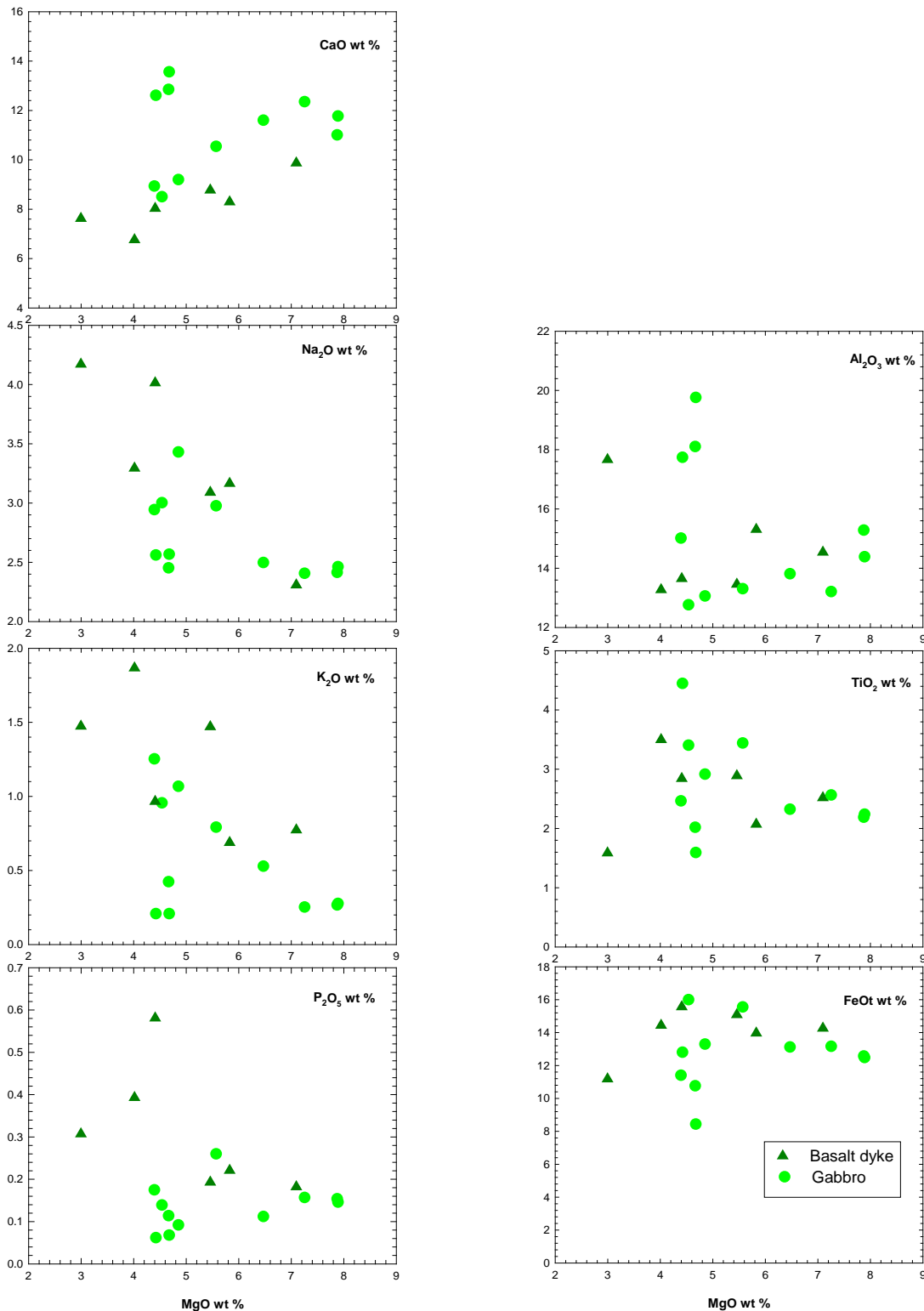
**Figure 4.4:** *Major element variation diagrams vs MgO of the Ambohiby Complex mafic rocks: (a) CaO, (b) Na$_2$O, (c) K$_2$O, (d) P$_2$O$_5$, (e) Al$_2$O$_3$, (f) TiO$_2$ and (g) FeO$_t$ Vs MgO (wt).*

*4.3.2 Trace and rare earth elements*

Figure 4.5 shows plots of $SiO_2$ (wt. %) versus trace elements for the Ambohiby mafic rocks. Mafic rocks show a positive trend for $SiO_2$ plotted against Nb (ppm) and Zr (ppm). All mafic rocks have relative poor correlations ($R^2$=0.04) for $SiO_2$ plotted against Zr/Nb ratio and La/Yb ratio ranging ~7-8 (Fig.4.5). Gabbroic samples have significantly higher concentrations of Sr (up to ~650 ppm) as compare to the basalts. $SiO_2$ plotted against Sr (ppm) shows a weak negative correlation for both gabbros and basalt dyke samples, whereas $SiO_2$ plotted against Rb (ppm) shows a weak positive correlation (Fig.4.5). On the bivariate plot of CaO against Sr (ppm), Sr (ppm) shows a positive relationship with CaO (Fig.4.6). On the bivariate plot of MgO against Sr (ppm), Sr shows strong positive correlations for all mafic rocks, whereas Ba (ppm) against Sr (ppm) shows negative correlations (Fig.4.6). Figure 4.7 shows plots of Zr (ppm) versus trace elements for all Ambohiby mafic rocks. In addition there is a strong positive correlation between Zr (ppm) and Nb (ppm), Zr (ppm) and Yb (ppm), as well as Zr (ppm) and Th (ppm).

Chondrite normalised REE diagrams for gabbros and basaltic dykes are shown in Figure 4.8. REE concentrations in gabbros are around 50 times chondritic levels, with a slight elevation in the LREEs and minor Eu anomalies (both positive and negative). One sample had a very pronounced negative Ce anomaly as compared to other gabbroic samples. REE concentrations in basaltic dykes are around 100 times chondritic levels. The basaltic dykes have no Eu anomalies except one sample that show a very weak negative Eu anomaly and a pronounced negative Ce anomaly. Basaltic dyke's on primitive mantle normalized spider diagrams shows very similar trend to the gabbros and shows positive Ba anomalies, and negative Rb anomalies. Two samples showed negative Sr anomalies (Fig.4.9).
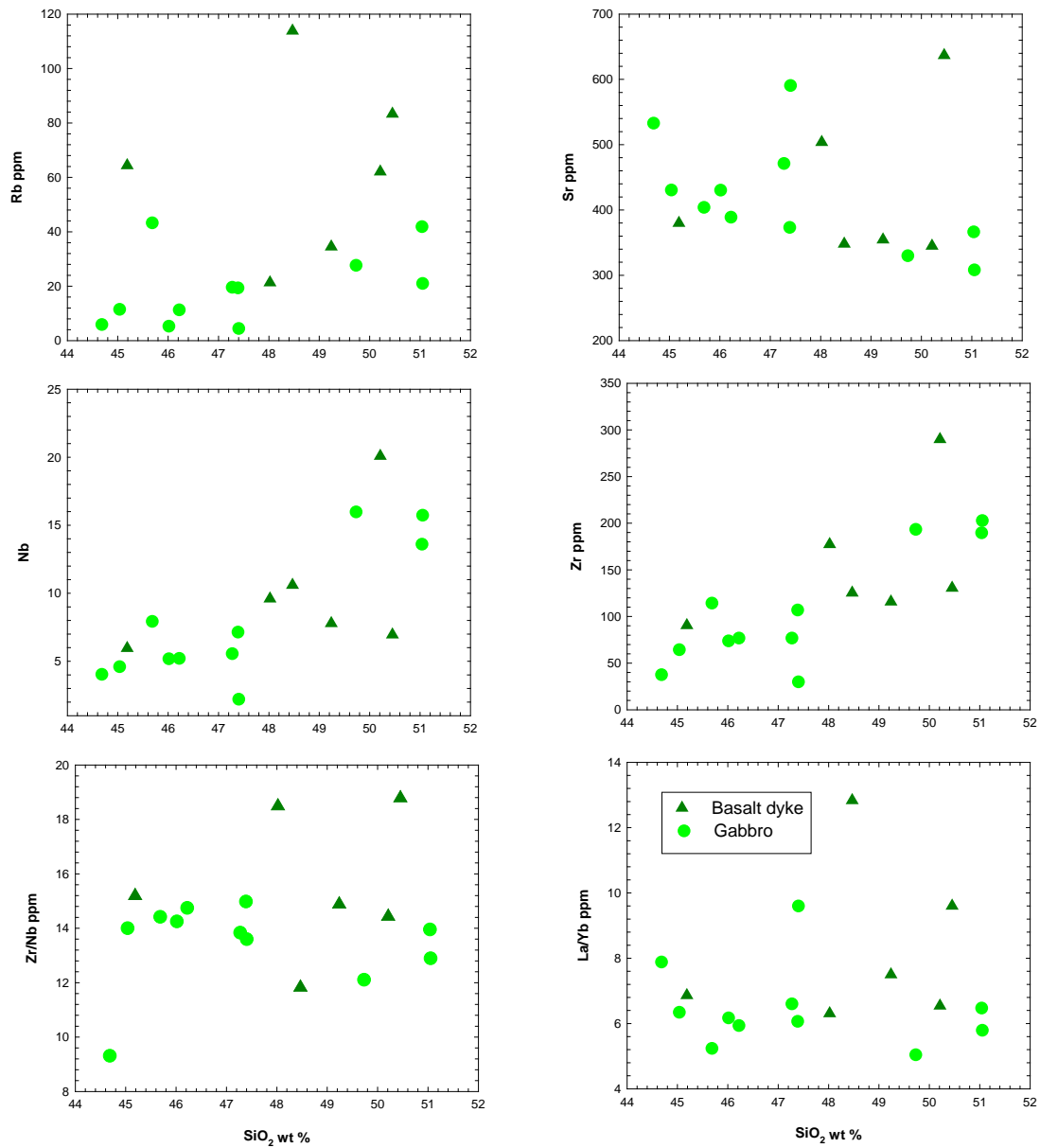
**Figure 4.5:** *Trace element variations for mafic rocks against wt% $SiO_2$: (a) Rb ppm vs wt%$SiO_2$ ppm; (b) Sr ppm vs wt% $SiO_2$, (c) Nb vs wt% $SiO_2$; (d), Zr ppm vs wt% $SiO_2$, (e) Zr/Nb ppm vs Wt%SiO2 ppm, (f) La/Yb ppm vs wt%$SiO_2$*
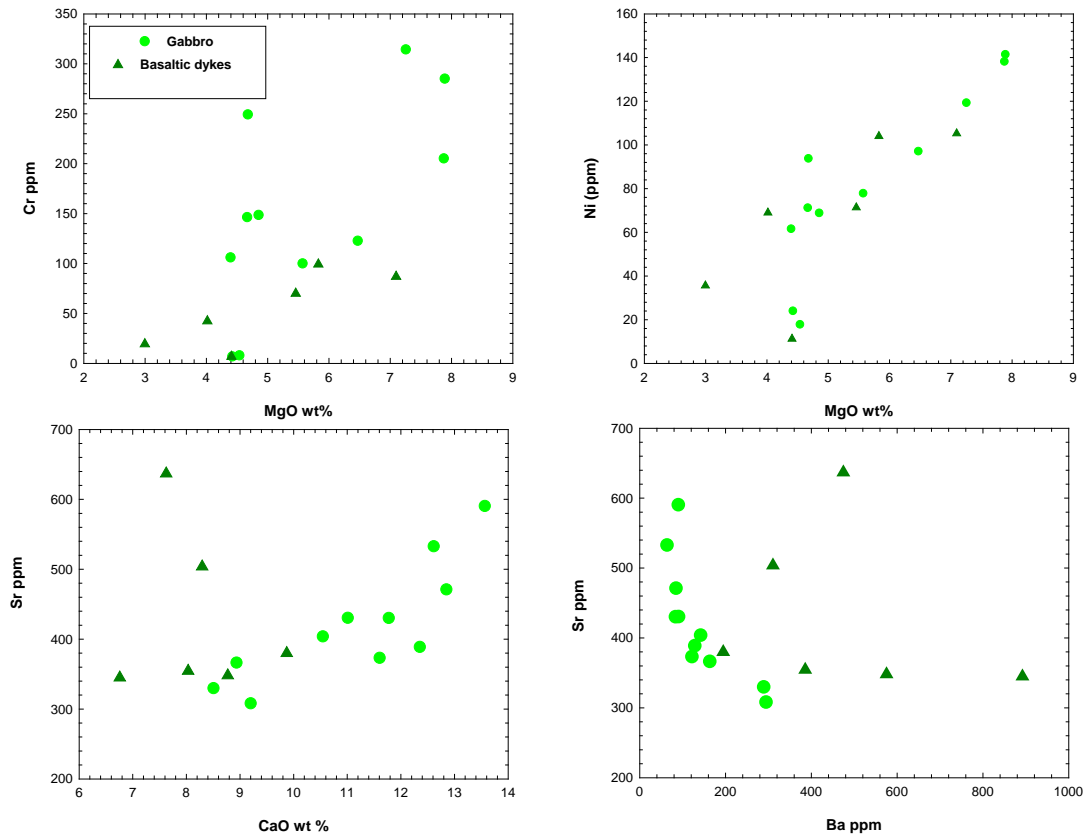
**Figure 4.6:** *Trace element variations for mafic rocks: (a) Cr ppm vs wt%MgO; (b) Ni ppm vs wt% MgO, (c) Sr vs wt% CaO; (d) Sr ppm vs Ba ppm.*
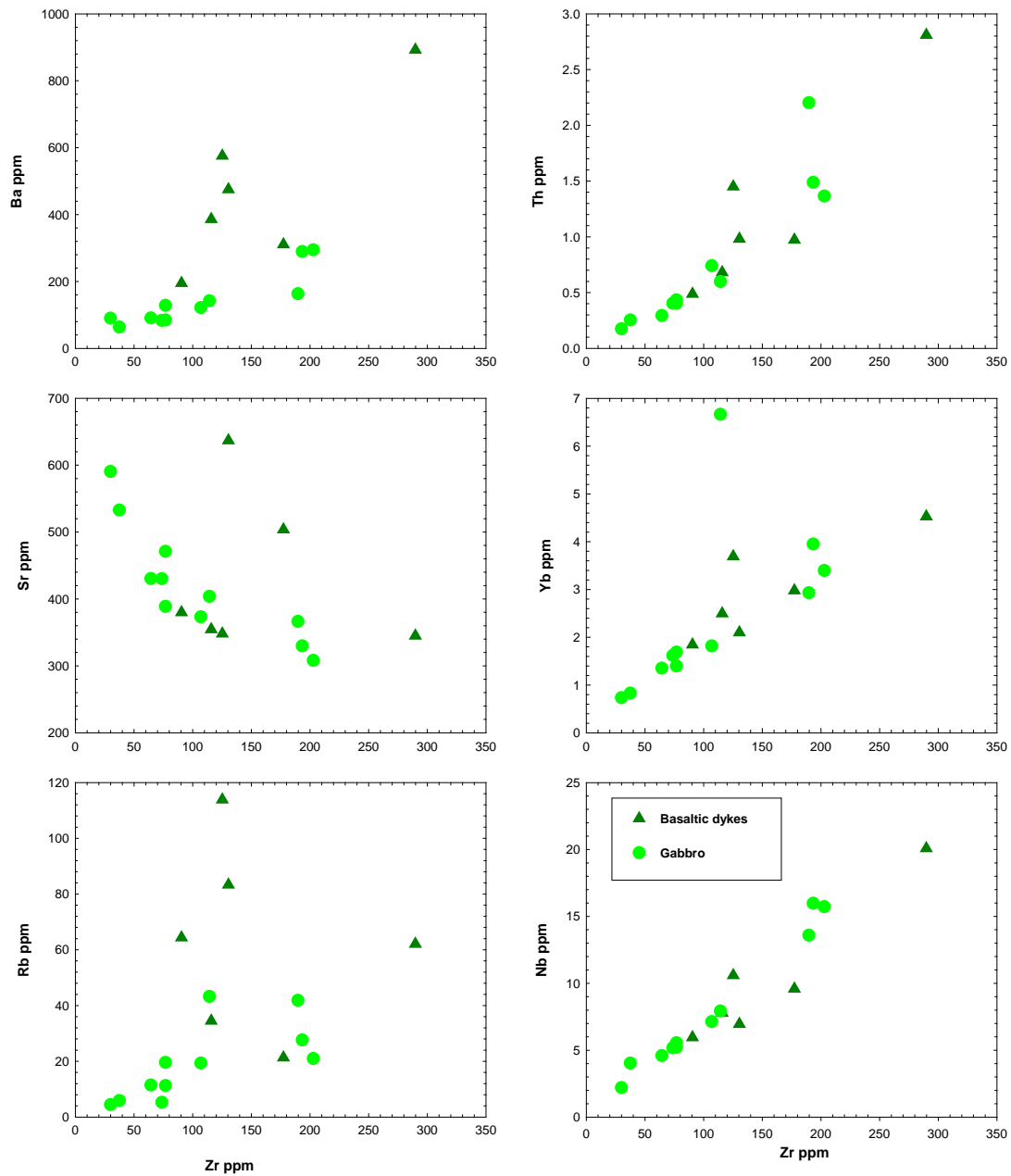
**Figure 4.7:** *Trace element variations for mafic rocks: (a) Ba ppm vs Zr ppm; (b) Th ppm vs Zr pmm, (c) Sr ppm vs Zr ppm; (d) Yb ppm vs Zr ppm, (e),Rb ppm vs Zr ppm, (f) Nb ppm vs Zr ppm*
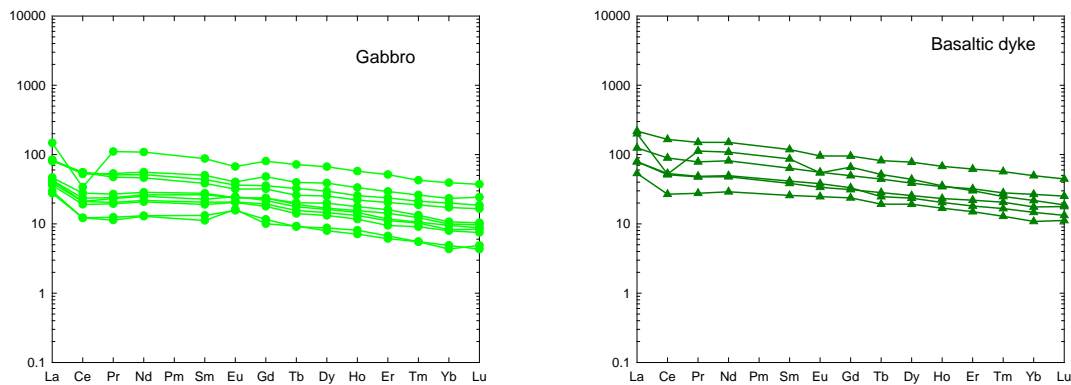
**Figure 4.8:** *Chondrite-normalized REE diagrams for gabbro, basaltic dykes. Chondrite normalization factors taken from Sun & McDonough (1989)*
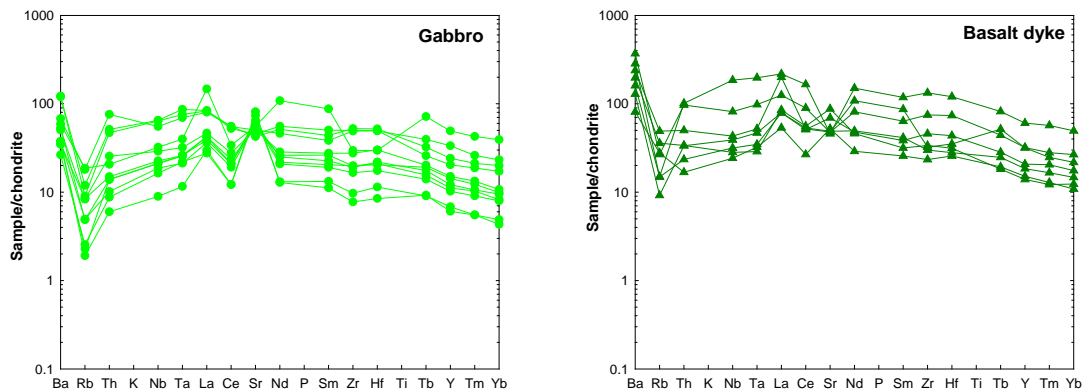


**Figure 4.9:** *Primitive-mantle-normalized spider diagrams for gabbro and basaltic dykes. Primitive-mantle normalization factors taken from Sun & McDonough (1989)*

## 4.4. Intermediate to felsic rocks

*4.4.1 Major elements*

Bivariate diagrams for intermediate to felsic rocks are shown in Figure 4.10 and 4.11. Intermediate rocks include monzonite and felsic rocks include alkali-syenite, micro-granite and medium-coarse grained granite as well felsic dyke samples. Felsic samples have the highest wt% $SiO_2$, ranging from ~58-74% (Fig.4.10). The Harker variation diagram versus $SiO_2$ indicates that the felsic rocks have higher wt% $Na_2O$ (up to 9%) and $K_2O$ (up to 6 %) as compared to the mafic rocks, however all the other elements tend to be lower. All felsic rocks show strong negative correlations between the bivariate plots for $SiO_2$ against CaO,

$TiO_2$, FeOt, MgO and $P_2O_5$, $Na_2O$ wt% (Fig. 4.10) whereas $SiO_2$ against $Al_2O_3$ shows weak negative correlations. All felsic rocks show strong positive correlations between $SiO_2$ against $K_2O$ wt % (Fig.4.10). The felsic rocks have very low MgO contents (< 1.0 wt %). Syenites, micro-granites, granites, and rhyolite dyke samples on the bivariate plots for MgO against other major elements, are plotted on the vertical pattern against the y-axis because they have very low MgO wt% concentration as compare to monzonite samples, which are scattered (Fig.4.11).

Monzonite samples are intermediate in composition and $SiO_2$ wt % contents range from 58.2 to 60.2 % (Fig.4.10). Harker variation diagrams (Fig.4.10) indicate a steep negative relationship between $SiO_2$ wt% and MgO, FeOt, $TiO_2$ and CaO wt%, and a positive relationship between $SiO_2$ wt% and $K_2O$ wt% and variable relationship between $SiO_2$ wt% and $P_2O_5$, $Na_2O$ and $Al_2O_3$ wt% (Fig.4.10). Two samples on the Harker variation diagram between $SiO_2$ wt% and $P_2O_5$ wt% contents are much elevated compared to the rest of the rock types with maximum concentrations around ~0.7wt%(Fig.4.10). On the bivariate plot for MgO wt% against other major elements, monzonite again displays an intermediate composition between mafic and the rest of the felsic rocks (i.e., alkali-syenites, micro-granite, granites and rhyolite dykes) (Fig.4.11) Furthermore, the bivariate plot versus MgO wt%, indicates a positive relationship with CaO, FeOt, $TiO_2$ and $K_2O$ wt% while $Al_2O_3$ and $Na_2O$ indicates a negative correlations (Fig.4.11)

Alkali-syenite, micro-granite, granite and rhyolite dyke samples compositionally, form a much consistent group with less internal variation in composition (Fig.4.10). They have highest wt% $SiO_2$ (~77 wt %) as compared to the rest of the Ambohiby Complex rock types. On the Harker variation diagram versus $SiO_2$ wt%, rhyolite dykes shows a negative correlations with MgO, CaO and $TiO_2$ wt% (Fig.4.10). Rhyolite dykes have lowest concentration of wt% MgO, CaO and $P_2O_5$ wt% (Fig.4.10).
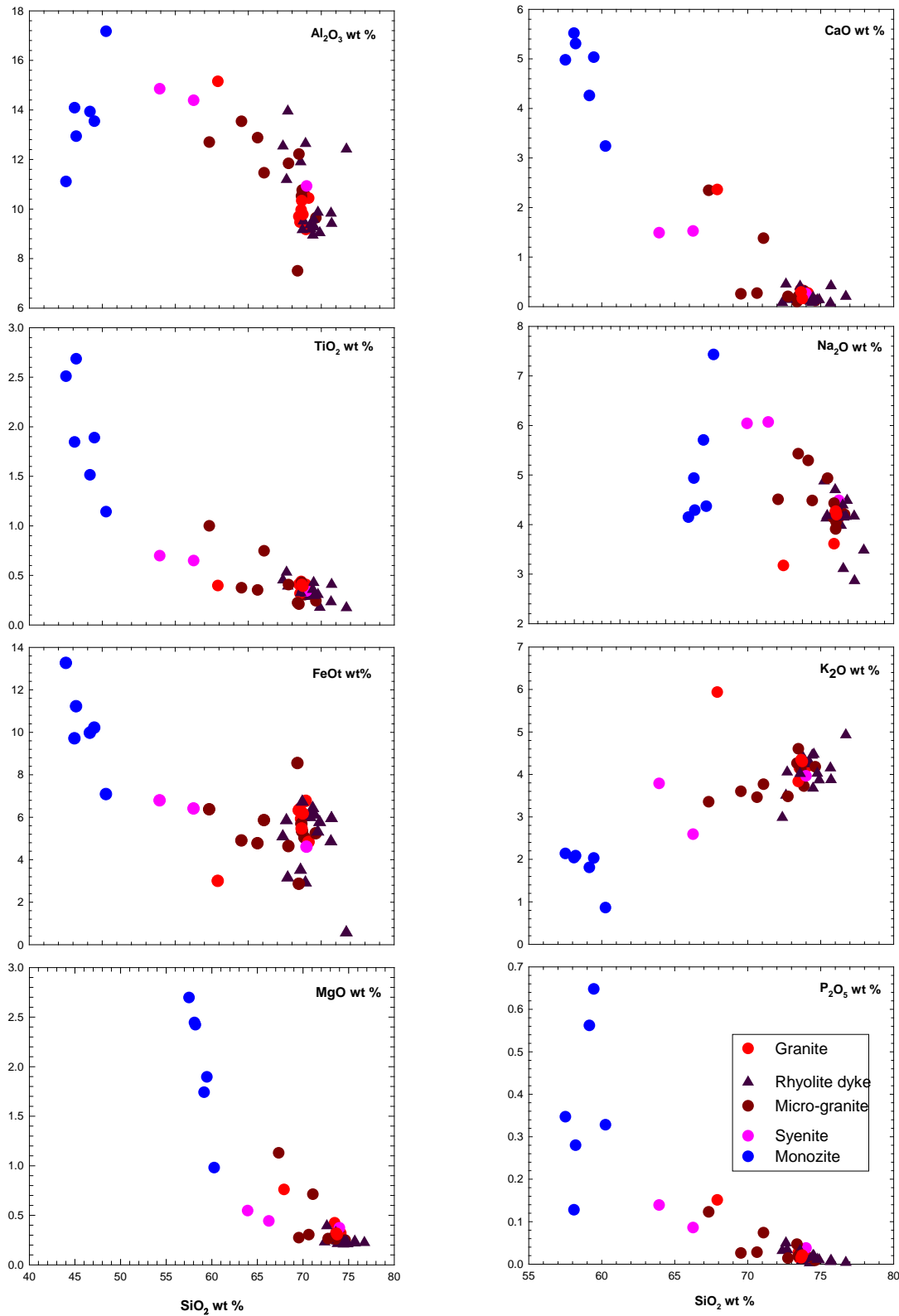
**Figure 4.10:** *Major element variation diagrams for Ambohiby intermediate to felsic rocks: (a) $Al_2O_3$, (b) $TiO_2$, (c) $Fe_2Ot$, (d) MgO,(e) CaO, (f) $Na_2O$ , (g) $K_2O$ and (h) $P_2O_5$ Vs $SiO_2$ (wt%) for all rock types within the complex.*
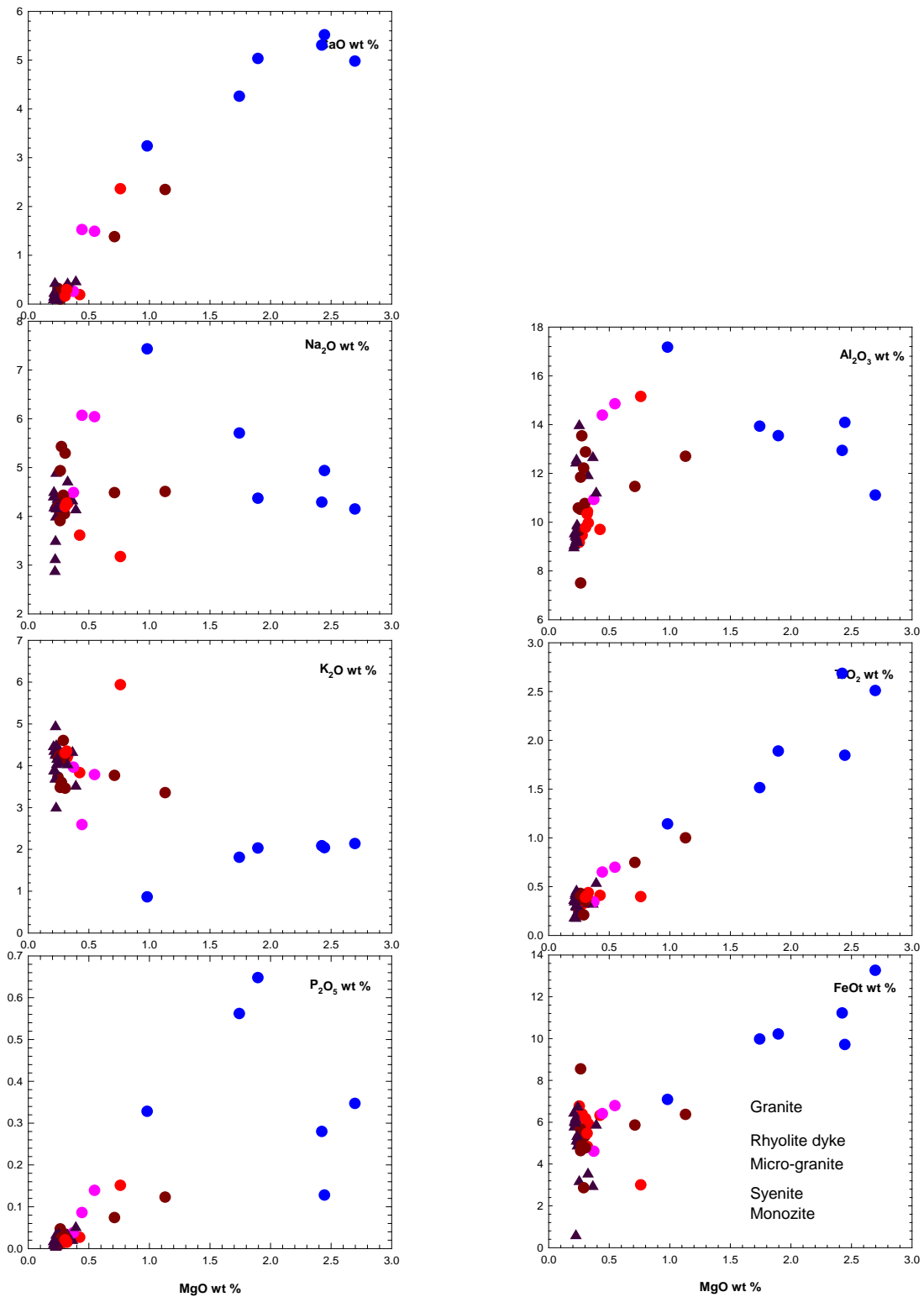
**Figure 4.11:** *Major element variation diagrams: (a) CaO, (b) Na$_2$O, (c) K$_2$O, (d) P$_2$O$_5$, (e) Al$_2$O$_3$, (f) TiO$_2$ and (g) FeO$_t$ Vs MgO (wt).*

*4.4.2 Trace elements and rare earth elements*

SiO$_2$ plotted against Sr (ppm) shows a strong negative correlation for both intermediate and felsic rocks of the Ambohiby complex (Fig.4.12), whereas SiO$_2$ plotted against Rb (ppm) shows positive correlations (Fig.4.12). On the bivariate plot of CaO against Sr (ppm), Sr (ppm) shows a positive relationship with CaO (Fig.4.13). On the bivariate MgO against Cr (ppm), all shows weak correlations, whereas Ba (ppm) against Sr (ppm) shows negative correlations (Fig.4.13). Figure 4.14 shows plots of Zr (ppm) versus trace elements for all Ambohiby intermediate and felsic rocks. There is a strong positive correlation between Zr (ppm) and Nb (ppm), Zr (ppm) and Yb (ppm), Zr (ppm) and Th (ppm) as well as Zr (ppm) and Rb (ppm) (Fig.4.14). There is a strong negative correlation between Zr (ppm) and Sr (ppm), as well as Zr (ppm) and Ba (ppm) (Fig.4.14).

The monzonite samples display similar trace element patterns to the gabbros (Fig.4.12 table 4.2). They have high Sr concentration (up to 313 ppm) as compared to the basalt dykes, alkali-syenites, micro-granites, granites and rhyolite dykes. On the bivariate plot versus SiO$_2$, Zr/Nb and La/Yb ratios are very similar to the gabbros; Zr (ppm) concentrations are higher (~500ppm) as compared to mafic rocks and furthermore correlate with higher SiO$_2$ wt% ranging from 56-62% (Fig.4.12). Chondrite normalised REE diagram for monzonite (Fig.4.15) show slight LREE enrichment and higher overall concentrations than the gabbro's with LREE around 100 times chondritic levels similar to that of the basaltic dyke samples. Furthermore, monzonite samples have weak negative Eu anomalies except one sample that display a very pronounced positive anomaly (Fig.4.15)

Alkali-syenites have very low concentration of Sr (ppm), Ba (ppm) and wt% CaO reflecting the lack of plagioclase feldspar and the dominance of alkali feldspar (Fig.4.12). Like Alkali-syenites, micro-granites have low concentration of Sr (< 200 ppm), but have high concentration of Ba up to ~700 ppm (Fig.4.12). REE concentrations in the syenites are 100 times chondritic levels but the patterns are relatively flat without obvious Eu anomalies present (Fig.4.13). While REE concentrations in micro-granites reach up to 1000 times Chondrite, but are more commonly sits around 200 times chondrite (Fig.4.13). REE concentrations in medium-coarse grained granite are around 100 times Chondrite and the HREE show flattest patterns of all the rock types from the Ambohiby Complex (Fig.4.13). Both micro-granites and granites show a weak negative Eu anomalies and one

sample show a negative Ce anomaly (Fig.4.13). In addition both micro-granites and granites samples show a pronounced negative Sr anomalies on a primitive mantle normalized trace element spider diagrams (Fig.4.14).

The rhyolite dykes have very similar trace-element characteristics to the granites, but the concentrations are slightly higher and variable to the granites (Fig.4.12). The rhyolite dykes are enriched in Zr (up to ~2800 ppm) and Zr/Nb ratio (up to ~ 19) and corresponds to the wt% $SiO_2$ concentrations and thus the degree of differentiation. On chondrite normalized REE diagrams, the REE concentrations are variable and range between 100 times chondritic values up to 1000 times chondritic values (Fig.4.15). The rhyolite dykes have moderate to strong negative Eu anomalies and relatively flat HREE patterns (Fig.4.15). Two samples show a positive Pr anomalies and the rest of the samples show a flat pattern. Like granites, rhyolite dykes shows negative Rb and Sr anomalies, on the spider diagram of primitive mantle normalized (Fig.4.16). However, few samples shows negative Ba anomalies (Fig.4.16)
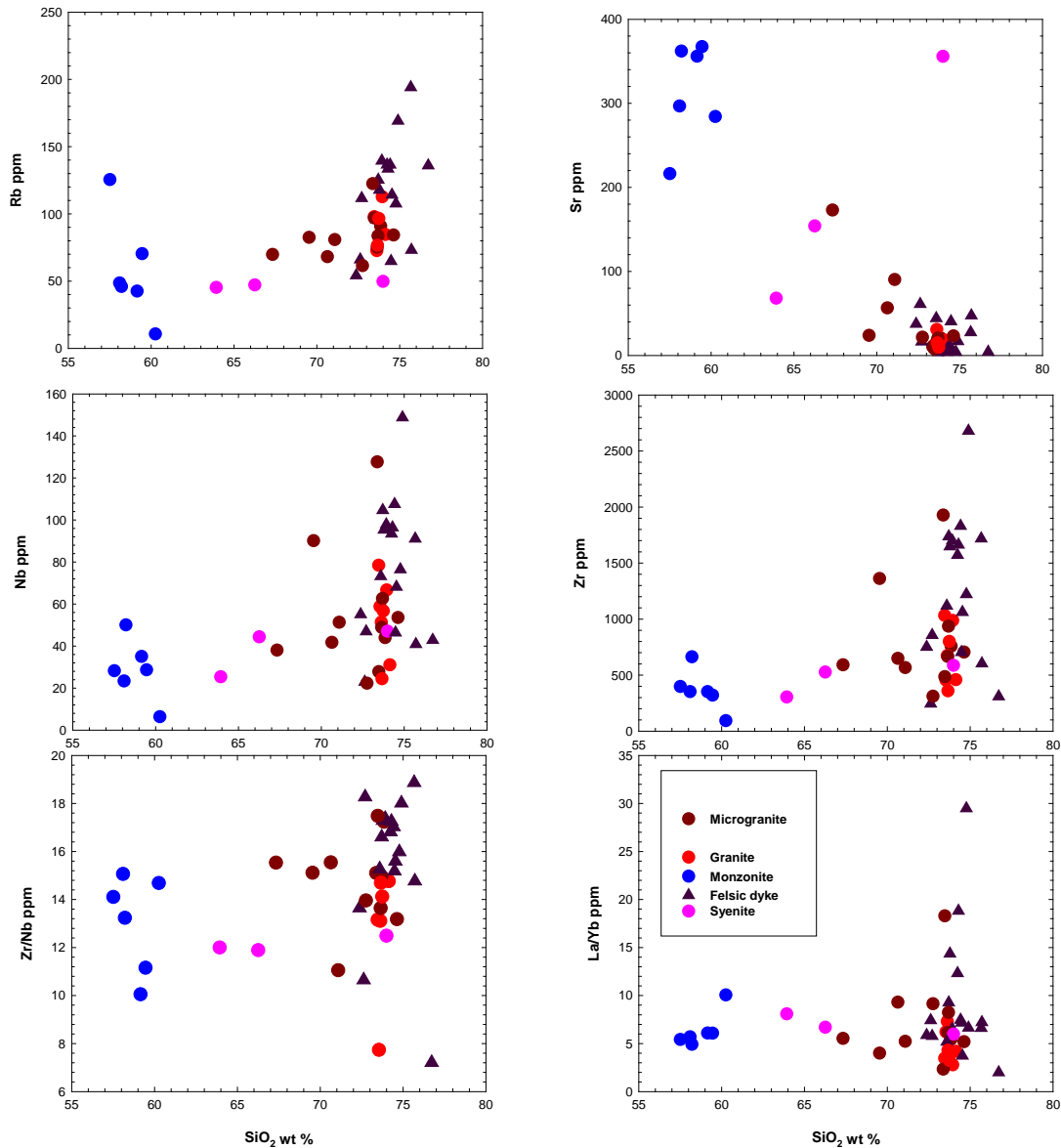
**Figure 4.12:** *Trace element variations for wt% SiO$_2$: (a) Rb ppm vs wt%SiO$_2$ ppm; (b) Sr ppm vs wt% SiO$_2$, (c) Nb vs wt% SiO$_2$; (d), Zr ppm vs wt% SiO$_2$, (e) Zr/Nb ppm vs Wt%SiO$_2$ ppm, (f) La/Yb ppm vs wt%SiO$_2$*
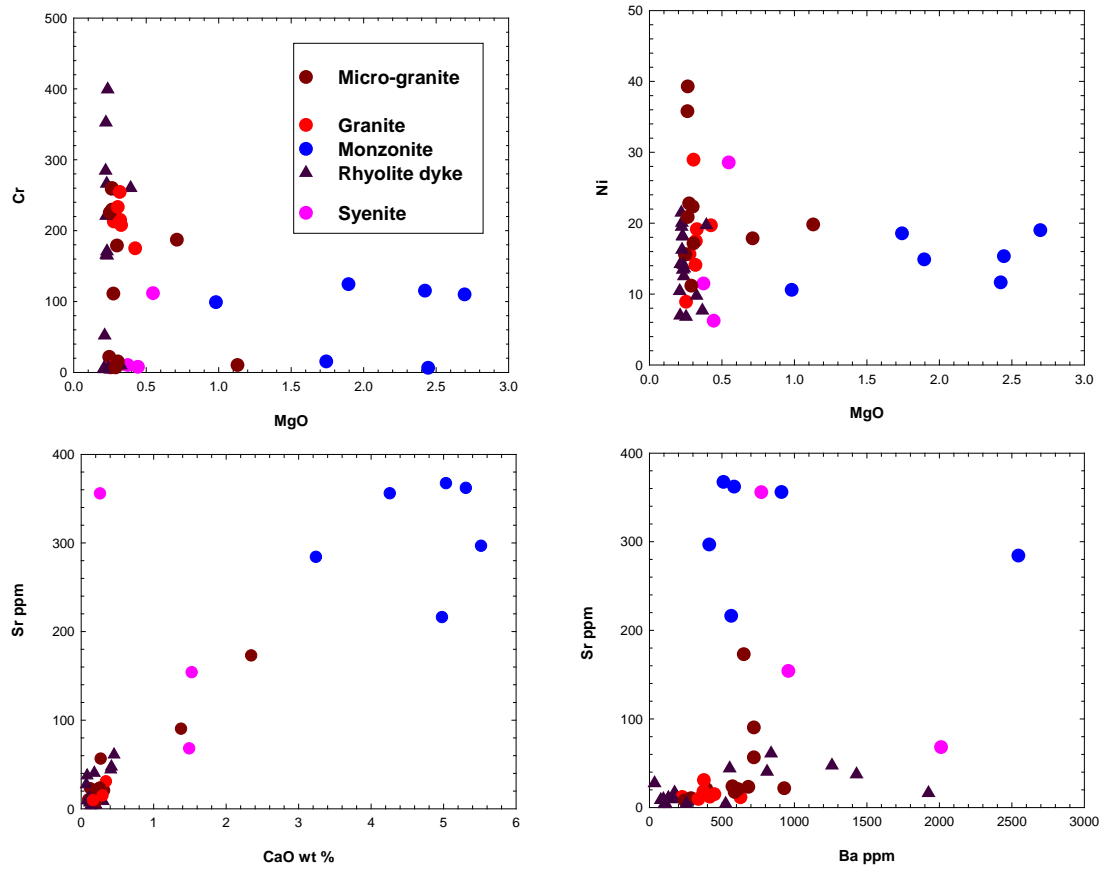
**Figure 4.13:** *Trace element variations for felsic rocks: (a) Cr ppm vs wt% MgO; (b) Ni ppm vs wt% MgO, (c) Sr vs wt% CaO; (d) Sr ppm vs Ba ppm.*
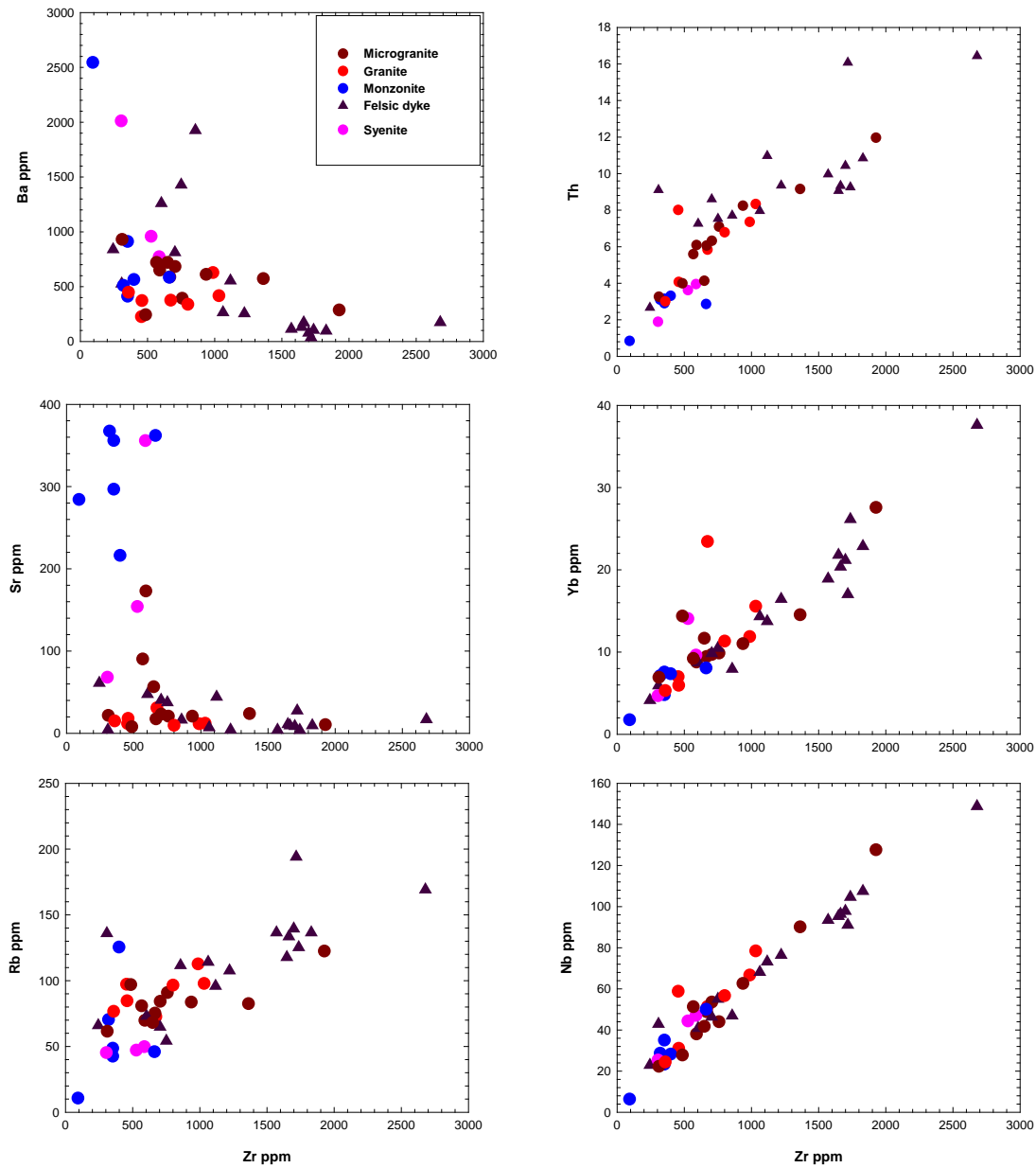
**Figure 4.14:** *Trace element variations against Zr (ppm) : (a) Ba ppm vs Zr ppm; (b) Th ppm vs Zr pmm, (c) Sr ppm vs Zr ppm; (d) Yb ppm vs Zr ppm, (e),Rb ppm vs Zr ppm, (f) Nb ppm vs Zr ppm*
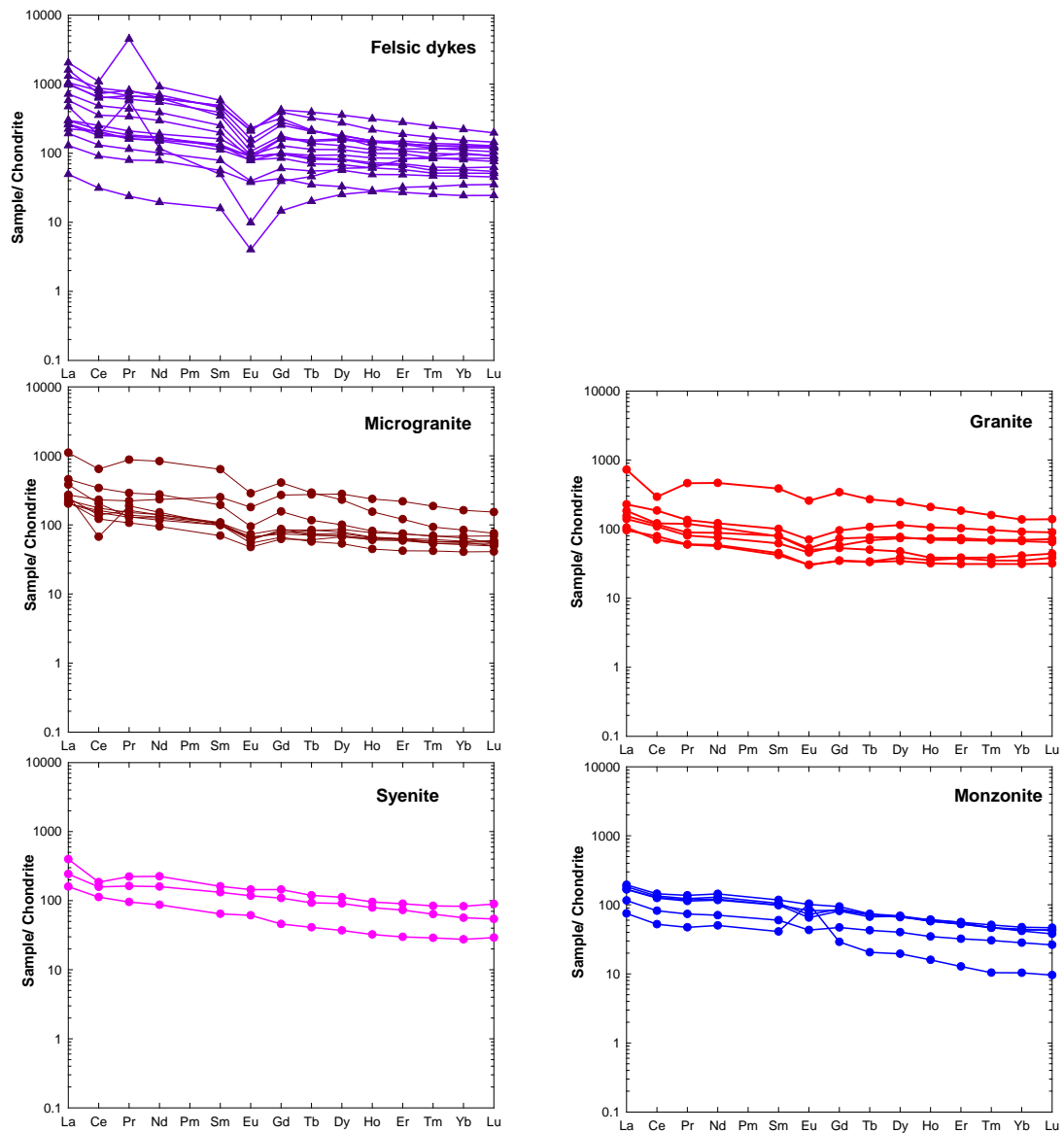
**Figure 4.15:** *Chondrite-normalized REE diagrams for monzonite, syenite, micro-granite, medium-coarse grained granite and rhyolite dyke samples. Chondrite normalization factors taken from Sun & McDonough (1989)*
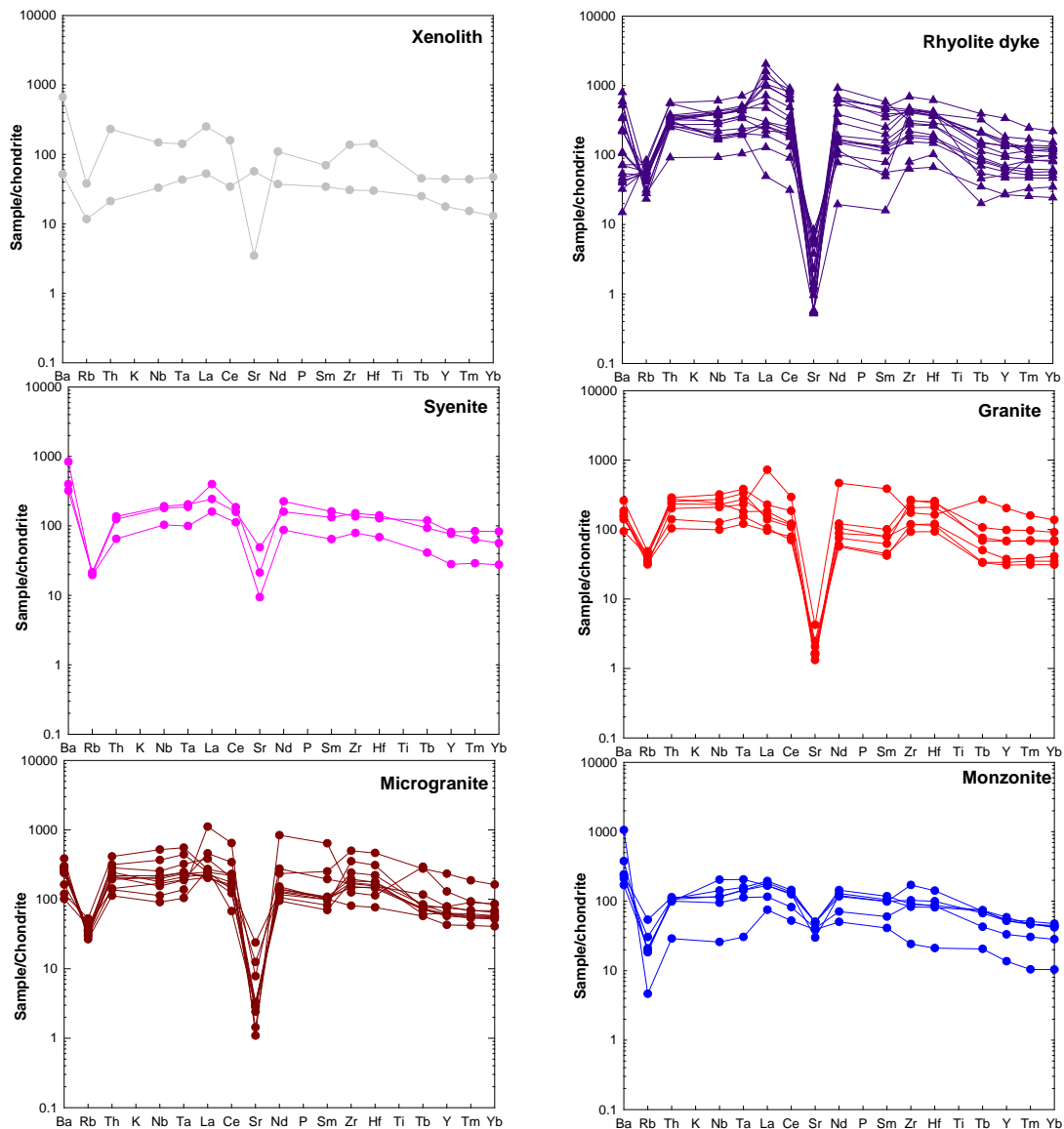
**Figure 4.16:** *Primitive-mantle-normalized spider diagrams for monzonite, microgranite, syenite, granite, rhyolite dykes and xenolith. Primitive-mantle normalization factors taken from Sun & McDonough (1989)*

## 4.5. Radiogenic isotopes

Radiogenic isotopes were determined on a selected sub-set of the Ambohiby Complex rocks to try to further constrain the age of the rocks and to constrain petrogenically their magmatic sources. Strontium and neodymium isotopes were selected for radiogenic analysis, since the Ambohiby Complex contains rocks that range from basic to intermediate in composition. 21 samples represented all five main rock types from the complex. The resultant strontium and neodymium is represented in Appendix1.5

### 4.5.1 Processing of Sr and Nd Isotope Data

The age of the rocks and their initial Sr and Nd isotope values were obtained using isochron plots and from the measured $^{87}Sr/^{86}Sr$ values, $^{87}Rb/^{86}Sr$ values were calculated using the equation:

$$^{87}Rb/^{86}Sr = (Rb/Sr) x (Ab^{87}Rb x WSr)/(Ab^{86}Sr x WRb) \qquad \text{Eq 1}$$

where $(Rb/Sr)$ is the ratio of the concentration of Rb and Sr in ppm in the rock, $Ab^{87}Rb$ is the atomic abundance of the $^{87}Rb$ isotope equal to 0.27835, $WSr$ is the atomic weight of Sr for the sample assuming the atomic mass of $^{84}Sr$ = 83.9134, $^{86}Sr$ = 85.9092, $^{87}Sr$ = 86.9088 and $^{88}Sr$ = 87.9056 amu and that the $^{86}Sr/^{88}Sr$ and $^{84}Sr/^{88}Sr$ ratios are equal to 0.119 and 0.006756 respectively (Faure, 1986).

The age of the rock samples was determined using the program Isoplot (Ludwig, 2008) and the measured $^{87}Sr/^{86}Sr$ values and the calculated $^{87}Rb/^{86}Sr$ values. Errors were calculated using the $2\sigma$ error values from the mass spectrometry for the measured $^{87}Sr/^{86}Sr$ values.

Initial $^{87}Sr/^{86}Sr$ values were determined using the equation

$$(^{87}Sr/^{86}Sr)_m = (^{87}Sr/^{86}Sr)_i + {}^{87}Rb/^{86}Sr(e^{\lambda t}-1) \qquad \text{Eq 2}$$

Where $m$ is the measured $^{87}Sr/^{86}Sr$ value, $i$ is the initial $^{87}Sr/^{86}Sr$ values, $\lambda$ is a constant with the value 1.42 x 10$^{-11}$ (Steiger and Jager, 1977) and $t$ is the age of the rocks. Initial values were calculated using two different ages since the Ambohiby Complex has not been conclusively dated. One is an age of 88 Ma which is derived from an Rb-Sr date on the Ambohitrosy Complex in the NW of Madagascar (Rasolofomanana, 1998). The other is an age of 90 Ma which is based on the Rb-Sr isochron determined in this study. These ages are consistent with a progressive breakup of Madagascar from India and extended

movement of Madagascar over the Marion Hot Spot plume for in excess of 30Ma as has been proposed by Torsvik *et al*. (1998) and Seward *et al*. (2004). The significance of these ages is discussed in more detail in chapter five

### 4.5.2. Results

*4.5.2.1 Isochron plots and the age of the Ambohiby Complex*

All selected plutonic subset of samples were plotted on the Rb-Sr isochron and yield an age of 90.0±2.4 Ma, Initial $^{87}Sr/^{86}Sr$ of 0.70376±0.00039and Mean Squared Weighted Deviates (MSWD) = 0.95 (Fig.4.17). The basalt and rhyolite dykes were excluded since the field relations have shown that the dykes mainly crosscut major rock types of the complex, indicating they are much younger than the main rock types of the complex.



Age = 90.0±2.4 Ma
Initial $^{87}Sr/^{86}Sr$ =0.70376±0.00039
MSWD = 0.95
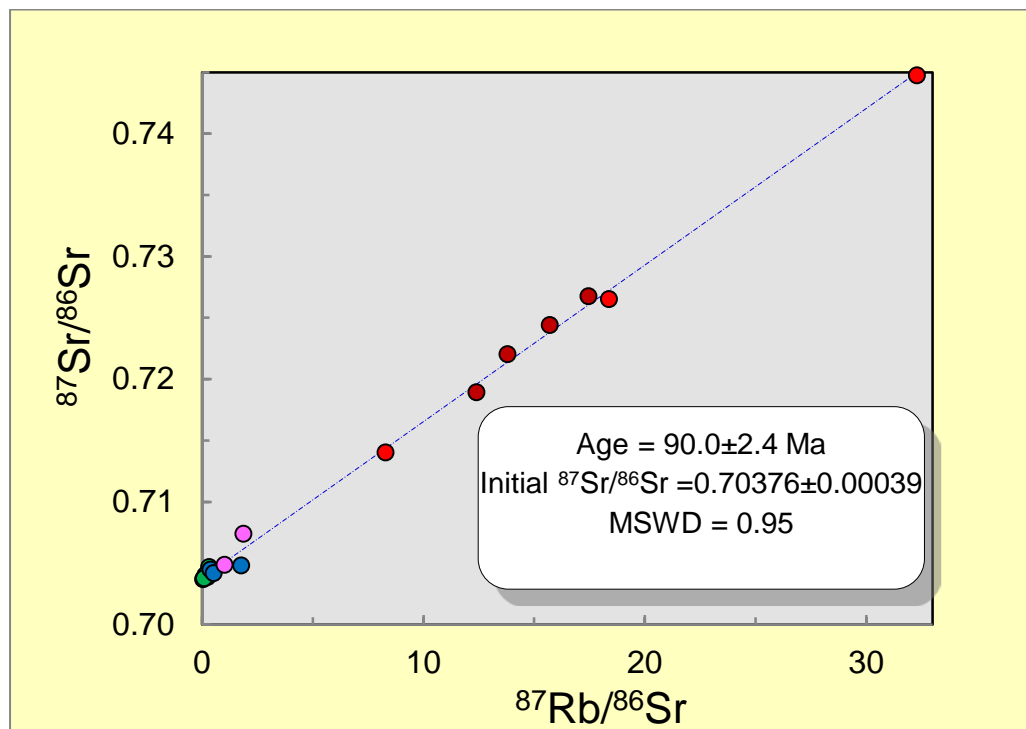
**Figure 4.17:** *Isochron plot for the Ambohiby Complex. The Rb-Sr isochron plot yielded an age of 90.0±2.4 Ma, $^{87}Sr/^{86}Sr_i$ of 0.70376±39 and MSWD = 0.95. Circles with green colour=gabbro; blue circle=monzonite; pink circle=alkali syenite; red circle=granite; and dark red circle= micro-granite. Extrusive samples were not included in this graph (Basalt and rhyolite dyke)*

It was not possible to determine ages using Sm-Nd isochrons because of the very significant errors associated with all isochron constructed (Fig.4.18). The constructed isochron had a very large error and estimated ages varied between 817 and 460Ma. These ages are not considered valid, given the relatively consistent results from Rb-Sr in this Study. Furthermore these ages are not consistent with any ages of the Cretaceous

ring Complexes of Madagascar (e.g. Storey *et al.,* 1995; Melluso *et al.,* 1997; Rasolofomanana, 1998). Although the data was re-analysed the interpretation could not be improved upon. It may be that the Sm-Nd data is being distorted by accessory phases controlling the Sm-Nd budget.
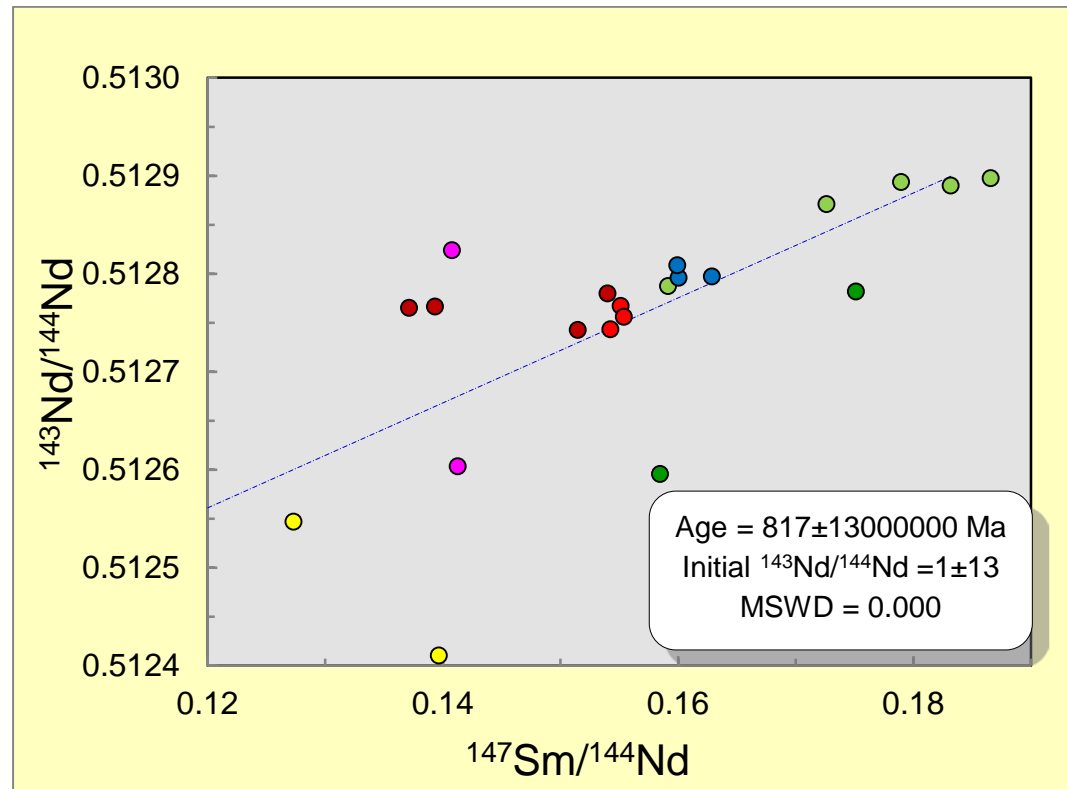


**Figure 4.18:** *Sm-Nd Isochron plot for the Ambohiby Complex. The data give unrealistic ages with high errors. Circles with green colour=gabbro; blue circle=monzonite; pink circle=alkali syenite; red circle=granite; dark red circle= micro-granite; dark green circle=mafic dyke; yellow circle=felsic dyke*

*4.5.2.2 Initial isotope values*

An important feature of the data from this study is that the gabbro show a very little variation in initial $^{143}Nd/^{144}Nd$ ratios (0.51269-0.51279), with $\varepsilon Nd$ values of mantle sources (average $\varepsilon Nd$= +5.83). Initial $^{87}Sr/^{86}Sr$ values are not varied, ranging from 0.70368 to 0.70428. Both the initial $^{143}Nd/^{144}Nd$ values and $^{87}Sr/^{86}Sr$ values of the gabbros samples clearly indicate that they are mantle derived in origin. Mafic dyke samples have a very

wide variation of initial $^{143}$Nd/$^{144}$Nd ratios (0.51250-0.51268) and $^{87}$Sr/$^{86}$Sr values ranging from 0.70626 to 0.71233. One basalt dyke sample sits on the continental crust while the other sample sits on "bulk earth" field.

Monzonite samples show a very little variation in initial $^{143}$Nd/$^{144}$Nd ratios (0.51270), with εNd values of mantle sources (average εNd= +3.49). Initial $^{87}$Sr/$^{86}$Sr values are not varied, ranging from 0.70271 to 0.70401. Alkali-syenite samples, show a very wide variation of initial $^{143}$Nd/$^{144}$Nd (0.51252- 0.51274) and $^{87}$Sr/$^{86}$Sr values are not varied ranging from 0.70378 to 0.70500. The micro-granites show a very little variation in initial $^{143}$Nd/$^{144}$Nd ratios (0.51265) and a wide variation in initial $^{87}$Sr/$^{86}$Sr values ranging from 0.70425 to 0.71123. Three micro-granite samples plot on the upper quadrant of "bulk earth" field, and one micro-granite plot on the depleted mantle enriched field. Granite samples show little variation in $^{143}$Nd/$^{144}$Nd values (0.51265) and have a wide variation in initial $^{87}$Sr/$^{86}$Sr values (0.70547-0.71524). Two granite samples plots on the "bulk earth" field, and one sample plot on the mantle depleted source field. The felsic dyke samples show very little variation in initial $^{143}$Nd/$^{144}$Nd values ranging from 0.5123 to 0.51247, indicating that is from continental crust in origin and has a very wide variation in initial $^{87}$Sr/$^{86}$Sr values (0.71244-0.81650).
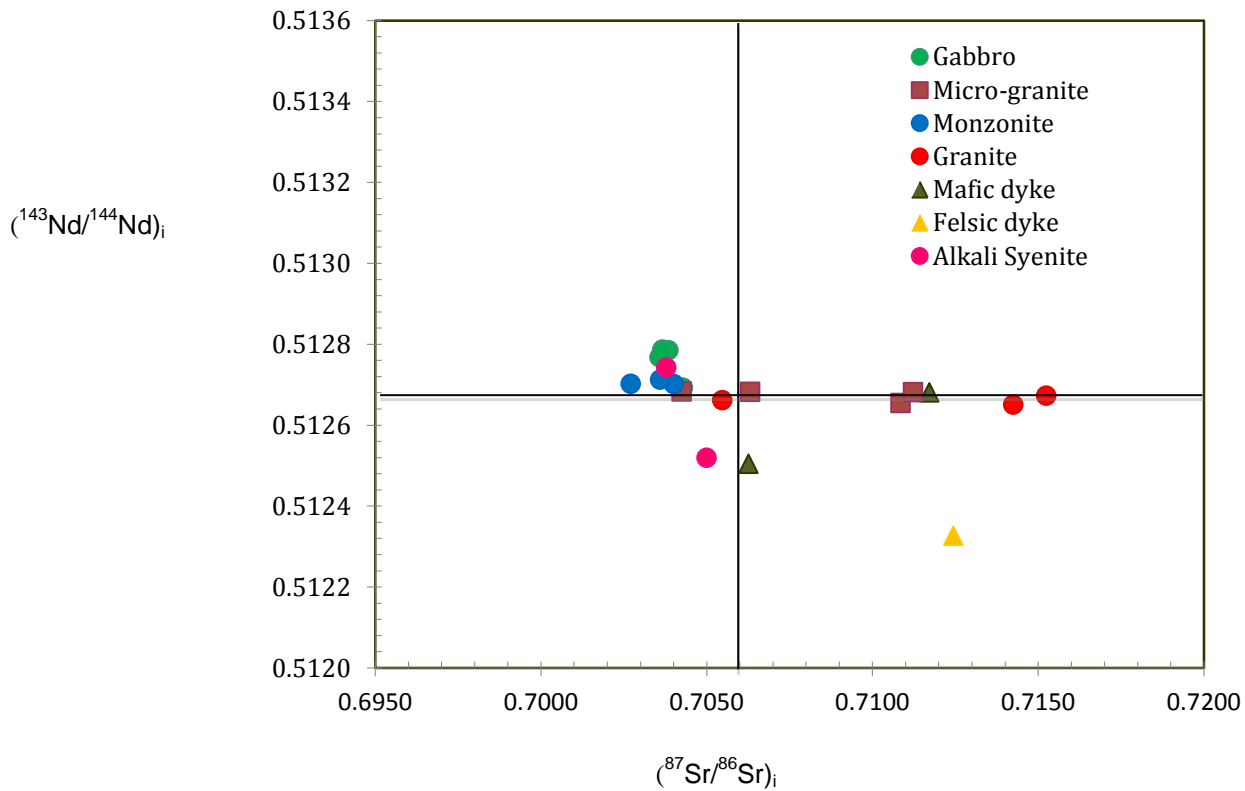
**Figure 4.19:** $^{143}Nd/^{144}Nd$ *vs* $^{87}Sr/^{86}Sr$ *initial isotope correlation diagram showing the relative positions of depleted and enriched mantle sources. The upper left quadrant represent most non-enriched mantle reservoirs while most crustal rocks will plot on the lower right quadrant. The upper and lower crust tends to plot in different positions in the crustal quadrant (from Depaolo and Wasserburg, 1979). The Gabbro and Mozonite samples plot on the upper left quadrant representing that they are mantle enriched, while the granites, mafic and felsic dykes samples plot on the upper right crustal quadrant and lower right quadrant.*

# CHAPTER 5: DISCUSSION

## 5.1 Introduction

The aim of this chapter is to investigate the magmatic source region that led to the formation of the Ambohiby Complex. First, investigate the petrogenetic relationship between different rocks types within the Ambohiby Complex in order to define the magmatic source region. Whole-rock geochemical patterns described in chapter 4, suggest that the Ambohiby rocks may have formed by a fractional crystallization process. All the Ambohiby complex rocks show that there is a constant negative correlation between CaO and $SiO_2$ that suggests fractionation of a mineral such as plagioclase and/or clinopyroxene. $TiO_2$ and FeOt also show decrease with an increase of $SiO_2$ while $Na_2O$ show positive correlations with $SiO_2$ at first and then negative correlations with $SiO_2$. An explanation for this change in correlation could be the start of Fe-Ti oxide fractionation. The fractional crystallization model is best described by the Rayleigh Law and this will be used to test if the most primitive Ambohiby Complex rocks (gabbros) can be used to produce the felsic end members (granites). In addition an assimilation-fractional crystallization (AFC) model (Bowen, 1928; DePaolo, 1981) will be used to test if the Ambohiby Complex rocks were contaminated by wallrock during their formation.

## 5.2 Comparisons of the Ambohiby complex with other Madagascan complexes

The Ambohiby is here compared to other Cretaceous Complexes on Madagascar to understand how its geochemical evolution compares to them. The following Cretaceous

complexes were selected for comparison with the Ambohiby Complex: Volcan de l'Androy Complex (Storey *et al.,* 1997, and Mahoney *et. al.,* 2008), the Antampombato-Ambatovy Complex (Melluso *et al.,* 2003 and Melluso *et al., 2005*), the Mailaka Complex (Melluso *et al.,* 2003), the Morondava volcanic province (Bardintzeff *et al.,* 2001), and the Tamatave sector (Melluso *et al.,* 2003). The Volcan de l'Androy is situated in the south eastern part of the island. The Antampondato-Ambatovy is located in the central eastern part of the island, and the Mailaka intrudes into the sedimentary rocks of the Morondava basin (Melluso et al., 2003) in the central western part of the island. The Morondava volcanic province is located in the south west of the island and the Tamatave located in the central eastern part of Madagascar (see Fig. 5.1). Selected major and trace elements from all the above-mentioned complexes of Madagascar and the Ambohiby Complex are shown in Figure 5.2, 5.3 and 5.4. Sr and Nd isotopes of the Ambohiby Complex, Antampondato-Ambatovy, Volcan de l'Androy and Mailaka Complex are shown in Figure 5. 5.
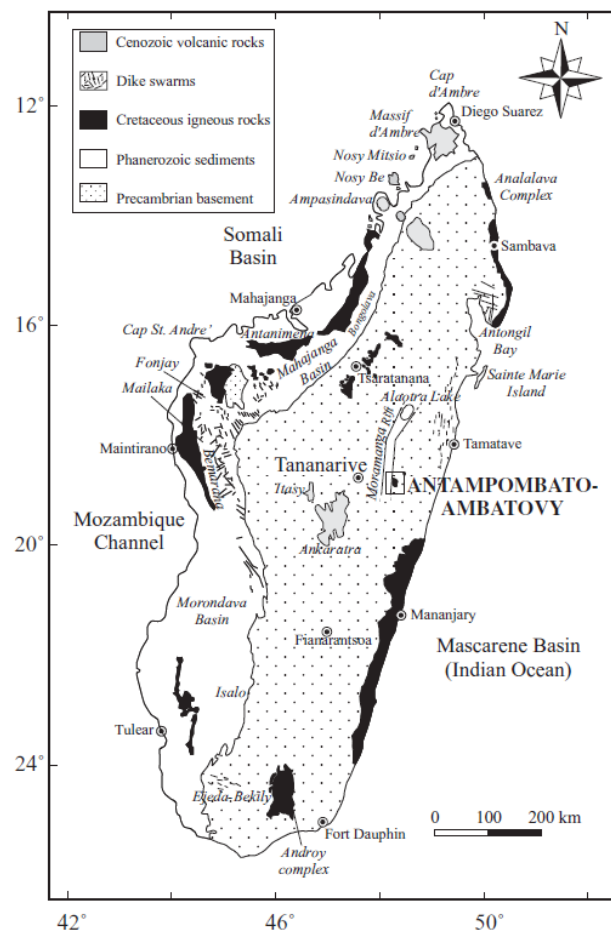


**Figure 5.1:** *Map of Madagascar showing the locations of Cretaceous igneous rocks. Modified after Melluso et al., 2005.*

### 5.2.1 Major and trace elements

The Ambohiby Complex, Volcan de l'Androy and, Antampombato-Ambatovy complex show very similar trends of decreasing CaO and MgO against $SiO_2$ (Fig 5.2). The Antampombato-Ambatovy Complex shows a similar trend to that seen in the Ambohiby Complex except that the Antampombato-Ambatovy Complex has more mafic rock samples with higher MgO and lower $SiO_2$ wt. % concentration than the Ambohiby Complex. The Morondava and Mailaka also shows a negative correlation between MgO and $SiO_2$, while Tamatave do not show much variation (Fig. 5.2). The decrease of CaO against $SiO_2$ can be explained by fractionation of plagioclase and clinopyroxene, which may also account for the negative Eu anomaly (Fig 4.15 & 16). For $TiO_2$ vs $SiO_2$ the Ambohiby Complex first shows a positive trend then a negative trend at approximately 55% $SiO_2$. The Mailaka and Morondava show positive trends of $TiO_2$ against $SiO_2$. $Al_2O_3$ vs $SiO_2$ shows the Ambohiby Complex has a decrease of $Al_2O_3$ as $SiO_2$ increases which levels out to a gentler slope at approximately 50% $SiO_2$, and then a slight increase of $Al_2O_3$ concentrations as $SiO_2$ increase, followed by a steep decrease at approximately 65% $SiO_2$. $Al_2O_3$ as silica increases suggests evolution by fractional crystallisation. The compositional similarities between Ambohiby and Volcan de l'Androy suggest that they were formed by similar magmatic processes. Though both complexes are geographically located far from each other with the Volcan de l'Androy located in the Southern tip of the island and Ambohiby Complex in the central part of the island, both shared similar geochemical characteristics.

Trace element variations show similar relationships. Figure 5.3 shows positive trends for Zr plotted against $SiO_2$ for the Ambohiby and Volcan de l'Androy Complex and the Morondava. This is presumably related to both complexes being related to fractionation of the accessory mineral zircon. The Ambohiby Complex, the Volcan de l'Androy Complex and the Antampombato-Ambatovy show increasing Nb as $SiO_2$ increases as well as increasing Rb as Zr increases (Fig.5.4).

**Figure 5.2***: Plots of major elements against SiO$_2$ wt. % for Tamatave, Mailaka, Antampombato-Ambatovy, Mailaka, Volcan de I' Androy, Morandava, and Ambohiby Complex*
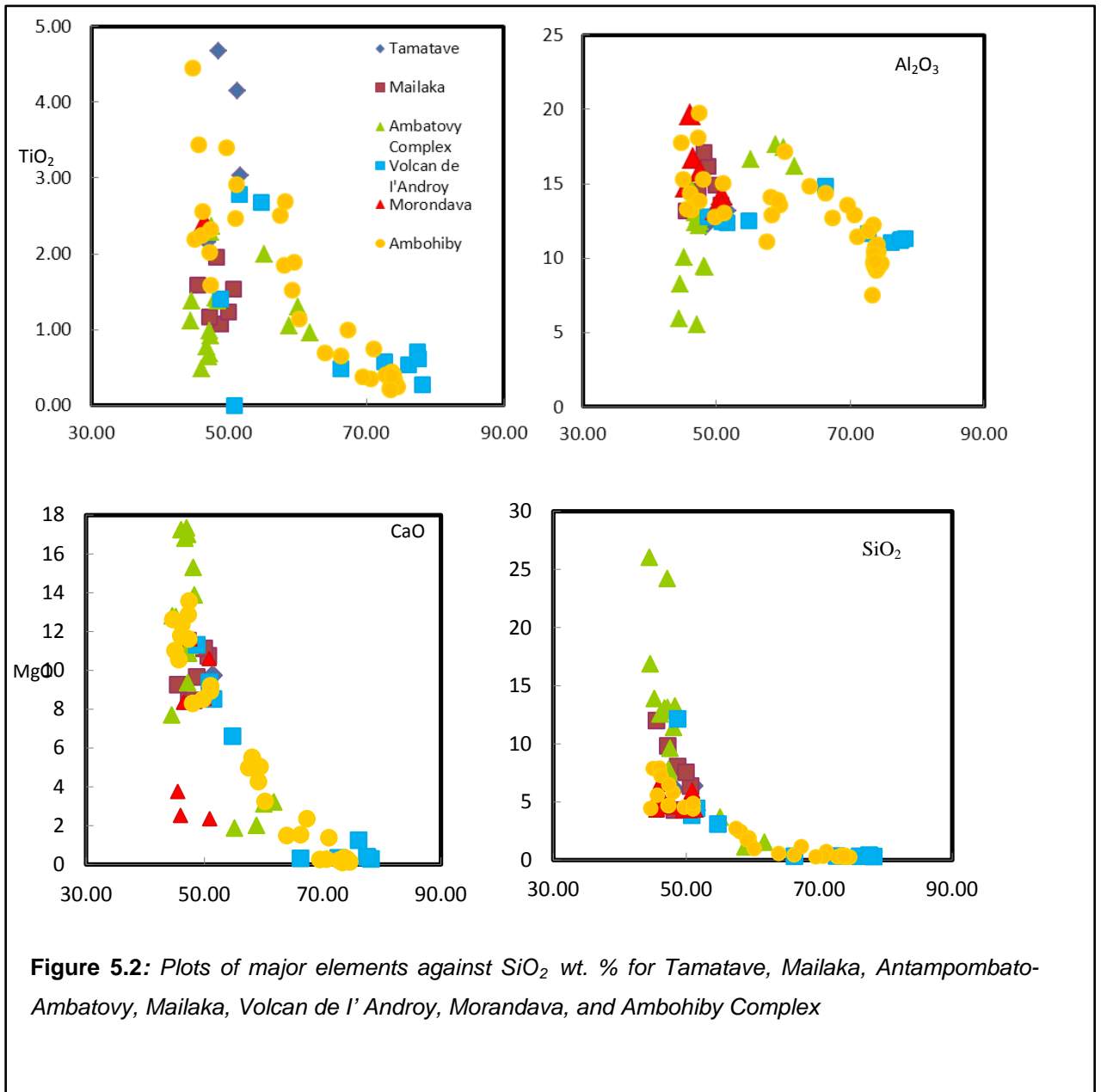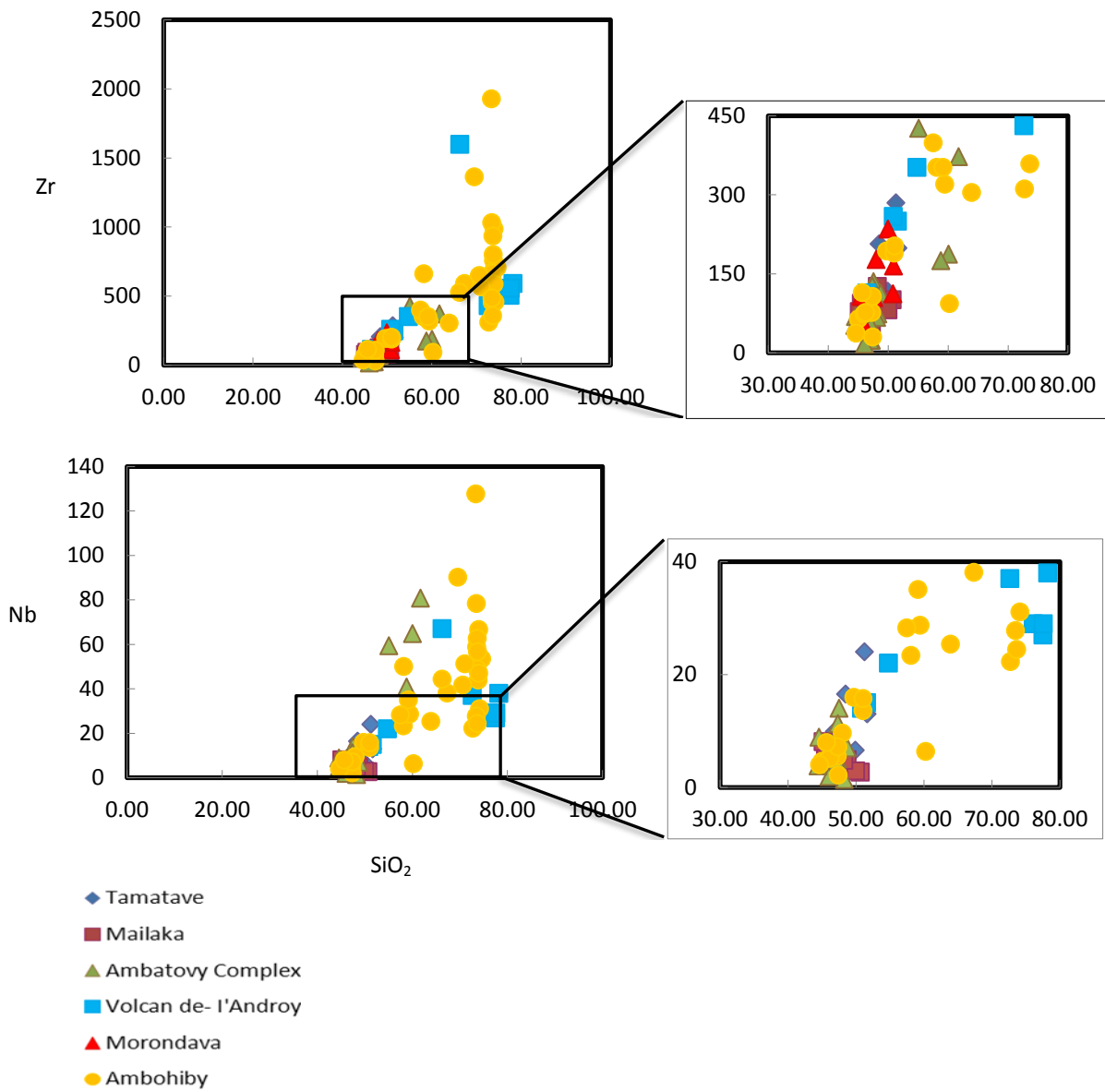
**Figure 5.3:** *Plots of trace elements against SiO$_2$ wt. % and against Zr (ppm) and Nb (ppm) for Volcan de l'Androy Complex, Tamatave, Antampombato-Ambatovy Complex, Mailaka Complex and Ambohiby Complex*
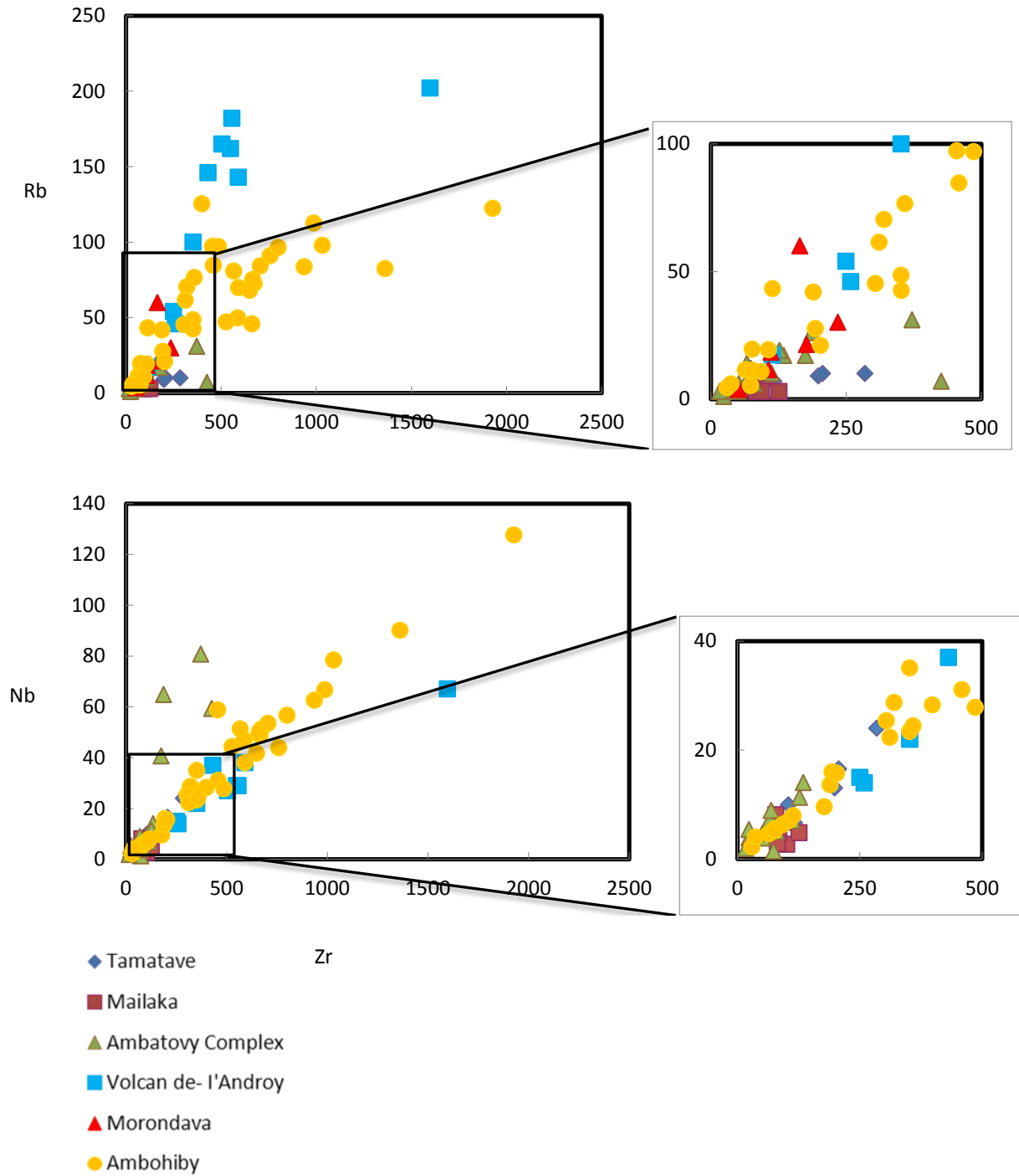
**Figure 5.4:** *Plots of trace element Zr (ppm) against Nb (ppm) and Rb (ppm) for, Volcan de l'Androy Complex, Tamatave, Antampombato-Ambatovy Complex, Mailaka Complex and Ambohiby Complex.*

### 5.2.2 Radiogenic isotopes

Figure 5.5 shows plotted initial Sr ratios against initial Nd values for the following Cretaceous complexes of Madagascar: Ambohiby, Tamatave (Melluso *et al.,* 2003), Mailaka (Melluso *et al.,* 2003), Maningoza Suite (Finkelstein, 2010), Volcan de l'Androy (Mahoney *et al.,* 2008), and Antampombato-Ambatovy Complex (Melluso *et al.,* 2005). Figure 5.5 shows that Antampombato-Ambatovy Complex, Tamatave Complex and the Ambohiby Complex plots within mantle-derived field. The Volcan de l'Androy and Maningoza Suite data shows a much wider variation in Sr and Nd initial ratios from mantle derived field up to bulk earth crust field, which indicates that their formation may have involved crustal contamination. In contrast the Antampomboto-Ambatovy and Ambohiby mafic samples plot within the mantle derived field. Only the mafic and felsic dyke samples of the Ambohiby Complex plot within the bulk earth crustal field, which indicates contamination may have occurred during their formation. The Mailaka plots within the continental crust field.

The Ambohiby Complex is located in the central part of the island and the Ambatovy Complex, located in the south east part of the island but share similar radiogenic isotope signatures indicating no crustal component. In addition both complexes have similar ages for the intrusion. This again supports an interpretation of a common magmatic history. The Volcan de l'Androy Complex and Maningoza suite show a much wider variation of initial Sr and Nd values as compared to the Ambohiby Complex. This suggests that that the Volcan de l'Androy and Maningoza Suite may have shared similar magmatic histories that involved wall-rock contamination during their formation.
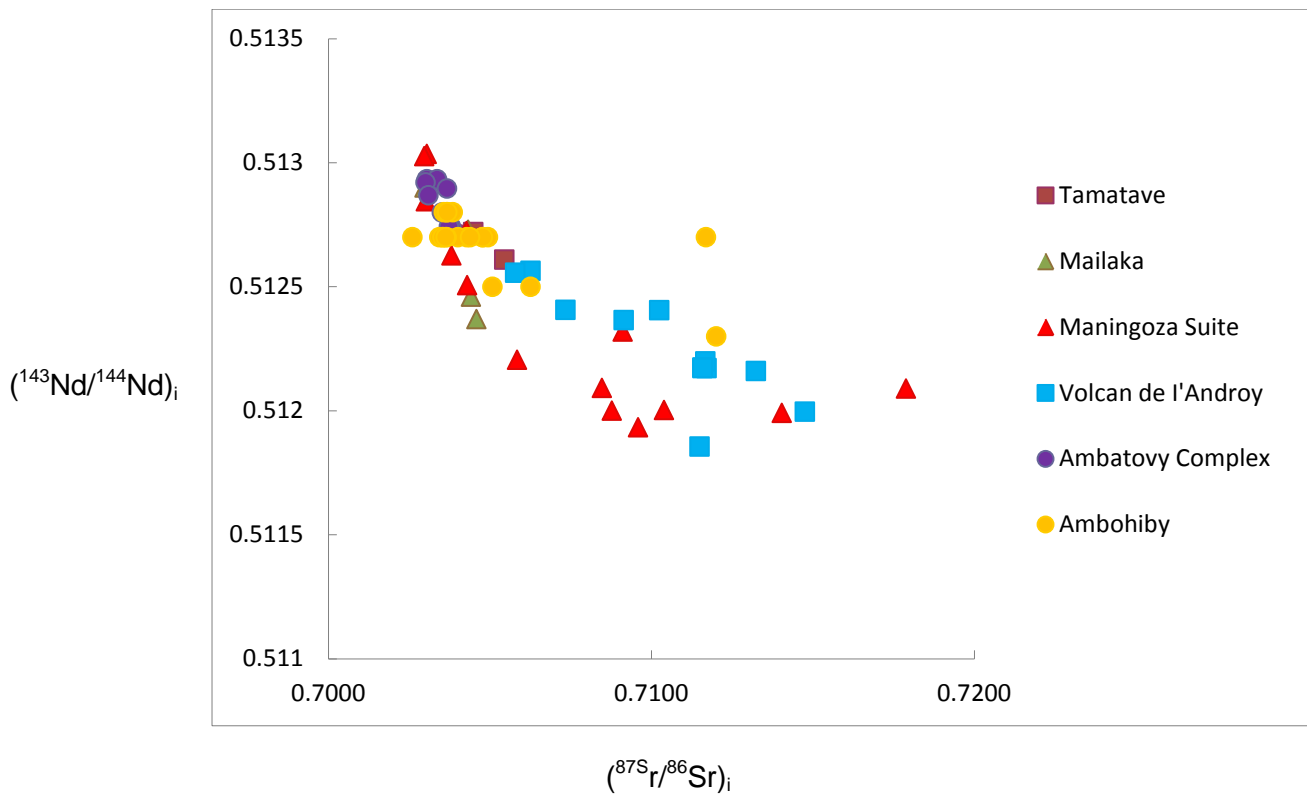
**Figure 5.5:** *Plot of Initial Sr against initial Nd for the Ambohiby Complex, Tamatave complex, Mailaka Complex, and Maningoza Suite*

## 5.3 Comparisons of the Ambohiby Complex with the Marion hotspot Plume

The Ambohiby Complex data is compared to the current Marion Hotspot data collected from Marion Island (Storey *et al.,* 1997). Several of the Madagascan complexes have been compared to Marion Hotspot plume including the Volcan de l'Androy complex, Mailaka, and Tamatave complex (Storey *et al.,* 1997). The importance of this section is to confirm if the Ambohiby complex was formed due to the Marion hotspot, which was underneath the southern tip of the Madagascan plate approximately 90 Ma ago. The location of the Ambohiby Complex is also an important factor when comparing to Marion Hotspot plume, since the Madagascan plate was in motion 90 Ma during the Gondwana break-up. If the Ambohiby complex does have geochemical characteristics similar to those of the Marion Hotspot, this information can be used to infer something about the position of the Marion Hotspot when the Ambohiby was being emplaced.

### 5.3.1 Major and trace elements

Figure 5.6 shows $SiO_2$ against $TiO_2$ and CaO for three Marion data and 15 Ambohiby plutonic rocks samples. Figure 5.6 indicates that the Marion Island data are similar to that of the Ambohiby Complex gabbros and not the Ambohiby Monzonites. Figure 5.7 shows a Chondrite normalized REE diagram of the Ambohiby plutonic rocks and the Marion data. The REE concentrations are variable with gabbro having the lowest Chondritic values below 100xchondrite, and the Marion data show a trend of high concentrations of LREE and then low HREE concentrations. The Marion data and the Ambohiby gabbros exhibit similar HREE trends (Fig.5.7). The monzonite, alkali syenite, and granites have REE concentrations above 100xchondritic values. The micro-granites and granites show depletion of Eu, indicative of plagioclase fractionation. Monzonite, alkali syenite, microgranite and granite display a slight decrease of HREE on the Chondrite normalized diagram compared to the LREE concentrations.
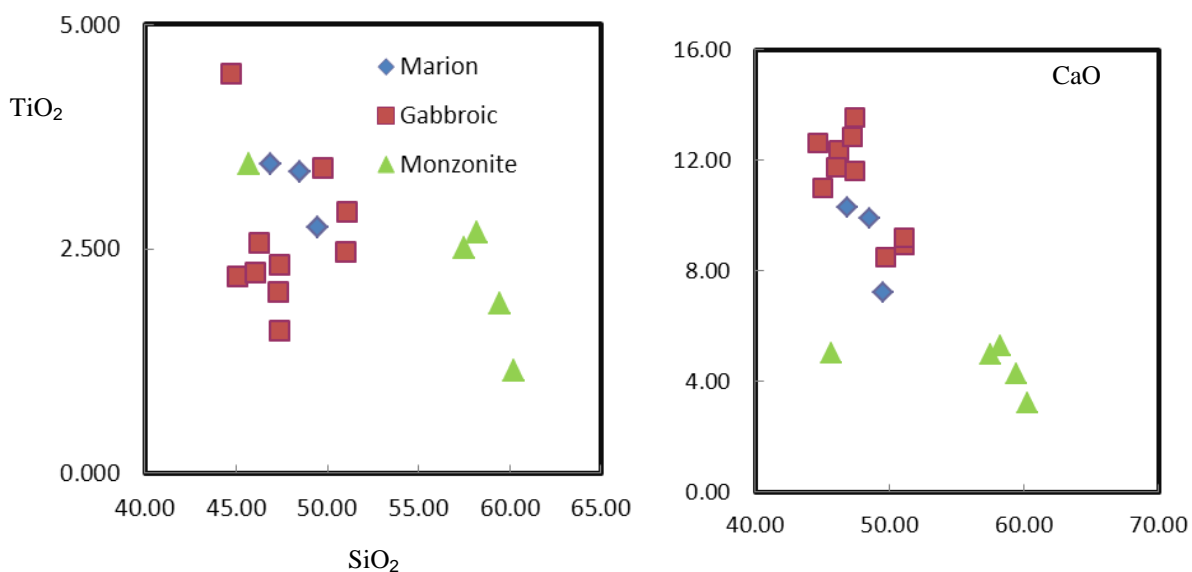


**Figure 5.6:** *Major element variation diagrams: (a) CaO, and $TiO_2$ for marion, and Ambohiby gabbroic and monzonite sampels*
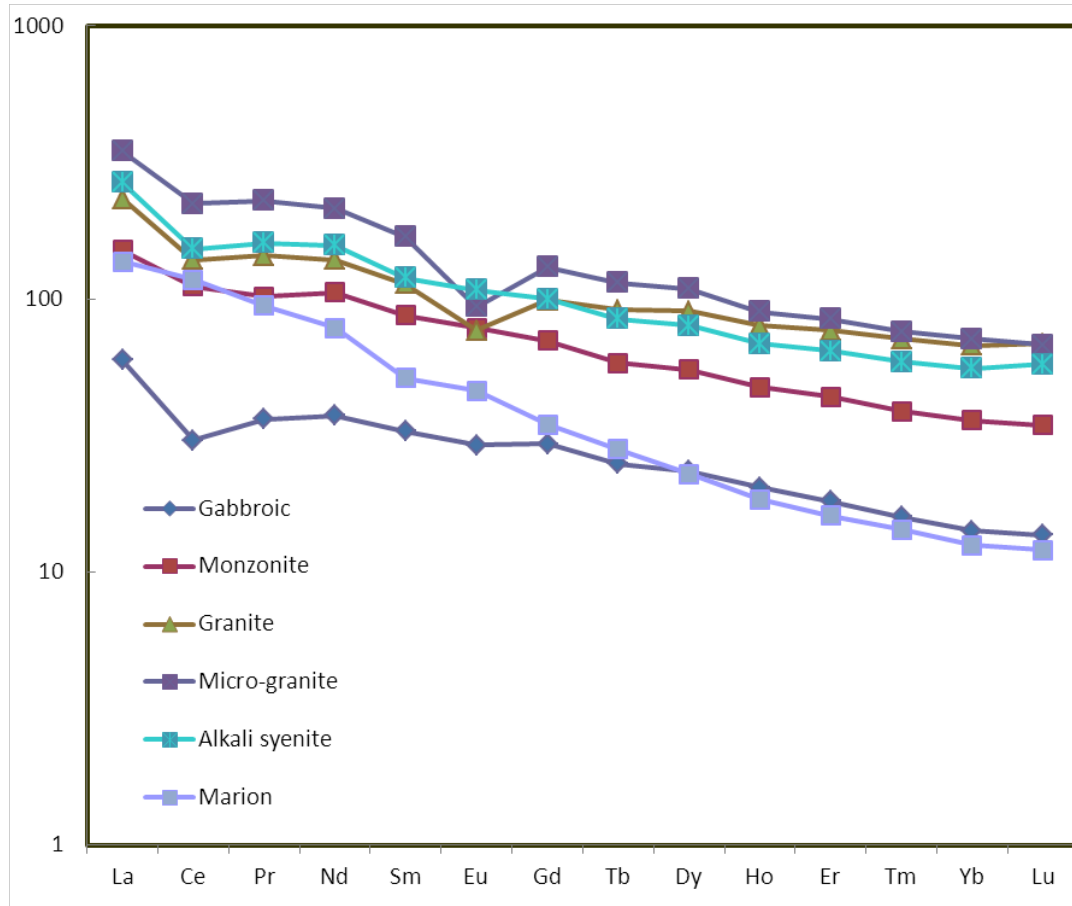
**Figure 5.7:** *Chondrite-normalized REE diagram for Marion, and Ambohiby Complex plutonic rocks-Gabbro, monzonite, alkali-syenite, microgranite and granite. Chondrite normalization factors taken from Sun & McDonough (1989)*

Figure 5.8 shows primitive-mantle-normalized spider diagram for the Marion and Ambohiby plutonic rocks. All of the Ambohiby rocks show Sr depletion while Marion samples do not show any depletion of Sr and display positive Nd anomalies. All Ambohiby plutonic rocks also display positive Nd anomalies. Both Marion and Ambohiby Complex gabbroic samples show a steep slope depletion of HREE on the primitive-mantle normalized diagram. This may indicate that both Marion and the gabbroic samples shared similar mineral background that consumed all the HREE in the melt, possibly garnet since it is compatible with HREE
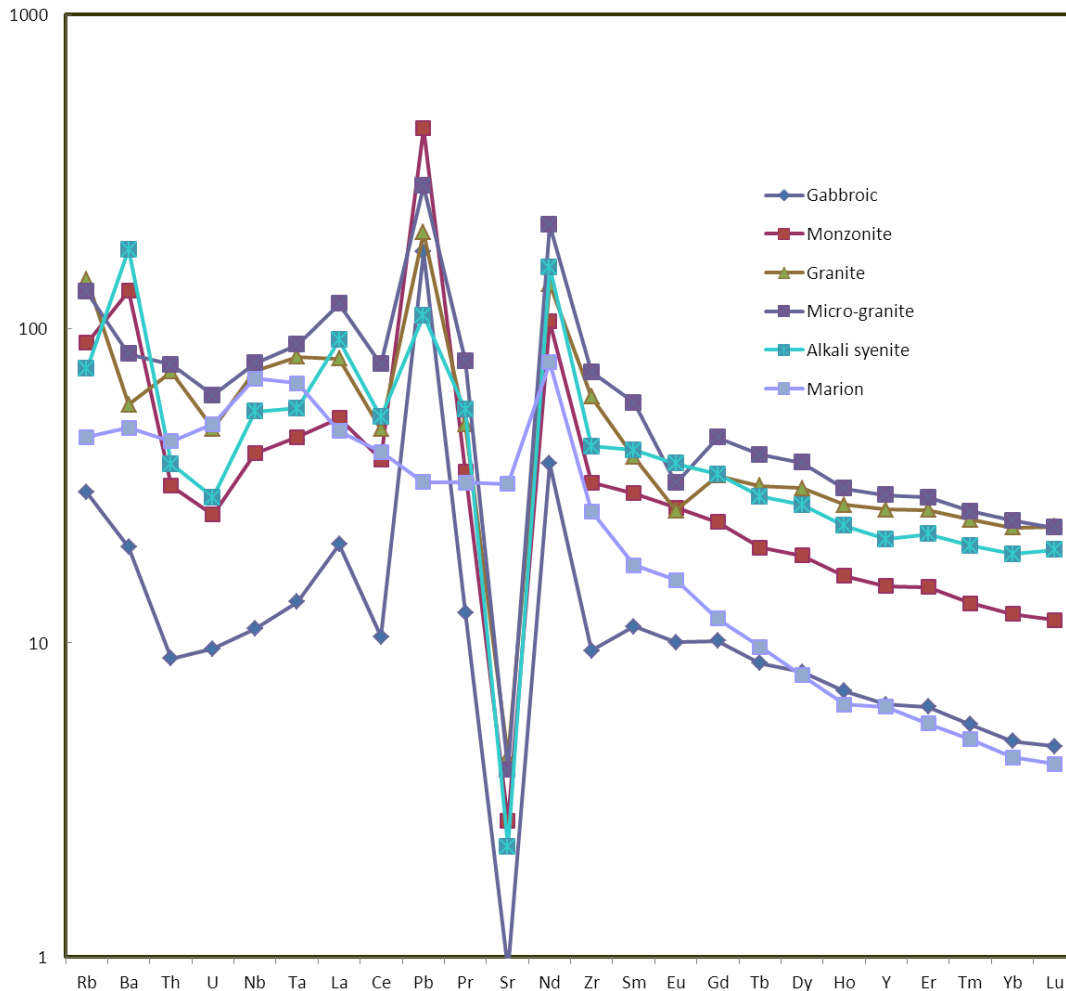
**Figure 5.8:** *Primitive-mantle-normalized spider diagrams for Marion, and Ambohiby plutonic rocks i.e. gabbro, monzonite, granite, syenite, and xenolith. Primitive-mantle normalization factors taken from Sun & McDonough (1989)*

### 5.3.2 Radiogenic isotope

Figure 5.9 shows plotted initial Sr and Nd ratios for the Ambohiby rocks as well as the Marion data (Storey *et al.,* 1997). Figure 5.9 show that the Marion data has high initial Nd values (0.512935) as compared to the Ambohiby rocks (ranging from 0.51240-0.51280). The gabbro and monzonite samples of the Ambohiby Complex show a very little variation in initial Nd and Sr ratios and plot in the mantle enriched field. The alkali-syenite samples show a very wide variation of initial Nd (0.512604- 0.51282) and less varied initial Sr values. Two micro-granite and granite samples plot in the crustal fields, while only one sample of both micro-granite and granite plot on the mantle enriched field**.** The samples on the crustal field may have been contaminated by surrounding rocks during their

formation. Both mafic and felsic dykes plot on the crustal field, indicating contamination during their formation.
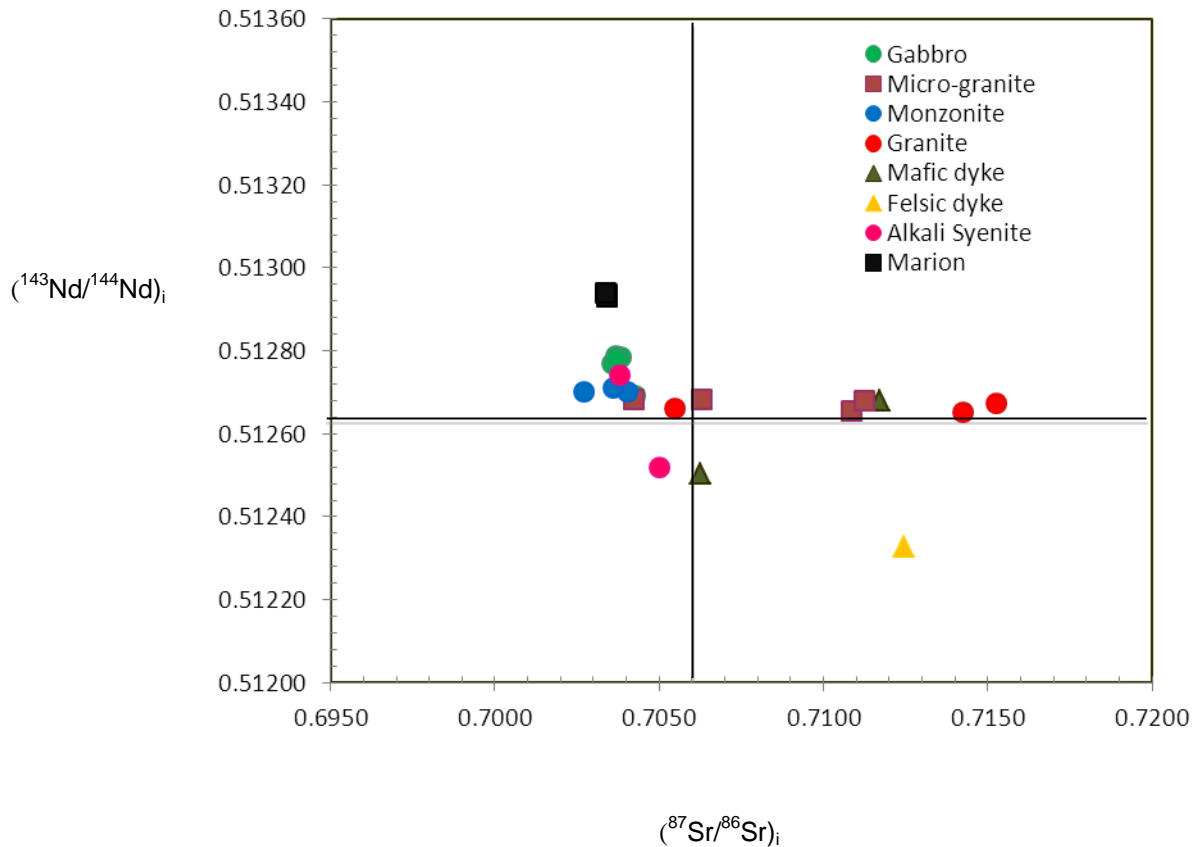


**Figure 5.9:** $^{143}Nd/^{144}Nd$ vs $^{87}Sr/^{86}Sr$ *initial isotope correlation diagram showing the relative positions of depleted and enriched mantle sources. The upper left quadrant represent most non-enriched mantle reservoirs while most crustal rocks will plot on the lower right quadrant. The upper and lower crust tends to plot in different positions in the crustal quadrant (from Depaolo and Wasserburg, 1979). The Marion data plot on the upper left quadrant representing that they are the most mantle enriched samples. Gabbro and Mozonite samples also plot on the upper left quadrant representing that they are mantle enriched, while the micro-granite, mafic and felsic dykes samples plot on the upper right crustal quadrant and lower right quadrant*

## 5.4 Summary

Although the Ambohiby Complex is geographically located in the central part of the island and the Volcan de l'Androy located in the southern part of the island as well as Antampombato-Ambatovy Complex located in central eastern part of the island, all three have similar geochemical characteristics. This suggests that all three complexes may have shared a common magmatic source. The tectonic reconstruction model of Storey *et al.,* (1995) suggests that the Marion Hotspot plume was underneath the southern tip of Madagascan plate between 120-90 Ma ago, which then led to the formation of the Volcan de l'Androy at 88 Ma. The Rb-Sr data of the Ambohiby Complex gave an age of 90±2.4 Ma for the intrusion, meaning that the Ambohiby Complex and the Volcan de l'Androy Complex are 2±2.4 Ma age apart, which also confirms that they may have shared the same magmatic source, possible Marion Hotspot plume. Based on the Chondrite normalized diagram (Fig.5.7) both the Ambohiby gabbroic samples and the Marion Hotspot data do show similar trend of HREE depletion. However there are significant differences in the LREE with the Marion Hotspot being more LREE enriched. From the major and trace geochemistry it is thus inconclusive as to the involvement of the Marion Hotspot in the formation of the Ambohiby Complex

## 5.5. Modelling

To better understand the petrogenesis of the Ambohiby Complex, modelling of the geochemical compositions was undertaken to see how the different rocks types are related to one another and what if any relationship there is to the Marion Hotspot Plume. The following models were considered: (1) a fractional crystallization model using trace and REEs; and (2) an assimilation and fractional crystallization (AFC) model using radiogenic isotopes.

### 5.5.1 Fractional Crystallization model

The amount of fractional crystallisation is investigated by the use of trace and rare earth elements. The actual trace element concentration of the most primitive rock sample of the Ambohiby Complex is used to estimate the felsic end member of the complex (granite) using an assumed mineral assemblage and appropriate partition coefficients. The partition coefficients for fractional crystallization model are shown in Table 5.1. Two mineral compositions were considered, one that involves olivine and one that does not. Olivine was not seen in thin-sections of the Ambohiby Complex mafic rocks but a model that includes a small amount of olivine appears to give a better fit to the trace element data. These two models are described and discussed below.

#### *5.5.1.1 Fractional crystallisation not involving olivine*

The bulk partition coefficient was calculated using the minerals clinopyroxene (45%), plagioclase (40%), phlogopite (10%) and magnetite (5%) and the partition coefficients given in Table 5.1. This mineral assemblage is based on the actual mineral concentrations in the most primitive gabbroic rock sample of the Ambohiby Complex. The mineral / melt partition coefficient for basaltic liquids were taken from the compilation of Rollinson (1993) using the data of Arth (1976). The following equation was used for calculating the bulk partition coefficient

$$D_i = x_1 Kd_1 + x_2 Kd_2 + x_3 Kd_3 + x_4 Kd_4 \qquad\qquad \text{eq (1)}$$

$D_i$ is the bulk partition coeffient for the element $i$, $x_1$ is the fraction of mineral *"1"* in the fractionating assemblage; $Kd_1$ is the relevant partition coefficient of mineral "*1*"

**Table 5.1:** Mineral partition coefficient for basaltic gabbroic liquid, from Rollinson (1993) and compilation from Arth (1976) and the **D** is the calculated *bulk partition coefficient. The mineral modes are indicated above.*

| Partition Coefficients | Clinopyroxene | Phlogopite | Plagioclase | Magnetite | D |
|---|---|---|---|---|---|
| **Rb** | 0.031 | 3.060 | 0.071 | | 0.380 |
| **Sr** | 0.060 | 0.081 | 1.830 | | 3.359 |
| **Ba** | 0.026 | 1.090 | 0.230 | | 0.511 |
| **K** | 0.038 | | 0.170 | | 0.313 |
| **Y** | 0.900 | 0.030 | 0.030 | 0.200 | 0.111 |
| **Ti** | 0.400 | 0.900 | 0.040 | 7.500 | 0.170 |
| **Zr** | 0.100 | 0.600 | 0.048 | 0.100 | 0.142 |
| **Hf** | 0.263 | | 0.051 | 2.000 | 0.109 |
| **Nb** | 0.005 | 1.000 | 0.010 | 0.400 | 0.100 |
| **Ta** | 0.013 | | | 1.000 | 0.001 |
| **Th** | 0.030 | | 0.010 | | 0.020 |
| **U** | 0.040 | | 0.010 | | 0.021 |
| **La** | 0.056 | | 0.380 | 1.500 | 0.699 |
| **Ce** | 0.150 | 0.034 | 0.120 | 1.300 | 0.231 |
| **Nd** | 0.310 | 0.032 | 0.081 | 1.000 | 0.169 |
| **Sm** | 0.500 | 0.031 | 0.072 | 1.100 | 0.164 |
| **Eu** | 0.510 | 0.030 | 0.340 | 0.600 | 0.655 |
| **Gd** | 0.610 | 0.030 | 0.063 | | 0.154 |
| **Dy** | 0.680 | 0.030 | 0.055 | | 0.144 |
| **Er** | 0.650 | 0.034 | 0.063 | | 0.157 |
| **Yb** | 0.620 | 0.042 | 0.067 | 0.900 | 0.163 |
| **Lu** | 0.560 | 0.046 | 0.060 | | 0.147 |
| **Ni** | 1.500 | | | 29.000 | 0.090 |
| **Co** | 0.500 | | | 7.400 | 0.030 |
| **V** | 1.350 | | | 26.000 | 0.081 |
| **Cr** | 34.000 | | | 153.000 | 2.040 |
| **Sc** | 1.700 | | | | 0.102 |
| **Mn** | 0.300 | | | | 0.018 |

To calculate fractional crystallization the Rayleigh fractionation equation is used

$$C_L/C_0 = F^{(D-1)} \qquad\qquad\qquad eq\ (2)$$

where $C_L$ is the concentration of the element in the liquid, $C_0$ is the concentration of the element in the initial liquid, F is the weight fraction of the remaining liquid, D, is the bulk partition coefficient.

Sample MC7042 was used as representative for the Ambohiby gabbroic rocks in order to complete the calculations for eq (2). After the calculations of the fractional crystallization, the model results of the concentration of the element in the liquid are Chondrite normalized using Sun and McDonough (1989) normalizing values. The results are shown in Figure 5.10 as well as the REE composition of one of the granites. The model seems to be a fairly good fit to the F value of around 0.1 An F value of 0.1 mean that the remaining melt of 10% after 90% fractional crystallization of gabbros has compositions very similar to the Ambohiby Complex. The close correlation based on the REE indicates that fractional crystallization of gabbroic parent magma could account for the range of rock types present in the Ambohiby Complex. The fit for this model improves when olivine is added into the model.
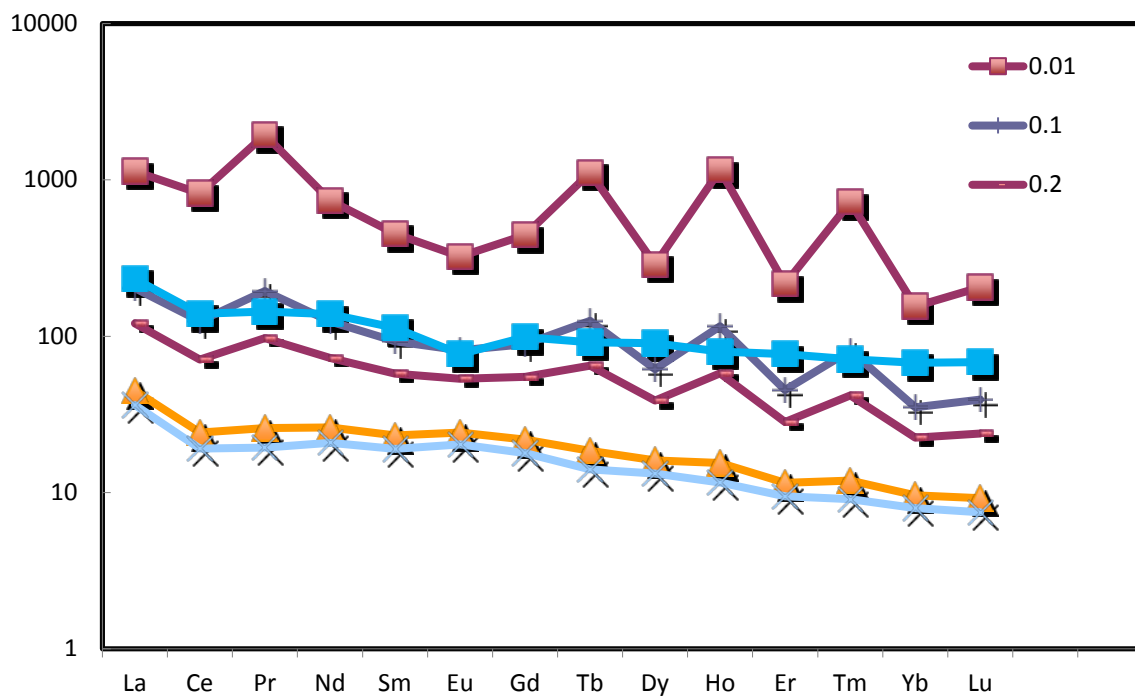


**Figure 5.10:** *REE plot comparing the actual felsic end member of the Ambohiby Complex value and calculated felsic end member using concentrations of La, Ce, Pr, Nd, Sm, Eu, Gd, Tb, Dy, Ho, Er, Tm, Yb and Lu of the following mineral assemblage; clinopyroxene, plagioclase, phlogopite and magnetite*

*5.5.1.2 Fractional crystallisation with olivine*

A second model was tested that includes small amounts of olivine and orthopyroxene in the parental mineral assemblage. The mineral assemblage modelled is plagioclase (66%), clinopyroxene (10%), orthopyroxene (10%), olivine (7%), phlogopite (5%) and magnetite (2%). The partition coefficients for this fractional crystallization model are shown in Table 5.2. Eq (1) for calculating the bulk partition coefficient was used as indicated above. Rayleigh fractionation using equation eq (2) was used to complete the fractional crystallization model calculations. The results for this fractional crystallization model were Chondrite normalised using Sun and McDonough (1989) normalizing values. Figure 5.11 show plots of fractionation at different fractional values as well as the actual felsic end member of the Ambohiby Complex (granite). The model show a very good fit to the F value of around 0.1 This mean that for the Ambohiby Complex gabbros to fractional crystalized minerals similar to those of the felsic end member of the complex, it has to fractionate 90%, and the remaining melt (10%) will have similar felsic end member of the Ambohiby Complex (granite). This model fits very well compared to the fractional crystallization model without olivine. The inclusions of small proportions of olivine, seems to play significant role toward the compositions of felsic end member of the Complex (granites).

**Table 5.2:** Mineral partition coefficient for basaltic gabbroic liquid, from Rollinson (1993) and compilation from Arth (1976) and the **D** is the calculated *bulk partition coefficient.* The mineral modes are indicated above.

| Partition Coefficients | Olivine | Opx | Cpx | Phlogopite | Plagioclase | Magnetite | D |
|---|---|---|---|---|---|---|---|
| Rb | 0.01 | 0.02 | 0.03 | 3.06 | 0.07 | 0.00 | 0.30 |
| Sr | 0.01 | 0.04 | 0.06 | 0.08 | 1.83 | 0.00 | 6.26 |
| Ba | 0.01 | 0.01 | 0.03 | 1.09 | 0.23 | 0.00 | 0.82 |
| K | 0.01 | 0.01 | 0.04 | 0.00 | 0.17 | 0.00 | 0.64 |
| Y | 0.01 | 0.18 | 0.90 | 0.03 | 0.03 | 0.20 | 1.76 |
| Ti | 0.02 | 0.10 | 0.40 | 0.90 | 0.04 | 7.50 | 0.88 |
| Zr | 0.01 | 0.18 | 0.10 | 0.60 | 0.05 | 0.10 | 0.36 |
| Hf | 0.01 | 0.00 | 0.26 | 0.00 | 0.05 | 2.00 | 0.00 |
| Nb | 0.01 | 0.15 | 0.01 | 1.00 | 0.01 | 0.40 | 0.06 |
| Ta | 0.00 | 0.00 | 0.01 | 0.00 | 0.00 | 1.00 | 0.00 |
| Th | 0.00 | 0.00 | 0.03 | 0.00 | 0.01 | 0.00 | 0.09 |
| U | 0.00 | 0.00 | 0.04 | 0.00 | 0.01 | 0.00 | 0.11 |
| La | 0.00 | 0.00 | 0.06 | 0.00 | 0.38 | 1.50 | 1.38 |
| Ce | 0.00 | 0.02 | 0.15 | 0.03 | 0.12 | 1.30 | 0.68 |
| Pr | 0.00 | 0.00 | 0.00 | 0.00 | 0.00 | 0.00 | 0.00 |
| Nd | 0.00 | 0.03 | 0.31 | 0.03 | 0.08 | 1.00 | 0.84 |
| Sm | 0.00 | 0.05 | 0.50 | 0.03 | 0.07 | 1.10 | 1.16 |
| Eu | 0.01 | 0.05 | 0.51 | 0.03 | 0.34 | 0.60 | 2.08 |
| Gd | 0.01 | 0.09 | 0.61 | 0.03 | 0.06 | 0.00 | 1.34 |
| Tb | 0.01 | 0.00 | 0.00 | 0.00 | 0.00 | 1.00 | 0.00 |
| Dy | 0.01 | 0.15 | 0.68 | 0.03 | 0.06 | 0.00 | 1.44 |
| Ho | 0.00 | 0.00 | 0.00 | 0.00 | 0.00 | 0.00 | 0.00 |
| Er | 0.03 | 0.23 | 0.65 | 0.03 | 0.06 | 0.00 | 1.42 |
| Tm | 0.00 | 0.00 | 0.00 | 0.00 | 0.00 | 1.00 | 0.00 |
| Yb | 0.03 | 0.34 | 0.62 | 0.04 | 0.07 | 0.90 | 1.39 |
| Lu | 0.03 | 0.42 | 0.56 | 0.05 | 0.06 | 0.00 | 1.26 |
| Ni | 5.90 | 5.00 | 1.50 | 0.00 | 0.00 | 29.00 | 3.50 |
| Co | 6.60 | 2.50 | 0.50 | 0.00 | 0.00 | 7.40 | 1.51 |
| V | 0.06 | 0.60 | 1.35 | 0.00 | 0.00 | 26.00 | 2.52 |
| Cr | 0.70 | 10.00 | 34.00 | 0.00 | 0.00 | 153.00 | 63.07 |
| Sc | 0.17 | 1.20 | 1.70 | 0.00 | 0.00 | 0.00 | 0.00 |
| Mn | 1.45 | 1.40 | 0.30 | 0.00 | 0.00 | 0.00 | 0.75 |
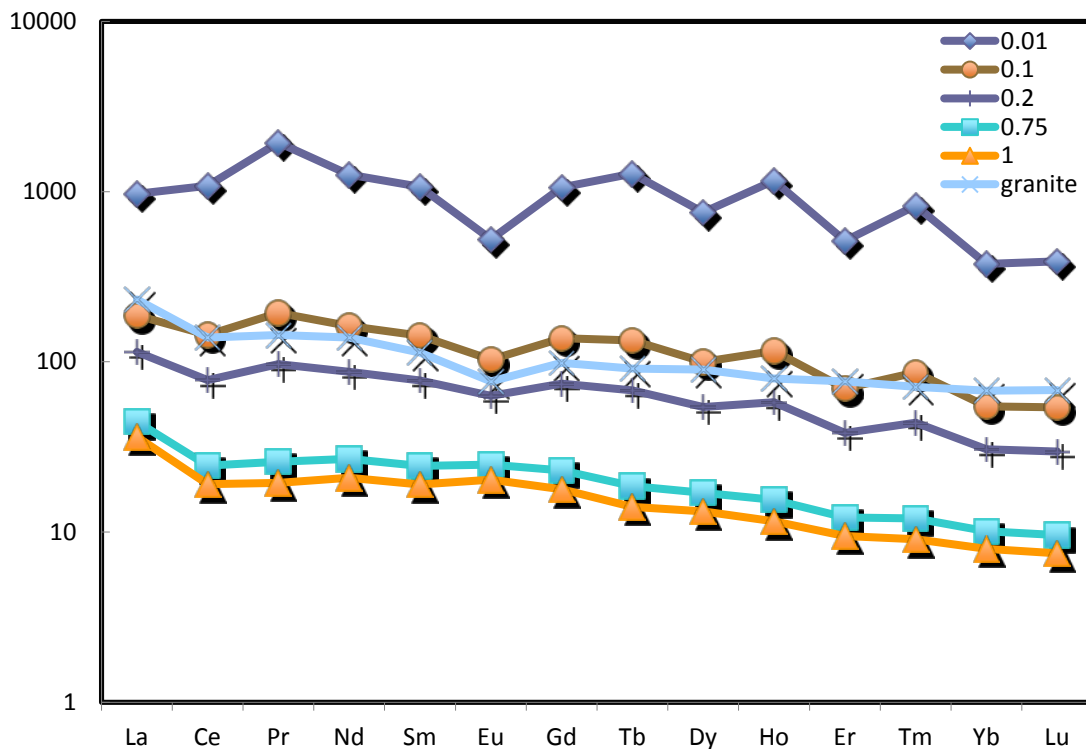
**Figure 5.11** *REE plot comparing the actual felsic end member of the Ambohiby Complex value and calculated felsic end member using concentrations of La, Ce, Pr, Nd, Sm, Eu, Gd, Tb, Dy, Ho, Er, Tm, Yb and Lu of the following mineral assemblage; olivine, orthopyroxene clinopyroxene, plagioclase, phlogopite and magnetite*

### 5.5.2 Assimilation-fractional crystallization (AFC) model

The AFC model is used to test for wall rock assimilation during the formation of the Ambohiby Complex. The Marion hotspot data (Storey *et al.,* 1997) is used as a starting material. Since the Marion Hotspot plume is the most possible magmatic source for this study. Due to lack of available radiogenic isotopes for the surrounding basement gneiss at this study area, several basement gneiss samples were selected from around Madagascar as a representative for the contaminant. The following equations for Sr and Nd ratios were used to determine how much mixing of each isotope ratio was needed to achieve the same values as felsic end members of the complex.

$$\left(\frac{^{143}Nd}{^{144}Nd}\right)_{Mix} = \frac{\left(\frac{^{143}Nd}{^{144}Nd}\right)_A Nd_A f + \left(\frac{^{143}Nd}{^{144}Nd}\right)_B Nd_B(1-f)}{Nd_A f + Nd_B(1-f)} [Eq(3)]$$

$$\left(\frac{{}^{87}Sr}{{}^{86}Sr}\right)_{Mix} = \frac{\left(\frac{{}^{87}Sr}{{}^{86}Sr}\right)_A Sr_A f + \left(\frac{{}^{87}Sr}{{}^{86}Sr}\right)_B Sr_B(1-f)}{Sr_A f + Sr_B(1-f)} \quad [Eq(4)]$$

Equations (3) and (4) are used to calculate the ${}^{143}$Nd/${}^{144}$Nd and ${}^{87}$Sr/${}^{86}$Sr ratios respectively of a mixture (mix) of components A and B where f is the weight fraction with f=1 being only component A and f=0 being only component B (Faure, 1986)

Table 5.3 shows Sr and Nd data for potential contaminants that are Archaean in age and related to Madagascar. Sr and Nd data was taken from Melluso *et al.,* (2001) on the Mailaka area for a Precambrian leucogranite. The Maevatanana gneisses represent the Archaean basement rocks of north-central Madagascar with Sr and Nd data taken from Tucker *et al.,* (1999b). Sr and Nd data for Precambrian rocks of the Indian Dharwar craton and Tanzania craton are included since are the Neoarchaean rocks of the Antananarivo Block and have been suggested to be associated with both of these cratons (Tucker *et al.,* 1999, Kroner *et al.,* 2000, Collins *et al.,* 2000, and Collins and Windley (2002). Sr and Nd data for the Dharwar tronalitic-trondhjemitic-granodioritic (TTG) basement was taken from Jayananda *et al.,* (2000) and data for the Tanzanian craton was taken from Möller *et al.,* (1998). The gneiss and BY6163 samples were taken from Macey (unpublished data) of the North Central Madagascar near the Ambohiby Complex

**Table 5.3:** Selected crustal/basement rocks for AFC model using the Sr and Nd concentrations as well as initial Sr ratios and initial Nd. Initial Sr and Nd ratios for Mailka, Leucogranite, mevatanana gneiss, Dhrwar TGG, and Tanzania Gneiss, are calculated to 93 Ma. The BY6163 (gneiss) from Central Madagascar are calculated to 88 Ma.

| Contaminant | Sr | ${}^{87}$Sr/${}^{86}$Sr | Nd | ${}^{143}$Nd/${}^{144}$Nd |
|---|---|---|---|---|
| Gneiss | 661.075 | 0.70608075 | 42.055 | 0.511078 |
| Mailka Leucogranite | 265.00 | 0.72111 | 16.4 | 0.51115 |
| Mevatanana gneiss | 216.00 | 0.72138 | 29.30 | 0.51131 |
| Dhrwar TGG | 322.0 | 0.72449 | 37.3 | 0.51072 |
| Tanzania Gneiss | 574.0 | 0.71853 | 21.5 | 0.51102 |
| BY6163 | 3.35 | 0701828244 | 21.9 | 0.51108909 |

The results of the AFC model are shown on Figure 5.12, which shows the plot of initial Sr ratio against initial Nd ratios with mixing curves of the contaminants. The Ambohiby plutonic rock samples are plotted on the graph to determine if they fit any of the mixing curves. The Ambohiby plutonic samples plotted are gabbroic, intermediate monzonite as well as felsic alkali syenites and granites samples. All Ambohiby plotted data did not fit on any of the mixing curves. It is concluded that the Ambohiby rocks do not show any likely mixing with the selected contaminant.

Figure 5.13 shows plot of Sr (ppm) against initial Sr ratios to see if the Ambohiby data fit on the straight-line of the plot. Data following a straight-line trend is normally taken to indicate mixing via a contamination type process. Figure 5.13 shows that only one sample fits on the straight line of the curve, which confirmed that the Ambohiby rocks were not involved in any AFC processes.
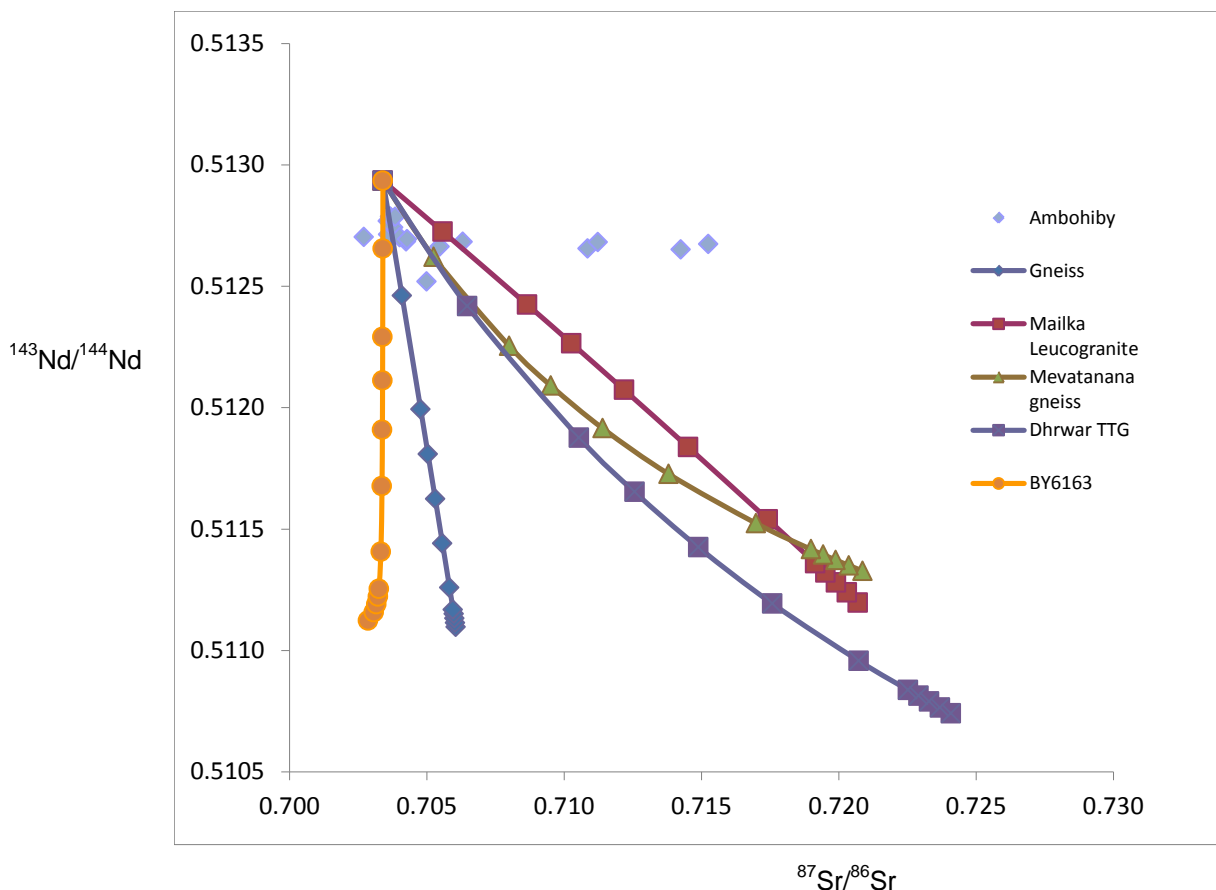


**Figure 5.12 :** *Plots of initial $^{143}Nd/^{144}Nd$ against $^{87}Sr/^{86}Sr$ showing the simple mixing between sample Marion island data and the partial melts of the possible contaminants*
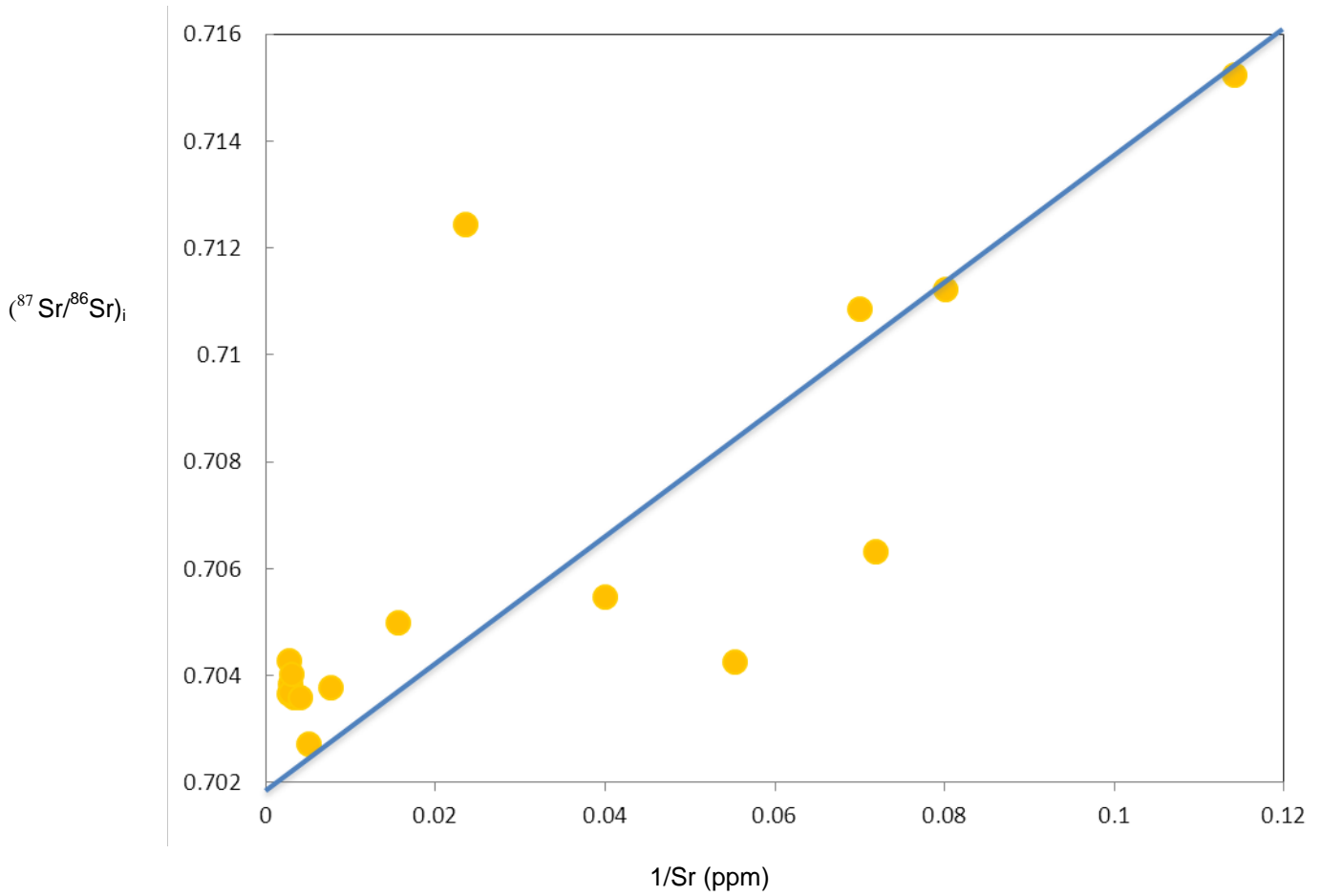
**Figure 5.13:** *The Ambohiby plutonic samples $^{87}Sr/^{86}Sr$ initial values are plotted against measured 1/Sr (ppm) to test for any mixing.*

## 5.6 Summary

Fractional crystallization model results fits well with the actual felsic compositions of the Ambohiby Complex. The Assimilation Fractional crystallization model did not fit well with the Ambohiby Complex data. The radiogenic isotope shows that two samples of both micro-granite and granite plot within the crustal field, which indicate that they may have been crustal contaminated, however the AFC model does not show any mixing curves that Ambohiby Complex rocks can fit at. This can be explained by lack of suitable contaminant for the Ambohiby Complex to produce a mixing curve that Ambohiby Complex rocks can fit-in.

# CHAPTER 6: CONCLUSIONS

The purpose of this study was to investigate the petrogenesis of the Ambohiby Complex, which is location in the central part of Madagascar. Previous studies related to ring complexes in Madagascar looked at the ring complexes in the south, east and west of the island but to date none have looked at the ring complexes in the central part of Madagascar. To investigate the petrogenesis, the rocks types were identified based on field relations and mineralogy and their distribution mapped. Major and trace elements as well as radiogenic isotopes were used to characterise the rocks geochemically, to confirm the field classification and to compare the Ambohiby to other ring complexes on Madagascar as well as the Marion Hotspot plume. The results of this work can be summarised as follows.

- Field relations established in this study indicate that a basement of Precambrian gneisses belonging to the Antananarivo Neoproterozoic Block underlies the Ambohiby Complex. The complex consists of the following intrusive rocks in chronological order: gabbro, monzonite, alkali syenite as well as granite. The complex is cross-cut by late extrusive mafic and felsic dykes.

- Rocks of the Ambohiby Complex are made up of variable amounts of pyroxenes, amphiboles and alkali feldspars, which generally have sodic compositions. Mafic rocks of the complex such as gabbro generally contain plagioclase, augite, arfvedsonite as the main primary phases, and biotite and chlorite as secondary phases. Felsic rocks of the complex such as granites generally contain alkali feldspars, quartz, arfvedsonite, aegirine, augite, microcline feldspars, and trace amounts of aenigmatite.

- Major element variation diagrams plotted against $SiO_2$ indicate that the mafic and felsic rocks are related by fractional crystallisation. All the complex rocks show that there is a constant negative correlation between CaO and $SiO_2$ that suggests fractionation of a plagioclase and/or clinopyroxene. Variation diagrams of trace elements Rb and Nb plotted against $SiO_2$ also suggest fractional crystallisation of plagioclase and accumulation of clinopyroxene.

- The mafic samples have low concentrations of REE and the felsic samples have low concentrations of HREE and high concentrations of LREE. Typically the felsic samples also show an increasing negative Eu anomaly indicating fractionation of plagioclase feldspars. The complex shows a similar pattern to the extrusive rocks where the mafic dyke samples have low concentrations of REE and the felsic dyke samples have low concentrations of HREE and high concentrations of LREE. Two gabbro samples show positive Eu anomalies, which may indicate accumulation of clinopyroxene, five gabbro samples show a flat Eu anomalies and the two samples with high LREE show a negative Eu anomalies. In addition gabbro samples also show depletion of HREE on the Chondrite normalized diagram.

- The Rb –Sr geochronology of the Ambohiby Complex gives an average age of 90.0±2.4 Ma and is consistent with the complex being emplaced during the Cretaceous. As expected, this confirms that the Ambohiby Complex is associated with the break-up of Gondwana. Sm- Nd data gave a very poorly constrained isochron and this may have been influenced by the Sm-Nd budget since the isotope data and the Sm-Nd concentration data were not acquired on the same dissolution. Therefore Sm-Nd ages were not considered correct for this study. The plot of $\varepsilon_{Nd}$ versus $^{87}Sr/^{86}Sr$ shows that gabbro samples are the most primitive samples of the complex although there is not a significant amount of variation and little evidence for a significant crustal component derived through contamination The exception to this are granites, basaltic and felsic dykes which indicate minor variable crustal contamination.

- The Ambohiby Complex shows similarities when compared to other Cretaceous igneous complexes located around Madagascar. Major element and trace element data for Volcan de l'Androy and Antampombato-Ambatovy Complex compares well

with the Ambohiby Complex data with similar correlations. The Volcan de l'Androy Complex is located in the southern part of the island and Antampombato-Ambatovy Complex located on the central eastern of the island. The later complex has a plume type geochemical signature possibly of the Marion Hotspot. As noted by Story *et al*., (1997) plate reconstructions models show that the hotspot was near the south eastern tip of Madagascar at 88 Ma.

- A fractional crystallization (FC) model involving 45% clinopyroxene + 40% plagioclase + 10% phlogopite + 5% Magnetite was used to generate the Ambohiby granites assuming 90% crystallisation of a melt with a composition of the Ambohiby gabbros. The Ambohiby gabbros are used as a proxy for the Marion Hotspot because of similarities in their heavy REE compositions. An AFC model could not be generated for the Ambohiby Complex using radiogenic isotopes because not suitable contaminant could be identified. For the FC model, the mineral assemblage that include olivine and orthopyroxene, plagioclase, magnetite and phlogopite gave a better 'fit' calculated felsic end member as compared to the mineral assemblage with clinopyroxene, plagioclase, magnetite and phlogopite. Olivine was therefore determined to be an important phase in the FC model although a small concentrations. This may explain why olivine was not identified in the thin-sections of Ambohiby Gabbros.

- The Ambohiby Complex has some geochemical characteristics that is similar to those of the Marion Hotspot Plume, particularly their similarities with the HREE. This may mean that the Marion Hotspot plume may have played a role towards the formation of the Ambohiby Complex. The LREE/HREE trend in the Marion Hotspot is different to that of the Ambohiby Complex and thus the role of the Marion Hotspot in the formation of the Ambohiby complex is inconclusive. However more work is recommended to further understand the processes that led to the formation of the Ambohiby Complex.

## REFERENCES

Abaa, S.I. (1984). Some geochemical chacteristics of alkaline rocks of the Mada Younger Granite complex, Nigeria. Journal of African Earth Sciences, **3** (1/2)115-121

Acharyya, A.K. (2000). Break up of Australia-India-Madagascar block, opening of Indian Ocean and continental accretion in Southeast Asia with special references to the characteristics of the Peri-Indian Collision Zone. Gondwana Research, **3**(4), 425-443

Ackermand, D., Windley, B.F. and Razafiniparany H. (1991). Kornerupine breakdown reactions in paragneisses from southern Madagascar. Mineralogical Magazine, **55**, 71-80

Agrawal, P.K., Pandey O.P and Negi J.P. (1992). Madagascar: a Continental fragment of the paleosuper Dharwar craton of India., Geology, **20**, 543-546

Almond, D.C. (1979) Younger Granite complexes of Sudan, In: Evolution and mineralization of the Arabian-Nubian Shield (Edited by Tahoun, S.A) Pergamon Press Oxford, **3**, 151-164

Alva-Valdivia, L.M., Goguitchaichvili, A., Urrutia-Fucugauchi, J., Riisager, J., Riisager, P. and Lopes, O.F. (2003) Palaeomagnetic poles and paleosecular variation of basalts from Parana Magmatic province, Brazil: Geomagnetic and geodynamic implications, Physics of the earth and planetary interiors, **138**, 183-196

Ashwal, L. and Tucker, R.D. (1999). Geology of Madagascar: A brief outline. Gondwana Research, **2**(3), 335-339

Arth J.G. (1976) Behaviour of trace elements during magmatic processes- a summary of theoretical models and their applications Journal of Research of the U. S. Geological Survey**, 4,** 41-47

Bailey, D.K. (1964). Crustal wrapping: a possible tectonic control of alkaline magmatism. Journal of Geophysical Research, **69**(6), 1103-1111

Bardintzeff J.M, Bonin B, Rasamimanana G, 2001. The Cretaceous Morondava volcanic province (west Madagascar): Mineralogical, petrological and geochemical aspects. Journal of African Earth Sciences, .**32** (2), 299-316

Bassias, Y. and Leclaire, L. (1990) The Davie Ridge in the Mozambique Channel: Crystalline basement and intraplate magmatism, N.jb.Geol.Palaont.Mh, 2, 67-90

Battistini, R. (1959). La structure du massif Volcanique de l Androy (Madagascar). Bulletin of Geological Society of France, **7**, 187-191

Batchelor, , R.A. and Bowden, P. (1985) Petrogenetic interpretation of granitoid rock series

using multicationic parameters. Chemical Geology **48**, 43–55.

Besairie, H. (1964) Madagascar, Carte Geologique. Tananarive servive Geologiqie de Madagascar

Besairie, H. (1968-1971) Description Geologique du massif ancient de Madagascar, Document Bureau Geologique Madagascar, no, 177, no 177a: centre nord et centre cord-est; 177b: region cotiere orientale; 177c: region centrale-systeme de graphite; 177d: region centrale-systeme du Vohibory; 177e: le sud; 177f: le nord. Bureau Geologique Madagascar, Antananarivo

Besarie, H. (1969) Description Geologique du massif ancient de Madagascar, Troisieme Volume: la region centrale. 1. Le Systeme du graphite, Groupe d' Ambatolampy. Documentation du Bureau Geologique, Tananarivo, Service Geologique de Madagascar, **177c,** 73

Bhattacharya,, S. and Kar, R. (2005) Petrological and Geochemical Constraints on the Evolution of the Akaline Complex of Koraput in the Eastern Ghats Granulite Belt, India, Gondwana Research (Gondwana Newsletter Section) **8**, 596-602

Bonin, B. (1986) Ring complexes and anorogenic magmatism studies in Geology, North Oxford Academic, Oxford, 188

Bonin, B. (1992) The role of Crust in the development of A-type alkali feldspar granites in within-plate bimodal alkaline magmatism. Bull. Ind. Geol. Assoc. **25**, 11-27

Bonin, B. (1996) A-type granite ring complexes: Mantle origin through crustal filters and the anorthosite-rapakivi magmatism connection. In: Demaiffe, D., (Ed.), Petrology and Geochemistry of Magmatic Suites of Rocks in the Continental and Oceanic

Crusts. A volume dedicated to Professor Jean Michot, Université Libre de Bruxelles-Royal Museum for Central Africa (Tervuren), 201-218

Bonin, B. (1998). Alkaline rocks and geodynamics. Journal of Earth Sciences, **7,**105-118

Boulanger J (1959) Les anorthosites de Madagascar. Ann Geol Madagascar **26**, 1-71

Bowden, P. (1985) The Geochemistry and mineralization of alkaline ring complexes in Africa (a Review), Journal of African Earth Sciences*,* **3**(1/2), 17-39

Bowen, N.L. (1928). The evolution of the igneous rocks. Princeton University Press., 1-334

Buchwalt, R., Tucker, R.D. and Dymeck, R.F. (2003) Geothermobarometry and U-Pb Geochronology of metapelitic granulites and politic migmatites from the Lokoho region, Northern Madagascar, American Mineralogist, **88**, 1753-1768

Buckland, W. (1821) Notice on the geological structure of a part of the island of Madagascar, Transactions of the Geological Society, **V**, 476-481

Chand, S. and Subrahmayam, C. (2003). Rifting between India and Madagascar-Mechanism and isostasy. Earth and Planetary Science Letters, **210**, 317-332

Claisse F. (1999). A New one step fusion technique for fusing metal powders, including Ferroalloys.

A new one-step fusion technique for fusing metal powders, including Ferroalloys

Coffin, M.F., Rabinowitz, P.D. and Houtz R.E. (1986) Crustal structure in the western Somali Basin, Geophysical Journal of the Royal Astronomical Society, **86**, 331-369

Coffin, M.F. and Rabinowitz, P.D. (1987) Reconstruction of Madagascar and Africa-evidence from the Davie fracture zone and Western Somali Basin, Journal of Geophysical Research, **92**, 9385-9406

Coffin, M.F. and Rabinowitz, P.D. (1988) Evolution of the conjugate East African-Madagascan margins and the western Somali Basin, Geological Society of America special paper, **226,** 78

Collins, A.S. (2000). The Tectonic evolution of Madagascar: Its place in the East African Orogen. Gondwana Research (Gondwana Newsletter Section*)*, 3(4),549-552

Collins, A.S. (2006). Madagascar and the amalgamation of Central Gondwana. Gondwana Research, **9**, 3-16

Collins, A.S., Windley, B., Kroner, A., Fitzsimons, I. and Hulscher, B. (2001) The Tectonic Architecture of Central Madagascar: Implication on the Evolution of the East African Orogeny, Gondwana Research, **4**(2), 152-153

Collins, A.S. and Windley, B.F. (2002). The tectonic evolution of central and northern Madagascar and its place in the final assembly of Gondwana. Journal of Geology, **110**, 325-340

Collins, A.S., Fitzsimons, I.C.W. and Razakamanana, T. (2003a), Structure of the eastern margin of the East African Orogen in Central Madagascar, Precambrian Research, **123**,111-133

Collins, A.S., John, S., Fitzsimons, I.C.W., Powell, C.M., Hulcher, B., Abello, J. and Razakamanana, T. (2003b) Neoproterozoic deformation in central Madagacar: a structural section through part of the East African Orogen. In: Yoshida, M., Windley B., Dasgupta S. (Eds.). Proterozoic East Gondwana: Supercontinent Assembly and Breakup, Special Publication of the Geological Society, London. **206**, 363-379

Collins, A.S., Kroner, A., Fitzsimons, I.C.W. and Razakamanana T. (2003c) Detrital footprint of the Mozambique ocean: U/Pb SHRIMP and Pb evaporation zircon geochronology of metasedimentary Gneisses in Eastern Madagascar, Tectonophysic*s*, **375**, 77-99

Collins, A.S. and Pisarevsky, S.A. (2005). Amalgamating Eastern Gondwana: The evolution of the Circum-Indian Orogen. Earth Science Reviews, **71**, 229-270

Cortillout, V., Feraud, G., Maluski, A., Vendamme, D., Mohean, M.G., Besse, J., (1988) Deccan flood basalts and the K/T boundary, Nature, **33**, 843-846

Cox, K.G, Bell, J.D. and Pankhurst, R.J. (1979). The Interpretation of Igneous Rocks.- George Allen and Unwin. 450

Crawford A.R. (1978) Narmada-Son lineament of India traced into Madagascar, Journal of Geological Society of India, **19**, 144-153

de Paolo, D.J. (1981). Trace element and isotopic effects of combined wallrock assimilation and fractional crystallization. Earth and Planetary Science Letters, **53**, 189-202

de Wit, M.J. (2003). Madagascar: Heads it's a Continent. Tails it's an Island. Annual Review of Earth Planetary Science, **31**, 213-248

de Wit , M.J., Jeffrey M., Bregh, H. and Nicolaysen, L. (1988). Geological map of sections of Gondwana reconstructed to their disposition ca 150 Ma. University of Witwatersrand, Johannesburg,

Dalziel, I.W.D; Mosher S. and Gahagan L.M. (2000). Laurentia-Kalahari Collision and assembly of Rodinia. Journal of Geology, **108**, 499-513

Davies, D.V and Davies, J.H. (2009) Thermally-driven mantle plumes reconcile multiple hot-spot observations, Earth and Planetary Science Letters, **278**, 50-54

Deer, W.A., Howie, R.A. and Zussman, J. (1963) Rock-Forming Minerals Volume2A Single-Chain Silicates, The Geological Society of London

Deer, W.A., Howie, R.A. and Zussman, J. (1997) Rock-Forming Minerals Volume2B Double-Chain Silicates, The Geological Society of London, 656

Dixey, F. (1960) The geology and geomorphology of Madagascar and a comparison with eastern Africa, Journal of geological Society of London, **116**, 255-268

Dostal, J., and Dupuy, C., Nicollet C and Cantagrel, J.M. (1992). Geochemistry and Petrogenesis of Upper Cretaceous basaltic rocks from southern Malagasy. Chemical Geology Journal, **97**, 199-146

Droop G.T.R (1987).A General equation for estimating Fe+ concentrations in ferromagnesium silicates and oxides from microprobe analysis, using stoichiometric criteria. Mineralogical Magazine, **51**, 431-435

Duncan, R.A. and Pyle, D.G. (1988) Rapid eruption of the Deccan basalts at the K/Tr boundary, Nature, **333**,841-843

Eby, G.N. (1990) The A-type granitoids: a review of their occurrence and chemical characteristics and speculations on their petrogenesis. Lithos, **26**, 115–134.

El Ramly, M.F. & Hussein, A.A.A. (1984). The ring complexes of the Eastern Desert of Egypt. Journal of African Earth Sciences, **3** (1/2), 77-82

Emmel, B., Jacobs, J., Kastowski, M. and Graser, G. (2005) Phanerozoic upper crustal tectono-thermal development of basement rocks from central Madagascar: Integrated fission-track and Structural study, Tectonophysics, **412**, 61-86

Ewart, A., Milner, S.C., Duncan, A.R. and Bailey, M. (2002). The Cretaceous Messum Igenous complex, S.W. Etendeka Namibia: reinterpretation in terms of a downsag-cauldron subsidence model. Journal of Volcanology and Geothermal Research, **114**, 251-273

Faure, G. (1986). Principles of Isotope Geology, Second Edition. John Willey & Sons, 229

Finkelstein, J (2010). The petrogenesis of the mesozoic Maningoza Suite igneous complexes, central west Madagascar. Dissertation presented for the degree of Master of Science, Department of Geological Sciences, University of Cape Town

Flores, G. (1984) The SE Africa triple junction and the drift of Madagascar, Journal of Petroleum Geology, **7**, 403-418

Gast, P.W. (1968). Trace element fractionation and the origin of tholeiitic and alkaline magma types. Geochim. Cosmochim. Acta, **32**, 1057-1068

Geiger, M., Clark, D.N and Mette, W. (2004) Reappraisal of the timing of the breakup of Gondwana based on sedimentological and seismic evidence from the Morondava Basin, Madagascar. Journal of African Earth Sciences, **38**(4), 363-381

Green, A.G. (1972) Sea floor spreading in the Mozambique Channel, Nature, **236**, 19-21

Gualda, G.A.R. and Vlach, S.R.F. (2007) The Serra da Graciosa A-Type Granites and Syenites, southern Brazil part 3: Magmatic evolution and post-magmatic breakdown of amphiboles of the alkaline association, Lithos, **93**, 328-339

Harris, C. (1995) Oxygen isotope geochemistry of the Mesozoic anorogenic complexes of the Damaraland, northwest Namibia: Evidence for crustal contamination and its effect on silica saturation. Contributions to Mineralogy and Petrology, **122**, 308-321

Harris, C., Marsh, J.S. and Milner, S.C. (1999). Petrology of the Alkaline Core of the Messum Igneous Complex, Namibia: Evidence for the Progressively Decreasing Effect of Crustal Contamination. Journal of Petrology, **40**(9), 1377-1397

Harris, C. and Ashwal, L. (2002) The origin of low $^{18}$O granites and related rocks from the Seychelles, Contrib. Mineral petrology, **143,** 366-376

Harris, N.B.W. (1982) The Petrogenesis of alkaline intrusives from Arabia and north-east and their implications for within-plate magmatism, Tectonophysics, **83**, 243-258

Harris, N.B.W. (1985) Alkaline complexes from the Arabian Shield, Journal of African Sciences, **3**(1/2), 83-88

Hart, S.R ., and Dunn, T. (1993). Experimental cpx/melt partitioning of 24 trace elements. Contributions to Mineralogy and Petrology Journal. **113**, 1-8

Hottin, G. (1976) Presentation et essai d'interpretation du Pre'cambrien de Madagascar. Bulletin du Bureau de Recherches Geologiques et Minieres IV (2$^{nd}$ series), 117-153

Janardhan, A.S. (1999). Southern granulite terrain, South of the Palghat Cauvery Shear Zone: Implications for India-Madagascar connection. Gondwana Research, **2**(3), 463-469

Jayananda, M., Moyen, J-F., Martin, H., Peucat, J-J., Auvray, B and Mahabaleswar, B (2000). Late Archaean (2550-2500) juvenile magmatism in the Eastern Dharwar

craton: Constraints from geochronology, Nd-Sr isotopes and whole rock geochemistry. Precambrian Research. **99**, 225-254

Janney, P. E., le Roex, A. P. & Carlson, R. W. (2005). Hafnium isotope and trace element constraints on the nature of mantle heterogeneity beneath the central Southwest Indian Ridge (138E to 478E). Journal of Petrology 46, 2427-2464

Jons, N., Schenk V., John, T. and Razakamanana, T. (2005) Relics of the Mozambique Ocean: geochemistry of the Vohibory Block (Madagascar).In: Wingate, M.T.D. and Pisarevsky, S.A (Eds), Supercontinents and Earth Evolution, Geological Society of Australia, Abstracts, Fremantle, 81, 133

Jourde, G. (1971) Essai de synthese structurale et stratigraphique de Precambrien malagache, Compte Rendu Societe Geologique France, 59-70

Jourde, G., Rasamoelina, D., Raveloson, S.A and Razanakolana, J. (1974). Geological map of the Milanoa-Vohemar area, W33-X33, 1:100000. Service Geologique de Madagasikara, Antananarivo

Kelemen, P.B., Dick, J.B., and Quick J.E. (1992). Formation of harzburgite by pervasive melt/rock reaction in the upper mantle. Nature, **358**, 635-641

Kelemen, P.B., Shimizu, N., and Dunn, T. (1993). Relative depletion of niobium in some arc magmas and the continental crust: Partitioning of K, Nb, La and Ce during melt/rock reaction in the upper mantle. Earth and Planetary Science Letters, **120**, 111-134

Kent, R.W., Pringle, M.S., Muller, R.D., Saunders, A.D. and Ghose N.C. (2002). 40Ar/39Ar geochronology of the Rajmahal basalts, India, and their relationship to the Kerguelen Plateau. Journal of Petrology, **43**, 1141-1153

Kroner, A., Braun, I. and Jaeckel, P. (1996) Zircon geochronology of anatectic melts and residues from a high-grade politic assemblage at Ihosy, southern Madagascar: evidence for Pan-African granulite metamorphism, Geological Magazines, **133**, 311-323

Kroner, A., Windley, B.F., Jaeckel, P., Collins, A.S., Brewer, T.S., Nemchin, A. and Razkamanana, T. (1999) New Zircon Ages for Precambrian Granites Gneisses and Granulites from Central and Southern Madagascar: Significance for Correlations in East Gondwana, Gondwana Research, **2**(3), 351-352

Kroner, A., Hegner, E., Collins, A.S., Windley, B.F., Brewer, T.S., Razakamanana, T. and Pidgeon, R.T. (2000) Age and magmatic history of the Antananarivo Block, central Madagascar, as derived from zircon geochronology and Nd isotopic systematic, American Journal of Sciences, **200**, 251-288

Kroner, A., Collins, A.S., Hegner, E., Willner, A.P., Muhongo, S. and Kehelpannala K.V.W. (2001) The East African Orogen: New Zircon and Nd ages and Implications for Rodenia and Gondwana Supercontinent, Gondwana research, **4(2),** 179-181

Kumar A, G., Pande, K., Venkatesan, T.R. and Bhaskar Rao, Y.J. (2001). The Karnataka late Cretaceous dikes as products of the Marion Hot spot at the Madagascar–India breakup event: Evidence from $^{40}Ar/^{39}Ar$ geochronology and geochemistry. Geophysical Research letters, **228**, 2715-2718

Kuritani, T., Kitagawa, H. and Nakamura, E. (2005) Assimilation and Fractional Crystallization Controlled by Transport process of Crustal melt: Implications from an Alkali Basalt-Dacite Suite from Rishiri Volcano, Japan, Journal of Petrology, **46** (7), 1421-1442

Le Bas, M.J., Le MaitrÎ, R.W., Streckeisen, A. and Zanettin, B. (1986) A chemical classification of volcanic rocks based on the total alkali–silica diagram. Journal of Petrology, **27,** 745–750.

Langmuir, C.H., Vocke R.D., Hanson G.N, and Hart S.R (1978) A general mixing equation with applications to icelandic basalts. Earth and Planetary Science Letters, **37**, 380-392

Lameyre, E.B.J. and Bonin, B. (1985). The structural setting of alkaline complexes. Journal of African Earth Sciences, **3**(1/2), 5-16

Lassen, B., Bridgwater, D., Bernstein, S. and Rosing, M. (2004). Assimilation and high-pressure fractional crystallization (AFC) recorded by Paleo-proterozoic mafic dykes, Southeast Greenland. Lithos, **72**, 1-18

Le Roex, A. P. & Lanyon, R. (1998). Isotope and trace element geochemistry of Cretaceous Damaraland lamprophyres and carbonatites, Northwest Namibia: evidence for plume–lithosphere interactions. Journal of Petrology, **39**, 1117–1146.

Loiselle,M.C. and Wones, D.R., (1979). Characteristics and origin of anorogenic granites. Abstract, Geological Society of America, **11**, 468

McElhinny, M.W., Embleton B.J.J., Daly, L. and Pozzi, J.P. (1976) Palaeomagnetic evidence for the location of Madagascar in Gondwanaland, Geology, **4**, 455-458

McKenzie, D. (1989). Some remarks on the movement of small melt fractions in the mantle. Earth and Planetary Science Letters, **95**, 53-72

Macey, P.H. (2009). Palaeozoic to recent Geology-Karoo Supergroup, Bermaraha Formatio, Ambohiby Complex, and Ankaratra Group, unpublished, 107-147

Mahoney, J. J., Nicollet, C. and Dupuy, C. (1991). Madagascar basalts: Tracking oceanic and continental sources. Earth and Planetary Science Letters, **104**, 305-363

Mahoney, J.J., le Roex, A. P., Peng, Z. X., Fisher, R. L. & Natland, J. H. (1992). Southwestern limits of Indian Oceanic Ridge Mantle and the origin of low 206Pb/204Pb MORB: Isotope systematics of the central Southwest Indian Ridge (178-508 E). Journal of Geophysical Research, **97**, 19771-19790

Mahoney, J.J., Saunders, A.D., Storey, M. and Randriamanantenasoa A. (2008). Geochemistry of the Volcan de l'Androy Basalt-Rhyolite Complex, Madagascar Cretaceous Igneous Province. Journal of Petrology, **49**(6), 1069-1096

Markl, G., Bauerle, J., Grujic, D., (2000). Metamorphic evolution of Pan-African granulite facies metapelites from Southern Madagascar, Precambrian Research, 102, 47-68

Martelat, J.E., Nicollect, C., Lardeaux, J.M., Vidal, G., Rakotondrazafy, R., (1997) Lithospheric tectonic structures developed under high-grade metamorphism in the southern part of Madagascar, Geodinamica Acta, 10-94-114

Martin, R.F. (2006) A-type of crustal origin ultimately result from open-system fenitization-type reactions in an extentional environment, Lithos*, **91**, 125-136

Meert, J.G., Nedelec, A., Hall, C., Wingate, M.T.D and Rakotondrazafy M. (2001). Paleomagnetism, geochronology and tectonic implications of the Cambrian-age Carion granite, Central Madagascar. Tectonophysics, **340** (1-2(, 1-21

Meert, J.G. and Van Der Voo, R. (1997). The assembly of Gondwana 800-450 Ma. Journal of Geodynamics, **23** (314), 223-235

Meert, J.G. and Tamrat, E. (2006). Paleomagnetic evidence for a stationary Marion hotspot: Additional paleomagnetic data from Madagascar. Gondwana Research, **10**, 340-348

Melluso, L., Morra, V., Brotzu, P., Razafiniparany, A., Ratrimo, V and Razafimahatratra, D. (1997). Geochemistry and Sr-isotopic composition of the Cretaceous flood basalt sequence of northern Madagascar: Petrogenetic and geodynamic implications. Journal of African Earth Sciences, **24**, 371-390

Melluso, L. and Morra, V (2000). Petrogenesis of Late Cenozoic Mafic-alkaline rocks of the Nosy Be archipelago (Northern Madagascar): relationships with the Comorean magmatism. Journal of Volcanology and Geothermal Research, **96** (1-2), 129-142

Melluso, L., Morra, V., Brotzu, P. and Mahoney, J.J. (2001) The Cretaceous Igneous Province of Madagascar: Geochemistry and petrogenesis of lavas and dykes from the central–western Sector, Journal of Petrology, **42** (7), 1249-1278

Melluso, L., Morra, V., Brotzu, P., Franciosi, L., Petteruti Lieberknecht, A.M. and Bennio, L. (2003). Geochemical provinciality in the Cretaceous magmatism of the northern Madagascar and mantle source implications. Journal of Geological Society London, **160**, 477-488

Melluso, L., Morra, V., Brotzu, P., Tommasini, S., Renna, M.R., Duncun, R.A., Franciosi, L. and D'Amellio, F. (2005), Geochronology and petrogenesis of the Cretaceous Antampombato-Ambatovy Complex and associated dyke swarm, Madagascar. Journal of Geology, **46**(10), 1963-1996

Macey, P.H., Miller, J.A., Armstrong, R.A., Ingram, B.A., Bisnath, A., Yibas, B., Frost-Killian, S., Chevallier, L., Finkelstein, J. and Haddon, I.G. (2009) Map Explanation of 1:100 000 scale sheets G41 – Ambohipaky, H41 – Bevary, G42 – Mangoboky, H42 – Bekodoka, G43 – Andolamasa, H43 - Andrafialava and parts of G40 – Ankasakasa, F40 - Saint-Andre, F41 – Betsalampy, H40 – Maroboaly-Sud, I40 – Soalala-Sud, I41 – Andranomavo, F42 – Marovoay Kely, I42 – Mahabe, F43 – Bebao, F44 – Antranogoaika, G44 – Morafeno, I43 – Ampoza, H44- Bemolanga and I44 Makaraingo. Ministère de L'Energie et des Mines – Project de Gouvernance des Ressources Minérales, Antananarivo, Madagascar and Council for Geoscience, Pretoria, South Africa.

Milner, S.C., Le Roex, A., Pand O'Connor, J.M. (1995) Age of Mesozoic igneous rocks in Northwestern Namibia, and their relationship to continental breakup, Journal of the Geological Society, London,1**52**, 97-104

Milner, S.C and le Roex A.P. (1996). Isotope characteristics of Okenyenya igneous complex, Northwestern Namibia: Constraints on the compositions of the early Tristan plume mantle and the origin of the EM 1 mantle component. Earth & planetary Science Letters, **141**, 277-291

Mingram, B., Trumbull, R.B., Littmann, S. and Gerstenberger, H. (2000). A petrogenetic study of anorogenic felsic magmatism in the Cretaceous Paresis ring complex, Namibia: Evidence for crust-mantle hybridization. Lithos, **54**, 1-22

Morgan, W.J. (1972). Plate motions and deep mantle convection. Geological Society of America Memoire, **132**, 7-22

Morgan, W.J. (1981) Hotspot tracks and the opening of the Atlantic and Indian Ocean, In The Sea, edited by Emiliani C., **7**, 443-487

Morimito, N., Fabries, J., Ferguson, A.K., Ginzburg, I.V., Ross, M., Seifer,t F.A. and Zussman, J. (1988) Nomenclature of Pyroxenes, Mineralogical Magazines, **52**, 535-550

Moller A., Mezger K, and Schenk V. (1998) Crustal Age Domains and the Evolution of the Continental Crust in the Mozambique Belt of Tanzania: Combined Sm–Nd, Rb–Sr, and Pb–Pb Isotopic Evidence. Journal of Petrology. 34(4);749-783

Muller, R.D., Royer J.Y. and Lawver, L.A. (1993) Revised plate motions relative to hotspots tracks, Geology, **21**, 275-278

Nedelec, A., Stephens, A. and Fallick, W.E. (1995) The Pan-african Stratoid granites of Madagascar: alkaline magmatism in a post-collisional extensional setting, Journal of Petrology, **36**, 1367-1391

Nicollect, C. (1990) Crustal evolution of the granulites of Madagascar, In: Vielzeuf, D., Vidal, P. (Eds.), Granulites and Crustal Evolution, Kluwer Academic Publishers, Dordrecht, 291-310

O'Halloran, D.A. (1985). Rase'd Dom migrating ring complex: A-type granites and syenites from the Bayuda Desert, Sudan. Journal of African Earth Sciences, **3**(1/2), 61-75

O'Neil Muller, D. and Steinberger, B. (2003) Geodynamic implications of moving Indian Ocean hotspots, Earth and planetary Science Letters, **215**, 151-168

Paquette, J. and Nedelec, A. (1998) A new insight into Pan-African tectonics in the East-West Gondwana collision zone by U-Pb zircon dating of granites from central Madagascar, Earth and Planetary Science Letters, 1**55**, 45-56

Paquette, J.L., Goncalves, P., Devouard, B. and Nicollect, C. (2004) Micro-drilling ID-TIMS U-Pb dating of single monazites: A new method to unravel complex poly-metamorphic evolutions, Application to the UHT granulites of Andriamena (North-Central Madagascar), Contributions to Mineralogy and Petrology, **147**, 110-122

Pique, A. (1999). The geological evolution of Madagascar: An introduction. Journal of African Earth Sciences, **28**(4), 919-930

Pearce, J.A., Harris, N.B.W. and Tindle, A.G. (1984). Trace-element discrimination diagrams for the tectonic interpretation of granitic rocks. Journal of Petrology, **25**,. 956–983.

Plummer, P.S. (1995) Ages and geological significance of the igneous rocks from Seychelles, Journal of African Earth Sciences, **20**(2), 91-101

Rasolofomanana, A.S. (1998) Les complexes annulaires de la province magmatique du Cap Saint André: Géologie, pétrologie et géodynamique. Thèse, Université Blaise Pascal.

Raval, Y. and Veeraswamy, K. (2003) India-Madagascar Separation: Breakup along a Pre-existing Mobile Belt and Chipping of the Craton, Gondwana Research, **6**(3), 467-485

Ray, J.S. (1998) Trace element and isotope evolution during concurrent assimilation, fractional crystallization, and liquid immiscibility of a carbonated silicate magma, Geochemica et Cosmochimica Acta, **62** (19/20), 3301-3306

Razvalyayev, A.V. and Shakhov, G.P. (1976) New data on ring intrusions of the Red Sea Rift zone, Dockl.Akad.Nauk, SSSR, **229**, 114-116

Reeves, C.V.B., Sahu, K and De wit, M. (2002). A re-examination of the paleo-position of Africa's eastern neighbours in Gondwana. Journal of African Earth Sciences, **34** (3-4), 101-108

Rollinson H.R. (1993) Using Geochemical data: Evaluation, Presentation, Interpretation. 102-170

Schandelmeier, H., Bremer, F and Holl H.G. (2004). Evolution of the Morondava rift basin of SW Madagascar -from wrench tectonics to normal extension. Journal of African Earth Sciences, **38**(4), 321-330

Schmitt, A.K., Emmermann R., Trumbull, R.B., Buhn B., and Henjes-kunst, F. (2000) Petrogenesis and Ar/Ar Geochemistry of the Brandberg Complex, Namibia: Evidence for major mantle contribution in Metaluminous and peralkaline granites, Journal of Petrology, **41**(8), 1207-1239

Scrutton, R.A., Heptonstall, W.B., Peacock J.H (1981) Constraints on the motion of Madagascar with respect to Africa, Marine Geology, **43**,1-20

Seward, D, D., Grujic, D. and Schreurs, G. (2004) An insight into the breakup of Gondwana: Identifying events through low-temperature thermochronology from the basement rocks of Madagascar. Tectonics, 23

Shands, S.J. (1922) The problem of the alkaline rocks, Proc.Geological Society of South Africa., **25**, 19-33

Shaw, D.M. (1970). Trace element fractionation during anatexis, Geochim.Cosmochim. Acta. **34**, 237-243

Shimizu, N., and Kushiro I. (1975) The partitioning of rare earth elements between garnet and liquid at high pressures: Preliminary experiments. Geophysical Research Letters. **2**, 414-416

Singer, B.S. and Kudo, A.M. (1986) Assimilation-fractional crystallization of Polvadera Group rocks in the Northwestern Jemez Volcanic Field, New Mexico, Contributions to Mineralogy and Petrology, **94**, 374-386

Sinha, M.C., Louden, K.E. and Parsons, B. (1981) The crustal structure of the Madagascar Ridge, Geophysical Journal of Royal Astronomical Society, **66,** 351-377

Skyes, L.R. (1978). Intraplate seismicity reactivation, reactivation of pre-existing zones of weakness, alkaline magmatism and other tectonism post-dating continental fragmentation. Review of Geophysical Space Physics, **16,** 621-688

Smith, A.G and Hallam, A. (1970). The fit of the Southern Continents, Nature, **225**, 139-144

Steiger, R.H and Jager E. (1977) Subcommission on geochronology: convention of the use of decay constants in geo- and cosmochronology. Earth & Planetary Science Letters, **36**, 359-362

Storey, M., Mahoney, J.J, Saunders, A.D., Duncan, R.A., Kelley, S.P. and Coffin M.F. (1995). Timing of hot spot-related volcanism and the breakup of Madagascar and India. Science, **267**, 852-855

Storey, M., Mahoney, J.J. and Saunders, A.D. (1997). Cretaceous basalts in Madagascar and the transition between plume and the continental lithosphere mantle sources. In Mahoney, J.J and Coffin M. (eds) Large Igneous Provinces: Continental, Oceanic and Planetary Flood Volcanism. American Geophysical Union Monograph, **100**, 95-122

Sun, S.S. and McDonough, W.F. (1989) Chemical and isotopic systematics of oceanic basalts: implications for mantle composition and processes. In: Saunders, A.D., Norry, M.J. (eds) Magmatism in the ocean basins, Geological Society, London, Special publications, **42**, 313-345

Tanaka, T., Togashi S., Kamioka H., Amakawa H., Kagami, H., Hamamoto T., Yuhara, M, Orihashi, Y, Yoneda, S., Shimizu, H., Kunimaru, T., Takahashi, K., Yanagi, , T, Nakano, T., Fujimaki H., Ryuichi, S., Asahara, Y., Tanimizu, M., Dragusanu, C., (2000) JNdi-1: A neodymium isotopic reference in consistency with LaJolla neodymium. Chemical Geology, 168, **3-4**, 279-281

Taylor, S.R and McLennan S.M. (1985) The continental Crust: Its composition and evolution. Blackwell, Oxford, 312

Torsvisk, T.H., Tucker, R.D., Ashwal L.D., Eide, E.A., Rakotosolofo, N.A. and De Wit, M.J. (1998) Late Cretaceous magmatism in Madagascar palaeomagnetic evidence for a stationary Marion hotspot, Earth & Planetary Science Letters, **164**, 221-234

Torsvisk, T.H., Tucker, R.D., Ashwal, L.D., Carter, L.M., Jamtveit, B., Vidyadharan, K.T., and Venkataramana, P. (2000). Late Cretaceous India-Madagascar fit and timing of break-up related magmatism. Terra Nova, **12**, 220-224

Trumbull, R.B., Harris, C., Frindt, S. and Wigand, M. (2003a) Oxygen and neodymium isotope evidence for source diversity in Cretaceous anorogenic granites from Namibia and implications for A-type granite genesis, Lithos, **73**, 21-40

Trumbull, R.B., Buhn, B., Romer, R.L. and Volker, F. (2003b) The Petrology of Basanite-Tephrite Intrusions in the Erongo Complex and Implications for a Plume Origin of Cretaceous Alkaline Complexes in Namibia, Journal of Petrology, **44**(1), 93-111

Tucker, R.D., Aswa, L.D., Handke, M.J, and Hamiton, M.A (1997). A geochronological overview of the Precambrian rocks of Madagascar: A record from the middle Archean to the late Neoproterozoic. In: Cox. R and Ashwal, L.D. 1997 (eds). Proceeding of UNESCO/IUGS/IGCP 348/368 International Field Workshop on Proterozoic Geology of Madagascar, Gondwana Research Group, Rand Africans University Miscellaneous Publication, **5**, 99-100

Tucker, R.D., Ashwal, L.D., Hamilton, M.A., Torsvik, T.H. and Carter L.M., (1999a) Neoproterozoic silicic magmatism of northern Madagascar, Seychelles, and NW India: Clues to Rodinia's assembly and dispersal, Geological Society of America, Abstracts with programs, **31**, 317

Tucker, R.D., Ashwal, L.D., Handke, M.J., Hamilton, M.A., Le Grange, M., Rambeloson, R.A (1999b) U-Pb Geochronology and isotope Geochemistry of the Archean and Proterozoic Rocks of North-Central Madagascar, Journal of Geology, **107**, 135-153

Vail, J.R (1984). Alkaline ring complexes in Sudan. Journal of African Earth Sciences, **3**(1/2), 51-59

Venkatesan, T.R., Pande, K. and Gopalan, K. (1993) Did Deccan volcanism pre-dates the K/Tr transition? Earth and Planetary Science Letters, **119**, 181-189

Walter, M.J., and Presnall D.C. (1994) Melting behavior of simplified lherzolite in the system $CaO-MgO-Al_2O_3-SiO_2-Na_2O$ from 7 to 35kbar. Journal of Petrology, **35,** 329-359.

Wescott, W.A. and Diggens, J.N (1998). Depositional history and stratigraphical evolution of the Sakamena group (Middle Karoo Supergroup) in the Southern Morondava Basin, Madagascar. Journal of African Earth Sciences, **27**(2-4), 461-479)

Whalen, J.B., Currue, K.L. and Chappel, B.W. (1987) A-type granites: geochemical characteristics, discrimination and petrogenesis. Contribributions, Mineralogical Petrology, **95**, 407–419.

Windley, K.H., Razafiniparany, A., Razakamanana, T. and Ackermand, D. (1994). Tectonic framework of the Precambrian of Madagascar and its Gondwana connections: A review and reappraisal. Geologische Rundschau, **83**, 642-659

Wood, D.A. (1980). The application of a Th–Hf– Ta diagram to problems of tectonomagmatic classification and to establishing the nature of crustal contamination of basaltic lavas of the British Tertiary volcanic province. Earth and Planetary Science Letters, **50**, 11–30.

Yoder Jr., H.S. (1973). Contemporaneous basaltic and rhyolitic magmas. American Mineralogist, **58,** 153-171

Yoshida, M., Rajesh, H.M. and Santosh M. (1999). Juxtaposition of India and Madagascar: A perspective. Gondwana Research, **2**(3), 449-462

Appendix 1.1: list of the geographic positions of all the collected Ambohiby Complex samples

| Reference Point | Rock type | Sample No | Latitude | Longitude | Freshness | No of Blocks | Polished | Covered slipped | Split | Crushed | Powder | XRF | ICP-MS | Rb-Sr | Nd-Sm |
|---|---|---|---|---|---|---|---|---|---|---|---|---|---|---|---|
| | | | | | | | **Thin Section** | | | | | **Geochemistry** | | **Radiogenic isotopes** | |
| CM7001 | Stromatic ortho-gneisses | MC7001 | -18,853 | 46,162 | Very Fresh | 1 | X | | X | X | X | X | X | | |
| CM7001 | Mafic dyke | MC7002 | -18,853 | 46,162 | Very Fresh | 1 | | X | X | X | X | X | X | X | X |
| CM7002 | Mafic dyke | MC7003 | -18,852 | 46,179 | | | X | X | | | | | | | |
| CM7002 | Micro-granite | MC7004 | -18,852 | 46,179 | very very Fresh | 1 | X | | X | X | X | X | X | | |
| CM7002 | Gabbroic xenolith | MC7005 | -18,852 | 46,179 | Very Fresh | 1 | X | | X | X | X | X | X | | |
| CM7003 | Micro-granite | MC7006 | -18,861 | 46,187 | Very Fresh | 1 | X | | X | X | X | X | X | X | X |
| CM7004 | Granite | MC7007 | -18,873 | 46,200 | not very weathered | | | | X | X | X | X | X | | |
| CM7005 | Monzonite | MC7008 | -18,867 | 46,178 | Very Fresh | 1 | X | | X | X | X | X | X | X | X |
| CM7006 | Felsic dyke | MC7009 | -18,868 | 46,178 | Very Fresh | 1 | X | | X | X | X | X | X | | |
| CM7007 | Granite | MC7010 | -18,873 | 46,180 | very Fresh | 1 | X | | X | X | X | X | X | | |
| CM7007 | Gabbroic xenolith | MC7010 | -18,873 | 46,180 | | 1 | X | | | | | | | | |
| CM7007 | Felsic dyke | MC7012 | -18,873 | 46,180 | Very Fresh | 1 | X | | X | X | X | X | X | | |
| CM7009 | Granite | MC7013 | -18,878 | 46,186 | Very weathered | 1 | X | | X | X | X | X | X | X | X |
| CM7008 | | MC7014 | -18,875 | 46,185 | | | | | | | | | | | |
| CM7010 | Gabbroic xenolith | MC7015 | -18,871 | 46,201 | fine | 1 | X | | X | X | X | X | X | | |
| CM7011 | Felsic dyke | MC7016 | -18,873 | 46,199 | Very Fresh | 1 | X | | X | X | X | X | X | | |
| CM7012 | Granite | MC7017 | -18,874 | 46,198 | Very Fresh | 2 | X | | X | X | X | X | X | | |
| CM7015 | Granite | MC7018 | -18,878 | 46,201 | | 1 | X | | X | X | X | X | X | X | X |
| CM7017 | Felsic dyke | MC7019 | -18,880 | 46,205 | Very Fresh | 1 | X | | X | X | X | X | X | X | X |
| CM7023 | Felsic dyke | MC7020 | -18,878 | 46,212 | | 1 | X | | X | X | X | X | X | | |
| CM7024 | Granite | MC7021 | -18,877 | 46,211 | bit weathered but still fresh | 1 | X | | X | X | X | X | X | X | X |
| CM7026 | Micro-granite | MC7022 | -18,874 | 46,209 | Very Fresh | 1 | X | | X | X | X | X | X | | |
| CM7032 | Felsic dyke | MC7023 | -18,878 | 46,233 | Very Fresh | 1 | X | | X | X | X | X | X | | |
| CM7033 | Micro-granite | MC7024A | -18,874 | 46,236 | fine | 1 | X | | X | X | X | X | X | X | X |
| CM7033 | Micro-granite | MC7024B | -18,874 | 46,236 | Very weathered | 1 | X | | | | | | | | |
| CM7034 | Micro-granite | MC7025 | -18,871 | 46,237 | Very weathered | 1 | X | | X | X | X | X | X | X | X |
| CM7036 | Alkali-syenite | MC7026 | -18,865 | 46,235 | Very Fresh | 1 | X | | X | X | X | X | X | | |
| CM7037 | Alkali-syenite | MC7027 | -18,863 | 46,228 | Very Fresh | 1 | X | | X | X | X | X | X | X | X |
| CM7038 | Mafic dyke | MC7028 | -18,867 | 46,223 | Very Fresh | 1 | X | | X | X | X | X | X | | |
| CM7038 | Alkali-syenite | MC7029 | -18,867 | 46,223 | fine | 1 | X | | X | X | X | X | X | | |
| CM7038 | | MC7029 | -18,867 | 46,223 | | 1 | X | | | | | | | | |
| CM7040 | Orthogneiss | MC7030 | -18,841 | 46,164 | Very Fresh | 1 | X | | X | X | X | X | X | | |
| CM7040 | Felsic dyke | MC7031 | -18,841 | 46,164 | Very Fresh | 1 | X | | X | X | X | X | X | X | X |
| CM7040 | Rhyolite dyke | MC7032 | -18,841 | 46,164 | Very Fresh | 1 | X | | X | X | X | X | X | X | X |

Appendix 1.1: list of the geographic positions of all the collected Ambohiby Complex samples

| Reference Point | Rock type | Sample No | Latitude | Longitude | Freshness | Sample Preparation — Thin Section — No of Blocks | Polished | Covered slipped | Split | Crushed | Powder | Geochemistry — XRF | ICP-MS | Radiogenic isotopes — Rb-Sr | Nd-Sm |
|---|---|---|---|---|---|---|---|---|---|---|---|---|---|---|---|
| CM7041 | Micro-granite | MC7033 | -18,840 | 46,162 | Very Fresh | 1 | X | | X | X | X | X | X | | |
| CM7041 | | MC7033 | -18,840 | 46,162 | | | | | X | X | X | X | X | | |
| CM7043 | Felsic dyke | MC7034 | -18,828 | 46,167 | fine but bit weathered | 1 | X | | X | X | X | X | X | | |
| CM7043 | Felsic dyke | MC7035 | -18,828 | 46,167 | fine | 1 | X | | X | X | X | X | X | | |
| CM7043 | Felsic dyke | MC7036 | -18,828 | 46,167 | very  Fresh | 1 | X | | X | X | X | X | X | X | X |
| CM7043 | Felsic dyke | MC7037 | -18,828 | 46,167 | | 1 | X | | | | | | | | |
| CM7043 | Felsic dyke | MC7038 | -18,828 | 46,167 | Fresh | 1 | X | | X | X | X | X | X | | |
| CM7045 | Monzonite | MC7039 | -18,848 | 46,169 | Very Fresh | 1 | X | | X | X | X | X | X | | |
| CM7046 | Monzonite | MC7040 | -18,848 | 46,168 | fine but bit weathered | 1 | X | | X | X | X | X | X | X | X |
| CM7046 | Monzonite | MC7041 | -18,848 | 46,168 | Very Fresh | 1 | X | | X | X | X | X | X | X | X |
| CM7048 | Gabbro | MC7042 | -18,868 | 46,161 | Very Fresh | 1 | X | | X | X | X | X | X | | |
| CM7049 | Felsic dyke | MC7043 | -18,869 | 46,163 | Very Fresh | 1 | X | | X | X | X | X | X | X | X |
| | Felsic dyke | MC7044 | | | Very Fresh | 1 | X | | X | X | X | X | X | | |
| CM7050 | Gabbro | MC7045 | -18,867 | 46,166 | Very Fresh | 1 | X | | X | X | X | X | X | X | X |
| CM7051 | Granite | MC7046 | -18,863 | 46,170 | | | | | | | | | | | |
| CM7051 | Felsic dyke | MC7047 | -18,863 | 46,170 | Very Fresh | 1 | X | | X | X | X | X | X | | |
| CM7053 | Gabbro | MC7048 | -18,869 | 46,171 | Very Fresh | 1 | X | | X | X | X | X | X | | |
| CM7054 | Gabbro | MC7049 | -18,871 | 46,171 | | | | | | | | | | | |
| CM7054 | Gabbro | MC7050 | -18,862 | 46,180 | Very Fresh | 1 | X | | X | X | X | X | X | X | X |
| CM7055 | Micro-granite | MC7051 | -18,862 | 46,180 | Fresh | 1 | X | | X | X | X | X | X | | |
| CM7055 | | | -18,862 | 46,180 | | 1 | X | | | | | | | | |
| CM7056 | Gabbro | MC7052 | -18,846 | 46,172 | Very  Fresh | | | | X | X | X | X | X | X | X |
| CM7057 | Felsic dyke | MC7053 | -18,849 | 46,173 | Very very  Fresh | 1 | X | | | | | | | | |
| CM7060 | Felsic dyke | MC7054 | -18,843 | 46,186 | Very Fresh | 1 | X | | X | X | X | X | X | | |
| CM7060 | Granite | MC7055 | -18,843 | 46,186 | Fresh | 1 | X | | X | X | X | X | X | | |
| CM7062 | Monzonite | MC7056 | -18,828 | 46,186 | Very Fresh | 1 | X | | X | X | X | X | X | | |
| CM7063 | Alkali-syenite | MC7057 | -18,819 | 46,198 | | 1 | X | | | | | | | | |
| CM7065 | Monzonite | MC7058 | -18,823 | 46,194 | Very Fresh | 1 | X | | X | X | X | X | X | | |
| CM7067 | Gabbro | MC7059 | -18,833 | 46,189 | Very Fresh | 1 | X | | X | X | X | X | X | | |
| CM7078 | Alkali-syenite | MC7060 | -18,851 | 46,214 | Very Fresh | 1 | X | | X | X | X | X | X | X | X |
| CM7081 | Micro-granite | MC7061 | -18,842 | 46,222 | Very very  Fresh | 1 | X | | X | X | X | X | X | | |
| CM7085 | Gabbro | MC7062 | -18,838 | 46,236 | Very Fresh | 1 | X | | X | X | X | X | X | | |
| CM7089 | Gabbro | MC7063 | -18,836 | 46,239 | Very very  Fresh | 1 | X | | X | X | X | X | X | X | X |
| CM7106 | Felsic dyke | MC7064 | -18,907 | 46,222 | Very Fresh | 1 | X | | X | X | X | X | X | | |

Appendix 1.1: list of the geographic positions of all the collected Ambohiby Complex samples

| Reference Point | Rock type | Sample No | Latitude | Longitude | Freshness | Sample Preparation | | | | | | Geochemistry | | Radiogenic isotopes | |
| | | | | | | No of Blocks | Thin Section | | Split | Crushed | Powder | XRF | ICP-MS | Rb-Sr | Nd-Sm |
| | | | | | | | Polished | Covered slipped | | | | | | | |
| CM7109 | Micro-granite | MC7065 | -18,884 | 46,173 | Fine | 1 | X | | X | X | X | X | X | | |
| CM7110 | Gabbro | MC7066 | -18,882 | 46,175 | Very Fresh | 1 | X | | X | X | X | X | X | X | X |
| CM7133 | Orthogneiss | MC7067 | -18,842 | 46,165 | Very Fresh | 1 | X | | X | X | X | X | X | | |
| CM7108 | Felsic dyke | MC7068 | -18,886 | 46,171 | | | | | | | | | | | |
| PD06001 | Mafic dyke | PD06001 | -18,854 | 46,159 | | 1 | | X | X | X | X | X | X | | |
| PD06001 | Orthogneiss | PD06002 | -18,854 | 46,159 | | 1 | | X | X | X | X | X | X | | |
| PD06001 | Felsic dyke | PD06003 | -18,854 | 46,159 | | 2 | | X | X | X | X | X | X | | |
| PD06002 | Gabbro | PD06004 | -18,853 | 46,170 | | 1 | | X | X | X | X | X | X | | |
| PD06003 | Felsic dyke | PD06005 | -18,851 | 46,176 | | 1 | | X | X | X | X | X | X | | |
| PD06004 | Micro-granite | PD06006 | -18,843 | 46,187 | | 1 | | X | X | X | X | X | X | | |
| PD06005 | Felsic dyke | PD06007 | -18,859 | 46,193 | | 2 | | X | X | X | X | X | X | | |
| PD06007 | Granite | PD06008 | -18,877 | 46,197 | | 1 | | X | X | X | X | X | X | | |
| PD06008 | Granite | PD06009 | -18,878 | 46,188 | | 1 | | X | X | X | X | X | X | | |
| PD06009 | Alkali-syenite | PD06010 | -18,867 | 46,179 | | 1 | | X | | | | | | | |
| PD06010 | Gabbro | PD06011 | -18,862 | 46,175 | | 1 | | X | | | | | | | |

## MC7001 – ORTHOGNEISS

| Grain size(mm) | Modal % | Mineral | Description |
|---|---|---|---|
| 1.0-1.5 | 40 | Alkali Feldspars | Non pleochroic (colourless), first order birefringence, straight extinction |
| 0.2-1.2 | 30 | Chlorite | Strongly pleochroic (colourless to light green), anomalous order birefringence |
| 0.2-1.2 | 14 | Biotite | Strongly pleochroic (pale yellow to brown), second order birefringence (pinkish blue), extinction angle of 24° |
| 0.5-1.0 | 10 | Quartz | Has undulose extinction |
| 0.7-1.5 | 4 | Muscovite | Non pleochroic (colourless), second order birefringence (pinkish to blue), extinction angle ranging from 33-37° |
| 1.0-1.5 | 2 | Plagioclase | Non pleochroic (colourless), first order birefringence, straight extinction |
| 0.1-0.5 | tr | Oxides | |
| 0.1-0.19 | tr | Zircon | Non pleochroic (colourless), third order birefringence (pinkish-blue) and hexagonal in shape |

**Texture:** This is a medium grained rock that consists of alkali feldspars, micas and quartz. This rock is characterized by alignment of minerals in groups. Micas indicate schollen or raft fabric. The alkali feldspars are altered to sericite and are very difficult to define the fabric of the feldspars since they are much altered. Biotite is flattened and is replaced by chlorite and there is no particular orientation of the grains. Some of the biotite exhibits pleochroic haloes that are attributed to the presence of inclusions of zircon. Oxides are associated with the micas and there is very minor occurrence of secondary oxides in feldspars.

**Rock type** Gneiss

## MC7002 – MAFIC DYKE

| Grain size(mm) | Modal % | Mineral | Description |
|---|---|---|---|
| 0.2-1.0 | 68 | Plagioclase | Non pleochroic (colourless), first order birefringence, straight extinction |
| 0.5-0.8 | 15 | Diopside | Weakly pleochroic (colourless to light brown) second order birefringence (yellowish blue), extinction angle 35-38° |
| 0.1-0.5 | 10 | Chlorite | Weakly pleochroic (light green to green), first order birefringence |
| 0.1-0.5 | 5 | Oxides | |
| 0.2-0.3 | 1 | Epidote | Weakly pleochroic (yellow to brown), first order birefringence |
| 0.1-0.2 | 1 | Sulphides | Anhedral |

**Texture:** This is a fine-grained basaltic rock that consists of elongated plagioclase feldspars, anhedral diopside, secondary epidote and chlorite. Anhedral diopside is replaced by chlorite. The diopside, epidote, and chlorite occur in plagioclase matrix. The oxides are subhedral and blocky while sulphides are anhedral and randomly distributed.

**Rock type**: Basalt

## MC7004 – MICRO-GRANITE

| Grain size(mm) | Modal % | Mineral | Description |
|---|---|---|---|
| 0.1-0.3 | 74 | Quartz | Non pleochroic (colourless), first order birefringence |
| 0.1-0.2 | 15 | Epidote | Strongly pleochroic (yellowish to green), second order birefringence (yellowish to orange), inclined extinction angle 26° |
| 0.1-0.2 | 10 | Arfvedsonite | Strongly pleochroic (dark blue to purple), second order birefringence (bluish to pink), straight extinction |
| 0.1-0.4 | 1 | Diopside | Non pleochroic (colourless), second order birefringence (yellowish pink), inclined extinction angle of 29° |

**Texture:** This is a very fine-grained felsic rock that consists of quartz, anhedral epidote, elongated needle-like arfvedsonite and trace amount of anhedral diopside. The arfvedsonite, epidote and diopside occur in quartz matrix and randomly distributed.

**Rock type:** Micro-granite

## MC7005 – GABBROIC XENOLITH

| Grain size(mm) | Modal % | Mineral | Description |
|---|---|---|---|
| 0.2-0.7 | 50 | Amphibole | Strongly pleochroic (pale-yellow to dark brown), second order birefringence, 124° cleavage angle, extinction angle 28-29° |
| 0.3-0.6 | 46 | Alkali feldspar | Non pleochroic (colourless), first order birefringence and has straight extinction |
| 0.4-0.5 | 2 | Augite | Weakly pleochroic (colourless to weak brown), second order birefringence (pinkish blue) |
| 0.3-0.5 | 1 | Chlorite | Weakly pleochroic (colourless to green), anomalous birefringence |
| 0.2-0.4 | 1 | Biotite | Weakly pleochroic (weak brown to brown), second order birefringence (pinkish blue), extinction angle of 24° |
| 0.3-.0.7 | tr | Oxides | |

**Texture:** This rock consists of anhedral amphibole alkali feldspars, augite, secondary chlorite, biotite and trace amount of oxides. The augite is replaced by amphibole, while amphibole is replaced by secondary chlorite and biotite. The feldspars are elongated and altered to sericite and consequently it is very difficult to identify the type of feldspar. This rock is similar to MC7049.

**Rock type:** Gabbro

## MC7006 – MICRO-GRANITE

| Grain size(mm) | Modal % | Mineral | Description |
|---|---|---|---|
| 0.3-2.2 | 50 | Mesoperthite feldspars | Non pleochroic (colourless), first order birefringence, and has straight extinction |
| 0.1-2.4 | 37 | Quartz | Non pleochroic (colourless), first order birefringence, undulose extinction |
| 0.3-1.2 | 5 | Aegirine | Strongly pleochroic (pale yellow to green), second order birefringence (greenish blue), inclined extinction angle =32-36° |
| 0.2-1.4 | 4 | Arfvedsonite | Strongly pleochroic (deep indigo blue to green), second order birefringence, extinction angle=39-42° |
| 0.2-0.5 | 3 | Augite | Non pleochroic (colourless), second order birefringence (pinkish blue), inclined extinction angle = 38° |
| 0.1-0.3 | 1 | Oxides | |
| 0.1-0.2 | tr | Zircon | Non pleochroic (colourless), third order birefringence (pinkish blue) and hexagonal in shape. |

**Texture:** This rock consists of mesoperthite feldspars, quartz, anhedral aegirine, anhedral arfvedsonite, sub-euhedral augite and secondary oxides. Mesoperthites are equigranular and there is no fabric pattern. Anhedral aegirine is replaced by arfvedsonites. Both oxides and zircons occur in arfvedsonite matrix
.

**Rock type:** Micro-granite

## MC7007 – GRANITE

| Grain size(mm) | Modal % | Mineral | Description |
|---|---|---|---|
| 1.7-3.0 | 64 | Mesoperthite | Non pleochroic (colourless), first order birefringence, straight extinction |
| 0.5-2.6 | 30 | Quartz | Has undulose extinction |
| 0.3-0.9 | 5 | Arfvedsonite | Strongly pleochroic (pale-yellowish-green to blue), second order birefringence (bluish pink), straight extinction |
| 0.5-1.2 | 1 | Plagioclase | Non pleochroic (colourless), first order birefringence, straight extinction and has polysynthetic twins |
| 0.2-0.5 | tr | Aenigmatite | Strongly pleochroic (red to brown), fourth order birefringence, |

**Texture:** This rock consists of mesoperthite, quartz, sub-euhedral arfvedsonite and minor amount of plagioclase. Arfvedsonite is zoned indicating compositional change during crystallization. There are trace amount of fine-grained aenigmatite and occurs in arfvedsonite matrix. This rock is very weathered and is similar to MC7006 and MC7029.

**Rock type:** Granite

### MC7008 – GABBRO

| Grain size(mm) | Modal % | Mineral | Description |
|---|---|---|---|
| 0.2-1.5 | 52 | Orthoclase | Non pleochroic (colourless), first order birefringence, straight extinction and has carlsbad twins |
| 0.3-0.5 | 30 | Augite | Weakly pleochroic (light brown to colourless), second order birefringence (bluish pink), inclined extinction angle= 38° |
| 0.4-1.2 | 7 | Biotite | Weakly pleochroic (light brown to dark brown), first order birefringence, extinction angle = 27° |
| 0.5-1.0 | 6 | Quartz | Has undulose extinction |
| 0.1-0.5 | 3 | Chlorite | Weakly pleochroic (light yellow to green), anomalous birefringence, |
| 0.3-0.4 | 2 | Plagioclase | Non pleochroic (colourless), first order birefringence and has polysynthetic twins |
| 0.2-0.5 | tr | Oxides | |

**Texture:** This is a medium grained gabbro that consists of much altered augite, orthoclase, plagioclase, secondary chlorite and biotite. The orthoclase is elongated, zoned, and has a bimodal grain size distribution. Chlorite is replacing both biotite and augite. The oxides occur as fine blocky grains and some display a spongy texture particularly in biotite grains. This rock is very weathered.

**Rock type:** Gabbro

### MC7009 – FELSIC DYKE

| Grain size(mm) | Modal % | Mineral | Description |
|---|---|---|---|
| 1.5-2.0 | 86 | Mesoperthites | Non pleochroic(colourless), first order birefringence, straight extinction |
| 1.3-2.0 | 4 | Orthoclase | Non pleochroic(colourless), first order birefringence, straight extinction |
| 0.1-0.6 | 3 | Biotite | Strongly pleochroic (pale yellow to brown), second order birefringence (orange to darkish pink) |
| 0.1-0.4 | 2 | Diopside | Non pleochroic (colourless), second order birefringence (pinkish blue), inclined extinction angle =25° |
| 0.2-1.6 | 2 | Quartz | |
| 0.1-0.3 | 1 | Aenigmatite | Strongly pleochroic (red to brown), fourth order birefringence |
| 0.2-0.4 | 1 | Chlorite | Weakly pleochroic (light yellow to green), first order birefringence, |
| 0.1-0.3 | 1 | Aegirine | Strongly pleochroic (brown to green), second order birefringence (bluish pink), straight extinction |
| 0.2-0.5 | tr | Oxides | |
| 0.0-0.1 | tr | Sericite | Non pleochroic (yellowish), second order birefringence |

**Texture:** This rock is comprised of mesoperthite, orthoclase, skeletal aegirine, fine-grained quartz, secondary chlorite, aenigmatite, as well as trace amount of oxides and sericite. Both mesoperthite and orthoclase are zoned while aegirine and diopside are anhedral, interstitial in feldspar matrix. The aegirine and diopside is replaced by biotite and chlorite. Feldspars and quartz display a granophyric

reaction texture. Aenigmatite occurs in biotite matrix. Oxides occur in diopside and aegirine matrix. Sericite occurs as an alteration product in feldspars matrix.
**Rock type:** Felsic dyke

## MC7010 – GRANITE

| Grain size(mm) | Modal % | Mineral | Description |
|---|---|---|---|
| 0.6-2.5 | 61 | Mesoperthite | Non pleochroic (colourless), first order birefringence, has straight extinction |
| 1.5-2.2 | 26 | Quartz | Has undulose extinction |
| 0.1-1.8 | 7 | Arfvedsonite | Strongly pleochroic (blue to green), second order birefringence (greenish yellow), straight extinction |
| 1.2-1.6 | 3 | Aegirine | Strongly pleochroic (brown to green), second order birefringence straight extinction |
| 0.1-0.4 | 2 | Augite | Non pleochroic (colourless), second order birefringence (bluish pink), straight extinction |
| 0.2-0.4 | 1 | Biotite | Moderate (brownish to dark brown), first order birefringence |
| 0.1-0.4 | tr | Aenigmatite | Strongly pleochroic (red to brown), fourth order birefringence and sub-euhedral. |

**Texture:** This rock consists of mesoperthite, quartz, anhedral arfvedsonite, aegirine, augite, trace amount of biotite and aenigmatite. Mesoperthite shows string texture. Augite is replaced by aegirine and arfvedsonite is zoned and is replacing aegirine. The biotite occurs along the cleavage plane of the arfvedsonite grains. This rock is similar to MC7010-1.

**Note:** This is a cover-slip thin section

**Rock type:** Granite

## MC7010-1 – GRANITE WITH A XENOLITH

### MC7010-1 – granite

| Grain size(mm) | Modal % | Mineral | Description |
|---|---|---|---|
| 1.0-1.5 | 60 | Mesoperthite | Non pleochroic (colourless), first order birefringence, straight extinction |
| 0.5-1.4 | 25 | Quartz | Has undulose extinction. |
| 0.2-1.4 | 7 | Arfvedsonite | Strongly pleochroic, (blue to green), second order birefringence (bluish-pink), extinction angle 31-38° |
| 0.7-1.4 | 3 | Aegirine | Strongly coloured (brown to green), second order birefringence, extinction angle 32° |
| 0.2-0.7 | 3 | Aegirine - Augite | Weakly pleochroic (colourless to weakly brown), second order birefringence (greenish pink) |

| 1.0-1.3 | 2 | Microcline feldspar | Non pleochroic (colourless), first order birefringence, straight extinction |
| 0.1-0.4 | tr | Aenigmatite | Strongly pleochroic (red to brown) fourth order birefringence and sub-euhedral. |

**Texture:** The rock consists of subhedral mesoperthite, arfvedsonite and minor amount of anhedral aegirine, aegirine-augite and microcline feldspars. Arfvedsonites are zoned and replacing aegirine as well as aegirine-augite. The microcline feldspars are subhedral and altered. Aenigmatite occurs in the core as well as in the cleavage plane of the arfvedsonite. This rock is similar to MC7007.

**Rock type:** Granite

### MC7010-2 –GRANITE

| Grain size(mm) | Modal % | Mineral | Description |
|---|---|---|---|
| 1.2-1.6 | 72 | Mesoperthite | Non pleochroic (colourless), first order birefringence, straight extinction |
| 0.2-1.6 | 20 | Quartz | showing undulose extinction |
| 0.4-1.6 | 5 | Arfvedsonite | Strongly pleochroic (pale yellow to bluish), second order birefringence (bluish-pink), straight extinction |
| 0.2-0.5 | 3 | Aegirine | Strongly coloured (brownish to dark green), second order birefringence, extinction angle 32° |
| 0.2-0.5 | 2 | Augite | Weakly pleochroic (colourless to weak brown), second order birefringence (bluish-green), straight extinction |
| 0.2-0.5 | tr | Aenigmatite | Strongly pleochroic (red-brown), fourth order birefringence sub-anhedral, |
| 0.1-0.19 | tr | Zircons | Non pleochroic (colourless), third order birefringence (bluish-pinkish orange), hexagonal in shape |

**Texture:** This rock consists of mesoperthite, arfvedsonite, fine-grained quartz and minor amount of interstitial aegirine and augite. Mesoperthite is prismatic to euhedral in shape. The arfvedsonite is subhedral and zoned displaying compositional change. The core of most arfvedsonite is altered by aenigmatite. Aegirine is anhedral and is replaced by arfvedsonite. This rock is similar to the MC7010 and MC7010-1.

**Rock type:** Granite

### MC7012 – GRANITE

| Grain size(mm) | Modal % | Mineral | Description |
|---|---|---|---|
| 1.0-2.9 | 77 | Orthoclase | Non pleochroic (colourless), first order birefringence, straight extinction |
| 0.5-1.2 | 10 | Quartz | undulose extinction |
| 0.2-0.7 | 4 | Augite | Non pleochroic (colourless) , second order birefringence (pinkish blue), inclined extinction angle =34° |

| 0.1-0.5 | 4 | Chlorite | Weakly pleochroic (light green to pale brown), second order birefringence |
|---------|---|----------|----------------------------------------------------------------------------|
| 0.4-1.5 | 3 | Biotite | Weakly pleochroic (light brown to dark brown), second order birefringence |
| 0.2-0.7 | 2 | Oxides | |
| 0.1-0.3 | tr | Sericite | |

**Texture:** This rock consists of orthoclase, fine-grained quartz, anhedral augite, and secondary biotite and chlorite. The orthoclase is prismatic, and altered to sericite. Anhedral augite is replaced by biotite and chlorite. Biotite is platy and displays a replacement texture reaction with chlorite. Oxides occur in augite as well as in the feldspar matrix and are randomly distributed. This rock is similar to MC7049.

**Note:** This is a cover-slip thin section

**Rock type:** Granite

## MC7012 – FELSIC DYKE

| Grain size(mm) | Modal % | Mineral | Description |
|----------------|---------|---------|-------------|
| 0.1-0.2 | 98 | Spherulites | Radiating arrays of crystalites fibres in fine quartz matrix |
| 0.1-0.2 | 1 | Quartz | |
| 1.2-1.5 | 1 | Orthoclase | Non pleochroic (colourless), first order birefringence, straight extinction |

**Texture:** This rock consists of rare orthoclase phenocrysts in a very fine-grained matrix dominated by radiating spherulites. This rock is very fine-grained and very difficult to identify other minerals due to fine grained texture; however the texture that is most dominant is spherulites (i.e. derivitification-high temperature environment)

**Rock type:** Rhyolite

## MC7013 –GRANITE

| Grain size(mm) | Modal % | Mineral | Description |
|----------------|---------|---------|-------------|
| 1.2-3.0 | 56 | Mesoperthite | Non pleochroic (colourless), first order birefringence, straight extinction |
| 0.3-3.0 | 26 | Quartz | Has undulose extinction |
| 0.2-0.8 | 10 | Arfvedsonite-richterite | Strongly pleochroic (green to blue), second order birefringence (bluish to pink), straight extinction |
| 0.2-0.5 | 4 | Augite | Weakly pleochroic (brown to colourless), second order birefringence (bluish-green), straight extinction |
| 0.1-0.3 | 3 | Sanidine | Non pleochroic (colourless), first order birefringence, straight extinction and has carlsbad twins |
| 0.2-0.8 | 1 | Aenigmatite | Strongly pleochroic (red to brown), fourth order birefringence |

**Texture:** This rock consists of mesoperthite, anhedral arfvedsonite-richterite, quartz, anhedral augite with minor amount of elongated sanidine and anhedral aenigmatite. Mesoperthite is prismatic and altered to sericite. Arfvedsonite-richterite is replacing augite and skeletal. Aenigmatite occurs in the core of arfvedsonite-richterite

**Rock type:** Granite

## MC7015 – MICROGRANITE XENOLITH IN GRANITE

| Grain size(mm) | Modal % | Mineral | Description |
|---|---|---|---|
| 0.5-1.2 | 60 | Alkali feldspar | Non pleochroic (colourless), first order birefringence, |
| 0.2-0.9 | 25 | Quartz | Has undulose extinction |
| 0.2-0.8 | 9 | Aegirine | Strongly pleochroic (pale yellow to strong green), second order birefringence, extinction angle 29-33° |
| 0.2-0.6 | 3 | Arfvedsonite | Strongly pleochroic (indigo to deep blue), second order birefringence, straight extinction |
| 0.3-0.6 | 2 | Plagioclase | Non pleochroic (colourless), first order birefringence, straight extinction |
| 0.1-0.3 | 1 | Oxides | |
| 0.1-0.13 | tr | Zircon | Non pleochroic (colourless), third order birefringence (bluish-pink), hexagonal to rectangle in shape |
| 0.1-0.13 | tr | Monazite | Non pleochroic (colourless), first order birefringence, inclined extinction angle |

**Texture:** This rock contains mesoperthite feldspars, quartz, anhedral aegirine, anhedral arfvedsonite, elongated plagioclase, oxides and trace amount of zircon and monazite. The mesoperthite has bimodal grains size distributions and anhedral aegirine is replaced by arfvedsonite, while oxides and zircons occur in arfvedsonite grains. Plagioclases are elongated and display polysynthetic twins. Monazite occurs in feldspar matrix.

**Rock type:** Micro-granite Xenolith

## MC7015 – MICROGRANITE -XENOLITH

| Grain size(mm) | Modal % | Mineral | Description |
|---|---|---|---|
| 0.5-1.2 | 62 | Alkali feldspar | Non pleochroic (colourless), first order birefringence, straight extinction |
| 0.2-0.9 | 28 | Quartz | Showing undulose extinction |
| 1.0-1.6 | 3 | Microcline | |
| 0.2-0.5 | 3 | Aegirine | Weakly pleochroic (pale yellow to green), second order birefringence, inclined extinction angle 34° |
| 0.2-0.4 | 1 | Arfvedsonite | Strongly pleochroic (blue to deep indigo blue), second order birefringence (blue), straight extinction |
| 0.3-0.6 | 2 | Plagioclase | Non pleochroic (colourless), first order birefringence, straight extinction a |
| 0.1-0.3 | tr | Oxides | |

| 0.1-0.3 | tr | Augite | Non pleochroic (colourless), second order birefringence (pinkish blue), straight extinction |

**Texture:** This rock consists of alkali feldspars, fine-grained quartz, anhedral aegirine, anhedral arfvedsonite, and trace amount of oxides, euhedral augite and orthopyroxene. Alkali feldspars are zoned, display a granophyric texture and have bimodal grains size distribution. Microcline feldspars display tartan twining. The plagioclase is elongated, has carlsbad twins and some plagioclases are altered to sericite. The orthoclase has reaction texture with plagioclase and most plagioclases are rimmed by orthoclase. Aegirine is being replaced by arfvedsonite and augite is interstitial in alkali feldspar matrix.

**Rock type:** Microgranite xenolith


## MC7016 – FELSIC DYKE

| Grain size(mm) | Modal % | Mineral | Description |
|---|---|---|---|
| 0.1-0.2 | 39 | Arfvedsonite | Strongly pleochroic (pale yellow to strong blue), second order birefringence (pinkish blue), extinction angle 31° |
| 0.1-0.6 | 60 | Quartz | Has undulose extinction |
| 0.5-1.4 | 1 | Orthoclase phenocrysts | Non pleochroic (colourless), first order birefringence, inclined extinction angle = 37° |

**Texture:** This is a very fine-grained rock with microcrystalline texture and euhedral orthoclase phenocrysts

**Rock type:** Rhyolite


## MC7017 – GRANITE

| Grain size(mm) | Modal % | Mineral | Description |
|---|---|---|---|
| 0.5-1.2 | 68 | Mesoperthite | Non pleochroic (colourless), first order birefringence, straight extinction |
| 1.0-2.5 | 24 | Quartz | Has undulose extinction |
| 0.2-1.3 | 7 | Arfvedsonite | Strongly pleochroic (greenish to blue), second order birefringence (bluish-pink), extinction angle 33° |
| 0.3-1.4 | 1 | Aegirine | Strongly pleochroic (brownish to deep green), second order birefringence, extinction angle 32° |
| 0.1-0.5 | tr | Plagioclase | Non pleochroic (colourless), first order birefringence, straight extinction |
| 0.1-0.5 | tr | Augite | Non pleochroic (colourless) second-order birefringence (pinkish to blue), extinction angle 32° |

**Texture:** This is a coarse-grained rock that consists of fine-grained quartz, mesoperthite, arfvedsonite and minor amount of plagioclase and anhedral augite. The mesoperthite is zoned and altered to

sericite. Some of the arfvedsonite grains are zoned indicating compositional variations and are replacing aegirine
**Rock type:** Granite

**MC7018 – GRANITE**

| Grain size(mm) | Modal % | Mineral | Description |
|---|---|---|---|
| 0.5-2.5 | 62 | Mesoperthite | Non pleochroic (colourless), first order birefringence, straight extinction |
| 0.3-1.5 | 30 | Quartz | |
| 0.4-1.4 | 5 | Arfvedsonite | Strongly pleochroic (pale brownish-green to blue), second order birefringence (pinkish orange), straight extinction |
| 0.2-0.5 | 2 | Plagioclase | Non pleochroic (colourless), first order birefringence, straight extinction |
| 0.3-0.9 | 1 | Aegirine | Strongly pleochroic (green to dark green), second order birefringence, inclined extinction angle=34 |
| 0.1-0.3 | tr | Augite | Non pleochroic (colourless) second order birefringence (pinkish blue), inclined extinction angle 26-28° |
| 0.2-0.6 | tr | Aenigmatite | Strongly pleochroic (red to brown), fourth order birefringence |

**Texture:** This rock consists of mesoperthite, quartz, anhedral aegirine, subhedral arfvedsonite, and trace amounts of aenigmatite. Arfvedsonite is zoned and replacing aegirine. The plagioclase is elongated, has polysynthetic twinning and occurs in association with mesoperthite as well as an inclusion in mesoperthite grains. Aenigmatite occur as a secondary product particularly in the core of the aegirine and rarely in arfvedsonite.

**Rock type:** Granite

**MC7019 – FELSIC DYKE**

| Grain size(mm) | Modal % | Mineral | Description |
|---|---|---|---|
| 0.1-0.2 | 98 | Amphibole? (actinolite/tremolite) | Strongly pleochroic (colourless to green), second order birefringence (pinkish blue), Needle-like, radiating arrays of fibrous (needle-like acicular)when XPL |
| 0.1-0.3 | 2 | Crystallites | |

**Texture:** This rock that is characterized by radiating needle-like arrays of amphibole fibrous displaying a spherical texture.

**Rock type:** Rhyolite

**MC7020 – FELSIC DYKE**

| Grain size(mm) | Modal % | Mineral | Description |
|---|---|---|---|
| 0.1-0.3 | 63 | Quartz | showing undulose extinction |

| | | | |
|---|---|---|---|
| 0.1-0.2 | 35 | Arfvedsonite | Strongly pleochroic (light green to deep blue), second order birefringence (bluish green). |
| 0..3-0.6 | 2 | K-feldspar phenocrysts | Non pleochroic (colourless), first order birefringence, straight extinction |

**Texture:** This rock is containing an intergrowth of quartz and K-feldspar phenocrysts. The arfvedsonite has needle-like shape and the k-feldspar phenocrysts are euhedral in shape. This rock is similar to MC7012

**Rock type:** Rhyolite

## MC7021 – GRANITE

| Grain size(mm) | Modal % | Mineral | Description |
|---|---|---|---|
| 0.5-2.7 | 60 | Mesoperthite | Non pleochroic (colourless), first order birefringence, straight extinction |
| 0.5-1.2 | 30 | Quartz | Has undulose extinction |
| 0.3-1.0 | 6 | Arfvedsonite | Strongly pleochroic (bluish to green), second order birefringence (pinkish blue), straight extinction |
| 0.2-0.5 | 4 | Plagioclase | Non pleochroic (colourless), first order birefringence, straight extinction, polysynthetic twinning |
| 0.1-0.3 | 1 | Oxides | Inclusion of oxides in arfvedsonite grains |
| 0.8-1.7 | 1 | Richterite | Strongly pleochroic (Indigo to deep blue), first order birefringence. |
| 0.1-0.3 | tr | Augite | Non pleochroic (colourless), second order birefringence (pinkish blue), straight extinction |
| 0.2-0.8 | tr | Aenigmatite | Strongly pleochroic (red to brown), fourth order birefringence |
| 0.1-0.19 | tr | Zircon | Non pleochroic (colourless), third order birefringence (bluish-pink), hexagonal to rectangle in shape |

**Texture:** This granite consists of mesoperthite, quartz, arfvedsonite, richterite, augite and oxides. Arfvedsonite is zoned indicating compositional change during crystallization. Richterite seems to be replaced by arfvedsonite. The Aenigmatite occurs as inclusions in arfvedsonite grains particularly in their cores

**Rock type:** Granite

## MC7022 – MICRO-GRANITE

| Grain size(mm) | Modal % | Mineral | Description |
|---|---|---|---|
| 0.3-0.6 | 60 | Mesoperthite | Non pleochroic (colourless), first order birefringence, straight extinction |
| 0.2-0.5 | 30 | Quartz | |

| Grain size(mm) | Modal % | Mineral | Description |
|---|---|---|---|
| 0.1-0.3 | 5 | Arfvedsonite | Strongly pleochroic (brownish-green to blue), first order birefringence, straight extinction |
| 0.1-0.3 | 1 | Oxides | anhedral |
| 0.1-0.19 | tr | Zircon | Non pleochroic (colourless), fourth order birefringence (bluish-pink), hexagonal to rectangle in shape |

**Texture:** This is a fine-grained rock comprised of mesoperthite, quartz, anhedral arfvedsonite, minor amount of oxides and trace amount of zircons. Mesoperthite is sub-anhedral, has string perthitic texture and bimodal grains size. The feldspar displays a granophyric texture. The arfvedsonite is interstitial and randomly distributed. Trace amount of zircons occurs in arfvedsonite grains.

**Rock type:** Micro-granite

## MC7023 – FELSIC DYKE

| Grain size(mm) | Modal % | Mineral | Description |
|---|---|---|---|
| 0.2-0.5 | 70 | Quartz | Has undulose extinction |
| 0.1-0.2 | 20 | Amphibole | Needle like weakly pleochroic (greenish to yellowish), second order birefringence (pinkish–blue) |
| 0.1-0.4 | 10 | Alkali feldspar | Sub-euhedral |

**Texture:** This is a volcanic rock that has gone through the process of devitrification. This rock is characterized by spherulites. This spherical texture consists of radiating arrays of crystal fibres. This rock consists of quartz, amphiboles and alkali feldspars. The quartz seems to be recrystalized and make up the matrix of this thin section.

**Rock type:** Rhyolite

## MC7024 –GRANITE

| Grain size(mm) | Modal % | Mineral | Description |
|---|---|---|---|
| 0.3-1.6 | 53 | Mesoperthite | Non pleochroic (colourless), first order birefringence, straight extinction |
| 0.5-2.1 | 40 | Quartz | Has undulose extinction |
| 0.4-0.8 | 3 | Arfvedsonite | Strongly pleochroic (green to blue), second order birefringence (pinkish blue), straight extinction |
| 0.3-0.8 | 2 | Plagioclase | Non pleochroic (colourless), first order birefringence, straight extinction |
| 0.3-0.5 | 1 | Aenigmatite | Strongly pleochroic (red to brown), fourth order birefringence |
| 0.1-0.2 | 1 | Augite | Non pleochroic (colourless), second order birefringence (bluish pink), straight extinction |

**Texture:** This granite consists of mesoperthite, fine-grained quartz, interstitial arfvedsonite, elongated plagioclase, anhedral aenigmatite as well as anhedral augite. The core of the arfvedsonite is altered by aenigmatite.

**Rock type:** Granite

## MC7024 – XENOLITH IN COARSE GRAINED GRANITE

| Grain size(mm) | Modal % | Mineral | Description |
|---|---|---|---|
| 0.1-0.9 | 49 | Mesoperthite | Non pleochroic (colourless), first order birefringence, straight extinction |
| 0.1-.07 | 30 | Quartz | |
| 0.2-0.5 | 10 | Aegirine | Strongly pleochroic (brown to dark green), second order birefringence, extinction angle =37° |
| 0.2-0.9 | 4 | Orthoclase | Non pleochroic (colourless), first order birefringence, straight extinction |
| 0.2-0.5 | 4 | Plagioclase | Non pleochroic (colourless), first order birefringence, straight extinction |
| 0.1-0.3 | 1 | Sanidine | Non pleochroic (colourless), first order birefringence, straight extinction and has carlsbad twins |
| 0.1-0.3 | 1 | Diopside | Non pleochroic (colourless), second order birefringence (bluish pink), straight extinction |
| 0.2-0.4 | 1 | Aenigmatite | Strongly pleochroic (red to brown), fourth order birefringence |

**Texture:** This xenolith consists of intercumulate mesoperthite, interstitial aegirine, fine-grained quartz, prismatic orthoclase, elongated plagioclase and minor amount of diopside and aenigmatite. Anhedral aegirine is replacing diopside and occurs in mesoperthite and quartz matrix.

**Rock type:** micro-granite Xenolith

## MC7025 – XENOLITH IN MEDIUM GRAINED GRANITE

| Grain size(mm) | Modal % | Mineral | Description |
|---|---|---|---|
| 0.2-1.2 | 66 | Orthoclase | Non pleochroic (colourless), first order birefringence, straight extinction |
| 0.2-0.5 | 20 | Arfvedsonite | Strongly pleochroic (green to blue), second order birefringence, inclined extinction angle 44° |
| 0.2-0.5 | 10 | Quartz | Has undulose extinction |
| 0.2-0.5 | 2 | Oxides | Non pleochroic (black), first order birefringence |
| 0.1-0.3 | 1 | Diopside | Weakly pleochroic (light brown to colourless), second order birefringence (greenish blue), straight extinction |
| 0.8-1.0 | 1 | Biotite | Weakly pleochroic (light brown to dark brown), second order birefringence |
| 0.1-0.3 | tr | Plagioclase | Non pleochroic (colourless), first order birefringence, straight extinction |
| 0.11-0.13 | tr | Zircon | Non pleochroic (colourless), third order birefringence (bluish- |

| | | | pink), hexagonal to rectangle in shape |
|---|---|---|---|

**Texture:** This is a medium grained xenolith containing intercumulate orthoclase, quartz, interstitial diopside, anhedral arfvedsonite, secondary biotite and minor amount of oxides. The orthoclase is elongated and displays carlsbad twins. Arfvedsonite is replaced by biotite. Diopside is anhedral, and occurs in quartz-feldspathic matrix.

NB: large alkali feldspar (0.4-1.6 mm wide surrounded by interstitial arfvedsonite)

**Rock type:** Xenolith

## MC7025 – GRANITE

| Grain size(mm) | Modal % | Mineral | Description |
|---|---|---|---|
| 0.5-2.5 | 66 | Alkali-feldspar | Non pleochroic (colourless), first order birefringence, straight extinction |
| 0.2-1.2 | 22 | Quartz | Has undulose extinction |
| 1.0-1.5 | 9 | Aegirine | Weakly pleochroic (brownish-green), second order birefringence, straight extinction |
| 0.3-0.6 | 2 | Aenigmatite | Strongly pleochroic (red to brown), fourth order birefringence |
| 0.1-0.9 | 1 | Arfvedsonite | Strongly coloured (deep indigo blue), second order birefringence (deep blue), inclined extinction angle=40-45° |
| 0.1-0.2 | 1 | Augite | Weakly pleochroic (colourless), second order birefringence (greenish blue), straight extinction |
| 0.11-0.13 | tr | Zircon | Non pleochroic (colourless), third order birefringence (bluish-pink), hexagonal to rectangle in shape |

**Texture:** This granite consists of cumulate feldspars, fine-grained quartz, anhedral arfvedsonite, sub-anhedral aegirine, minor amount of aenigmatite and accessory zircons. The arfvedsonite is zoned and the core is filled with aenigmatite. The aegirine is replaced by arfvedsonite. This rock is very weathered

**Rock type:** Granite

## MC7026 – ALKALI-SYENITE

| Grain size(mm) | Modal % | Mineral | Description |
|---|---|---|---|
| 0.2-1.7 | 87 | Orthoclase | Non pleochroic (colourless), first order birefringence, straight extinction |
| 0.2-1.0 | 6 | Quartz | |

| 0.2-0.6 | 3 | Ferro-edenite | Strongly pleochroic (brownish-greenish to blue), second order birefringence, extinction angle 26° |
| 0.3-0.5 | 2 | Augite | Non pleochroic (colourless), second order birefringence (pinkish blue), inclined extinction angle=30-37° |
| 0.1-0.5 | 1 | Oxides | Non pleochroic (black), first order birefringence |
| 0.1-0.9 | 1 | Chlorite | Strongly pleochroic (colourless to green), first order birefringence |
| 0.11-0.13 | tr | Zircon | Non pleochroic (colourless), third order birefringence (bluish-pink), hexagonal to rectangle in shape |

**Texture:** This rock consists of intercumulate alkali feldspars, quartz, anhedral ferro-edenite, interstitial augite as well as secondary oxides. The alkali feldspars are prismatic and have granophyric texture. The augite is replaced by ferro-edenite. The oxides occur mostly in ferro-edenite grains and rarely in feldspar matrix. The chlorite is replacing ferro-edenite. The zircons are scattered all around the thin section.

**Rock type:** Akali-syenite

## MC7027 – ALKALI-SYENITE

| Grain size(mm) | Modal % | Mineral | Description |
|---|---|---|---|
| 0.2-1.5 | 71 | Orthoclase | Non pleochroic (colourless), first order birefringence, straight extinction |
| 0.2-0.7 | 15 | Ferro-edenite | Strongly coloured (brownish-green to blue), second order birefringence, straight extinction |
| 0.1-0.4 | 6 | Augite | Non pleochroic (colourless), second order birefringence (blue-pink), inclined straight extinction angle=37° |
| 0.2-0.6 | 4 | Quartz | |
| 0.2-0.9 | 2 | Plagioclase | Non pleochroic (colourless), first order birefringence, straight extinction |
| 0.2-0.4 | 1 | Oxides | |

| 0.1-05 | 1 | Aenigmatite | Strongly pleochroic (red to brown), fourth order birefringence |
|--------|---|-------------|----------------------------------------------------------------|

**Texture:** This rock consists of alkali feldspars, fine-grained quartz, anhedral ferro-edenite, interstitial augite, elongated plagioclase as well as secondary oxides. This rock display granophyric texture. The ferro-edenite is zoned and is replacing augite. Aenigmatite occurs around augite grains

**Rock type:** Akali-syenite

## MC7028 – MAFIC DYKE

| Grain size(mm) | Modal % | Mineral | Description |
|----------------|---------|---------|-------------|
| 0.2-1.0 | 61 | Orthoclase | Non pleochroic (colourless), first order birefringence, straight extinction |
| 1.0-2.1 | 15 | Clinopyroxene | Weakly pleochroic (colourless to light brown), second order birefringence (bluish-pink), inclined extinction angle 33° |
| 0.1-0.6 | 10 | Hornblende | Strongly pleochroic (greenish to pale brown), second order birefringence (orange to blue), extinction angle 37° |
| 0.3-0.6 | 7 | Plagioclase | Non pleochroic (colourless), first order birefringence, straight extinction |
| 0.2-0.6 | 4 | Quartz | Has undulose extinction |
| 0.1-0.3 | 2 | Biotite | Weakly pleochroic (dark brownish to brown), second order birefringence, platy and replacing hornblende |
| 0.1-0.4 | 1 | Oxides | Fine sub-euhedral |

**Texture:** This is a medium grained rock containing intercumulate alkali feldspar, elongated plagioclase, anhedral clinopyroxenes, hornblende, secondary biotite, quartz and minor amount of oxides. Most of the orthoclase is zoned while most clino-pyroxene grains are rimmed by hornblende indicating a replacement texture. The plagioclases display polysythetic twins. The biotite is replacing hornblende grains. This thin section is similar to MC7002 and MC7049.

**Rock type:** Basalt

## MC7029 – QUARTZ PORPHYRIC LEUCOCRATIC SYENITE

| Grain size(mm) | Modal % | Mineral | Description |
|---|---|---|---|
| 0.4-1.6 | 79 | Alkali feldspars | Non pleochroic (colourless), first order birefringence, straight extinction |
| 0.3-1.7 | 15 | Quartz | sub-euhedral and has undulose extinction |
| 0.2-0.6 | 3 | Arfvedsonite | Strongly pleochroic (brownish-green to blue), second order birefringence, inclined extinction angle 32° |
| 0.1-0.4 | 2 | Augite | Non pleochroic (colourless), Second order birefringence (pinkish to blue), straight extinction |
| 0.2-0.9 | 1 | Oxides | Fined grained |

**Texture:** This leucocratic rock consists of alkali feldspars, quartz, minor amount of arfvedsonite and diopside. Alkali feldspars and quartz shows bimodal grain size distribution. The alkali feldspars display a mesoperthitic texture and some of the grains are zoned. The oxides consist of two different morphologies, first type is fine blocky texture and second type is skeletal (spongy) texture and occurs mostly in arfvedsonite grains.

**Rock type:** Alkali-Syenite

## MC7029 –ALAKLI- SYENITE

| Grain size(mm) | Modal % | Mineral | Description |
|---|---|---|---|
| 0.4-1.5 | 79 | Orthoclase | Non pleochroic (colourless), first order birefringence, straight extinction |
| 0.3-1.5 | 15 | Quartz | Has undulose extinction |
| 0.2-0.6 | 3 | Arfvedsonite | Strongly pleochroic (brownish-green to blue), second order birefringence, inclined extinction angle 28° |
| 0.1-0.4 | 2 | Augite | Weakly pleochroic (colourless), second order birefringence (pinkish to blue), inclined extinction angle 26° |

| 0.2-0.9 | 1 | Oxides | Fined grained |

**Texture:** This is a medium grained leucocratic rock containing bimodal grain size distribution of orthoclase and quartz. The anhedral arfvedsonite and subhedral diopside occur as interstitial in orthoclase matrix. Oxides occur mostly in arfvedsonite grains and randomly distributed throughout the thin section. Oxides display a re-melting texture (spongy texture) in orthoclase matrix.

**Rock type:** Alkali-syenite

## MC7030 – ORTHOGNEISS

| Grain size(mm) | Modal % | Mineral | Description |
|---|---|---|---|
| 0.4-1.4 | 70 | Plagioclase | Non pleochroic (colourless), first order birefringence, straight extinction and has polysynthetic twins |
| 0.5-1.6 | 10 | Orthoclase | Non pleochroic (colourless), first order birefringence, straight extinction |
| 0.2 – 0.4 | 10 | Biotite | Strongly pleochroic (light brown to dark brown), second order birefringence, straight extinction |
| 0.2-0.7 | 5 | Quartz | Has undulose extinction |
| 0.4-0.8 | 4 | Hornblende | Strongly pleochroic (greenish to greenish-brown), second order birefringence (dark green to orange), inclined extinction angle 31° |
| 0.1-0.4 | 1 | Diopside | Weakly pleochroic (colourless to light cream), second order birefringence (pink to blue) |
| 0.1-0.2 | tr | Zircon | Weakly pleochroic (colourless), third order birefringence |

**Texture:** This rock is containing plagioclase, orthoclase, elongated platy biotite, quartz, anhedral hornblende and minor amount of diopside and accessory zircons. This rock displays a myrmekite texture as well as granophyric texture. There is no sense of grains orientation except that the biotites are elongated and always align in the same direction (dextral sense of shear). The diopside is sub-euhedral and skeletal. Trace amount of zircon occurs in biotite and feldspar matrix.

**Rock type:** Gneiss

## MC7031 – FELSIC DYKE

| Grain size(mm) | Modal % | Mineral | Description |
|---|---|---|---|
| 0.1-0.7 | 65 | Quartz | undulose extinction |

| 0.3-.1.2 | 5 | Alkali-feldspar | Non pleochroic (colourless), first order birefringence, straight extinction |
| 0.2-0.7 | 30 | Crystal fibrous | Spherulites consists of radiating arrays of crystal fibre |

**Texture:** This rock contains fine-grained recrystalized quartz, K-feldspar phenocrysts and is characterized by spherulites, which indicate that was formed at high-temperature.

**Rock type:** Rhyolite

## MC7032 – FELSIC DYKE

| Grain size(mm) | Modal % | Mineral | Description |
|---|---|---|---|
| 0.1-0.3 | 98 | Quartz | Has undulose extinction |
| 0.2-0.4 | 2 | K-feldspar | This is sub-euhedral phenocrysts |

**Texture:** This is a rhyolite rock containing intergrowth of quartz and K-feldspar phenocryst

**Rock type:** Rhyolite

## MC7033 – MICRO-GRANITE

| Grain size(mm) | Modal % | Mineral | Description |
|---|---|---|---|
| 0.1-0.6 | 62 | K-feldspar | Non pleochroic (colourless), first order birefringence, straight extinction |
| 0.1-0.4 | 15 | Augites | Weakly pleochroic (colourless), second order birefringence (pinkish orange), straight extinction |
| 0.2-1.2 | 13 | Arfvedsonite | Strongly pleochroic (pale-yellow to greenish-blue), second order birefringence (greenish-blue orange), straight extinction |
| 0.4-1.0 | 10 | | Has undulose extinction |

**Texture:** This rock consists of fine-grained recrystalized quartz, anhedral and elongated augite anhedral arfvedsonite and minor amount of alkali –feldspar. The feldspars display perthitic to mesoperthite texture. The augite is replaced by arfvedsonite.

**Rock type:** Micro-granite

## MC7034 – FELSIC DYKE

| Grain size(mm) | Modal % | Mineral | Description |
|---|---|---|---|
| 0.1-0.2 | 59 | Alkali Feldspar | Non pleochroic (colourless), first order birefringence, straight extinction |

| 0.1-03 | 36 | Quartz | showing undulose extinction |
|---|---|---|---|
| 0.5-1.3 | 4 | K-feldspar phenocrysts | Non pleochroic (colourless), first order birefringence, straight extinction |
| 0.1-0.2 | 1 | Pyroxene | Weakly pleochroic (colourless), second order birefringence (pinkish blue), straight extinction |
| 0.1-0.5 | tr | Aenigmatite | Strongly pleochroic (red to-brown), fourth order birefringence |

**Texture:** This is a rhyolite rock containing K-feldspar phenocrysts, elongated alkali feldspars and euhedral pyroxene. Aenigmatite randomly distributed through the section

**Rock type:** Rhyolite

## MC7035 – FELSIC DYKE

| Grain size(mm) | Modal % | Mineral | Description |
|---|---|---|---|
| 0.1-0.2 | 55 | Quartz | Very fine-grained and has undulose extinction |
| 0.1-0.4 | 40 | K-feldspar | Elongated fined grained |
| 0.2-0.5 | 5 | Spherulites | |

**Texture:** This is a very fine-grained rock and very difficult to identify minerals.

**Rock type:** Rhyolite

## MC7036 – MAFIC DYKE

| Grain size(mm) | Modal % | Mineral | Description |
|---|---|---|---|
| 0.1-0.3 | 40 | Alkali feldspar | Non pleochroic (colourless), first order birefringence, straight extinction |
| 0.1-0.5 | 31 | Chlorite | Weakly pleochroic (brownish to light green), first order birefringence, extinction angle 32°. |
| 0.2-0.3 | 24 | Diopside | Weakly pleochroic (colourless), second order birefringence (bluish-pink), straight extinction |
| 0.1-0.3 | 5 | Oxides | Some of the oxides are elongated and some are sub-euhedral and randomly orientated. |

**Texture:** This is a medium grained rock consisting mainly of elongated alkali feldspars, anhedral diopside, secondary chlorite and minor amount of elongated oxides. The feldspar is altered to sericite. This is a very weathered rock and is similar to MC7002.

**Rock type:** Basalt

## MC7037 – FELSIC DYKE

| Grain size(mm) | Modal % | Mineral | Description |
|---|---|---|---|
| 0.3-0.6 | 95 | Crystalites | Fibres crystals displaying radiating arrays under XPL |
| 0.2-1.3 | 5 | K-feldspar phenocrysts | Non pleochroic (colourless), first order birefringence, straight extinction |

**Texture:** This rock contains feldspar phenocrysts set on spherulites matrix. The spherulites seem to have formed from either quartz or/and feldspars. Alkali feldspars are coarse sub-euhedral in shape and altered. Some of the phenocrysts seem to be dislocated.

**Rock type:** Rhyolite

## MC7038 – FELSIC DYKE

| Grain size(mm) | Modal % | Mineral | Description |
|---|---|---|---|
| 0.3-0.4 | 75 | Alkali feldspar | Non pleochroic (colourless), first order birefringence, straight extinction |
| 0.1-0.3 | 20 | Quartz | |
| 0.4-0.6 | 3 | Orthoclase-phenocrysts | Non pleochroic (colourless), first order birefringence, straight extinction |
| 0.1-0.3 | 1 | Oxides | Fine sub-euhedral oxides |
| 0.1-0.2 | 1 | Aegirine | Weakly pleochroic (brownish green), second order birefringence (pinkish-orange), straight extinction |

**Texture:** This rock consists of tabular orthoclase phenocrysts, elongated alkali feldspars that have carlsbad twins. There is minor amount of interstitial aegirine, and secondary oxides

**Rock type:** Rhyolite

## MC7039 – MONZONITE

| Grain size(mm) | Modal % | Mineral | Description |
|---|---|---|---|
| 0.3-1.6 | 59 | Alkali feldspar | Non pleochroic (colourless), first order birefringence, straight extinction |
| 0.3-1.2 | 14 | Ferro-edenite | Strongly pleochroic (brown to green blue), second order birefringence, straight extinction |
| 0.5-1.5 | 13 | Plagioclase | Non pleochroic (colourless), first order birefringence, straight extinction |
| 0.3-0.7 | 5 | Quartz | |

| 0.4-1.5 | 4 | Ferro-augite-ferro-hedenbergite | Weakly pleochroic (colourless to light brown), second order birefringence), inclined extinction angle 32° |
|---|---|---|---|
| 0.2-1.2 | 3 | Oxides | Fined grained |
| 0.2-0.4 | 2 | Chlorite | Weakly pleochroic (light green to brown), first order birefringence |
| 0.1-0.13 | tr | Zircon | Non pleochroic (colourless), third order birefringence (bluish pink) |

**Texture:** This is medium grained rock containing elongated alkali feldspar that has perthitic texture, plagioclase, and minor amount of ferro-augite, and secondary chlorite and oxides. The ferro-augite and ferro-hedenbergite are replaced by ferro-edenite. Chlorite is replacing both ferro-augite and ferro-edenite. The oxide consists of two different morphologies, first type is fine blocky texture and second type is skeletal (spongy) texture and occurs mostly in ferro-edenite grains. Accessory minerals include zircons and monazite and are randomly distributed.

**Rock type:** Monzonite

**MC7040 – MONZONITE**

| Grain size(mm) | Modal % | Mineral | Description |
|---|---|---|---|
| 0.6-1.6 | 60 | Mesoperthite | Non pleochroic (colourless), first order birefringence, straight extinction |
| 0.4-1.0 | 20 | Plagioclase | Non pleochroic (colourless), first order birefringence, straight extinction |
| 0.4-1.2 | 15 | Ferro-edenite | Strongly pleochroic (pale brown to green), second order birefringence, inclined extinction angle 40° |
| 0.2-0.9 | 2 | Ferro-augite | Weakly pleochroic (colourless to light brown), second order birefringence (orange to pink), straight extinction |
| 0.3-0.7 | 2 | Quartz | |
| 0.2-1.2 | 1 | Oxides | |

**Texture:** This rock consists of mesoperthite feldspar, ferro-edenite, interstitial ferro-augite, minor amount of quartz and oxides. The core of the alkali feldspar displays a plagioclase with polysynthetic twinning while the rim is completely mesoperthite. The ferro-edenite is replacing the ferro-augite. The

oxide consists of two different morphologies, first type is fine blocky texture and second type is skeletal (spongy) texture and occurs mostly in ferro-edenite grains.

**Rock type:** Monzonite

## MC7041 – MONZONITE

| Grain size(mm) | Modal % | Mineral | Description |
|---|---|---|---|
| 0.3-1.6 | 60 | Alkali feldspars | Non pleochroic (colourless), first order birefringence, straight extinction |
| 0.3-1.5 | 15 | Ferro-edenite | Strongly pleochroic, (light brown to green), second order birefringence (orange), straight extinction |
| 0.2-0.5 | 9 | Ferro-augite | Weakly pleochroic (light brown to colourless) second order birefringence (greenish pink), straight extinction and euhedral |
| 0.3-0.7 | 4 | Quartz | |
| 0.1-0.4 | 1 | Chlorite | Weakly pleochroic (brown to light green), second order birefringence |
| 0.2-1.2 | 1 | Oxides | |

**Texture:** This is a very altered rock, which consists of feldspars that are altered to sericite, skeletal ferro-augite and ferro-edenite. The ferro-edenite seem to be replacing ferro-augite while the chlorite is replacing ferro-edenite. The oxide consists of two different morphologies, first type is fine blocky texture and second type is skeletal (spongy) texture and occurs mostly in ferro-edenite grains. This rock is similar to MC7039 and MC7040

**Rock type**: Monzonite

## MC7042 – GABBRO

| Grain size(mm) | Modal % | Mineral | Description |
|---|---|---|---|
| 0.5-1.7 | 66 | Alkali feldspars | Non pleochroic (colourless), first order birefringence, straight extinction |
| 0.2-1.0 | 20 | Chlorite | Weakly pleochroic (light green to light brown), second |

| Grain size(mm) | Modal % | Mineral | Description |
|---|---|---|---|
| | | | order birefringence |
| 0.3-0.7 | 6 | Augite | Weakly pleochroic (colourless) second order birefringence (bluish-pink), inclined extinction angle 25° |
| 0.1-0.6 | 5 | Biotite | Weakly pleochroic (dark brown), second order birefringence, straight extinction |
| 0.3-1.4 | 3 | Oxides | |

**Texture:** This rock consists of elongated plagioclase feldspars, augite, secondary chlorite, biotite and oxides. The alkali feldspars have anorthite composition of 55% and are altered to sericite. The augites are replaced by chlorite and biotite. There are two different morphologies of oxides. (1). Regional fine-grained sub-euhedral grain. (2) Reaction product –spongy texture.

**Rock type:** Gabbro

## MC7043 – FELSIC DYKE

| Grain size(mm) | Modal % | Mineral | Description |
|---|---|---|---|
| 0.1-0.3 | 92 | Alkali feldspar | Non pleochroic (colourless), first order birefringence, straight extinction |
| 0.2-0.4 | 6 | Chlorite | Weakly pleochroic (light green), first order birefringence |
| 0.1-0.4 | 1 | Quartz | |
| 0.1-0.3 | 1 | Oxides | Randomly distributed |

**Texture:** This rock consists mainly of tabular/elongated alkali feldspars, and minor amount of oxides.

**Rock type:** Rhyolite

## MC7044 – FELSIC DYKE

| Grain size(mm) | Modal % | Mineral | Description |
|---|---|---|---|
| 0.1-0.7 | 65 | Quartz | |
| 0.2-0.7 | 30 | Crystal fibrous | Strongly pleochroic (brown to blue), first order birefringence, spherulites consist of radiating arrays of crystal fibre. |
| 0.2-0.6 | 5 | Arfvedsonite | Strongly pleochroic (green to blue), second order birefringence, very altered & difficult to measure the extinction angle |

**Texture:** This rock contains fine-grained recrystalized quartz, spherulites as well as minor amount of arfvedsonite. The texture of this rock indicates that was formed due to the process of devitrification**.**

**Rock type**: Rhyolite

## MC7045 – GABBRO

| Grain size(mm) | Modal % | Mineral | Description |
|---|---|---|---|

| 0.2-1.2 | 49 | Plagioclase | Non pleochroic (colourless), first order birefringence, straight extinction |
|---------|-----|-------------|------------------------------------------------------------------------------|
| 0.2-0.9 | 30 | Augite | Weakly pleochroic (colourless to weakly brown), second order birefringence (pink to blue), inclined extinction angle =26° |
| 0.3-0.8 | 15 | Chlorite | Weakly pleochroic (light green to brown), first order birefringence |
| 0.2-0.7 | 5 | Biotite | Strongly pleochroic (light brown to dark brown), second order birefringence, straight extinction |
| 0.1-0.7 | 1 | Oxides | |

**Texture:** This is a coarse-grained rock consist of elongated plagioclase, skeletal augite, and minor amount of chlorite and biotite. Both chlorite and biotite seem to be replacing augite. Oxides are randomly distributed.

**Rock type:** Gabbro

## MC7046 – GRANITE

| Grain size(mm) | Modal % | Mineral | Description |
|----------------|---------|---------|-------------|
| 0.2-1.7 | 60 | Mesoperthite | Non pleochroic (colourless), first order birefringence, straight extinction |
| 0.2-1.5 | 35 | Quartz | Has undulose extinction |
| 0.3-1.3 | 3 | Arfvedsonite | Strongly pleochroic (greenish-brown to blue), second order birefringence (greenish pink), straight extinction |
| 0.2-0.5 | 1 | Augite | Weakly pleochroic (colourless to weakly brown), second order birefringence (pink to blue), inclined extinction angle=37° |
| 0.1-0.9 | 1 | Aenigmatite | Strongly pleochroic (red to brown), fourth order birefringence |
| 0.3-0.5 | tr | Oxides | |

**Texture:** This is a coarse-grained rock consisting of coarse-grained mesoperthite feldspar, fine euhedral quartz, arfvedsonite and minor amount of skeletal augite, aenigmatite and oxides. The arfvedsonite is zoned indicating compositional change.

**Rock type:** Granite

## MC7047 – FELSIC DYKE

| Grain size(mm) | Modal % | Mineral | Description |
|----------------|---------|---------|-------------|
| 0.2-1.4 | 62 | Mesoperthite | Non pleochroic (colourless), first order birefringence, straight extinction |
| 0.1-0.5 | 30 | Quartz | |
| 0.3-1.2 | 5 | Orthoclase | Non pleochroic (colourless), first order birefringence, straight extinction |

| 0.2-0.6 | 2 | Hornblende | Strongly coloured (dark-green to brown), second order birefringence, inclined extinction angle 36° |
| 0.1-0.14 | 1 | Diopside | Weakly pleochroic (colourless to weakly brown), second order birefringence (pink to blue), inclined extinction angle 43° |
| 0.2-0.4 | tr | Aenigmatite | Strongly pleochroic (red to brown), fourth order birefringence |

**Texture:** This is a medium grained rock consisting of mesoperthite, quartz, orthoclase, hornblende and minor amount of diopside and aenigmatite. The mesoperthite show bimodal grain size distribution, while the hornblende occurs as interstitial in feldspathic matrix. Aenigmatite occurs in the core of the hornblende grains.

**Rock type:** Rhyolite

## MC7048 – GABBRO

| Grain size(mm) | Modal % | Mineral | Description |
|---|---|---|---|
| 0.2-1.6 | 69 | Plagioclase | Non pleochroic (colourless), first order birefringence, straight extinction |
| 0.1-0.3 | 18 | Augite | Weakly pleochroic (colourless to light brown), second order birefringence, (yellowish light), straight extinction |
| 0.4-1.3 | 10 | Orthoclase | Non pleochroic (colourless), first order birefringence, straight extinction |
| 0.2-0.3 | 2 | Chlorite | Weakly pleochroic (weak green to green), first order birefringence |
| 0.1-0.4 | 1 | Biotite | Weakly pleochroic (brown to weak brown), second order birefringence |
| 0.1-0.5 | tr | Oxides | |
| 0.1-0.3 | tr | Aenigmatite | Strongly pleochroic (red to brown), fourth order birefringence |

**Texture:** This rock consists of elongated plagioclase, orthoclase, and augite. The plagioclases are prismatic, zoned and randomly distributed. The augite is replaced by chlorite and biotite. Oxides display a spongy texture while the aenigmatite is randomly distributed.

**Rock type:** Gabbro

## MC7049 – GABBRO

| Grain size(mm) | Modal % | Mineral | Description |
|---|---|---|---|
| 0.5- 1.8 | 28 | Arfvedsonite | Strongly pleochroic (brown to dark green), 120° cleavage angle, second order birefringence, extinction angle=20° |
| 0.3-0.5 | 27 | Orthoclase | Non pleochroic (colourless), first order birefringence, straight extinction |

| 0.3-0.5 | 21 | Plagioclase | Non pleochroic (colourless), first order birefringence, straight extinction |
|---|---|---|---|
| 0.2-0.6 | 20 | Augite | Weakly pleochroic (colourless to light brown), second order birefringence, (yellowish light), inclined extinction angle=28° |
| 0.3-0.4 | 2 | Quartz | |
| 0.1-0.5 | 1 | Chlorite | Weakly Pleochroic (colourless to light green), second order birefringence |
| 0.2-0.4 | 1 | Oxides | |
| 0.1-0.3 | tr | Sericite | Non pleochroic (colourless), second order birefringence |
| 0.1-0.14 | tr | Zircon | Non pleochroic (colourless), third order birefringence (bluish pink) |

**Texture:** This rock consists mainly of plagioclase, arfvedsonite, skeletal augite and minor amount of quartz. The plagioclases are elongated, strongly zoned and altered to sericite. Some of the plagioclase displays a triple junction. The arfvedsonite seem to be replacing augite while chlorite is replacing arfvedsonite.

**Rock type:** gabbro

**MC7050 – GABBRO**

| Grain size(mm) | Modal % | Mineral | Description |
|---|---|---|---|
| 0.3-0.5 | 45 | Plagioclase | Non pleochroic (colourless), first order birefringence, straight extinction |
| 0.4-1.2 | 31 | Arfvedsonite | Strongly pleochroic (greenish- brown to blue), 120° cleavage angle, second order birefringence, extinction angle 20° |
| 0.2-0.6 | 10 | Augite | Weakly pleochroic (colourless to light brown), second order birefringence, (yellowish light), inclined extinction angle 28° |
| 0.3-0.4 | 7 | Quartz | |
| 0.3-0.5 | 5 | Orthoclase | Non pleochroic (colourless), first order birefringence, straight extinction |
| 0.1-0.5 | 2 | Chlorite | Weakly pleochroic (colourless to light green), first order birefringence |
| 0.1-0.3 | tr | Sericite | Non pleochroic (colourless), second order birefringence |
| 0.1-0.4 | tr | Oxides | Non pleochroic (black), first order birefringence |

**Texture:** This rock consists of elongated plagioclase, orthoclase, arfvedsonite, skeletal augite, and minor amount of oxides. The plagioclase and orthoclase is strongly zoned, display polysynthetic twins. Some of the plagioclase displays a triple junction. The arfvedsonite seem to be replacing augite. The chlorite is replacing both arfvedsonite and clinopyroxene. This rock is similar to MC7049

**Rock type:** Gabbro

## MC7051 – MICRO-GRANITE WITH A XENOLITH

## MC7051 – MICRO-GRANITE

| Grain size(mm) | Modal % | Mineral | Description |
|---|---|---|---|
| 0.2-1.1 | 60 | Mesoperthite | Non pleochroic (colourless), first order birefringence, straight extinction |
| 0.2-0.8 | 22 | Quartz | |
| 0.2-0.6 | 15 | Arfvedsonite | Strongly pleochroic (dark green to brown), second order birefringence |
| 0.2-0.4 | 3 | Augite | Non pleochroic (colourless) second order birefringence, inclined extinction angle=27° |

**Texture:** This medium grained rock consists of mesoperthite, quartz, interstitial augite as well as anhedral arfvedsonite. The mesoperthite is anhedral and has bimodal grain size distribution. Quartz has bimodal grain size distribution.

**Rock type:** Micro-granite

## MC7051-1 MICRO-GRANITE

| Grain size(mm) | Modal % | Mineral | Description |
|---|---|---|---|
| 0.2-1.2 | 60 | Mesoperthite | Non pleochroic (colourless), first order birefringence, straight extinction |
| 0.1-0.8 | 25 | Quartz | |
| 0.1-1.3 | 10 | Aegirine | Strongly pleochroic, (dark green to brown), second order birefringence, extinction angle 32° |
| 0.1-0.5 | 5 | Augite | Weakly pleochroic (colourless) second order birefringence (pinkish orange), inclined extinction angle=34° |
| 0.2-0.3 | tr | Aenigmatite | Strongly pleochroic (red to brown), fourth order birefringence |
| 0.5-0.5 | tr | Oxides | |

**Texture:** This is a medium grained rock that consists of mesoperthite, fine-grained quartz, aegirine, euhedral augite and trace amount of aenigmatite and oxides. The mesoperthite display bead and string texture.

**Rock type:** Micro-granite

## MC7051-2 – MICRO-GRANITE

| Grain size(mm) | Modal % | Mineral | Description |
|---|---|---|---|

| 0.2-1.2 | 55 | Mesoperthite | Non pleochroic (colourless), first order birefringence, straight extinction |
|---|---|---|---|
| 0.1-0.8 | 30 | Quartz | |
| 0.1-1.3 | 10 | Arfvedsonite | Strongly pleochroic, (brownish-green to slightly blue) first order birefringence, extinction angle 32° |
| 0.1-0.5 | 3 | Augite | Weakly pleochroic (colourless) second order birefringence (pinkish orange), inclined extinction angle 34° |
| 0.5-0.5 | 2 | Oxides | |
| 0.2-0.3 | tr | Aenigmatite | Strongly pleochroic (red to brown), fourth order birefringence |

**Texture:** This rock consists of mesoperthite, quartz, arfvedsonite and minor amount of augite, aenigmatite and oxides. Mesoperthite has bead and string texture. Oxides occur in arfvedsonite grains and randomly distributed.

**Rock type:** Micro-granite

**MC7052 – GABBRO**

| Grain size(mm) | Modal % | Mineral | Description |
|---|---|---|---|
| 0.1-0.9 | 49 | Plagioclase | Non pleochroic (colourless), first order birefringence, straight extinction |
| 0.3-1.3 | 40 | Augite | Weakly pleochroic (creamish brown), second order birefringence (pink-yellowish to blue). Inclined extinction angle=35° |
| 0.2-0.8 | 5 | Biotite | Weakly pleochroic (brown to light brown), first order birefringence, inclined extinction angle |
| 0.1-0.6 | 4 | Chlorite | Weakly pleochroic (light green to medium green), first order birefringence |
| 0.1-0.5 | 1 | Oxides | |
| 0.1-0.2 | 1 | Sulphides | |

**Texture:** This is a medium grained rock that consists of altered augite, elongated plagioclase, and secondary biotite and chlorite. The plagioclases are elongated display polysynthetic twinning and have bimodal grains size distribution. The augites are replaced by biotite, while biotite is replaced by chlorite. There is minor amount of sulphides and are randomly distributed.

**Rock type:** Gabbro

**MC7053 – FELSIC DYKE**

| Grain size(mm) | Modal % | Mineral | Description |
|---|---|---|---|
| 0.1-0.2 | 70 | Alkali feldspar | Non pleochroic (colourless), first order birefringence, straight extinction |
| 0.1-0.5 | 15 | Quartz | Showing undulose extinction |

| 0.1-0.4 | 15 | Epidote | Weakly pleochroic (light brownish to green), second order birefringence (pinkish-blue), extinction angle 33° |

**Texture:** This dyke is containing alkali feldspar, quartz and minor amount of epidote. This rock has Graphic (granophyric) texture.

**Rock type:** Trachyte

## MC7054 – FELSIC DYKE

| Grain size(mm) | Modal % | Mineral | Description |
|---|---|---|---|
| 0.1-0.3 | 85 | Quartz | |
| 0.1-0.4 | 6 | Feldspar phenocrysts | Non pleochroic (colourless), first order birefringence, straight extinction |
| 0.1-0.2 | 5 | Aegirine | Strongly pleochroic (green to brown), second order birefringence (bluish-pink), straight extinction |
| 0.1-0.2 | 4 | Richterite | Non pleochroic (blue), second order birefringence, straight extinction |

**Texture:** This rock consists of feldspar phenocrysts set in a fine quartz matrix. The alkali feldspars phenocrysts are prismatic and sub-euhedral and have granophyric texture. Richterite has a needle like shape and randomly distributed

**Rock type:** Rhyolite

## MC7055 – GRANITE

| Grain size(mm) | Modal % | Mineral | Description |
|---|---|---|---|
| 0.5-1.5 | 75 | Orthoclase | Non pleochroic (colourless), first order birefringence, straight extinction |
| 0.1-0.4 | 20 | Quartz | Has undulose extinction |
| 0.1-0.5 | 3 | Hornblende | Weakly pleochroic (brownish), second order birefringence, and difficult to measure the extinction angle, because is very altered |
| 0.2-0.4 | 1 | Plagioclase | Non pleochroic (colourless), first order birefringence, straight extinction |
| 0.1-0.5 | 1 | Aenigmatite | Strongly pleochroic (red to brown), fourth order birefringence |

**Texture:** This rock consists of orthoclase, fine-grained quartz and minor amount of hornblende and plagioclase. The orthoclase has carlsbad twins while the plagioclase has polysynthetic twins

**Rock type:** Granite

## MC7056 – MONZONITE

| Grain size(mm) | Modal % | Mineral | Description |
|---|---|---|---|
| 0.1-1.5 | 60 | Alkali feldspar | Non pleochroic (colourless), first order birefringence, straight extinction |
| 0.1-0.5 | 15 | Ferro-edenite | Strongly pleochroic (green to brown), second order birefringence (pinkish blue), 120° cleavage angle and extinction angle =40°, |
| 0.1-0.8 | 4 | Ferro-augite | Weakly pleochroic (colourless), second order birefringence (bluish-light to dark-purple), inclined extinction angle =33⁻35° |
| 0.1-0.5 | 2 | Chlorite | Weakly pleochroic (light to medium green), first order birefringence |
| 0.1-0.4 | 1 | Quartz | Has undulose extinction |
| 0.1-0.4 | 1 | Biotite | Weakly pleochroic (light brown to dark brown), first order birefringence |

**Texture:** This rock consists of alkali feldspar, interstitial ferro-augite, ferro-edenite and minor amount of secondary chlorite and biotite. The alkali feldspars display carlsbad twins. The ferro-edenite seem to be replacing ferro-augite. The ferro-edenite is replaced by biotite and chlorite.

**Rock type:** Monzonite

## MC7057 – ALKALI-SYENITE

| Grain size(mm) | Modal % | Mineral | Description |
|---|---|---|---|
| 0.1-1.2 | 74 | Orthoclase | Non pleochroic (colourless), first order birefringence, straight extinction |
| 0.1-1.3 | 15 | Microcline feldspar | Non pleochroic (colourless), first order birefringence, straight extinction |
| 0.2-0.5 | 10 | Arfvedsonite | Strongly pleochroic (brownish-green to blue), second order birefringence (pinkish blue), extinction angle=30° |
| 0.1-0.5 | 1 | Aenigmatite | Weakly pleochroic (pale yellow to red), fourth order birefringence, extinction angle 26° |

**Texture:** This rock consists of alkali feldspar, minor amount of interstitial arfvedsonite and aenigmatite. The orthoclase is elongated, interconnected and arfvedsonite is altered by aenigmatite.
**Rock type:** Alkali-syenite

## MC7058 – MONZONITE

| Grain size(mm) | Modal % | Mineral | Description |
|---|---|---|---|
| 0.1-1.6 | 91 | Alkali feldspar | Non pleochroic (colourless), first order birefringence, straight extinction |
| 0.2-0.6 | 6 | Ferro augite | Weakly pleochroic (colourless), second order birefringence (pinkish blue) extinction angle=35° |
| 0.1-0.6 | 1 | Plagioclase | None pleochroic (colourless), first order birefringence, straight extinction |
| 0.1-0.4 | 1 | Chlorite | Weakly pleochroic (light green), first order birefringence |
| 0.1-0.5 | 1 | Aenigmatite | Strongly pleochroic (red to brown), fourth order birefringence |

**Texture:** This rock consists of alkali feldspar, interstitial ferro-augite, secondary chlorite and aenigmatite. The alkali feldspars are interconnected and randomly distributed. The plagioclases are elongated and display polysynthetic twins. The ferro-augite grains are euhedral and fractured. Chlorite is replacing ferro-augite and aenigmatite occurs in ferro-augite grains.

**Rock type:** Monzonite

## MC7059 – GABBRO

| Grain size(mm) | Modal % | Mineral | Description |
|---|---|---|---|
| 0.3-1.2 | 59 | Plagioclase | Non pleochroic (colourless), first order birefringence, straight extinction |
| 0.2-0.9 | 30 | Augite | Non pleochroic (colourless) second order birefringence, inclined extinction angle 32° |
| 0.2-0.4 | 5 | Biotite | Weakly pleochroic (brown to dark brown), second order birefringence, extinction angle 31° |
| 0.2-0.4 | 5 | Chlorite | Weakly pleochroic (colourless to light green), second order birefringence, extinction angle 27° |
| 0.1-0.3 | 1 | Oxides | |

**Texture:** This rock consists of elongated plagioclase, augite, secondary biotite and chlorite and minor amount of oxides. The plagioclases display polysynthetic twins and have bimodal grain size distribution. The augites are sub-euhedral to anhedral and are replaced by biotite and chlorite. The oxides have a blocky texture and occur in and near augite grains.

**Rock type:** Gabbro

## MC7060 – ALKALI-SYENITE

| Grain size(mm) | Modal % | Mineral | Description |
|---|---|---|---|
| 0.2-1.0 | 78 | Alkali feldspars (mesoperthite) | Non pleochroic (colourless), first order birefringence, straight extinction |
| 0.5-1.6 | 5 | Orthoclase | Non pleochroic (colourless), first order birefringence, straight extinction |
| 0.3-0.6 | 6 | Aegirine | Non pleochroic (green), second order birefringence (green), straight extinction |
| 0.2-0.5 | 3 | Biotite | Strongly pleochroic (pale yellow to dark brown), second order birefringence, extinction angle 35° |
| 0.1-0.2 | 3 | Quartz | |
| 0.2-1.0 | 2 | Augite | Non pleochroic (colourless), second order birefringence (bluish), extinction angle=36° |
| 0.1-0.3 | 2 | Ferro-edenite | Strongly pleochroic (light-blue to deep blue), second order birefringence, extinction angle=32° |
| 0.1-0.4 | 1 | Aenigmatite | Strongly pleochroic (red to brown), fourth order birefringence |
| 0.1-0.15 | tr | Plagioclase | Non pleochroic (colourless), first order birefringence, straight extinction |

**Texture:** This rock consists of alkali feldspars, orthoclase, plagioclase, aegirine, mica (biotite), Augite, ferro-edenite and secondary aenigmatite. The mesoperthite show bimodal grain size and the orthoclase is zoned and have carlsbad twins. The Augite seems to be replaced by aegirine, while aegirine is replaced by ferro-edenite and mica (biotite).

**Rock type:** Alkali-syenite

## MC7061 – MICRO-GRANITE

| Grain size(mm) | Modal % | Mineral | Description |
|---|---|---|---|
| 0.2-1.0 | 60 | Alkali feldspars | Non pleochroic (colourless), first order birefringence, straight extinction |

| 0.1-0.5 | 30 | Quartz | |
|---|---|---|---|
| 0.3-0.6 | 7 | Aegirine | Weakly pleochroic (pale yellow to green), second order birefringence (green), straight extinction |
| 0.1-0.3 | 3 | Arfvedsonite | Strongly pleochroic (brown to deep indigo blue), second order birefringence, extinction angle 29° |

**Texture:** This rock consists of coarse-grained alkali feldspars, fine quartz, aegirine and magnesia arfvedsonite. The aegirine is anhedral and is replaced by magnesia arfvedsonite.

**Rock type:** Micro-granite

## MC7062 – GABBRO

| Grain size(mm) | Modal % | Mineral | Description |
|---|---|---|---|
| 0.3-1.2 | 78 | Plagioclase | Non pleochroic (colourless), first order birefringence and straight extinction |
| 0.3-0.6 | 15 | Augite | Non pleochroic (colourless), first order birefringence, inclined extinction angle=27° |
| 0.1-0.2 | 3 | Biotite | Weakly pleochroic (light brown to brown), second order birefringence, straight extinction |
| 0.1-0.15 | 2 | Chlorite | Moderate pleochroic (brown to light green), first order birefringence |
| 0.3-0.9 | 2 | Oxides | |
| 0.1-0.15 | tr | Accessory? | Non pleochroic (brown), first order birefringence |

**Texture:** This rock consists of plagioclase, augite, minor amount of biotite and chlorite. The augite is anhedral and is replaced by biotite and chlorite. The oxide occurs in and near augite grains. The accessory mineral is fine-grained and hexagonal in shape and occurs in plagioclase matrix.

**Rock type:** Gabbro

## MC7063 – GABBRO

| Grain size(mm) | Modal % | Mineral | Description |
|---|---|---|---|
| 0.2-0.6 | 64 | Alkali feldspar | Non pleochroic (colourless), first order birefringence, straight extinction |
| 0.3-0.5 | 30 | Augite | Non pleochroic (colourless), second order birefringence (bluish-yellow), inclined extinction angle 32° |
| 0.2-0.6 | 5 | Oxides | |
| 0.1-0.3 | 1 | Biotite | Weakly pleochroic (light brown to brown), second order birefringence, straight extinction |
| 01-0.17 | tr | Accessory | Non pleochroic (brown to red), first order birefringence |

**Texture:** This medium grained rock consists of alkali feldspar, augite, oxides and secondary biotite. The alkali feldspar is elongated and some of the plagioclase display polysynthetic twinning. The augites are very altered and replaced by biotite. The oxide consists of two different morphologies, first type is fine blocky texture and second type is skeletal (spongy) texture and these textures occur in augite grains. The accessory mineral is fine-grained and hexagonal in shape and occurs in augite and plagioclase matrix.

**Rock type:** Gabbro

## MC7064 – FELSIC DYKE

| Grain size(mm) | Modal % | Mineral | Description |
|---|---|---|---|
| 0.1-0.3 | 87 | Alkali feldspar | Non pleochroic (colourless), first order birefringence, straight extinction |
| 0.1-0.3 | 5 | Pyroxenes | Non pleochroic (colourless), second order birefringence (bluish-yellow), inclined extinction angle 32° |
| 0.1-0.4 | 5 | Oxides | |
| 0.1-0.2 | 3 | Aenigmatite | Strongly pleochroic (red to brown), fourth order birefringence |

**Texture:** This rock consists of elongated feldspar, interstitial pyroxenes and secondary oxides.

**Rock type:** Rhyolite

## MC7065 – MICRO-GRANITE

| Grain size(mm) | Modal % | Mineral | Description |
|---|---|---|---|
| 0.1-.0.6 | 70 | Alkali feldspar | Non pleochroic (colourless), first order birefringence, straight extinction |
| 0.2-0.5 | 15 | Aegirine | Strongly pleochroic (pale yellow to greenish-blue), second order birefringence (greenish blue), inclined extinction angle=28° |
| 0.2-0.5 | 7 | Quartz | |
| 0.2-0.5 | 4 | Richterite | Moderate pleochroic (blue to deep blue), second order birefringence (deep blue), straight extinction |
| 0.2-0.5 | 3 | Diopside | Non pleochroic (colourless), second order birefringence (bluish-yellow), straight extinction |
| 0.1-0.4 | 1 | Aenigmatite | Strongly pleochroic (red to brown), fourth order birefringence |

**Texture:** This medium grained rock consists of mesoperthite, quartz, diopside, aegirine, richterite and minor amount of aenigmatite. Diopside is replaced by aegirine and aegirine seem to be in the process of being replaced by richterite.

**Rock type:** Micro-granite

**MC7065 – MICRO-GRANITE**

| Grain size(mm) | Modal % | Mineral | Description |
|---|---|---|---|
| 0.1-.0.6 | 67 | Alkali feldspar | Non pleochroic (colourless), first order birefringence, straight extinction |
| 0.2-0.5 | 15 | Aegirine | Strongly pleochroic (pale-yellow to greenish-blue), second order birefringence (greenish blue), inclined extinction angle=28° |
| 0.2-0.5 | 10 | Quartz | |
| 0.2-0.5 | 4 | Richterite | Moderate pleochroic (blue to deep indigo blue), second order birefringence (deep blue to ), straight extinction |
| 0.2-0.5 | 3 | Diopside-Hedenbergite | Non pleochroic (colourless), second order birefringence (bluish-yellow), straight extinction |
| 0.1-0.4 | 1 | Aenigmatite | Strongly pleochroic (red to brown), fourth order birefringence |

**Texture:** This rock consists of mesoperthite, quartz, diopside-hedenbergite, aegirine, richterite and minor amount of aenigmatite. Diopside is replaced by aegirine. Aegirine seem to be in the process of being replaced by the richterite.

**Rock type:** Micro-granite

**MC7066 – GABBRO**

| Grain size(mm) | Modal % | Mineral | Description |
|---|---|---|---|
| 0.3-0.6 | 67 | Plagioclase | Non pleochroic (colourless), first order birefringence, straight extinction |
| 0.3-0.6 | 20 | Augite | Non pleochroic (colourless), first order birefringence, inclined extinction angle=30° |
| 0.1-0.15 | 6 | Chlorite | Moderate pleochroic (colourless to light green), first order birefringence |
| 0.1-0.2 | 5 | Biotite | Weakly pleochroic (colourless to brown), second order birefringence, straight extinction |
| 0.3-0.9 | 2 | Oxides | |

**Texture:** This medium grained rock consists of elongated plagioclase, sub-euhedral pyroxenes and secondary chlorite and biotite. The plagioclases have bimodal grain size and have polysynthetic twins. The augites seem very unstable and are replaced by biotite and chlorite. The oxide consists of two different morphologies, first type is fine blocky texture and second type is skeletal (spongy) texture and these textures occur in augite and plagioclase matrix. The accessory mineral is hexagonal in shape and occurs in augite and plagioclase matrix.

**Rock type:** Gabbro

### MC7067 – ORTHOGNEISS

| Grain size(mm) | Modal % | Mineral | Description |
|---|---|---|---|
| 0.3-1.3 | 71 | Orthoclase | Non pleochroic (colourless), first order birefringence, straight extinction |
| 0.2-0.7 | 20 | Quartz | showing undulose extinction |
| 0.3-0.6 | 5 | Biotite | Strongly pleochroic (brown to dark brown), second order birefringence, straight extinction |
| 0.1-0.15 | 2 | Chlorite | Moderate pleochroic (colourless to light green), second order birefringence |
| 0.1-0.4 | 1 | Pyroxene | Non pleochroic (colourless), second order birefringence (bluish pink), inclined extinction angle=34° |
| 0.2-0.3 | 1 | Oxides | |
| 0.1-0.14 | tr | Zircon | Non pleochroic (colourless), third order birefringence (bluish pink) |

**Texture:** This medium grained rock consists of orthoclase, quartz, pyroxene, elongated biotite and chlorite. Most of the pyroxene grains are altered and seem to be filled with oxides. The pyroxenes are replaced by chlorite and biotite. Minor amount of zircon are seen throughout the section.

**Rock type:** Gneiss

### PD06001 –FELSIC DYKE

| Grain size(mm) | Modal % | Mineral | Description |
|---|---|---|---|
| 0.1-0.3 | 88 | Alkali feldspars | Non pleochroic (colourless), first order birefringence, straight extinction |
| 0.1-0.5 | 8 | Chlorite | Moderate pleochroic (colourless to light green), first order birefringence |
| 0.1-0.3 | 3 | Oxides | |
| 0.1-0.3 | 1 | Epidote | Weakly pleochroic (colourless to light yellow), second order birefringence (bluish green), straight extinction |

**Texture:** This rock consists of alkali feldspars, chlorite, epidote and oxides. The feldspars are elongated and altered to sericite. Chlorite and epidote are randomly distributed.

**Rock type:** Rhyolite

### PD06002 – ORTHOGNEISS

| Grain size(mm) | Modal % | Mineral | Description |
|---|---|---|---|
| 0.3-0.9 | 69 | Microcline feldspars | Non pleochroic (colourless), first order birefringence, straight extinction |

| Grain size(mm) | Modal % | Mineral | Description |
|---|---|---|---|
| 0.3-0.6 | 15 | Orthoclase | Not pleochroic (colourless), first order birefringence, straight extinction |
| 0.2-0.5 | 10 | Quartz | has undulose extinction |
| 0.2-0.4 | 5 | Biotite | Moderate pleochroic (light brown to brown), second order birefringence (greenish blue), straight extinction |
| 0.1-0.35 | 1 | Pyroxene | Non pleochroic (colourless), second order birefringence (bluish pink), inclined extinction angle=34° |
| 0.1-0.14 | tr | Zircon | Non pleochroic (colourless), third order birefringence (bluish pink) |

**Texture:** This medium grained rock consists of microcline feldspars, orthoclase, quartz, biotite, pyroxene and accessory zircon. The microclines are sub-euhedral and have bimodal grain size. The orthoclases are coarse-grained and altered to sericite. The biotites are elongated and seem to be replacing anhedral pyroxene grains. Zircon is hexagonal in shape and occurs in biotite grains and alkali feldspars matrix.

**Rock type:** Gneiss

## PD06003 – FELSIC DYKE

| Grain size(mm) | Modal % | Mineral | Description |
|---|---|---|---|
| 0.1-0.3 | 84 | Alkali feldspars | Non pleochroic (colourless), first order birefringence, straight extinction |
| 0.1-0.2 | 8 | Chlorite | Moderate pleochroic (colourless to light green), first order birefringence |
| 0.1-0.3 | 3 | Epidote | Weakly pleochroic (pale-yellow to colourless), second order birefringence (pinkish to orange), straight extinction |
| 0.1-0.3 | 3 | Oxides | |
| 0.2-0.6 | 1 | Orthoclase Phenocrysts | Non pleochroic (colourless), first order birefringence, straight extinction |
| 0.1-0.4 | 1 | Nepheline | Non pleochroic (colourless), first order birefringence and uniaxial |

**Texture:** This rock consists of orthoclase phenocrysts in alkali feldspars and chlorite matrix. The alkali feldspars are elongated and chlorites are randomly distributed. The epidote is anhedral

**Rock type:** Rhyolite

## PD06004 – GABBRO

| Grain size(mm) | Modal % | Mineral | Description |
|---|---|---|---|

| 0.2-0.7 | 49 | Alkali feldspars | Non pleochroic (colourless), first order birefringence, straight extinction |
|---|---|---|---|
| 0.2-0.5 | 35 | Aegirine | Strongly pleochroic (brown to greenish brown), second order birefringence (orange), straight extinction |
| 0.2-0.4 | 8 | Augite | Non pleochroic (colourless) second order birefringence, straight extinction |
| 0.1-0.3 | 5 | Chlorite | Moderate pleochroic (colourless to light green), first order birefringence |
| 0.1-0.3 | 3 | oxides | |

**Texture:** This rock consists of elongated feldspars, aegirine, augite and chlorite. The augite seems to be replaced by aegirine and chlorite. The oxide consists of two different morphologies, first type is fine blocky texture and second type is skeletal (spongy) texture and these textures occur in pyroxene and plagioclase matrix.

**Rock type:** Gabbro

## PD06005 – FELSIC DYKE

| Grain size(mm) | Modal % | Mineral | Description |
|---|---|---|---|
| 0.2-0.5 | 69 | Alkali feldspar | Non pleochroic (colourless), first order birefringence, straight extinction |
| 0.2-0.4 | 13 | Diopside | Non pleochroic (colourless) second order birefringence, straight extinction |
| 0.2-0.4 | 10 | Biotite | Weakly pleochroic (light brown to brown), second order birefringence (orange), straight extinction |
| 0.3-0.5 | 5 | Quartz | |
| 0.2-0.5 | 3 | Chlorite | Moderate pleochroic (pale yellow to light green), second order birefringence |
| 0.2-0.4 | tr | Oxides | |

**Texture:** This rock consists of alkali feldspars, diopside, quartz and secondary biotite and chlorite. The diopside is replaced by biotite and chlorite. The oxides are blocky

**Rock type:** Rhyolite

## PD06007 – FELSIC DYKE

| Grain size(mm) | Modal % | Mineral | Description |
|---|---|---|---|

| 0.1-0.17 | 95 | Needle like-mineral | Pleochroic (dark black to blue), first order birefringence. |
| 0.2-0.4 | 2 | Alkali feldspar phenocrysts | Non pleochroic (colourless), first order birefringence, straight extinction |
| 0.1-0.17 | 1 | Quartz | Quartz |
| 0.1-0.3 | 1 | Epidote | Weakly pleochroic (pale-yellow to green), second order birefringence (pinkish to orange), inclined extinction angle=33° |
| 0.1-0.3 | 1 | Aegirine | Non pleochroic (green), second order birefringence (greenish pink), straight extinction |

**Texture:** This is a very fine-grained porphyric dyke, consists of feldspar phenocrysts in quartz-needle-like mineral matrix. There is minor occurrence of epidote and aegirine in quartz needle-like mineral matrix. The alkali feldspar phenocrysts display a granophyric texture.

**Rock type:** Rhyolite

### PD06008 – GRANITE

| Grain size(mm) | Modal % | Mineral | Description |
|---|---|---|---|
| 0.2-0.8 | 60 | Mesoperthite | Non pleochroic (colourless), first order birefringence, straight extinction and has carlsbad twins |
| 0.3-0.5 | 30 | Quartz | Has undulose extinction |
| 0.3-0.6 | 5 | Aegirine | Strongly pleochroic (brownish to green), second order birefringence (greenish), inclined extinction angle=26° |
| 0.3-0.7 | 3 | Arfvedsonite | Moderate pleochroic (light blue to deep blue), second order birefringence (pinkish blue) and has straight extinction |
| 0.2-0.4 | 2 | Aenigmatite | Strongly pleochroic (red to brown), fourth order birefringence |

**Texture:** This rock consists of mesoperthite, quartz, zoned aegirine and arfvedsonite. The arfvedsonite mostly occurs as a rim in aegirine grains. There is Xenolith phenocrysts that display a spherulites texture in quartz matrix. Aenigmatite occurs in the core of aegirine grains.

**Rock type:** Granite

### PD06008 – XENOLITH IN GRANITE

| Grain size(mm) | Modal % | Mineral | Description |
|---|---|---|---|

| 0.2-0.5 | 80 | Mesoperthite | Non pleochroic (colourless), first order birefringence, straight extinction |
| 0.3-0.5 | 12 | Quartz | Showing undulose extinction |
| 0.3-0.6 | 6 | Arfvedsonite | Strongly pleochroic (brownish green to blue), second order birefringence (greenish), straight extinction |
| 02-0.4 | 1 | Aegirine | Non pleochroic (green), second order birefringence (pinkish blue), straight extinction |
| 0.2-0.3 | 1 | Aenigmatite | Strongly pleochroic (red to brown), fourth order birefringence |

**Texture:** This rock consists of medium grained mesoperthite, quartz, arfvedsonite, aegirine and aenigmatite. Most of the mesoperthite grains has carlsbad twins and randomly distributed while arfvedsonite is zoned and aegirine is anhedral in shape.

**Rock type:** Syenite

**PD06009 – GRANITE**

| Grain size(mm) | Modal % | Mineral | Description |
|---|---|---|---|
| 0.2-0.8 | 60 | Mesoperthite | Non pleochroic (colourless), first order birefringence, straight extinction |
| 0.3-0.5 | 28 | Quartz | Showing undulose extinction |
| 03-0.7 | 4 | Arfvedsonite | Moderate pleochroic (brown-green to blue), second order birefringence (pinkish blue), straight extinction |
| 0.3-0.6 | 3 | Aegirine | Strongly Pleochroic (brown to green), second order birefringence (greenish), inclined extinction angle=34° |
| 0.2-0.4 | 2 | Augite | Non pleochroic (colourless), second order birefringence (pinkish-blue), straight extinction |
| 0.13-0.2 | 1 | Apatite | Non pleochroic (colourless), first order birefringence, straight extinction |
| 0.13-0.25 | 1 | Titanite | Non pleochroic (colourless), second order birefringence, inclined extinction angle |
| 0.2-0.4 | 1 | Aenigmatite | Strongly pleochroic (red to brown), fourth order birefringence |

**Texture:** This rock consists of mesoperthite, fine-grained quartz, zoned arfvedsonite, aegirine, augite, aenigmatite and accessory minerals such as apatite and titanite. Arfvedsonite seem to be replacing aegirine

**Rock type:** Granite

**PD060010 – ALKALI-SYENITE**

| Grain size(mm) | Modal % | Mineral | Description |
|---|---|---|---|
| 0.3-0.5 | 90 | Alkali feldspars | Non pleochroic (colourless), first order birefringence, |

| Grain size(mm) | Modal % | Mineral | Description |
|---|---|---|---|
| | | | straight extinction |
| 0.2-0.5 | 5 | Quartz | |
| 0.2-0.6 | 3 | Biotite | Weakly pleochroic (light brown to brown), second order birefringence, straight extinction |
| 0.2-0.3 | 2 | Diopside | Non pleochroic (colourless), second order birefringence (orange), straight extinction |
| 0.2-0.4 | tr | Oxides | |
| 0.1-0.14 | tr | Zircon | Non pleochroic (colourless), third order birefringence (bluish pink) |

**Texture:** This rock consists of alkali feldspars, fine-grained quartz, diopside, secondary biotite, oxides as well as zircons. The alkali feldspars are zoned and have bimodal grains size distribution. Biotite is replacing diopside. Oxides occur in biotite grains and zircons are seen in feldspars matrix.

**Rock type:** Alkali-syenite

## PD060011 – GABBRO

| Grain size(mm) | Modal % | Mineral | Description |
|---|---|---|---|
| 0.2-0.7 | 35 | Alkali feldspars | Non pleochroic (colourless), first order birefringence, straight extinction |
| 0.2-0.4 | 53 | Augite | Not pleochroic (colourless) second order birefringence, inclined extinction angle=30° |
| 0.1-0.3 | 7 | Chlorite | Moderate pleochroic (colourless to light green),second order birefringence |
| 0.2-0.3 | 3 | Biotite | Moderate pleochroic (light brown to dark brown), second order birefringence (bluish-pink), straight extinction |
| 0.1-0.3 | 2 | Oxides | |

**Texture:** This rock consists of elongated feldspars, augite, secondary biotite and chlorite. The augite is replaced by biotite and chlorite. The oxide consists of two different morphologies, first type is fine blocky texture and second type is skeletal (spongy) texture and these textures occur in augite and feldspar matrix.

**Rock type:** Gabbro

Appendix 1.3 : Mineral Chemistry Analysis:  Orthopyroxene and Augite analysis
Re-calculated to 6O

| Thin Section | MC7002 | MC7002 | MC7002 | MC7039 | MC7039 | MC7039 |
|---|---|---|---|---|---|---|
| Circle No | C3 | C4 | C4 | | | |
| Location | core | core | core | | | |
| | | | | | | |
| **Wt % oxides** | | | | | | |
| SiO$_2$ | 49.95 | 49.25 | 48.65 | 49.89 | 49.96 | 49.96 |
| TiO$_2$ | 1.71 | 1.96 | 2.23 | 0.13 | 0.18 | 0.11 |
| Al$_2$O$_3$ | 3.91 | 4.86 | 5.34 | 0.81 | 0.77 | 0.89 |
| Cr$_2$O$_3$ | 0.00 | 0.00 | 0.00 | 0.00 | 0.00 | 0.00 |
| FeO | 10.65 | 10.73 | 11.14 | 35.97 | 36.18 | 36.08 |
| MnO | 0.23 | 0.14 | 0.19 | 0.96 | 0.97 | 0.95 |
| MgO | 12.77 | 13.00 | 12.41 | 1.12 | 1.09 | 1.16 |
| CaO | 19.31 | 19.59 | 19.49 | 11.10 | 11.00 | 10.99 |
| Na$_2$O | 0.53 | 0.53 | 0.48 | 0.21 | 0.25 | 0.25 |
| K$_2$O | 0.00 | 0.00 | 0.02 | 0.08 | 0.09 | 0.08 |
| **Total** | **99.06** | **100.06** | **99.93** | **100.27** | **100.48** | **100.47** |
| | | | | | | |
| | | | | | | |
| Si | 1.89 | 1.84 | 1.83 | 2.08 | 2.08 | 2.08 |
| Al | 0.11 | 0.16 | 0.17 | -0.08 | -0.08 | -0.08 |
| S T-site | 2.00 | 2.00 | 2.00 | 2.00 | 2.00 | 2.00 |
| | | | | | | |
| Al | 0.06 | 0.06 | 0.07 | 0.12 | 0.12 | 0.12 |
| Ti | 0.05 | 0.06 | 0.06 | 0.00 | 0.01 | 0.00 |
| Mg | 0.60 | 0.60 | 0.58 | 0.04 | 0.04 | 0.05 |
| Fe | 0.28 | 0.28 | 0.29 | 0.80 | 0.80 | 0.80 |
| Mn | 0.01 | 0.00 | 0.01 | 0.03 | 0.03 | 0.03 |
| S M1-site | 1.00 | 1.00 | 1.00 | 1.00 | 1.00 | 1.00 |
| | | | | | | |
| Fe/Mg | 0.17 | 0.17 | 0.17 | 0.37 | 0.37 | 0.37 |
| | | | | | | |
| Fe | 0.06 | 0.06 | 0.06 | 0.46 | 0.46 | 0.46 |
| Mg | 0.12 | 0.12 | 0.12 | 0.03 | 0.02 | 0.03 |
| Ca | 0.78 | 0.79 | 0.78 | 0.50 | 0.49 | 0.49 |
| Na | 0.04 | 0.04 | 0.03 | 0.02 | 0.02 | 0.02 |
| K | 0.00 | 0.00 | 0.00 | 0.00 | 0.00 | 0.00 |
| S M2-site | 1.00 | 1.00 | 1.00 | 1.00 | 1.00 | 1.00 |
| | | | | | | |
| **Endmember calculation** | | | | | | |
| Wo (Ca) | 0.47 | 0.47 | 0.47 | 0.37 | 0.37 | 0.37 |
| En (Mg) | 0.36 | 0.36 | 0.35 | 0.03 | 0.03 | 0.03 |
| Fs (Fe) | 0.17 | 0.17 | 0.18 | 0.60 | 0.60 | 0.60 |

Appendix 1.3: Mineral Chemistry analysis: Aegirine and Ferrohedenbergite
Recalculated to 6O

| Thin Section No | MC7015 | MC7015 | MC7015 | MC7015 | MC7015 | MC7015 | MC7015 | MC7015 | MC7015 | MC7015 | MC7015 | MC7015 | MC7015 | MC7015 | MC7015 | MC7015 | MC7015 |
|---|---|---|---|---|---|---|---|---|---|---|---|---|---|---|---|---|---|
| Circle No | C1 | C1 | C1 | C1 | C2 | C2 | C2 | C2 | C2 | C2 | C3 | C3 | C3 | C3 | C3 | C3 | C3 |
| Location | core | core | core | core | core | core | core | core | | | | core | core | core | core | core | core |
| **Wt % oxides** | | | | | | | | | | | | | | | | | |
| $SiO_2$ | 53.49 | 53.52 | 54.42 | 53.27 | 54.53 | 54.71 | 53.65 | 53.45 | 53.56 | 53.40 | 53.41 | 53.77 | 53.06 | 53.51 | 54.20 | 54.00 | 54.20 |
| $TiO_2$ | 1.77 | 1.07 | 1.16 | 0.86 | 1.55 | 1.98 | 1.31 | 1.16 | 1.19 | 1.92 | 1.65 | 1.01 | 2.21 | 1.49 | 0.86 | 0.46 | 0.49 |
| $Al_2O_3$ | 0.39 | 0.39 | 0.42 | 0.37 | 0.37 | 0.49 | 0.34 | 0.42 | 0.40 | 0.52 | 0.38 | 0.51 | 0.42 | 0.44 | 0.37 | 0.40 | 0.46 |
| $Cr_2O_3$ | 0.00 | 0.00 | 0.00 | 0.00 | 0.00 | 0.00 | 0.00 | 0.00 | 0.00 | 0.00 | 0.00 | 0.00 | 0.00 | 0.00 | 0.00 | 0.00 | 0.00 |
| $Fe_2O_3$ | 32.31 | 33.30 | 32.97 | 33.24 | 32.27 | 32.31 | 32.74 | 33.04 | 32.83 | 32.28 | 32.07 | 32.59 | 31.38 | 32.21 | 34.16 | 34.83 | 34.42 |
| FeO | 29.08 | 29.96 | 29.67 | 29.91 | 29.04 | 29.07 | 29.46 | 29.73 | 29.54 | 29.04 | 28.86 | 29.32 | 28.23 | 28.98 | 30.73 | 31.34 | 30.97 |
| MnO | 0.21 | 0.21 | 0.42 | 0.23 | 0.42 | 0.42 | 0.13 | 0.00 | 0.10 | 0.26 | 0.33 | 0.34 | 0.21 | 0.21 | 0.18 | 0.13 | 0.11 |
| MgO | 0.13 | 0.14 | 0.15 | 0.17 | 0.17 | 0.17 | 0.09 | 0.00 | 0.06 | 0.14 | 0.18 | 0.23 | 0.07 | 0.17 | 0.14 | 0.01 | 0.09 |
| CaO | 1.02 | 0.82 | 0.39 | 0.61 | 0.25 | 0.23 | 1.97 | 1.88 | 2.61 | 1.44 | 0.30 | 0.25 | 1.57 | 1.45 | 0.19 | 0.15 | 0.16 |
| $Na_2O$ | 12.08 | 12.09 | 12.80 | 12.42 | 12.80 | 12.75 | 11.63 | 11.56 | 11.15 | 11.82 | 12.64 | 12.71 | 11.98 | 11.89 | 12.82 | 12.83 | 12.80 |
| $K_2O$ | 0.02 | 0.03 | 0.05 | 0.02 | 0.00 | 0.00 | 0.00 | 0.00 | 0.00 | 0.00 | 0.00 | 0.00 | 0.00 | 0.00 | 0.00 | 0.00 | 0.00 |
| **Total** | **101.42** | **101.56** | **102.78** | **101.19** | **102.37** | **103.05** | **101.87** | **101.52** | **101.90** | **101.77** | **100.96** | **101.41** | **100.89** | **101.37** | **102.91** | **102.80** | **102.72** |
| | | | | | | | | | | | | | | | | | |
| Si | 2.00 | 1.99 | 1.99 | 1.98 | 2.00 | 2.00 | 2.00 | 2.00 | 2.00 | 1.99 | 1.99 | 1.99 | 1.99 | 2.00 | 1.98 | 1.98 | 1.99 |
| $Al^{IV}$ | 0.00 | 0.01 | 0.01 | 0.02 | 0.00 | 0.00 | 0.00 | 0.00 | 0.00 | 0.01 | 0.01 | 0.01 | 0.01 | 0.00 | 0.02 | 0.02 | 0.01 |
| S T-site | 2.00 | 2.00 | 2.00 | 2.00 | 2.00 | 2.00 | 2.00 | 2.00 | 2.00 | 2.00 | 2.00 | 2.00 | 2.00 | 2.00 | 2.00 | 2.00 | 2.00 |
| | | | | | | | | | | | | | | | | | |
| $Al^{VI}$ | 0.02 | 0.01 | 0.01 | 0.00 | 0.02 | 0.02 | 0.01 | 0.02 | 0.02 | 0.01 | 0.01 | 0.02 | 0.01 | 0.02 | 0.00 | 0.00 | 0.01 |
| Ti | 0.05 | 0.03 | 0.03 | 0.02 | 0.04 | 0.05 | 0.04 | 0.03 | 0.03 | 0.05 | 0.05 | 0.03 | 0.06 | 0.04 | 0.02 | 0.01 | 0.01 |
| $Fe^{3+}$ | 0.76 | 0.81 | 0.84 | 0.86 | 0.80 | 0.77 | 0.75 | 0.75 | 0.72 | 0.74 | 0.82 | 0.85 | 0.75 | 0.76 | 0.88 | 0.91 | 0.89 |
| Mg | 0.01 | 0.01 | 0.01 | 0.01 | 0.01 | 0.01 | 0.01 | 0.00 | 0.00 | 0.01 | 0.01 | 0.01 | 0.00 | 0.01 | 0.01 | 0.00 | 0.00 |
| $Fe^{2+}$ | 0.17 | 0.14 | 0.11 | 0.10 | 0.13 | 0.14 | 0.19 | 0.19 | 0.22 | 0.18 | 0.11 | 0.10 | 0.18 | 0.17 | 0.09 | 0.08 | 0.09 |
| S M1-site | 1.00 | 1.00 | 1.00 | 1.00 | 1.00 | 1.00 | 1.00 | 1.00 | 1.00 | 1.00 | 1.00 | 1.00 | 1.00 | 1.00 | 1.00 | 1.00 | 1.00 |
| | | | | | | | | | | | | | | | | | |
| $Fe^{2+}$ | 0.08 | 0.09 | 0.06 | 0.07 | 0.06 | 0.07 | 0.08 | 0.09 | 0.08 | 0.08 | 0.06 | 0.07 | 0.06 | 0.07 | 0.08 | 0.08 | 0.08 |
| Ca | 0.04 | 0.03 | 0.02 | 0.02 | 0.01 | 0.01 | 0.08 | 0.08 | 0.10 | 0.06 | 0.01 | 0.01 | 0.06 | 0.06 | 0.01 | 0.01 | 0.01 |
| Na | 0.88 | 0.87 | 0.91 | 0.90 | 0.91 | 0.90 | 0.84 | 0.84 | 0.81 | 0.85 | 0.91 | 0.91 | 0.87 | 0.86 | 0.91 | 0.91 | 0.91 |
| *S M2-site* | 1.00 | 0.99 | 0.98 | 0.99 | 0.99 | 0.99 | 1.00 | 1.00 | 1.00 | 0.99 | 0.99 | 0.99 | 0.99 | 0.99 | 0.99 | 1.00 | 1.00 |

Appendix 1.3: Mineral Chemistry analysis: Aegirine and Ferrohedenbergite
Recalculated to 6O

| Thin Section No | MC7015 | MC7015 | MC7015 | MC7015 | MC7015 | MC7015 | MC7015 | MC7015 | MC7015 | MC7015 | MC7015 | MC7015 | MC7015 | MC7015 | MC7015 | MC7015 | MC7015 |
|---|---|---|---|---|---|---|---|---|---|---|---|---|---|---|---|---|---|
| Circle No | C1 | C1 | C1 | C1 | C2 | C2 | C2 | C2 | C2 | C2 | C3 | C3 | C3 | C3 | C3 | C3 | C3 |
| Location | core | core | core | core | core | core | core | core | | | | core | core | core | core | core | core |
| Endmember calculation | | | | | | | | | | | | | | | | | |
| Wo (Ca) | 0.19 | 0.18 | 0.12 | 0.18 | 0.07 | 0.06 | 0.29 | 0.28 | 0.31 | 0.23 | 0.09 | 0.09 | 0.26 | 0.24 | 0.07 | 0.07 | 0.06 |
| En (Mg) | 0.03 | 0.04 | 0.06 | 0.07 | 0.06 | 0.06 | 0.02 | 0.00 | 0.01 | 0.03 | 0.07 | 0.11 | 0.02 | 0.04 | 0.07 | 0.00 | 0.05 |
| Fs (Fe) | 0.78 | 0.78 | 0.82 | 0.75 | 0.87 | 0.89 | 0.69 | 0.72 | 0.68 | 0.74 | 0.84 | 0.81 | 0.72 | 0.72 | 0.86 | 0.92 | 0.89 |

Appendix 1.3: Mineral Chemistry analysis: Aegirine and Ferrohedenbergite
Recalculated to 6O

| Thin Section No | MC7015 | MC7015 | MC7015 | MC7015 | MC717 |
|---|---|---|---|---|---|
| Circle No | C3 | C5 | C5 | C5 | C1 |
| Location | core | core | core | core | core |
| Wt % oxides | | | | | |
| $SiO_2$ | 54.25 | 54.31 | 53.79 | 54.15 | 53.64 |
| $TiO_2$ | 1.39 | 0.44 | 1.53 | 1.63 | 1.25 |
| $Al_2O_3$ | 0.41 | 0.41 | 0.44 | 0.44 | 0.32 |
| $Cr_2O_3$ | 0.00 | 0.00 | 0.00 | 0.00 | 0.00 |
| $Fe_2O_3$ | 33.60 | 34.77 | 32.14 | 32.19 | 33.21 |
| FeO | 30.24 | 31.29 | 28.92 | 28.96 | 29.88 |
| MnO | 0.18 | 0.19 | 0.24 | 0.23 | 0.11 |
| MgO | 0.12 | 0.01 | 0.20 | 0.21 | 0.04 |
| CaO | 0.53 | 0.20 | 0.82 | 0.99 | 1.76 |
| $Na_2O$ | 12.59 | 12.70 | 12.43 | 12.27 | 11.59 |
| $K_2O$ | 0.00 | 0.00 | 0.00 | 0.00 | 0.00 |
| Total | 103.08 | 103.03 | 101.57 | 102.11 | 101.90 |
| | | | | | |
| Si | 1.99 | 1.99 | 2.00 | 2.00 | 2.00 |
| $Al^{IV}$ | 0.01 | 0.01 | 0.00 | 0.00 | 0.00 |
| S T-site | 2.00 | 2.00 | 2.00 | 2.00 | 2.00 |
| | | | | | |
| $Al^{VI}$ | 0.01 | 0.01 | 0.02 | 0.02 | 0.01 |
| Ti | 0.04 | 0.01 | 0.04 | 0.05 | 0.03 |
| $Fe^{3+}$ | 0.83 | 0.88 | 0.80 | 0.77 | 0.75 |
| Mg | 0.01 | 0.00 | 0.01 | 0.01 | 0.00 |
| $Fe^{2+}$ | 0.13 | 0.10 | 0.13 | 0.16 | 0.20 |
| S M1-site | 1.00 | 1.00 | 1.00 | 1.00 | 1.00 |
| | | | | | |
| $Fe^{2+}$ | 0.08 | 0.08 | 0.07 | 0.07 | 0.09 |
| Ca | 0.02 | 0.01 | 0.03 | 0.04 | 0.07 |
| Na | 0.89 | 0.90 | 0.89 | 0.88 | 0.84 |
| *S M2-site* | 0.99 | 0.99 | 0.99 | 0.99 | 1.00 |

Appendix 1.3: Mineral Chemistry analysis: Aegirine and Ferrohedenbergite
Recalculated to 6O

| Thin Section No | MC7015 | MC7015 | MC7015 | MC7015 | MC717 |
|---|---|---|---|---|---|
| Circle No | C3 | C5 | C5 | C5 | C1 |
| Location | core | core | core | core | core |
| Endmember calc | | | | | |
| Wo (Ca) | 0.14 | 0.07 | 0.18 | 0.19 | 0.26 |
| En (Mg) | 0.04 | 0.01 | 0.06 | 0.05 | 0.01 |
| Fs (Fe) | 0.82 | 0.92 | 0.75 | 0.76 | 0.73 |

Appendix 1.3: Mineral Chemistry analysis: Sodic amphibole

Re calculated to 16O

| Thin Section | MC7015 | MC7015 | MC7015 | MC7010-1 | MC7010-1 | MC7010-1 | MC7010-1 | MC7010-1 | MC7010-1 | MC7010-1 | MC7010-1 | MC7010-1 | MC7010-1 | MC7010-1 | MC7010-1 | MC7010-1 | MC7010-1 |
|---|---|---|---|---|---|---|---|---|---|---|---|---|---|---|---|---|---|
| Circle No | C1 | C1 | C2 | C1 | C1 | C1 | C1 | C1 | C1 | C1 | C1 | C1 | C1 | C1 | C1 | C1 | C1 |
| Location | | | | core | core | core | core | core | core | core | rim | rim | core | core | core | core | core |
| **Wt % oxides** | | | | | | | | | | | | | | | | | |
| SiO2 | 55.80 | 59.55 | 55.61 | 50.96 | 52.26 | 51.11 | 49.65 | 50.86 | 50.44 | 50.14 | 51.70 | 51.38 | 51.11 | 51.50 | 50.89 | 51.05 | 51.35 |
| TiO2 | 0.48 | 0.43 | 0.35 | 1.88 | 2.15 | 2.14 | 1.25 | 1.29 | 1.24 | 1.22 | 1.96 | 1.95 | 2.03 | 1.92 | 1.41 | 1.20 | 1.34 |
| Al2O3 | 0.37 | 2.99 | 0.36 | 0.32 | 0.25 | 0.28 | 0.72 | 0.91 | 0.85 | 0.77 | 0.30 | 0.33 | 0.27 | 0.28 | 0.26 | 0.19 | 0.19 |
| Fe2O3 | 0.00 | 0.00 | 0.00 | 0.00 | 0.00 | 0.00 | 0.00 | 0.00 | 0.00 | 0.00 | 0.00 | 0.00 | 0.00 | 0.00 | 0.00 | 0.00 | 0.00 |
| FeO | 20.78 | 17.41 | 20.85 | 32.80 | 33.06 | 32.45 | 32.28 | 32.69 | 32.82 | 32.94 | 32.54 | 32.72 | 32.66 | 32.51 | 33.20 | 33.03 | 33.14 |
| MnO | 3.67 | 2.98 | 3.23 | 0.80 | 0.73 | 0.78 | 0.66 | 0.67 | 0.67 | 0.63 | 0.71 | 0.67 | 0.71 | 0.72 | 0.87 | 0.88 | 0.85 |
| MgO | 5.06 | 4.23 | 5.16 | 0.25 | 0.31 | 0.25 | 1.50 | 1.59 | 1.55 | 1.55 | 0.26 | 0.28 | 0.27 | 0.28 | 0.32 | 0.29 | 0.35 |
| CaO | 0.05 | 0.00 | 0.10 | 0.26 | 0.30 | 0.31 | 3.02 | 3.23 | 3.07 | 3.20 | 0.24 | 0.25 | 0.26 | 0.26 | 0.37 | 0.43 | 0.44 |
| Na2O | 9.15 | 8.29 | 9.17 | 8.34 | 8.25 | 7.98 | 6.68 | 6.75 | 6.70 | 6.69 | 8.31 | 8.13 | 8.27 | 8.15 | 7.77 | 7.65 | 7.62 |
| K2O | 3.74 | 3.89 | 3.88 | 1.55 | 1.87 | 1.88 | 1.25 | 1.25 | 1.25 | 1.20 | 1.70 | 1.74 | 1.62 | 1.64 | 2.18 | 2.37 | 2.35 |
| Total | 99.10 | 99.76 | 98.70 | 97.15 | 99.19 | 97.16 | 97.01 | 99.24 | 98.59 | 98.31 | 97.71 | 97.46 | 97.19 | 97.26 | 97.27 | 97.09 | 97.63 |
| | | | | | | | | | | | | | | | | | |
| Si | 8.00 | 8.00 | 8.00 | 8.00 | 8.00 | 8.00 | 8.00 | 8.00 | 8.00 | 8.00 | 8.00 | 8.00 | 8.00 | 8.00 | 8.00 | 8.00 | 8.00 |
| S T-site | 8.00 | 8.00 | 8.00 | 8.00 | 8.00 | 8.00 | 8.00 | 8.00 | 8.00 | 8.00 | 8.00 | 8.00 | 8.00 | 8.00 | 8.00 | 8.00 | 8.00 |
| | | | | | | | | | | | | | | | | | |
| AlVI | 0.06 | 0.47 | 0.06 | 0.06 | 0.05 | 0.05 | 0.14 | 0.17 | 0.16 | 0.14 | 0.05 | 0.06 | 0.05 | 0.05 | 0.05 | 0.03 | 0.03 |
| Ti | 0.05 | 0.04 | 0.04 | 0.22 | 0.25 | 0.25 | 0.15 | 0.15 | 0.15 | 0.15 | 0.23 | 0.23 | 0.24 | 0.22 | 0.17 | 0.14 | 0.16 |
| Fe3+ | 2.33 | 1.96 | 2.35 | 1.06 | 1.17 | 1.12 | 0.00 | 0.00 | 0.00 | 0.00 | 1.29 | 1.19 | 1.11 | 1.32 | 1.15 | 1.36 | 1.33 |
| Fe2+ | 0.17 | 0.00 | 0.16 | 3.24 | 3.07 | 3.13 | 4.35 | 4.30 | 4.35 | 4.39 | 2.92 | 3.07 | 3.16 | 2.91 | 3.21 | 2.96 | 2.98 |
| Mg | 1.08 | 0.85 | 1.11 | 0.06 | 0.07 | 0.06 | 0.36 | 0.37 | 0.37 | 0.37 | 0.06 | 0.07 | 0.06 | 0.07 | 0.07 | 0.07 | 0.08 |
| Mn | 0.45 | 0.34 | 0.39 | 0.11 | 0.09 | 0.10 | 0.09 | 0.09 | 0.09 | 0.08 | 0.09 | 0.09 | 0.09 | 0.09 | 0.12 | 0.12 | 0.11 |
| S C-site | 4.13 | 3.66 | 4.11 | 4.75 | 4.69 | 4.71 | 5.09 | 5.08 | 5.12 | 5.14 | 4.64 | 4.70 | 4.72 | 4.66 | 4.77 | 4.69 | 4.70 |
| | | | | | | | | | | | | | | | | | |
| Ca | 0.01 | 0.00 | 0.02 | 0.04 | 0.05 | 0.05 | 0.52 | 0.54 | 0.52 | 0.55 | 0.04 | 0.04 | 0.04 | 0.04 | 0.06 | 0.07 | 0.07 |
| Na | 1.99 | 2.00 | 1.98 | 1.96 | 1.95 | 1.95 | 1.48 | 1.46 | 1.48 | 1.45 | 1.96 | 1.96 | 1.96 | 1.96 | 1.94 | 1.93 | 1.93 |
| S B-site | 2.00 | 2.00 | 2.00 | 2.00 | 2.00 | 2.00 | 2.00 | 2.00 | 2.00 | 2.00 | 2.00 | 2.00 | 2.00 | 2.00 | 2.00 | 2.00 | 2.00 |
| | | | | | | | | | | | | | | | | | |
| Na | 0.55 | 0.16 | 0.57 | 0.58 | 0.50 | 0.47 | 0.61 | 0.60 | 0.58 | 0.61 | 0.53 | 0.50 | 0.55 | 0.50 | 0.43 | 0.40 | 0.37 |
| K | 0.68 | 0.67 | 0.71 | 0.31 | 0.37 | 0.37 | 0.26 | 0.25 | 0.25 | 0.24 | 0.34 | 0.35 | 0.32 | 0.33 | 0.44 | 0.47 | 0.47 |
| S A-site | 1.24 | 0.83 | 1.28 | 0.89 | 0.86 | 0.85 | 0.86 | 0.85 | 0.83 | 0.86 | 0.87 | 0.84 | 0.88 | 0.82 | 0.87 | 0.87 | 0.84 |

Appendix 1.3: Mineral Chemistry analysis: Sodic amphibole

Re calculated to 16O

| Thin Section | MC7010-1 | MC7010-1 | MC7010-1 | MC7010-1 | MC7010-1 | MC7010-1 | MC7010-1 | MC7010-1 | MC7010-1 | MC7010-1 | MC7010-1 | MC7010-1 | MC7010-1 | MC7010-1 | MC7010-1 | MC7010-1 | MC7010-1 |
|---|---|---|---|---|---|---|---|---|---|---|---|---|---|---|---|---|---|
| Circle No | C1 | C1 | C1 | C1 | C1 | C2 | C2 | C2 | C2 | C2 | C2 | C2 | C2 | C2 | C2 | C2 | C3 |
| Location | core | core | rim | rim | rim | rim | core | core | core | core | core | rim | | | core | rim | rim |
| **Wt % oxides** | | | | | | | | | | | | | | | | | |
| SiO2 | 52.23 | 51.78 | 51.16 | 51.87 | 51.52 | 53.78 | 53.78 | 52.17 | 53.31 | 53.51 | 53.02 | 54.74 | 54.30 | 53.99 | 53.35 | 54.16 | 51.28 |
| TiO2 | 1.28 | 1.41 | 1.72 | 1.59 | 1.93 | 0.60 | 0.64 | 0.58 | 0.69 | 0.65 | 0.59 | 3.87 | 0.64 | 0.63 | 0.67 | 3.07 | 1.44 |
| Al2O3 | 0.17 | 0.25 | 0.36 | 0.26 | 0.17 | 0.34 | 0.38 | 0.35 | 0.42 | 0.40 | 0.39 | 0.34 | 0.39 | 0.40 | 0.39 | 0.40 | 0.30 |
| Fe2O3 | 0.00 | 0.00 | 0.00 | 0.00 | 0.00 | 0.00 | 0.00 | 0.00 | 0.00 | 0.00 | 0.00 | 0.00 | 0.00 | 0.00 | 0.00 | 0.00 | 0.00 |
| FeO | 33.68 | 33.66 | 33.21 | 33.41 | 33.28 | 29.67 | 28.89 | 28.37 | 29.01 | 29.35 | 29.19 | 26.69 | 29.51 | 29.53 | 28.98 | 27.28 | 32.99 |
| MnO | 0.85 | 0.88 | 0.76 | 0.77 | 0.73 | 0.20 | 0.27 | 0.32 | 0.28 | 0.24 | 0.18 | 0.29 | 0.20 | 0.22 | 0.28 | 0.24 | 0.71 |
| MgO | 0.26 | 0.31 | 0.20 | 0.32 | 0.27 | 0.18 | 0.72 | 0.60 | 0.65 | 0.43 | 0.36 | 0.23 | 0.29 | 0.40 | 0.47 | 0.21 | 0.64 |
| CaO | 0.38 | 0.38 | 0.24 | 0.27 | 0.21 | 3.82 | 5.17 | 4.97 | 4.87 | 4.83 | 4.52 | 1.92 | 4.41 | 4.43 | 4.30 | 1.93 | 0.40 |
| Na2O | 7.84 | 7.76 | 8.10 | 8.24 | 8.06 | 10.40 | 9.68 | 9.44 | 9.58 | 9.61 | 10.27 | 11.81 | 10.21 | 10.03 | 10.05 | 11.65 | 8.02 |
| K2O | 2.29 | 2.22 | 1.73 | 1.73 | 1.71 | 0.00 | 0.08 | 0.12 | 0.13 | 0.03 | 0.00 | 0.01 | 0.03 | -0.01 | 0.00 | 0.01 | 1.75 |
| Total | 98.99 | 98.65 | 97.47 | 98.45 | 97.88 | 98.98 | 99.61 | 96.92 | 98.94 | 99.05 | 98.53 | 99.90 | 99.99 | 99.63 | 98.49 | 98.95 | 97.53 |
| | | | | | | | | | | | | | | | | | |
| Si | 8.00 | 8.00 | 8.00 | 8.00 | 8.00 | 8.00 | 8.00 | 8.00 | 8.00 | 8.00 | 8.00 | 8.00 | 8.00 | 8.00 | 8.00 | 8.00 | 8.00 |
| S T-site | 8.00 | 8.00 | 8.00 | 8.00 | 8.00 | 8.00 | 8.00 | 8.00 | 8.00 | 8.00 | 8.00 | 8.00 | 8.00 | 8.00 | 8.00 | 8.00 | 8.00 |
| | | | | | | | | | | | | | | | | | |
| AlVI | 0.03 | 0.05 | 0.07 | 0.05 | 0.03 | 0.06 | 0.07 | 0.06 | 0.07 | 0.07 | 0.07 | 0.06 | 0.07 | 0.07 | 0.07 | 0.07 | 0.05 |
| Ti | 0.15 | 0.16 | 0.20 | 0.18 | 0.23 | 0.07 | 0.07 | 0.07 | 0.08 | 0.07 | 0.07 | 0.43 | 0.07 | 0.07 | 0.08 | 0.34 | 0.17 |
| Fe3+ | 1.45 | 1.25 | 1.13 | 1.26 | 1.21 | 1.83 | 1.48 | 1.45 | 1.45 | 1.57 | 1.48 | 1.48 | 1.75 | 1.67 | 1.64 | 1.59 | 1.16 |
| Fe2+ | 2.86 | 3.10 | 3.21 | 3.04 | 3.11 | 1.86 | 2.11 | 2.19 | 2.19 | 2.10 | 2.20 | 1.78 | 1.88 | 1.99 | 2.00 | 1.78 | 3.14 |
| Mg | 0.06 | 0.07 | 0.05 | 0.07 | 0.06 | 0.04 | 0.16 | 0.14 | 0.14 | 0.10 | 0.08 | 0.05 | 0.06 | 0.09 | 0.11 | 0.05 | 0.15 |
| Mn | 0.11 | 0.12 | 0.10 | 0.10 | 0.10 | 0.02 | 0.03 | 0.04 | 0.04 | 0.03 | 0.02 | 0.04 | 0.02 | 0.03 | 0.04 | 0.03 | 0.09 |
| S C-site | 4.66 | 4.74 | 4.76 | 4.71 | 4.74 | 3.88 | 3.93 | 3.95 | 3.97 | 3.94 | 3.93 | 3.83 | 3.86 | 3.92 | 3.92 | 3.86 | 4.77 |
| | | | | | | | | | | | | | | | | | |
| Ca | 0.06 | 0.06 | 0.04 | 0.04 | 0.04 | 0.61 | 0.82 | 0.82 | 0.78 | 0.77 | 0.73 | 0.30 | 0.70 | 0.70 | 0.69 | 0.30 | 0.07 |
| Na | 1.94 | 1.94 | 1.96 | 1.96 | 1.96 | 1.39 | 1.18 | 1.18 | 1.22 | 1.23 | 1.27 | 1.70 | 1.30 | 1.30 | 1.31 | 1.70 | 1.93 |
| S B-site | 2.00 | 2.00 | 2.00 | 2.00 | 2.00 | 2.00 | 2.00 | 2.00 | 2.00 | 2.00 | 2.00 | 2.00 | 2.00 | 2.00 | 2.00 | 2.00 | 2.00 |
| | | | | | | | | | | | | | | | | | |
| Na | 0.39 | 0.39 | 0.50 | 0.51 | 0.46 | 1.61 | 1.62 | 1.62 | 1.57 | 1.56 | 1.73 | 1.65 | 1.61 | 1.59 | 1.61 | 1.64 | 0.49 |
| K | 0.45 | 0.44 | 0.34 | 0.34 | 0.34 | 0.00 | 0.02 | 0.02 | 0.02 | 0.01 | 0.00 | 0.00 | 0.01 | 0.00 | 0.00 | 0.00 | 0.35 |
| S A-site | 0.84 | 0.82 | 0.84 | 0.85 | 0.80 | 1.61 | 1.63 | 1.65 | 1.60 | 1.57 | 1.73 | 1.65 | 1.62 | 1.58 | 1.61 | 1.64 | 0.84 |

Appendix 1.3: Mineral Chemistry analysis: Sodic amphibole

Re calculated to 16O

| Thin Section | MC7010-1 | MC7010-1 | MC7010-1 | MC7010-1 | MC7010-1 | MC7010-1 | MC7010-1 | MC7010-1 | MC7010-1 | MC7010-1 | MC7015 | MC7015 | MC7015 | MC7015 | MC7015 | MC7015 | MC7017 |
|---|---|---|---|---|---|---|---|---|---|---|---|---|---|---|---|---|---|
| Circle No | C3 | C3 | C3 | C3 | C3 | C3 | C3 | C3 | C3 | C4 | C3 | C3 | C3 | C3 | C3 | C3 | C1 |
| Location | core | core | core | core | core | core | core | core | core | core | | | core | | | | |
| **Wt % oxides** | | | | | | | | | | | | | | | | | |
| SiO2 | 50.03 | 49.79 | 50.99 | 51.06 | 50.79 | 50.89 | 50.38 | 50.89 | 50.38 | 51.25 | 55.31 | 54.84 | 54.85 | 54.75 | 54.81 | 54.36 | 52.54 |
| TiO2 | 1.30 | 1.26 | 1.94 | 1.92 | 1.90 | 1.16 | 1.18 | 1.16 | 1.18 | 0.99 | 0.59 | 0.59 | 0.54 | 0.60 | 0.63 | 0.67 | 2.18 |
| Al2O3 | 0.86 | 0.79 | 0.37 | 0.46 | 0.30 | 0.88 | 0.71 | 0.88 | 0.71 | 0.16 | 0.78 | 0.40 | 0.59 | 0.45 | 0.46 | 0.63 | 0.20 |
| Fe2O3 | 0.00 | 0.00 | 35.96 | 0.00 | 0.00 | 0.00 | 0.00 | 0.00 | 0.00 | 0.00 | 0.00 | 0.00 | 0.00 | 0.00 | 0.00 | 0.00 | 0.00 |
| FeO | 31.30 | 32.03 | | 32.46 | 32.34 | 32.88 | 32.84 | 32.88 | 32.84 | 33.22 | 21.31 | 20.53 | 20.07 | 20.94 | 20.80 | 20.27 | 32.62 |
| MnO | 0.67 | 0.68 | 0.67 | 0.71 | 0.73 | 0.71 | 0.74 | 0.71 | 0.74 | 0.61 | 1.92 | 2.92 | 3.14 | 2.94 | 3.02 | 3.09 | 0.81 |
| MgO | 1.81 | 1.67 | 0.36 | 0.38 | 0.45 | 1.21 | 1.15 | 1.21 | 1.15 | 0.47 | 6.06 | 5.33 | 5.45 | 5.35 | 5.01 | 5.37 | 0.52 |
| CaO | 3.46 | 3.45 | 0.27 | 0.30 | 0.29 | 2.61 | 2.84 | 2.61 | 2.84 | 0.37 | 0.09 | 0.02 | 0.05 | 0.00 | 0.07 | 0.10 | 0.35 |
| Na2O | 6.43 | 6.61 | 8.13 | 8.24 | 8.25 | 7.00 | 6.88 | 7.00 | 6.88 | 7.62 | 9.44 | 9.11 | 9.11 | 8.98 | 8.83 | 8.88 | 8.39 |
| K2O | 1.22 | 1.26 | 1.59 | 1.64 | 1.63 | 1.38 | 1.30 | 1.38 | 1.30 | 2.60 | 3.58 | 3.58 | 3.67 | 3.66 | 3.61 | 3.66 | 1.63 |
| Total | **97.06** | **97.55** | **100.28** | **97.16** | **96.67** | **98.73** | **98.02** | **98.73** | **98.02** | **97.29** | **99.08** | **97.31** | **97.46** | **97.66** | **97.25** | **97.02** | **99.25** |
| Si | 8.00 | 8.00 | 8.00 | 8.00 | 8.00 | 8.00 | 8.00 | 8.00 | 8.00 | 8.00 | 8.00 | 8.00 | 8.00 | 8.00 | 8.00 | 8.00 | 8.00 |
| S T-site | **8.00** | **8.00** | **8.00** | **8.00** | **8.00** | **8.00** | **8.00** | **8.00** | **8.00** | **8.00** | **8.00** | **8.00** | **8.00** | **8.00** | **8.00** | **8.00** | **8.00** |
| AlVI | 0.16 | 0.15 | 0.07 | 0.08 | 0.06 | 0.16 | 0.13 | 0.16 | 0.13 | 0.03 | 0.13 | 0.07 | 0.10 | 0.08 | 0.08 | 0.11 | 0.04 |
| Ti | 0.16 | 0.15 | 0.23 | 0.23 | 0.23 | 0.14 | 0.14 | 0.14 | 0.14 | 0.12 | 0.06 | 0.06 | 0.06 | 0.07 | 0.07 | 0.07 | 0.25 |
| Fe3+ | 0.05 | 0.00 | 0.00 | 1.04 | 1.06 | 0.27 | 0.23 | 0.27 | 0.23 | 1.45 | 1.77 | 2.24 | 2.14 | 2.11 | 2.29 | 2.01 | 1.24 |
| Fe2+ | 4.13 | 4.30 | 0.00 | 3.21 | 3.20 | 4.05 | 4.13 | 4.05 | 4.13 | 2.89 | 0.81 | 0.26 | 0.31 | 0.45 | 0.25 | 0.48 | 2.92 |
| Mg | 0.43 | 0.40 | 0.08 | 0.09 | 0.11 | 0.28 | 0.27 | 0.28 | 0.27 | 0.11 | 1.31 | 1.16 | 1.18 | 1.16 | 1.09 | 1.18 | 0.12 |
| Mn | 0.09 | 0.09 | 0.09 | 0.09 | 0.10 | 0.09 | 0.10 | 0.09 | 0.10 | 0.08 | 0.24 | 0.36 | 0.39 | 0.36 | 0.37 | 0.38 | 0.10 |
| S C-site | **5.02** | **5.10** | **0.47** | **4.75** | **4.74** | **5.00** | **5.01** | **5.00** | **5.01** | **4.67** | **4.32** | **4.16** | **4.18** | **4.23** | **4.15** | **4.24** | **4.66** |
| Ca | 0.59 | 0.59 | 0.05 | 0.05 | 0.05 | 0.44 | 0.48 | 0.44 | 0.48 | 0.06 | 0.01 | 0.00 | 0.01 | 0.00 | 0.01 | 0.01 | 0.06 |
| Na | 1.41 | 1.41 | 1.95 | 1.95 | 1.95 | 1.56 | 1.52 | 1.56 | 1.52 | 1.94 | 1.99 | 2.00 | 1.99 | 2.00 | 1.99 | 1.99 | 1.94 |
| S B-site | **2.00** | **2.00** | **2.00** | **2.00** | **2.00** | **2.00** | **2.00** | **2.00** | **2.00** | **2.00** | **2.00** | **2.00** | **2.00** | **2.00** | **2.00** | **2.00** | **2.00** |
| Na | 0.59 | 0.65 | 0.52 | 0.55 | 0.57 | 0.57 | 0.60 | 0.57 | 0.60 | 0.37 | 0.66 | 0.58 | 0.58 | 0.54 | 0.51 | 0.55 | 0.53 |
| K | 0.25 | 0.26 | 0.32 | 0.33 | 0.33 | 0.28 | 0.26 | 0.28 | 0.26 | 0.52 | 0.66 | 0.67 | 0.68 | 0.68 | 0.67 | 0.69 | 0.32 |
| S A-site | **0.83** | **0.91** | **0.84** | **0.88** | **0.89** | **0.85** | **0.86** | **0.85** | **0.86** | **0.89** | **1.32** | **1.24** | **1.27** | **1.23** | **1.18** | **1.24** | **0.85** |

Appendix 1.3: Mineral Chemistry analysis: Sodic amphibole
Re calculated to 16O

| Thin Section | MC7015 | MC7015 | MC7015 | MC7015 | MC7015 | MC7015 | MC7015 | MC7015 | MC7015 | MC7017 | MC7017 | MC7017 | MC7017 | MC7017 | MC7017 | MC7017 | MC7017 |
|---|---|---|---|---|---|---|---|---|---|---|---|---|---|---|---|---|---|
| Circle No | C1 | C1 | C2 | C3 | C3 | C3 | C3 | C3 | C3 | C1 | C2 | C2 | C2 | C2 | C2 | C4 | C1 |
| Location | | | | | | core | | | | | | | | | | | core |
| **Wt % oxides** | | | | | | | | | | | | | | | | | |
| SiO2 | 55.80 | 59.55 | 55.61 | 55.31 | 54.84 | 54.85 | 54.75 | 54.81 | 54.36 | 52.54 | 51.53 | 51.11 | 53.49 | 52.15 | 51.33 | 51.76 | 51.76 |
| TiO2 | 0.48 | 0.43 | 0.35 | 0.59 | 0.59 | 0.54 | 0.60 | 0.63 | 0.67 | 2.18 | 2.15 | 2.04 | 2.18 | 2.04 | 2.00 | 1.38 | 2.15 |
| Al2O3 | 0.37 | 2.99 | 0.36 | 0.78 | 0.40 | 0.59 | 0.45 | 0.46 | 0.63 | 0.20 | 0.30 | 0.37 | 0.32 | 0.36 | 0.45 | 0.70 | 0.29 |
| Fe2O3 | 0.00 | 0.00 | 0.00 | 0.00 | 0.00 | 0.00 | 0.00 | 0.00 | 0.00 | 0.00 | 0.00 | 0.00 | 0.00 | 0.00 | 0.00 | 0.00 | 0.00 |
| FeO | 20.78 | 17.41 | 20.85 | 21.31 | 20.53 | 20.07 | 20.94 | 20.80 | 20.27 | 32.62 | 32.01 | 32.38 | 33.94 | 33.07 | 32.09 | 32.46 | 32.24 |
| MnO | 3.67 | 2.98 | 3.23 | 1.92 | 2.92 | 3.14 | 2.94 | 3.02 | 3.09 | 0.81 | 0.78 | 0.78 | 0.88 | 0.79 | 0.78 | 0.70 | 0.80 |
| MgO | 5.06 | 4.23 | 5.16 | 6.06 | 5.33 | 5.45 | 5.35 | 5.01 | 5.37 | 0.52 | 0.57 | 0.55 | 0.38 | 0.51 | 0.53 | 0.92 | 0.57 |
| CaO | 0.05 | 0.00 | 0.10 | 0.09 | 0.02 | 0.05 | 0.00 | 0.07 | 0.10 | 0.35 | 0.35 | 0.40 | 0.37 | 0.36 | 0.32 | 1.89 | 0.37 |
| Na2O | 9.15 | 8.29 | 9.17 | 9.44 | 9.11 | 9.11 | 8.98 | 8.83 | 8.88 | 8.39 | 8.27 | 8.14 | 8.61 | 8.23 | 8.19 | 7.76 | 8.44 |
| K2O | 3.74 | 3.89 | 3.88 | 3.58 | 3.58 | 3.67 | 3.66 | 3.61 | 3.66 | 1.63 | 1.78 | 1.64 | 1.75 | 1.68 | 1.65 | 1.42 | 1.59 |
| Total | **99.10** | **99.76** | **98.70** | **99.08** | **97.31** | **97.46** | **97.66** | **97.25** | **97.02** | **99.25** | **97.74** | **97.40** | **101.93** | **99.19** | **97.32** | **98.97** | **98.20** |
| Si | 8.00 | 8.00 | 8.00 | 8.00 | 8.00 | 8.00 | 8.00 | 8.00 | 8.00 | 8.00 | 8.00 | 8.00 | 8.00 | 8.00 | 8.00 | 8.00 | 8.00 |
| S T-site | **8.00** | **8.00** | **8.00** | **8.00** | **8.00** | **8.00** | **8.00** | **8.00** | **8.00** | **8.00** | **8.00** | **8.00** | **8.00** | **8.00** | **8.00** | **8.00** | **8.00** |
| AlVI | 0.06 | 0.47 | 0.06 | 0.13 | 0.07 | 0.10 | 0.08 | 0.08 | 0.11 | 0.04 | 0.05 | 0.07 | 0.06 | 0.06 | 0.08 | 0.13 | 0.05 |
| Ti | 0.05 | 0.04 | 0.04 | 0.06 | 0.06 | 0.06 | 0.07 | 0.07 | 0.07 | 0.25 | 0.25 | 0.24 | 0.25 | 0.24 | 0.23 | 0.16 | 0.25 |
| Fe3+ | 2.33 | 1.96 | 2.35 | 1.77 | 2.24 | 2.14 | 2.11 | 2.29 | 2.01 | 1.24 | 1.09 | 0.97 | 1.02 | 1.05 | 1.09 | 0.75 | 1.07 |
| Fe2+ | 0.17 | 0.00 | 0.16 | 0.81 | 0.26 | 0.31 | 0.45 | 0.25 | 0.48 | 2.92 | 3.06 | 3.27 | 3.23 | 3.19 | 3.09 | 3.45 | 3.09 |
| Mg | 1.08 | 0.85 | 1.11 | 1.31 | 1.16 | 1.18 | 1.16 | 1.09 | 1.18 | 0.12 | 0.13 | 0.13 | 0.08 | 0.12 | 0.12 | 0.21 | 0.13 |
| Mn | 0.45 | 0.34 | 0.39 | 0.24 | 0.36 | 0.39 | 0.36 | 0.37 | 0.38 | 0.10 | 0.10 | 0.10 | 0.11 | 0.10 | 0.10 | 0.09 | 0.10 |
| S C-site | **4.13** | **3.66** | **4.11** | **4.32** | **4.16** | **4.18** | **4.23** | **4.15** | **4.24** | **4.66** | **4.70** | **4.78** | **4.74** | **4.76** | **4.72** | **4.79** | **4.71** |
| Ca | 0.01 | 0.00 | 0.02 | 0.01 | 0.00 | 0.01 | 0.00 | 0.01 | 0.01 | 0.06 | 0.06 | 0.07 | 0.06 | 0.06 | 0.05 | 0.31 | 0.06 |
| Na | 1.99 | 2.00 | 1.98 | 1.99 | 2.00 | 1.99 | 2.00 | 1.99 | 1.99 | 1.94 | 1.94 | 1.93 | 1.94 | 1.94 | 1.95 | 1.69 | 1.94 |
| S B-site | **2.00** | **2.00** | **2.00** | **2.00** | **2.00** | **2.00** | **2.00** | **2.00** | **2.00** | **2.00** | **2.00** | **2.00** | **2.00** | **2.00** | **2.00** | **2.00** | **2.00** |
| Na | 0.55 | 0.16 | 0.57 | 0.66 | 0.58 | 0.58 | 0.54 | 0.51 | 0.55 | 0.53 | 0.55 | 0.54 | 0.56 | 0.51 | 0.53 | 0.64 | 0.59 |
| K | 0.68 | 0.67 | 0.71 | 0.66 | 0.67 | 0.68 | 0.68 | 0.67 | 0.69 | 0.32 | 0.35 | 0.33 | 0.33 | 0.33 | 0.33 | 0.28 | 0.31 |
| S A-site | **1.24** | **0.83** | **1.28** | **1.32** | **1.24** | **1.27** | **1.23** | **1.18** | **1.24** | **0.85** | **0.90** | **0.86** | **0.89** | **0.84** | **0.85** | **0.92** | **0.90** |

Appendix 1.3: Mineral Chemistry analysis: Sodic amphibole
Re calculated to 16O

| Thin Section | MC7017 | MC7017 | MC7017 | MC7017 | MC7017 | MC7017 | MC7017 | MC7017 | MC7017 | MC7017 | MC7017 | MC7017 | MC7017 | MC7017 | MC7017 | MC7017 | MC7018 |
|---|---|---|---|---|---|---|---|---|---|---|---|---|---|---|---|---|---|
| Circle No | C1 | C1 | C1 | C1 | C1 | C1 | C2 | C2 | C2 | C2 | C2 | C2 | C2 | C2 | C2 | C2 | |
| Location | core | core | rim | rim | core | core | core | core | core | core | core | core | core | | | | |
| **Wt % oxides** | | | | | | | | | | | | | | | | | |
| SiO2 | 51.76 | 53.09 | 52.12 | 52.14 | 52.73 | 52.35 | 51.51 | 52.59 | 52.29 | 52.82 | 52.28 | 52.59 | 52.54 | 53.21 | 52.75 | 52.36 | 52.20 |
| TiO2 | 2.15 | 2.13 | 2.38 | 2.29 | 2.03 | 2.08 | 2.20 | 2.25 | 2.24 | 2.31 | 2.41 | 2.30 | 2.39 | 2.43 | 2.26 | 2.23 | 0.76 |
| Al2O3 | 0.29 | 0.34 | 0.23 | 0.29 | 0.32 | 0.22 | 0.30 | 0.23 | 0.28 | 0.37 | 0.29 | 0.27 | 0.28 | 0.00 | 0.00 | 0.26 | 0.48 |
| Fe2O3 | 0.00 | 0.00 | 0.00 | 0.00 | 0.00 | 0.00 | 0.00 | 0.00 | 0.00 | 0.00 | 0.00 | 0.00 | 0.00 | 0.00 | 0.00 | 0.00 | 0.00 |
| FeO | 32.24 | 33.04 | 32.48 | 32.74 | 33.20 | 32.90 | 32.42 | 33.07 | 33.07 | 33.06 | 32.68 | 32.52 | 32.81 | 32.89 | 33.18 | 32.67 | 29.14 |
| MnO | 0.80 | 0.82 | 0.94 | 0.87 | 0.83 | 0.87 | 1.02 | 1.04 | 1.00 | 1.04 | 0.95 | 0.92 | 0.92 | 0.89 | 0.88 | 0.84 | 0.26 |
| MgO | 0.57 | 0.50 | 0.56 | 0.54 | 0.58 | 0.56 | 0.24 | 0.22 | 0.24 | 0.21 | 0.27 | 0.29 | 0.30 | 0.34 | 0.55 | 0.53 | 0.16 |
| CaO | 0.37 | 0.38 | 0.70 | 0.43 | 0.27 | 0.33 | 0.68 | 0.62 | 0.70 | 0.59 | 0.70 | 0.64 | 0.73 | 0.71 | 0.37 | 0.39 | 5.46 |
| Na2O | 8.44 | 8.45 | 7.92 | 8.06 | 8.10 | 8.39 | 7.82 | 7.94 | 7.94 | 8.15 | 8.11 | 8.07 | 8.01 | 7.49 | 8.32 | 8.29 | 9.07 |
| K2O | 1.59 | 1.56 | 1.73 | 1.78 | 1.70 | 1.60 | 1.97 | 1.95 | 2.06 | 2.03 | 2.04 | 2.00 | 2.05 | 2.12 | 1.74 | 1.67 | 0.00 |
| Total | 98.20 | 100.31 | 99.07 | 99.15 | 99.77 | 99.30 | 98.16 | 99.89 | 99.82 | 100.57 | 99.74 | 99.59 | 100.03 | 100.07 | 100.04 | 99.24 | 97.53 |
| | | | | | | | | | | | | | | | | | |
| Si | 8.00 | 8.00 | 8.00 | 8.00 | 8.00 | 8.00 | 8.00 | 8.00 | 8.00 | 8.00 | 8.00 | 8.00 | 8.00 | 8.00 | 8.00 | 8.00 | 8.00 |
| S T-site | 8.00 | 8.00 | 8.00 | 8.00 | 8.00 | 8.00 | 8.00 | 8.00 | 8.00 | 8.00 | 8.00 | 8.00 | 8.00 | 8.00 | 8.00 | 8.00 | 8.00 |
| | | | | | | | | | | | | | | | | | |
| AlVI | 0.05 | 0.06 | 0.04 | 0.05 | 0.06 | 0.04 | 0.05 | 0.04 | 0.05 | 0.07 | 0.05 | 0.05 | 0.05 | 0.00 | 0.00 | 0.05 | 0.09 |
| Ti | 0.25 | 0.24 | 0.27 | 0.26 | 0.23 | 0.24 | 0.26 | 0.26 | 0.26 | 0.26 | 0.28 | 0.26 | 0.27 | 0.27 | 0.26 | 0.26 | 0.09 |
| Fe3+ | 1.07 | 1.20 | 1.01 | 1.02 | 1.20 | 1.13 | 1.04 | 1.15 | 1.00 | 1.04 | 0.97 | 1.19 | 1.02 | 1.44 | 1.18 | 1.12 | 1.29 |
| Fe2+ | 3.09 | 2.96 | 3.16 | 3.18 | 3.01 | 3.08 | 3.17 | 3.06 | 3.23 | 3.15 | 3.21 | 2.95 | 3.15 | 2.69 | 3.03 | 3.05 | 2.44 |
| Mg | 0.13 | 0.11 | 0.13 | 0.12 | 0.13 | 0.13 | 0.06 | 0.05 | 0.05 | 0.05 | 0.06 | 0.07 | 0.07 | 0.08 | 0.13 | 0.12 | 0.04 |
| Mn | 0.10 | 0.10 | 0.12 | 0.11 | 0.11 | 0.11 | 0.13 | 0.13 | 0.13 | 0.13 | 0.12 | 0.12 | 0.12 | 0.11 | 0.11 | 0.11 | 0.03 |
| S C-site | 4.71 | 4.68 | 4.74 | 4.75 | 4.74 | 4.72 | 4.71 | 4.69 | 4.72 | 4.70 | 4.70 | 4.63 | 4.69 | 4.60 | 4.70 | 4.71 | 3.98 |
| | | | | | | | | | | | | | | | | | |
| Ca | 0.06 | 0.06 | 0.11 | 0.07 | 0.04 | 0.05 | 0.11 | 0.10 | 0.11 | 0.10 | 0.12 | 0.10 | 0.12 | 0.11 | 0.06 | 0.06 | 0.90 |
| Na | 1.94 | 1.94 | 1.89 | 1.93 | 1.96 | 1.95 | 1.89 | 1.90 | 1.89 | 1.90 | 1.88 | 1.90 | 1.88 | 1.89 | 1.94 | 1.94 | 1.10 |
| S B-site | 2.00 | 2.00 | 2.00 | 2.00 | 2.00 | 2.00 | 2.00 | 2.00 | 2.00 | 2.00 | 2.00 | 2.00 | 2.00 | 2.00 | 2.00 | 2.00 | 2.00 |
| | | | | | | | | | | | | | | | | | |
| Na | 0.59 | 0.53 | 0.47 | 0.47 | 0.43 | 0.54 | 0.47 | 0.44 | 0.47 | 0.49 | 0.52 | 0.48 | 0.48 | 0.30 | 0.50 | 0.52 | 1.59 |
| K | 0.31 | 0.30 | 0.34 | 0.35 | 0.33 | 0.31 | 0.39 | 0.38 | 0.40 | 0.39 | 0.40 | 0.39 | 0.40 | 0.41 | 0.34 | 0.33 | 0.00 |
| S A-site | 0.90 | 0.83 | 0.81 | 0.82 | 0.76 | 0.85 | 0.86 | 0.82 | 0.87 | 0.88 | 0.92 | 0.87 | 0.88 | 0.70 | 0.84 | 0.84 | 1.59 |

Appendix 1.3: Mineral Chemistry analysis: Sodic amphibole
Re calculated to 16O

| Thin Section | MC7018 | MC7018 | MC7018 | MC7018 | MC7018 | MC7018 | MC7018 | MC7018 | MC7018 | MC7018 | MC7018 | MC7018 | MC7018 | MC7018 | MC7018 | MC7018 | MC7018 |
|---|---|---|---|---|---|---|---|---|---|---|---|---|---|---|---|---|---|
| Circle No | | | | | | C2 | C2 | C2 | C2 | C2 | C2 | C3 | C3 | C4 | C4 | C4 | C4 |
| Location | | | | | | core | rim | core | | | rim | core | core | core | core | core | core |
| **Wt % oxides** | | | | | | | | | | | | | | | | | |
| SiO2 | 52.26 | 50.14 | 51.67 | 50.96 | 49.97 | 53.04 | 51.79 | 52.42 | 52.44 | 52.34 | 52.81 | 52.50 | 53.74 | 50.35 | 51.88 | 51.17 | 50.17 |
| TiO2 | 0.44 | 1.45 | 1.56 | 1.47 | 1.42 | 0.37 | 1.29 | 0.77 | 0.35 | 0.45 | 1.10 | 0.69 | 0.79 | 1.46 | 1.57 | 1.48 | 1.43 |
| Al2O3 | 0.39 | 0.97 | 1.00 | 0.99 | 0.91 | 0.40 | 0.75 | 0.48 | 0.47 | 0.34 | 0.50 | 0.25 | 0.35 | 0.97 | 1.01 | 0.99 | 0.91 |
| Fe2O3 | 0.00 | 0.00 | 0.00 | 0.00 | 0.00 | 0.00 | 0.00 | 0.00 | 0.00 | 0.00 | 0.00 | 0.00 | 0.00 | 0.00 | 0.00 | 0.00 | 0.00 |
| FeO | 28.58 | 29.76 | 31.01 | 30.36 | 29.88 | 29.37 | 33.14 | 29.28 | 28.72 | 28.77 | 28.97 | 29.07 | 29.67 | 29.90 | 31.16 | 30.50 | 30.02 |
| MnO | 0.30 | 0.71 | 0.70 | 0.69 | 0.64 | 0.41 | 0.71 | 0.26 | 0.29 | 0.30 | 0.28 | 0.18 | 0.15 | 0.71 | 0.71 | 0.69 | 0.65 |
| MgO | 0.40 | 2.91 | 3.06 | 2.91 | 2.95 | 0.57 | 1.18 | 0.16 | 0.41 | 0.36 | 0.19 | 0.13 | 0.23 | 2.93 | 3.08 | 2.94 | 2.97 |
| CaO | 5.57 | 4.01 | 4.23 | 4.10 | 3.97 | 9.09 | 2.38 | 5.47 | 6.76 | 5.97 | 4.55 | 3.66 | 3.62 | 4.02 | 4.24 | 4.11 | 3.98 |
| Na2O | 9.22 | 6.36 | 6.44 | 6.39 | 6.29 | 7.43 | 7.24 | 9.18 | 8.61 | 9.02 | 10.01 | 10.31 | 10.72 | 6.43 | 6.51 | 6.46 | 6.37 |
| K2O | 0.00 | 1.13 | 1.13 | 1.15 | 1.16 | 0.00 | 1.40 | 0.00 | 0.00 | 0.00 | 0.00 | 0.00 | 0.00 | 1.13 | 1.14 | 1.16 | 1.16 |
| Total | 97.17 | 97.42 | 100.80 | 99.02 | 97.19 | 100.67 | 99.88 | 98.02 | 98.05 | 97.55 | 98.42 | 96.79 | 99.29 | 97.89 | 101.29 | 99.50 | 97.65 |
| | | | | | | | | | | | | | | | | | |
| Si | 8.00 | 8.00 | 8.00 | 8.00 | 8.00 | 8.00 | 8.00 | 8.00 | 8.00 | 8.00 | 8.00 | 8.00 | 8.00 | 8.00 | 8.00 | 8.00 | 8.00 |
| S T-site | 8.00 | 8.00 | 8.00 | 8.00 | 8.00 | 8.00 | 8.00 | 8.00 | 8.00 | 8.00 | 8.00 | 8.00 | 8.00 | 8.00 | 8.00 | 8.00 | 8.00 |
| | | | | | | | | | | | | | | | | | |
| AlVI | 0.07 | 0.18 | 0.18 | 0.18 | 0.17 | 0.07 | 0.14 | 0.09 | 0.09 | 0.06 | 0.09 | 0.05 | 0.06 | 0.18 | 0.18 | 0.18 | 0.17 |
| Ti | 0.05 | 0.17 | 0.18 | 0.17 | 0.17 | 0.04 | 0.15 | 0.09 | 0.04 | 0.05 | 0.12 | 0.08 | 0.09 | 0.17 | 0.18 | 0.17 | 0.17 |
| Fe3+ | 1.44 | 0.00 | 0.00 | 0.00 | 0.00 | 0.74 | 0.47 | 1.27 | 1.24 | 1.38 | 1.32 | 1.80 | 1.68 | 0.00 | 0.00 | 0.00 | 0.00 |
| Fe2+ | 2.21 | 3.97 | 4.02 | 3.99 | 4.00 | 2.96 | 3.81 | 2.47 | 2.42 | 2.29 | 2.35 | 1.91 | 2.01 | 3.97 | 4.02 | 3.99 | 4.00 |
| Mg | 0.09 | 0.69 | 0.71 | 0.68 | 0.70 | 0.13 | 0.27 | 0.04 | 0.09 | 0.08 | 0.04 | 0.03 | 0.05 | 0.69 | 0.71 | 0.68 | 0.71 |
| Mn | 0.04 | 0.10 | 0.09 | 0.09 | 0.09 | 0.05 | 0.09 | 0.03 | 0.04 | 0.04 | 0.04 | 0.02 | 0.02 | 0.10 | 0.09 | 0.09 | 0.09 |
| S C-site | 3.91 | 5.11 | 5.18 | 5.12 | 5.13 | 4.00 | 4.93 | 3.98 | 3.92 | 3.91 | 3.96 | 3.88 | 3.91 | 5.12 | 5.18 | 5.12 | 5.14 |
| | | | | | | | | | | | | | | | | | |
| Ca | 0.91 | 0.68 | 0.70 | 0.69 | 0.68 | 1.47 | 0.39 | 0.89 | 1.10 | 0.98 | 0.74 | 0.60 | 0.58 | 0.68 | 0.70 | 0.69 | 0.68 |
| Na | 1.09 | 1.32 | 1.30 | 1.31 | 1.32 | 0.53 | 1.61 | 1.11 | 0.90 | 1.02 | 1.26 | 1.40 | 1.42 | 1.32 | 1.30 | 1.31 | 1.32 |
| S B-site | 2.00 | 2.00 | 2.00 | 2.00 | 2.00 | 2.00 | 2.00 | 2.00 | 2.00 | 2.00 | 2.00 | 2.00 | 2.00 | 2.00 | 2.00 | 2.00 | 2.00 |
| | | | | | | | | | | | | | | | | | |
| Na | 1.65 | 0.65 | 0.63 | 0.63 | 0.63 | 1.64 | 0.56 | 1.61 | 1.65 | 1.65 | 1.68 | 1.64 | 1.67 | 0.67 | 0.65 | 0.65 | 0.65 |
| K | 0.00 | 0.23 | 0.22 | 0.23 | 0.24 | 0.00 | 0.28 | 0.00 | 0.00 | 0.00 | 0.00 | 0.00 | 0.00 | 0.23 | 0.22 | 0.23 | 0.24 |
| S A-site | 1.65 | 0.88 | 0.86 | 0.86 | 0.87 | 1.64 | 0.84 | 1.61 | 1.65 | 1.65 | 1.68 | 1.64 | 1.67 | 0.89 | 0.87 | 0.88 | 0.88 |

Appendix 1.3: Mineral Chemistry analysis: Sodic amphibole
Re calculated to 16O

| Thin Section | MC7018 | MC7018 | MC7018 | MC7018 | MC7018 | MC7018 | MC7018 | MC7018 | MC7018 | MC7018 | MC7018 | MC7018 | MC7018 | MC7018 | MC7018 | MC7018 |
|---|---|---|---|---|---|---|---|---|---|---|---|---|---|---|---|---|
| Circle No | C1 | C1 | C1 | C1 | C2 | C2 | C2 | C2 | C2 | C2 | C4 | C4 | C4 | C4 | C4 | C4 |
| Location | core | core | core | core | core | core | core | core | rim | rim | core | core | rim | rim | rim | rim |
| **Wt % oxides** | | | | | | | | | | | | | | | | |
| SiO2 | 53.39 | 53.50 | 52.78 | 53.14 | 51.27 | 51.99 | 51.89 | 51.48 | 52.34 | 52.82 | 50.42 | 50.55 | 52.99 | 52.18 | 52.15 | 52.24 |
| TiO2 | 2.00 | 0.47 | 0.42 | 0.55 | 1.41 | 0.35 | 0.34 | 0.36 | 0.44 | 0.95 | 1.49 | 1.51 | 1.42 | 1.34 | 1.28 | 1.33 |
| Al2O3 | 0.40 | 0.28 | 0.37 | 0.35 | 0.67 | 0.39 | 0.32 | 0.26 | 0.45 | 0.50 | 0.95 | 0.92 | 0.45 | 0.50 | 0.38 | 0.36 |
| Fe2O3 | 0.00 | 0.00 | 0.00 | 0.00 | 0.00 | 0.00 | 0.00 | 0.00 | 0.00 | 0.00 | 0.00 | 0.00 | 0.00 | 0.00 | 0.00 | 0.00 |
| FeO | 27.49 | 28.77 | 28.27 | 28.68 | 33.16 | 28.51 | 27.99 | 28.18 | 28.43 | 28.47 | 29.61 | 29.77 | 32.07 | 31.62 | 31.57 | 31.63 |
| MnO | 0.18 | 0.27 | 0.22 | 0.23 | 0.67 | 0.39 | 0.36 | 0.42 | 0.31 | 0.17 | 0.67 | 0.69 | 0.72 | 0.68 | 0.67 | 0.66 |
| MgO | 0.22 | 0.76 | 0.79 | 0.60 | 1.12 | 0.59 | 0.45 | 0.60 | 0.37 | 0.23 | 2.90 | 2.90 | 1.54 | 1.45 | 1.48 | 1.43 |
| CaO | 3.44 | 6.07 | 5.81 | 5.26 | 2.31 | 8.85 | 8.59 | 9.39 | 7.44 | 4.54 | 4.04 | 4.03 | 1.57 | 1.55 | 1.12 | 1.19 |
| Na2O | 11.05 | 9.20 | 9.54 | 9.50 | 7.37 | 7.35 | 7.59 | 7.12 | 8.33 | 9.93 | 6.54 | 6.37 | 7.86 | 7.56 | 7.95 | 7.88 |
| K2O | 0.00 | 0.00 | 0.00 | 0.00 | 1.48 | 0.00 | 0.00 | 0.00 | 0.00 | 0.00 | 1.10 | 1.13 | 1.81 | 1.83 | 1.82 | 1.89 |
| Total | 98.18 | 99.33 | 98.20 | 98.32 | 99.46 | 98.40 | 97.53 | 97.80 | 98.11 | 97.59 | 97.71 | 97.86 | 100.42 | 98.68 | 98.42 | 98.60 |
| Si | 8.00 | 8.00 | 8.00 | 8.00 | 8.00 | 8.00 | 8.00 | 8.00 | 8.00 | 8.00 | 8.00 | 8.00 | 8.00 | 8.00 | 8.00 | 8.00 |
| S T-site | 8.00 | 8.00 | 8.00 | 8.00 | 8.00 | 8.00 | 8.00 | 8.00 | 8.00 | 8.00 | 8.00 | 8.00 | 8.00 | 8.00 | 8.00 | 8.00 |
| AlVI | 0.07 | 0.05 | 0.07 | 0.06 | 0.12 | 0.07 | 0.06 | 0.05 | 0.08 | 0.09 | 0.18 | 0.17 | 0.08 | 0.09 | 0.07 | 0.07 |
| Ti | 0.23 | 0.05 | 0.05 | 0.06 | 0.17 | 0.04 | 0.04 | 0.04 | 0.05 | 0.11 | 0.18 | 0.18 | 0.16 | 0.15 | 0.15 | 0.15 |
| Fe3+ | 1.54 | 1.43 | 1.34 | 1.55 | 0.32 | 0.81 | 1.04 | 0.71 | 1.14 | 1.56 | 0.00 | 0.00 | 0.98 | 1.06 | 1.17 | 1.17 |
| Fe2+ | 1.91 | 2.17 | 2.25 | 2.06 | 4.01 | 2.86 | 2.56 | 2.96 | 2.50 | 2.05 | 3.93 | 3.94 | 3.06 | 2.99 | 2.88 | 2.88 |
| Mg | 0.05 | 0.17 | 0.18 | 0.14 | 0.26 | 0.13 | 0.10 | 0.14 | 0.08 | 0.05 | 0.69 | 0.68 | 0.35 | 0.33 | 0.34 | 0.33 |
| Mn | 0.02 | 0.03 | 0.03 | 0.03 | 0.09 | 0.05 | 0.05 | 0.05 | 0.04 | 0.02 | 0.09 | 0.09 | 0.09 | 0.09 | 0.09 | 0.09 |
| S C-site | 3.81 | 3.90 | 3.91 | 3.90 | 4.96 | 3.97 | 3.86 | 3.95 | 3.89 | 3.87 | 5.06 | 5.07 | 4.73 | 4.72 | 4.69 | 4.68 |
| Ca | 0.55 | 0.97 | 0.94 | 0.85 | 0.39 | 1.46 | 1.42 | 1.56 | 1.22 | 0.74 | 0.69 | 0.68 | 0.25 | 0.25 | 0.18 | 0.20 |
| Na | 1.45 | 1.03 | 1.06 | 1.15 | 1.61 | 0.54 | 0.58 | 0.44 | 0.78 | 1.26 | 1.31 | 1.32 | 1.75 | 1.75 | 1.82 | 1.80 |
| S B-site | 2.00 | 2.00 | 2.00 | 2.00 | 2.00 | 2.00 | 2.00 | 2.00 | 2.00 | 2.00 | 2.00 | 2.00 | 2.00 | 2.00 | 2.00 | 2.00 |
| Na | 1.76 | 1.64 | 1.75 | 1.62 | 0.61 | 1.65 | 1.69 | 1.71 | 1.69 | 1.65 | 0.70 | 0.64 | 0.55 | 0.50 | 0.55 | 0.53 |
| K | 0.00 | 0.00 | 0.00 | 0.00 | 0.30 | 0.00 | 0.00 | 0.00 | 0.00 | 0.00 | 0.22 | 0.23 | 0.35 | 0.36 | 0.36 | 0.37 |
| S A-site | 1.76 | 1.64 | 1.75 | 1.62 | 0.91 | 1.65 | 1.69 | 1.71 | 1.69 | 1.65 | 0.92 | 0.87 | 0.90 | 0.86 | 0.90 | 0.90 |

Appendix 1.3 : Mineral Chemistry Analysis :Fero-edenite analysis

| Thin Section | MC7026 | MC7026 | MC7026 | MC7026 | MC7026 | MC7026 | MC7026 | MC7026 | MC7026 | MC7026 | MC7026 | MC7026 | MC7026 | MC7026 | MC7026 | MC7026 | MC7026 | MC7026 | MC7026 | MC7026 | MC7026 | MC7026 | MC7039 | MC7039 | MC7039 | MC7039 | MC7039 | MC7039 | MC7039 |
|---|---|---|---|---|---|---|---|---|---|---|---|---|---|---|---|---|---|---|---|---|---|---|---|---|---|---|---|---|---|
| Circle No | C1 | C1 | C1 | C1 | C1 | C1 | C1 | C1 | C2 | C2 | C2 | C3 | C3 | C3 | C3 | C3 | C4 | C4 | C4 | C4 | C4 | C4 | C1 | C1 | C1 | C1 | C1 | C1 | C1 |
| Location | core | core | core | core | core | rim | rim | rim | core | core | core | core | core | core | core | core | core | core | core | rim | rim | rim | | | | | | | |
| **Wt % oxides** | | | | | | | | | | | | | | | | | | | | | | | | | | | | | |
| $SiO_2$ | 48.97 | 49.30 | 47.42 | 47.24 | 47.92 | 47.10 | 47.82 | 47.77 | 50.86 | 51.83 | 47.21 | 47.60 | 49.05 | 48.10 | 47.20 | 46.01 | 47.66 | 48.21 | 47.88 | 47.86 | 48.04 | 47.76 | 47.01 | 47.44 | 47.20 | 47.72 | 47.43 | 49.14 | 48.51 |
| $TiO_2$ | 1.04 | 0.94 | 0.92 | 0.86 | 0.79 | 0.93 | 0.83 | 0.66 | 0.15 | 0.13 | 0.95 | 1.09 | 0.82 | 0.79 | 1.04 | 1.15 | 0.83 | 0.65 | 0.88 | 0.73 | 0.64 | 0.56 | 1.27 | 1.16 | 1.21 | 1.15 | 1.27 | 0.47 | 0.93 |
| $Al_2O_3$ | 3.00 | 2.96 | 2.81 | 2.88 | 2.72 | 3.10 | 3.23 | 2.92 | 1.17 | 0.88 | 2.89 | 3.24 | 2.45 | 2.38 | 3.05 | 3.65 | 2.98 | 2.75 | 2.76 | 2.69 | 2.86 | 2.66 | 4.11 | 4.04 | 3.86 | 4.05 | 3.96 | 3.01 | 4.16 |
| $Fe_2O_3$ | 0.00 | 0.00 | 0.00 | 0.00 | 0.00 | 0.00 | 0.00 | 0.00 | 0.00 | 0.00 | 0.00 | 0.00 | 0.00 | 0.00 | 0.00 | 0.00 | 0.00 | 0.00 | 0.00 | 0.00 | 0.00 | 0.00 | 0.00 | 0.00 | 0.00 | 0.00 | 0.00 | 0.00 | 0.00 |
| FeO | 32.48 | 32.53 | 31.46 | 31.67 | 30.95 | 31.02 | 30.98 | 30.96 | 29.16 | 27.72 | 31.09 | 32.06 | 32.00 | 31.23 | 31.38 | 31.69 | 30.42 | 31.20 | 30.80 | 30.97 | 30.90 | 31.19 | 26.56 | 26.86 | 26.89 | 26.31 | 26.95 | 25.13 | 24.02 |
| MnO | 0.73 | 0.71 | 0.67 | 0.67 | 0.68 | 0.65 | 0.63 | 0.68 | 0.99 | 0.93 | 0.70 | 0.65 | 0.59 | 0.64 | 0.74 | 0.67 | 0.64 | 0.75 | 0.65 | 0.72 | 0.78 | 0.71 | 0.57 | 0.52 | 0.55 | 0.53 | 0.57 | 0.57 | 0.53 |
| MgO | 3.37 | 3.26 | 3.15 | 3.36 | 3.76 | 3.37 | 3.56 | 3.98 | 4.41 | 5.31 | 3.16 | 3.03 | 3.92 | 3.89 | 3.34 | 2.89 | 3.98 | 3.66 | 3.67 | 3.61 | 3.77 | 3.70 | 7.41 | 7.48 | 7.55 | 7.60 | 7.12 | 8.34 | 8.89 |
| CaO | 7.18 | 7.17 | 6.97 | 7.09 | 7.13 | 7.45 | 7.36 | 7.25 | 9.99 | 10.30 | 6.91 | 7.22 | 6.86 | 6.76 | 7.08 | 7.65 | 7.28 | 7.13 | 6.98 | 7.08 | 7.21 | 7.04 | 9.14 | 8.82 | 9.03 | 9.36 | 9.37 | 9.68 | 9.65 |
| $Na_2O$ | 2.92 | 2.94 | 2.84 | 2.99 | 3.06 | 2.72 | 2.72 | 2.83 | 0.70 | 0.62 | 3.11 | 3.28 | 3.11 | 3.17 | 2.86 | 2.76 | 2.93 | 2.65 | 2.86 | 2.69 | 2.67 | 2.66 | 1.83 | 1.77 | 1.60 | 1.78 | 1.70 | 1.45 | 1.64 |
| $K_2O$ | 0.90 | 0.93 | 0.87 | 0.77 | 0.72 | 0.81 | 0.80 | 0.78 | 0.28 | 0.17 | 0.81 | 0.84 | 0.71 | 0.74 | 0.86 | 0.83 | 0.79 | 0.82 | 0.72 | 0.77 | 0.74 | 0.76 | 0.47 | 0.48 | 0.48 | 0.46 | 0.44 | 0.31 | 0.53 |
| 2 | 100.59 | 100.73 | 97.11 | 97.52 | 97.73 | 97.13 | 97.92 | 97.81 | 97.70 | 97.88 | 96.80 | 99.01 | 99.51 | 97.69 | 97.55 | 97.29 | 97.51 | 97.81 | 97.20 | 97.12 | 97.59 | 97.04 | 98.37 | 98.58 | 98.36 | 98.96 | 98.80 | 98.09 | 98.86 |
| **Normalised with separate $Fe^{3+}$ and $Fe^{2+}$** | | | | | | | | | | | | | | | | | | | | | | | | | | | | | |
| Si | 7.39 | 7.44 | 7.43 | 7.37 | 7.44 | 7.38 | 7.40 | 7.39 | 7.86 | 7.94 | 7.43 | 7.36 | 7.44 | 7.45 | 7.36 | 7.25 | 7.40 | 7.45 | 7.45 | 7.45 | 7.44 | 7.43 | 7.06 | 7.08 | 7.07 | 7.12 | 7.11 | 7.35 | 7.17 |
| Ti | 0.12 | 0.11 | 0.11 | 0.10 | 0.09 | 0.11 | 0.10 | 0.08 | 0.02 | 0.02 | 0.11 | 0.13 | 0.09 | 0.09 | 0.12 | 0.14 | 0.10 | 0.08 | 0.10 | 0.09 | 0.07 | 0.07 | 0.14 | 0.13 | 0.14 | 0.13 | 0.14 | 0.05 | 0.10 |
| Si | 7.39 | 7.44 | 7.43 | 7.37 | 7.44 | 7.38 | 7.40 | 7.39 | 7.86 | 7.94 | 7.43 | 7.36 | 7.44 | 7.45 | 7.36 | 7.25 | 7.40 | 7.45 | 7.45 | 7.45 | 7.44 | 7.43 | 7.06 | 7.08 | 7.07 | 7.12 | 7.11 | 7.35 | 7.17 |
| $Al^{IV}$ | 0.53 | 0.53 | 0.52 | 0.53 | 0.50 | 0.57 | 0.59 | 0.53 | 0.14 | 0.06 | 0.54 | 0.59 | 0.44 | 0.43 | 0.56 | 0.68 | 0.55 | 0.50 | 0.51 | 0.49 | 0.52 | 0.49 | 0.73 | 0.71 | 0.68 | 0.71 | 0.70 | 0.53 | 0.73 |
| Ti | 0.07 | 0.04 | 0.05 | 0.10 | 0.07 | 0.05 | 0.01 | 0.08 | 0.00 | 0.00 | 0.04 | 0.05 | 0.09 | 0.09 | 0.08 | 0.08 | 0.05 | 0.05 | 0.05 | 0.05 | 0.04 | 0.07 | 0.14 | 0.13 | 0.14 | 0.13 | 0.14 | 0.05 | 0.10 |
| $Fe^{3+}$ | 0.00 | 0.00 | 0.00 | 0.00 | 0.00 | 0.00 | 0.00 | 0.01 | 0.00 | 0.00 | 0.00 | 0.00 | 0.02 | 0.03 | 0.00 | 0.00 | 0.00 | 0.00 | 0.00 | 0.00 | 0.00 | 0.01 | 0.07 | 0.08 | 0.12 | 0.04 | 0.04 | 0.07 | 0.00 |
| S T-site | 8.00 | 8.00 | 8.00 | 8.00 | 8.00 | 8.00 | 8.00 | 8.00 | 8.00 | 8.00 | 8.00 | 8.00 | 8.00 | 8.00 | 8.00 | 8.00 | 8.00 | 8.00 | 8.00 | 8.00 | 8.00 | 8.00 | 8.00 | 8.00 | 8.00 | 8.00 | 8.00 | 8.00 | 8.00 |
| $Al^{VI}$ | 0.00 | 0.00 | 0.00 | 0.00 | 0.00 | 0.00 | 0.00 | 0.00 | 0.07 | 0.10 | 0.00 | 0.00 | 0.00 | 0.00 | 0.00 | 0.00 | 0.00 | 0.00 | 0.00 | 0.00 | 0.00 | 0.00 | 0.00 | 0.00 | 0.00 | 0.00 | 0.00 | 0.00 | 0.00 |
| Ti | 0.05 | 0.07 | 0.06 | 0.00 | 0.03 | 0.06 | 0.09 | 0.00 | 0.02 | 0.02 | 0.08 | 0.07 | 0.00 | 0.00 | 0.04 | 0.06 | 0.04 | 0.03 | 0.03 | 0.03 | 0.03 | 0.00 | 0.00 | 0.00 | 0.00 | 0.00 | 0.00 | 0.00 | 0.00 |
| $Fe^{3+}$ | 1.09 | 1.03 | 1.03 | 1.10 | 1.01 | 0.96 | 1.00 | 1.14 | 0.47 | 0.33 | 0.94 | 0.91 | 1.18 | 1.12 | 1.08 | 0.97 | 1.00 | 1.13 | 1.06 | 1.10 | 1.12 | 1.20 | 1.23 | 1.37 | 1.35 | 1.15 | 1.16 | 1.02 | 1.09 |
| $Fe^{2+}$ | 3.01 | 3.07 | 3.09 | 3.03 | 3.00 | 3.11 | 3.01 | 2.86 | 3.30 | 3.22 | 3.15 | 3.23 | 2.86 | 2.90 | 3.01 | 3.21 | 2.95 | 2.90 | 2.94 | 2.93 | 2.88 | 2.85 | 2.03 | 1.90 | 1.90 | 2.09 | 2.18 | 2.05 | 1.88 |
| Mg | 0.76 | 0.73 | 0.74 | 0.78 | 0.87 | 0.79 | 0.82 | 0.92 | 1.02 | 1.21 | 0.74 | 0.70 | 0.89 | 0.90 | 0.78 | 0.68 | 0.92 | 0.84 | 0.85 | 0.84 | 0.87 | 0.86 | 1.66 | 1.66 | 1.68 | 1.69 | 1.59 | 1.86 | 1.96 |
| Mn | 0.09 | 0.09 | 0.09 | 0.09 | 0.09 | 0.09 | 0.08 | 0.09 | 0.13 | 0.12 | 0.09 | 0.09 | 0.08 | 0.08 | 0.10 | 0.09 | 0.08 | 0.10 | 0.09 | 0.09 | 0.10 | 0.09 | 0.07 | 0.07 | 0.07 | 0.07 | 0.07 | 0.07 | 0.07 |
| S M123-site | 5.00 | 5.00 | 5.00 | 5.00 | 5.00 | 5.00 | 5.00 | 5.00 | 5.00 | 5.00 | 5.00 | 5.00 | 5.00 | 5.00 | 5.00 | 5.00 | 5.00 | 5.00 | 5.00 | 5.00 | 5.00 | 5.00 | 5.00 | 5.00 | 5.00 | 5.00 | 5.00 | 5.00 | 5.00 |
| $Fe^{2+}$ | 0.00 | 0.00 | 0.00 | 0.00 | 0.00 | 0.00 | 0.00 | 0.00 | 0.00 | 0.00 | 0.00 | 0.00 | 0.00 | 0.00 | 0.00 | 0.00 | 0.00 | 0.00 | 0.00 | 0.00 | 0.00 | 0.00 | 0.00 | 0.00 | 0.00 | 0.00 | 0.00 | 0.00 | 0.00 |
| Mn | 0.00 | 0.00 | 0.00 | 0.00 | 0.00 | 0.00 | 0.00 | 0.00 | 0.00 | 0.00 | 0.00 | 0.00 | 0.00 | 0.00 | 0.00 | 0.00 | 0.00 | 0.00 | 0.00 | 0.00 | 0.00 | 0.00 | 0.00 | 0.00 | 0.00 | 0.00 | 0.00 | 0.00 | 0.00 |
| Ca | 1.19 | 1.18 | 1.20 | 1.21 | 1.21 | 1.28 | 1.25 | 1.23 | 1.67 | 1.70 | 1.19 | 1.22 | 1.15 | 1.15 | 1.21 | 1.32 | 1.24 | 1.21 | 1.19 | 1.21 | 1.23 | 1.21 | 1.51 | 1.45 | 1.50 | 1.54 | 1.54 | 1.59 | 1.57 |
| Na | 0.81 | 0.82 | 0.80 | 0.79 | 0.79 | 0.72 | 0.75 | 0.77 | 0.21 | 0.19 | 0.81 | 0.78 | 0.85 | 0.85 | 0.79 | 0.68 | 0.76 | 0.79 | 0.81 | 0.79 | 0.77 | 0.79 | 0.49 | 0.53 | 0.48 | 0.46 | 0.46 | 0.41 | 0.43 |
| S M4-site | 2.00 | 2.00 | 2.00 | 2.00 | 2.00 | 2.00 | 2.00 | 2.00 | 1.88 | 1.89 | 2.00 | 2.00 | 2.00 | 2.00 | 2.00 | 2.00 | 2.00 | 2.00 | 2.00 | 2.00 | 2.00 | 2.00 | 2.00 | 1.98 | 1.97 | 2.00 | 2.00 | 2.00 | 2.00 |
| Na | 0.07 | 0.06 | 0.08 | 0.14 | 0.15 | 0.12 | 0.08 | 0.10 | 0.00 | 0.00 | 0.16 | 0.22 | 0.09 | 0.13 | 0.10 | 0.18 | 0.14 | 0.02 | 0.07 | 0.04 | 0.05 | 0.03 | 0.06 | 0.00 | 0.00 | 0.07 | 0.05 | 0.02 | 0.05 |
| K | 0.18 | 0.18 | 0.18 | 0.16 | 0.14 | 0.16 | 0.16 | 0.16 | 0.06 | 0.03 | 0.17 | 0.17 | 0.14 | 0.15 | 0.18 | 0.17 | 0.16 | 0.17 | 0.15 | 0.16 | 0.15 | 0.15 | 0.09 | 0.10 | 0.10 | 0.09 | 0.09 | 0.06 | 0.10 |
| S A-site | 0.24 | 0.25 | 0.26 | 0.30 | 0.30 | 0.28 | 0.24 | 0.26 | 0.06 | 0.03 | 0.32 | 0.39 | 0.23 | 0.28 | 0.27 | 0.35 | 0.30 | 0.19 | 0.22 | 0.20 | 0.19 | 0.18 | 0.15 | 0.10 | 0.10 | 0.16 | 0.14 | 0.08 | 0.15 |

Appendix 1.3 : Mineral Chemistry Analysis :Fero-edenite analysis

| Thin Section | MC7039 | MC7039 | MC7039 | MC7039 | MC7039 | MC7039 | MC7039 | MC7039 | MC7039 | MC7039 | MC7039 | MC7039 | MC7039 | MC7039 | MC7039 | MC7039 | MC7039 | MC7039 | MC7039 | MC7039 | MC7039 |
|---|---|---|---|---|---|---|---|---|---|---|---|---|---|---|---|---|---|---|---|---|---|
| Circle No | C1 | C1 | C1 | C1 | C2 | C2 | C2 | C2 | C1 | C1 | C1 | C1 | C1 | C1 | C1 | C1 | C1 | C1 | C1 | C1 | C1 |
| Location | | | | | | | | | core | core | core | core | core | core | core | rim | rim | rim | core | core | core |
| **Wt % oxides** | | | | | | | | | | | | | | | | | | | | | |
| SiO$_2$ | 49.56 | 48.78 | 46.48 | 46.26 | 46.61 | 46.36 | 46.83 | 46.74 | 48.56 | 47.82 | 47.41 | 47.16 | 47.62 | 47.62 | 47.59 | 46.64 | 47.20 | 46.80 | 47.27 | 47.27 | 46.94 |
| TiO$_2$ | 0.96 | 0.93 | 1.30 | 1.36 | 1.23 | 1.11 | 1.16 | 1.13 | 1.26 | 1.30 | 1.35 | 1.36 | 1.38 | 1.38 | 1.24 | 1.33 | 1.26 | 1.30 | 1.15 | 1.18 | 1.25 |
| Al$_2$O$_3$ | 4.07 | 3.91 | 4.78 | 4.80 | 4.48 | 5.02 | 4.58 | 4.28 | 4.77 | 4.64 | 5.06 | 5.03 | 4.64 | 4.95 | 4.97 | 4.94 | 4.85 | 4.74 | 4.67 | 4.64 | 5.02 |
| Fe$_2$O$_3$ | 0.00 | 0.00 | 0.00 | 0.00 | 0.00 | 0.00 | 0.00 | 0.00 | 0.00 | 0.00 | 0.00 | 0.00 | 0.00 | 0.00 | 0.00 | 0.00 | 0.00 | 0.00 | 0.00 | 0.00 | 0.00 |
| FeO | 24.31 | 23.97 | 26.81 | 27.48 | 27.07 | 27.31 | 27.42 | 27.36 | 26.15 | 25.25 | 25.72 | 25.57 | 26.29 | 25.96 | 25.76 | 25.25 | 25.18 | 25.72 | 25.55 | 25.33 | 25.72 |
| MnO | 0.50 | 0.47 | 0.49 | 0.55 | 0.56 | 0.52 | 0.42 | 0.56 | 0.37 | 0.43 | 0.45 | 0.45 | 0.50 | 0.46 | 0.47 | 0.44 | 0.45 | 0.50 | 0.49 | 0.46 | 0.44 |
| MgO | 9.05 | 9.02 | 7.29 | 6.78 | 7.02 | 6.76 | 6.99 | 7.00 | 7.88 | 7.82 | 7.38 | 7.22 | 7.17 | 7.23 | 7.34 | 7.09 | 7.36 | 7.07 | 7.29 | 7.33 | 7.25 |
| CaO | 9.80 | 9.63 | 9.19 | 9.34 | 9.32 | 9.42 | 9.30 | 8.91 | 9.37 | 9.24 | 9.24 | 9.13 | 9.04 | 9.22 | 9.41 | 9.27 | 9.37 | 9.07 | 8.83 | 9.01 | 9.12 |
| Na$_2$O | 1.73 | 1.71 | 1.87 | 2.01 | 1.79 | 1.82 | 1.96 | 1.63 | 1.77 | 1.65 | 1.91 | 1.76 | 1.78 | 1.72 | 1.73 | 1.59 | 1.68 | 1.76 | 1.73 | 1.69 | 1.73 |
| K$_2$O | 0.48 | 0.48 | 0.62 | 0.59 | 0.56 | 0.63 | 0.61 | 0.53 | 0.54 | 0.51 | 0.56 | 0.56 | 0.55 | 0.58 | 0.66 | 0.56 | 0.51 | 0.51 | 0.41 | 0.50 | 0.55 |
| 2 | 100.46 | 98.90 | 98.83 | 99.17 | 98.64 | 98.95 | 99.26 | 98.15 | 100.66 | 98.66 | 99.07 | 98.23 | 98.96 | 99.12 | 99.16 | 97.09 | 97.86 | 97.48 | 97.38 | 97.40 | 98.02 |
| | | | | | | | | | | | | | | | | | | | | | |
| **Normalised with s** | | | | | | | | | | | | | | | | | | | | | |
| Si | 7.21 | 7.21 | 6.96 | 6.95 | 7.01 | 6.97 | 7.01 | 7.03 | 7.09 | 7.11 | 7.06 | 7.08 | 7.10 | 7.09 | 7.09 | 7.09 | 7.11 | 7.09 | 7.12 | 7.14 | 7.06 |
| Ti | 0.10 | 0.10 | 0.15 | 0.15 | 0.14 | 0.13 | 0.13 | 0.13 | 0.14 | 0.15 | 0.15 | 0.15 | 0.15 | 0.15 | 0.14 | 0.15 | 0.14 | 0.15 | 0.13 | 0.13 | 0.14 |
| | | | | | | | | | | | | | | | | | | | | | |
| Si | 7.21 | 7.21 | 6.96 | 6.95 | 7.01 | 6.97 | 7.01 | 7.03 | 7.09 | 7.11 | 7.06 | 7.08 | 7.10 | 7.09 | 7.09 | 7.09 | 7.11 | 7.09 | 7.12 | 7.14 | 7.06 |
| Al$^{IV}$ | 0.70 | 0.68 | 0.84 | 0.85 | 0.79 | 0.89 | 0.81 | 0.76 | 0.82 | 0.81 | 0.89 | 0.81 | 0.81 | 0.87 | 0.87 | 0.89 | 0.86 | 0.85 | 0.83 | 0.83 | 0.89 |
| Ti | 0.09 | 0.10 | 0.15 | 0.15 | 0.14 | 0.13 | 0.13 | 0.13 | 0.09 | 0.07 | 0.05 | 0.03 | 0.09 | 0.05 | 0.04 | 0.02 | 0.03 | 0.07 | 0.05 | 0.04 | 0.06 |
| Fe$^{3+}$ | 0.00 | 0.01 | 0.05 | 0.04 | 0.05 | 0.02 | 0.05 | 0.08 | 0.00 | 0.00 | 0.00 | 0.00 | 0.00 | 0.00 | 0.00 | 0.00 | 0.00 | 0.00 | 0.00 | 0.00 | 0.00 |
| S T-site | 8.00 | 8.00 | 8.00 | 8.00 | 8.00 | 8.00 | 8.00 | 8.00 | 8.00 | 8.00 | 8.00 | 8.00 | 8.00 | 8.00 | 8.00 | 8.00 | 8.00 | 8.00 | 8.00 | 8.00 | 8.00 |
| | | | | | | | | | | | | | | | | | | | | | |
| Al$^{VI}$ | 0.00 | 0.00 | 0.00 | 0.00 | 0.00 | 0.00 | 0.00 | 0.00 | 0.00 | 0.00 | 0.00 | 0.00 | 0.00 | 0.00 | 0.00 | 0.00 | 0.00 | 0.00 | 0.00 | 0.00 | 0.00 |
| Ti | 0.02 | 0.00 | 0.00 | 0.00 | 0.00 | 0.00 | 0.00 | 0.00 | 0.05 | 0.07 | 0.10 | 0.12 | 0.07 | 0.11 | 0.10 | 0.13 | 0.12 | 0.08 | 0.08 | 0.09 | 0.09 |
| Fe$^{3+}$ | 1.03 | 1.06 | 1.28 | 1.19 | 1.21 | 1.22 | 1.18 | 1.39 | 1.19 | 1.15 | 1.08 | 1.10 | 1.17 | 1.10 | 1.04 | 1.04 | 1.01 | 1.12 | 1.23 | 1.13 | 1.17 |
| Fe$^{2+}$ | 1.92 | 1.90 | 2.03 | 2.22 | 2.14 | 2.20 | 2.20 | 1.97 | 2.00 | 1.99 | 2.13 | 2.11 | 2.10 | 2.13 | 2.16 | 2.17 | 2.16 | 2.13 | 1.99 | 2.06 | 2.06 |
| Mg | 1.96 | 1.99 | 1.63 | 1.52 | 1.58 | 1.52 | 1.56 | 1.57 | 1.71 | 1.73 | 1.64 | 1.62 | 1.59 | 1.60 | 1.63 | 1.61 | 1.65 | 1.60 | 1.64 | 1.65 | 1.63 |
| Mn | 0.06 | 0.06 | 0.06 | 0.07 | 0.07 | 0.07 | 0.05 | 0.07 | 0.05 | 0.05 | 0.06 | 0.06 | 0.06 | 0.06 | 0.06 | 0.06 | 0.06 | 0.06 | 0.06 | 0.06 | 0.06 |
| S M123-site | 5.00 | 5.00 | 5.00 | 5.00 | 5.00 | 5.00 | 5.00 | 5.00 | 5.00 | 5.00 | 5.00 | 5.00 | 5.00 | 5.00 | 5.00 | 5.00 | 5.00 | 5.00 | 5.00 | 5.00 | 5.00 |
| | | | | | | | | | | | | | | | | | | | | | |
| Fe$^{2+}$ | 0.00 | 0.00 | 0.00 | 0.00 | 0.00 | 0.00 | 0.00 | 0.00 | 0.00 | 0.00 | 0.00 | 0.00 | 0.00 | 0.00 | 0.00 | 0.00 | 0.00 | 0.00 | 0.00 | 0.00 | 0.00 |
| Mn | 0.00 | 0.00 | 0.00 | 0.00 | 0.00 | 0.00 | 0.00 | 0.00 | 0.00 | 0.00 | 0.00 | 0.00 | 0.00 | 0.00 | 0.00 | 0.00 | 0.00 | 0.00 | 0.00 | 0.00 | 0.00 |
| Ca | 1.56 | 1.56 | 1.52 | 1.55 | 1.55 | 1.56 | 1.53 | 1.48 | 1.50 | 1.51 | 1.51 | 1.50 | 1.48 | 1.51 | 1.54 | 1.54 | 1.55 | 1.51 | 1.47 | 1.49 | 1.51 |
| Na | 0.44 | 0.44 | 0.48 | 0.45 | 0.45 | 0.44 | 0.47 | 0.49 | 0.50 | 0.49 | 0.49 | 0.50 | 0.52 | 0.49 | 0.46 | 0.46 | 0.45 | 0.49 | 0.52 | 0.51 | 0.49 |
| S M4-site | 2.00 | 2.00 | 2.00 | 2.00 | 2.00 | 2.00 | 2.00 | 1.97 | 2.00 | 2.00 | 2.00 | 2.00 | 2.00 | 2.00 | 2.00 | 2.00 | 2.00 | 2.00 | 1.98 | 2.00 | 2.00 |
| | | | | | | | | | | | | | | | | | | | | | |
| Na | 0.06 | 0.06 | 0.08 | 0.15 | 0.08 | 0.10 | 0.12 | 0.00 | 0.02 | 0.00 | 0.08 | 0.03 | 0.01 | 0.02 | 0.05 | 0.02 | 0.05 | 0.04 | 0.00 | 0.00 | 0.02 |
| K | 0.09 | 0.09 | 0.12 | 0.12 | 0.11 | 0.12 | 0.12 | 0.11 | 0.10 | 0.10 | 0.11 | 0.11 | 0.11 | 0.11 | 0.13 | 0.11 | 0.10 | 0.10 | 0.08 | 0.10 | 0.11 |
| S A-site | 0.15 | 0.16 | 0.20 | 0.26 | 0.19 | 0.23 | 0.24 | 0.11 | 0.12 | 0.10 | 0.18 | 0.14 | 0.12 | 0.13 | 0.17 | 0.13 | 0.15 | 0.14 | 0.08 | 0.10 | 0.13 |

Appendix 1.3: Mineral Chemistry analysis for feldspars
Recalculated to 8O

| Thin Section | MC7002 | MC7002 | MC7002 | MC7002 | MC7002 | MC7002 | MC7004 | MC7004 | MC7004 | MC7004 | MC7004 | MC7004 | MC710-1 | MC710-1 | MC710-1 | MC710-1 | MC710-1 |
|---|---|---|---|---|---|---|---|---|---|---|---|---|---|---|---|---|---|
| Circle No | C1 | C1 | C1 | C1 | C4 | C4 | C1 | C1 | C1 | C1 | C1 | C1 | C1 | C1 | C1 | C1 | C1 |
| Location | core | core | core | core | core | core | core | core | core | core | core | core | core | core | core | rim | rim |
| **wt%** | | | | | | | | | | | | | | | | | |
| SiO2 | 52.57 | 64.52 | 52.27 | 52.82 | 54.92 | 54.24 | 68.40 | 65.10 | 65.93 | 66.07 | 66.23 | 65.92 | 68.51 | 68.01 | 69.23 | 69.20 | 68.83 |
| Al2O3 | 30.72 | 19.32 | 30.96 | 30.49 | 28.38 | 28.64 | 16.21 | 17.32 | 17.54 | 17.57 | 17.57 | 17.58 | 19.33 | 19.06 | 19.66 | 19.74 | 18.94 |
| Fe2O3 | 0.68 | 0.09 | 0.62 | 0.76 | 0.85 | 0.85 | 0.24 | 0.15 | 0.28 | 0.26 | 0.14 | 0.08 | 0.30 | 0.48 | 0.14 | 0.30 | 0.81 |
| MgO | 0.21 | 0.04 | 0.19 | 0.20 | 0.15 | 0.19 | 0.00 | 0.00 | 0.03 | 0.08 | 0.03 | 0.01 | 0.05 | 0.00 | 0.01 | 0.00 | 0.00 |
| CaO | 12.56 | 0.50 | 12.64 | 12.00 | 10.27 | 10.77 | 0.00 | 0.00 | 0.00 | 0.00 | 0.00 | 0.00 | 0.00 | 0.00 | 0.00 | 0.00 | 0.00 |
| Na2O | 3.71 | 0.49 | 3.65 | 3.89 | 4.78 | 4.53 | 1.47 | 0.21 | 0.37 | 0.26 | 0.36 | 0.31 | 10.40 | 10.42 | 10.78 | 10.87 | 10.55 |
| K2O | 0.11 | 14.59 | 0.11 | 0.15 | 0.16 | 0.14 | 13.47 | 16.50 | 16.51 | 16.39 | 16.63 | 16.52 | 0.00 | 0.20 | 0.00 | 0.00 | 0.00 |
| Total | 100.56 | 99.54 | 100.43 | 100.30 | 99.50 | 99.35 | 99.79 | 99.28 | 100.66 | 100.63 | 100.95 | 100.43 | 98.59 | 98.18 | 99.82 | 100.11 | 99.12 |
| | | | | | | | | | | | | | | | | | |
| Si | 2.38 | 3.00 | 2.37 | 2.40 | 2.50 | 2.48 | 3.17 | 3.04 | 3.03 | 3.04 | 3.04 | 3.04 | 3.07 | 3.05 | 3.05 | 3.04 | 3.07 |
| Al | 1.64 | 1.06 | 1.65 | 1.63 | 1.52 | 1.54 | 0.89 | 0.95 | 0.95 | 0.95 | 0.95 | 0.96 | 1.02 | 1.01 | 1.02 | 1.02 | 0.99 |
| S T-site | 4.02 | 4.06 | 4.03 | 4.03 | 4.03 | 4.02 | 4.06 | 3.99 | 3.99 | 4.00 | 3.99 | 4.00 | 4.08 | 4.06 | 4.07 | 4.06 | 4.06 |
| | | | | | | | | | | | | | | | | | |
| Ca | 0.61 | 0.03 | 0.61 | 0.58 | 0.50 | 0.53 | 0.00 | 0.00 | 0.00 | 0.00 | 0.00 | 0.00 | 0.00 | 0.00 | 0.00 | 0.00 | 0.00 |
| Na | 0.33 | 0.04 | 0.32 | 0.34 | 0.42 | 0.40 | 0.13 | 0.02 | 0.03 | 0.02 | 0.03 | 0.03 | 0.90 | 0.91 | 0.92 | 0.93 | 0.91 |
| K | 0.01 | 0.87 | 0.01 | 0.01 | 0.01 | 0.01 | 0.80 | 0.98 | 0.97 | 0.96 | 0.97 | 0.97 | 0.00 | 0.01 | 0.00 | 0.00 | 0.00 |
| S A-site | 0.94 | 0.93 | 0.94 | 0.93 | 0.93 | 0.94 | 0.93 | 1.00 | 1.00 | 0.99 | 1.00 | 1.00 | 0.90 | 0.92 | 0.92 | 0.93 | 0.91 |
| | | | | | | | | | | | | | | | | | |
| **Endmember calculation** | | | | | | | | | | | | | | | | | |
| An (Ca) | 0.65 | 0.03 | 0.65 | 0.62 | 0.54 | 0.56 | 0.00 | 0.00 | 0.00 | 0.00 | 0.00 | 0.00 | 0.00 | 0.00 | 0.00 | 0.00 | 0.00 |
| Ab (Na) | 0.35 | 0.05 | 0.34 | 0.37 | 0.45 | 0.43 | 0.14 | 0.02 | 0.03 | 0.02 | 0.03 | 0.03 | 1.00 | 0.99 | 1.00 | 1.00 | 1.00 |
| Or (K) | 0.01 | 0.93 | 0.01 | 0.01 | 0.01 | 0.01 | 0.86 | 0.98 | 0.97 | 0.98 | 0.97 | 0.97 | 0.00 | 0.01 | 0.00 | 0.00 | 0.00 |

Appendix 1.3: Mineral Chemistry analysis for feldspars
Recalculated to 8O

| Thin Section | MC710-1 | MC710-1 | MC710-1 | MC710-1 | MC710-1 | MC710-1 | MC710-1 | MC710-1 | MC710-1 | MC710-1 | MC710-1 | MC710-1 | MC710-1 | MC7015 | MC7015 | MC7015 | MC7015 | MC7015 |
|---|---|---|---|---|---|---|---|---|---|---|---|---|---|---|---|---|---|---|
| Circle No | C1 | C1 | C1 | C2 | C2 | C2 | C3 | C3 | C3 | C4 | C4 | C4 | C4 | C1 | C1 | C1 | C1 | C1 |
| Location | rim | core | core | core | core | core | core | core | core | core | core | core | core | core | core | core | rim | rim |
| **wt%** | | | | | | | | | | | | | | | | | | |
| SiO2 | 68.23 | 68.03 | 65.97 | 65.95 | 64.60 | 65.96 | 65.51 | 64.73 | 64.88 | 65.08 | 65.26 | 68.86 | 64.58 | 68.31 | 68.86 | 68.55 | 70.22 | 68.81 |
| Al2O3 | 19.44 | 18.95 | 18.72 | 18.92 | 18.56 | 18.96 | 18.61 | 18.23 | 18.33 | 18.13 | 18.14 | 19.53 | 18.39 | 19.08 | 19.23 | 19.09 | 19.71 | 19.09 |
| Fe2O3 | 0.14 | 0.63 | 0.18 | 0.24 | 0.21 | 0.15 | 0.44 | 0.29 | 0.31 | 0.52 | 0.71 | 0.18 | 0.43 | 1.11 | 1.20 | 1.10 | 0.97 | 1.04 |
| MgO | 0.00 | 0.02 | 0.00 | 0.01 | 0.01 | 0.01 | 0.00 | 0.00 | 0.00 | 0.03 | 0.00 | 0.01 | 0.05 | 0.00 | 0.00 | 0.00 | 0.00 | 0.00 |
| CaO | 0.00 | 0.00 | 0.00 | 0.00 | 0.00 | 0.00 | 0.00 | 0.00 | 0.00 | 0.00 | 0.00 | 0.00 | 0.00 | 0.00 | 0.00 | 0.00 | 0.00 | 0.00 |
| Na2O | 10.54 | 10.47 | 0.33 | 0.34 | 0.28 | 0.37 | 0.37 | 0.37 | 0.32 | 0.41 | 0.40 | 10.67 | 0.33 | 10.54 | 10.30 | 10.38 | 7.57 | 10.26 |
| K2O | 0.02 | 0.18 | 15.34 | 15.53 | 14.98 | 15.39 | 15.42 | 15.24 | 15.39 | 15.29 | 15.32 | 0.01 | 15.37 | 0.05 | 0.06 | 0.06 | 0.05 | 0.10 |
| Total | 98.37 | 98.28 | 100.54 | 100.98 | 98.64 | 100.84 | 100.35 | 98.85 | 99.23 | 99.45 | 99.82 | 99.26 | 99.15 | 99.08 | 99.64 | 99.18 | 98.51 | 99.30 |
| | | | | | | | | | | | | | | | | | | |
| Si | 3.05 | 3.05 | 3.04 | 3.03 | 3.04 | 3.03 | 3.03 | 3.04 | 3.03 | 3.04 | 3.04 | 3.05 | 3.02 | 3.05 | 3.06 | 3.06 | 3.22 | 3.07 |
| Al | 1.03 | 1.00 | 1.02 | 1.02 | 1.03 | 1.03 | 1.01 | 1.01 | 1.01 | 1.00 | 0.99 | 1.02 | 1.01 | 1.00 | 1.01 | 1.00 | 1.07 | 1.00 |
| S T-site | 4.08 | 4.06 | 4.06 | 4.05 | 4.07 | 4.06 | 4.04 | 4.04 | 4.04 | 4.03 | 4.03 | 4.07 | 4.03 | 4.05 | 4.07 | 4.06 | 4.29 | 4.07 |
| | | | | | | | | | | | | | | | | | | |
| Ca | 0.00 | 0.00 | 0.00 | 0.00 | 0.00 | 0.00 | 0.00 | 0.00 | 0.00 | 0.00 | 0.00 | 0.00 | 0.00 | 0.00 | 0.00 | 0.00 | 0.00 | 0.00 |
| Na | 0.91 | 0.91 | 0.03 | 0.03 | 0.03 | 0.03 | 0.03 | 0.03 | 0.03 | 0.04 | 0.04 | 0.92 | 0.03 | 0.91 | 0.89 | 0.90 | 0.67 | 0.89 |
| K | 0.00 | 0.01 | 0.90 | 0.91 | 0.90 | 0.90 | 0.91 | 0.91 | 0.92 | 0.91 | 0.91 | 0.00 | 0.92 | 0.00 | 0.00 | 0.00 | 0.00 | 0.01 |
| S A-site | 0.92 | 0.92 | 0.93 | 0.94 | 0.92 | 0.94 | 0.94 | 0.95 | 0.95 | 0.95 | 0.95 | 0.92 | 0.95 | 0.91 | 0.89 | 0.90 | 0.68 | 0.89 |
| | | | | | | | | | | | | | | | | | | |
| Endmember c | | | | | | | | | | | | | | | | | | |
| An (Ca) | 0.00 | 0.00 | 0.00 | 0.00 | 0.00 | 0.00 | 0.00 | 0.00 | 0.00 | 0.00 | 0.00 | 0.00 | 0.00 | 0.00 | 0.00 | 0.00 | 0.00 | 0.00 |
| Ab (Na) | 1.00 | 0.99 | 0.03 | 0.03 | 0.03 | 0.04 | 0.04 | 0.04 | 0.03 | 0.04 | 0.04 | 1.00 | 0.03 | 1.00 | 1.00 | 1.00 | 1.00 | 0.99 |
| Or (K) | 0.00 | 0.01 | 0.97 | 0.97 | 0.97 | 0.96 | 0.96 | 0.96 | 0.97 | 0.96 | 0.96 | 0.00 | 0.97 | 0.00 | 0.00 | 0.00 | 0.00 | 0.01 |

Appendix 1.3: Mineral Chemistry analysis for feldspars
Recalculated to 8O

| Thin Section | MC7015 | MC7015 | MC7015 | MC7015 | MC7015 | MC7015 | MC7015 | MC7015 | MC7015 | MC7015 | MC7015 | MC7015 | MC7015 | MC7015 | MC7015 | MC7015 | MC7017 | MC7017 |
|---|---|---|---|---|---|---|---|---|---|---|---|---|---|---|---|---|---|---|
| Circle No | C1 | C1 | C3 | C3 | C3 | C3 | C3 | C1 | C1 | C1 | C1 | C1 | C1 | C1 | C1 | C1 | C1 | C1 |
| Location | rim | rim | | | | | | core | core | rim | rim | rim | core | rim | rim | rim | core | core |
| wt% | | | | | | | | | | | | | | | | | | |
| SiO2 | 68.02 | 68.37 | 68.39 | 69.71 | 69.51 | 68.25 | 67.87 | 65.60 | 65.51 | 64.79 | 65.31 | 64.93 | 65.85 | 65.63 | 66.11 | 65.81 | 69.22 | 70.28 |
| Al2O3 | 19.16 | 19.26 | 18.65 | 18.97 | 19.19 | 18.81 | 18.67 | 17.92 | 17.96 | 17.56 | 17.56 | 17.53 | 17.79 | 17.91 | 18.22 | 17.81 | 19.02 | 19.28 |
| Fe2O3 | 1.06 | 1.06 | 1.21 | 1.23 | 1.22 | 1.13 | 1.16 | 0.77 | 0.72 | 1.25 | 1.13 | 1.10 | 0.78 | 0.81 | 0.39 | 0.94 | 0.78 | 0.88 |
| MgO | 0.00 | 0.00 | 0.04 | 0.02 | 0.03 | 0.00 | 0.00 | 0.00 | 0.00 | 0.00 | 0.00 | 0.02 | 0.00 | 0.00 | 0.00 | 0.00 | 0.03 | 0.00 |
| CaO | 0.00 | 0.00 | 0.00 | 0.00 | 0.00 | 0.01 | 0.01 | 0.00 | 0.00 | 0.00 | 0.00 | 0.00 | 0.00 | 0.00 | 0.00 | 0.00 | 0.00 | 0.00 |
| Na2O | 10.41 | 10.23 | 9.64 | 8.78 | 10.72 | 10.45 | 10.61 | 0.73 | 0.65 | 0.58 | 0.61 | 0.52 | 0.73 | 0.77 | 0.71 | 0.71 | 8.57 | 6.63 |
| K2O | 0.12 | 0.10 | 0.12 | 0.04 | 0.11 | 0.05 | 0.17 | 14.32 | 14.55 | 14.88 | 14.67 | 14.79 | 14.60 | 14.51 | 14.56 | 14.68 | 0.10 | 0.09 |
| Total | 98.76 | 99.02 | 98.05 | 98.74 | 100.78 | 98.68 | 98.51 | 99.33 | 99.38 | 99.05 | 99.28 | 98.88 | 99.75 | 99.63 | 100.00 | 99.95 | 97.72 | 97.16 |
| | | | | | | | | | | | | | | | | | | |
| Si | 3.04 | 3.06 | 3.10 | 3.17 | 3.05 | 3.06 | 3.04 | 3.07 | 3.06 | 3.04 | 3.06 | 3.05 | 3.06 | 3.06 | 3.07 | 3.06 | 3.17 | 3.30 |
| Al | 1.01 | 1.01 | 1.00 | 1.02 | 0.99 | 0.99 | 0.99 | 0.99 | 0.99 | 0.97 | 0.97 | 0.97 | 0.98 | 0.98 | 1.00 | 0.98 | 1.03 | 1.07 |
| S T-site | 4.05 | 4.07 | 4.10 | 4.18 | 4.04 | 4.05 | 4.03 | 4.05 | 4.05 | 4.01 | 4.03 | 4.02 | 4.04 | 4.04 | 4.06 | 4.03 | 4.20 | 4.36 |
| | | | | | | | | | | | | | | | | | | |
| Ca | 0.00 | 0.00 | 0.00 | 0.00 | 0.00 | 0.00 | 0.00 | 0.00 | 0.00 | 0.00 | 0.00 | 0.00 | 0.00 | 0.00 | 0.00 | 0.00 | 0.00 | 0.00 |
| Na | 0.90 | 0.89 | 0.85 | 0.77 | 0.91 | 0.91 | 0.92 | 0.07 | 0.06 | 0.05 | 0.06 | 0.05 | 0.07 | 0.07 | 0.06 | 0.06 | 0.76 | 0.60 |
| K | 0.01 | 0.01 | 0.01 | 0.00 | 0.01 | 0.00 | 0.01 | 0.85 | 0.87 | 0.89 | 0.88 | 0.89 | 0.87 | 0.86 | 0.86 | 0.87 | 0.01 | 0.01 |
| S A-site | 0.91 | 0.89 | 0.86 | 0.78 | 0.92 | 0.91 | 0.93 | 0.92 | 0.93 | 0.94 | 0.93 | 0.94 | 0.93 | 0.93 | 0.93 | 0.93 | 0.77 | 0.61 |
| | | | | | | | | | | | | | | | | | | |
| Endmember c | | | | | | | | | | | | | | | | | | |
| An (Ca) | 0.00 | 0.00 | 0.00 | 0.00 | 0.00 | 0.00 | 0.00 | 0.00 | 0.00 | 0.00 | 0.00 | 0.00 | 0.00 | 0.00 | 0.00 | 0.00 | 0.00 | 0.00 |
| Ab (Na) | 0.99 | 0.99 | 0.99 | 1.00 | 0.99 | 1.00 | 0.99 | 0.07 | 0.06 | 0.06 | 0.06 | 0.05 | 0.07 | 0.07 | 0.07 | 0.07 | 0.99 | 0.99 |
| Or (K) | 0.01 | 0.01 | 0.01 | 0.00 | 0.01 | 0.00 | 0.01 | 0.93 | 0.94 | 0.94 | 0.94 | 0.95 | 0.93 | 0.93 | 0.93 | 0.93 | 0.01 | 0.01 |

Appendix 1.3: Mineral Chemistry analysis for feldspars
Recalculated to 8O

| Thin Section | MC7017 | MC7017 | MC7017 | MC7017 | MC7017 | MC7017 | MC7017 | MC7017 | MC7017 | MC7017 | MC7017 | MC7017 | MC7017 | MC7018 | MC7018 | MC7018 | MC7018 | MC7018 |
|---|---|---|---|---|---|---|---|---|---|---|---|---|---|---|---|---|---|---|
| Circle No | C1 | C1 | C1 | C1 | C2 | C2 | C2 | C2 | C2 | C2 | C2 | C2 | C2 | C1 | C1 | C1 | C1 | C1 |
| Location | core | core | core | core | core | core | core | core | core | core | core | core | core | core | core | core | core | core |
| **wt%** | | | | | | | | | | | | | | | | | | |
| SiO2 | 71.87 | 73.33 | 71.27 | 64.58 | 66.00 | 64.81 | 65.02 | 65.59 | 64.86 | 64.86 | 65.86 | 65.58 | 64.49 | 65.78 | 66.37 | 65.62 | 65.45 | 67.38 |
| Al2O3 | 19.66 | 19.89 | 19.64 | 18.47 | 18.95 | 18.54 | 18.68 | 18.56 | 18.42 | 18.43 | 18.79 | 18.80 | 18.57 | 18.20 | 17.61 | 18.01 | 18.29 | 17.61 |
| Fe2O3 | 0.92 | 0.92 | 0.80 | 0.15 | 0.15 | 0.10 | 0.11 | 0.15 | 0.15 | 0.00 | 0.28 | 0.32 | 0.23 | 0.54 | 0.76 | 0.69 | 0.59 | 0.28 |
| MgO | 0.02 | 0.04 | 0.06 | 0.03 | 0.06 | 0.05 | 0.05 | 0.01 | 0.02 | 0.01 | 0.00 | 0.00 | 0.03 | 0.07 | 0.03 | 0.02 | 0.03 | 0.02 |
| CaO | 0.00 | 0.00 | 0.00 | 0.00 | 0.00 | 0.00 | 0.00 | 0.00 | 0.00 | 0.00 | 0.00 | 0.00 | 0.00 | 0.00 | 0.00 | 0.00 | 0.00 | 0.00 |
| Na2O | 5.94 | 5.31 | 8.83 | 0.47 | 0.47 | 0.47 | 0.53 | 0.45 | 0.51 | 0.49 | 0.53 | 0.49 | 0.52 | 0.31 | 0.30 | 0.26 | 0.26 | 0.31 |
| K2O | 0.13 | 0.11 | 0.25 | 15.30 | 15.10 | 14.87 | 15.09 | 15.07 | 14.89 | 14.97 | 15.14 | 14.98 | 14.77 | 14.59 | 14.91 | 15.39 | 15.54 | 14.79 |
| Total | 98.54 | 99.59 | 100.85 | 99.00 | 100.74 | 98.84 | 99.47 | 99.82 | 98.85 | 98.76 | 100.60 | 100.17 | 98.60 | 99.49 | 99.97 | 99.98 | 100.16 | 100.38 |
| | | | | | | | | | | | | | | | | | | |
| Si | 3.34 | 3.40 | 3.17 | 3.02 | 3.04 | 3.04 | 3.02 | 3.05 | 3.04 | 3.04 | 3.03 | 3.03 | 3.03 | 3.08 | 3.09 | 3.05 | 3.03 | 3.12 |
| Al | 1.08 | 1.09 | 1.03 | 1.02 | 1.03 | 1.02 | 1.02 | 1.02 | 1.02 | 1.02 | 1.02 | 1.03 | 1.03 | 1.00 | 0.97 | 0.99 | 1.00 | 0.96 |
| S T-site | 4.42 | 4.48 | 4.19 | 4.04 | 4.06 | 4.06 | 4.05 | 4.06 | 4.06 | 4.06 | 4.05 | 4.06 | 4.06 | 4.08 | 4.06 | 4.04 | 4.03 | 4.09 |
| | | | | | | | | | | | | | | | | | | |
| Ca | 0.00 | 0.00 | 0.00 | 0.00 | 0.00 | 0.00 | 0.00 | 0.00 | 0.00 | 0.00 | 0.00 | 0.00 | 0.00 | 0.00 | 0.00 | 0.00 | 0.00 | 0.00 |
| Na | 0.54 | 0.48 | 0.76 | 0.04 | 0.04 | 0.04 | 0.05 | 0.04 | 0.05 | 0.04 | 0.05 | 0.04 | 0.05 | 0.03 | 0.03 | 0.02 | 0.02 | 0.03 |
| K | 0.01 | 0.01 | 0.01 | 0.91 | 0.89 | 0.89 | 0.90 | 0.89 | 0.89 | 0.90 | 0.89 | 0.88 | 0.89 | 0.87 | 0.89 | 0.91 | 0.92 | 0.87 |
| S A-site | 0.54 | 0.48 | 0.77 | 0.96 | 0.93 | 0.93 | 0.94 | 0.93 | 0.94 | 0.94 | 0.94 | 0.93 | 0.93 | 0.90 | 0.91 | 0.94 | 0.94 | 0.90 |
| | | | | | | | | | | | | | | | | | | |
| Endmember c | | | | | | | | | | | | | | | | | | |
| An (Ca) | 0.00 | 0.00 | 0.00 | 0.00 | 0.00 | 0.00 | 0.00 | 0.00 | 0.00 | 0.00 | 0.00 | 0.00 | 0.00 | 0.00 | 0.00 | 0.00 | 0.00 | 0.00 |
| Ab (Na) | 0.99 | 0.99 | 0.98 | 0.04 | 0.05 | 0.05 | 0.05 | 0.04 | 0.05 | 0.05 | 0.05 | 0.05 | 0.05 | 0.03 | 0.03 | 0.03 | 0.02 | 0.03 |
| Or (K) | 0.01 | 0.01 | 0.02 | 0.96 | 0.95 | 0.95 | 0.95 | 0.96 | 0.95 | 0.95 | 0.95 | 0.95 | 0.95 | 0.97 | 0.97 | 0.97 | 0.98 | 0.97 |

Appendix 1.3: Mineral Chemistry analysis for feldspars
Recalculated to 8O

| Thin Section | MC7026 | MC7026 | MC7026 | MC7026 | MC7026 | MC7026 | MC7026 | MC7026 | MC7026 | MC7026 | MC7026 | MC7026 | MC7026 | MC7026 | MC7026 | MC7037 | MC7037 | MC7037 |
|---|---|---|---|---|---|---|---|---|---|---|---|---|---|---|---|---|---|---|
| Circle No | C1 | C1 | C1 | C2 | C2 | C2 | C2 | C2 | C4 | C4 | C4 | C4 | C4 | C4 | C4 | C1 | C1 | C1 |
| Location | core | core | core | core | core | core | core | core | core | core | core | core | core | core | core | | | |
| **wt%** | | | | | | | | | | | | | | | | | | |
| SiO2 | 69.80 | 69.75 | 69.17 | 68.59 | 69.07 | 64.79 | 64.90 | 64.52 | 69.25 | 69.55 | 69.17 | 69.69 | 66.00 | 66.01 | 66.53 | 69.65 | 69.18 | 68.85 |
| Al2O3 | 19.80 | 19.70 | 19.82 | 19.72 | 19.76 | 18.92 | 18.70 | 18.52 | 19.95 | 19.92 | 19.73 | 19.95 | 18.70 | 18.78 | 18.77 | 19.27 | 19.08 | 19.09 |
| Fe2O3 | 0.28 | 0.28 | 0.20 | 0.08 | 0.05 | 0.00 | 0.00 | 0.00 | 0.14 | 0.06 | 0.23 | 0.10 | 0.22 | 0.04 | 0.43 | 0.01 | 0.03 | 0.01 |
| MgO | 0.02 | 0.00 | 0.05 | 0.03 | 0.02 | 0.01 | 0.02 | 0.00 | 0.04 | 0.05 | 0.06 | 0.03 | 0.03 | 0.00 | 0.05 | 0.12 | 0.01 | 0.01 |
| CaO | 0.00 | 0.03 | 0.05 | 0.07 | 0.03 | 0.00 | 0.00 | 0.00 | 0.09 | 0.18 | 0.06 | 0.06 | 0.00 | 0.00 | 0.00 | 0.48 | 0.54 | 0.47 |
| Na2O | 10.78 | 10.84 | 10.64 | 10.61 | 10.63 | 0.65 | 0.27 | 0.26 | 10.52 | 10.64 | 10.60 | 10.83 | 1.11 | 0.41 | 0.60 | 11.31 | 11.07 | 11.13 |
| K2O | 0.17 | 0.23 | 0.16 | 0.11 | 0.12 | 14.90 | 15.18 | 15.19 | 0.22 | 0.13 | 0.21 | 0.09 | 14.30 | 15.41 | 14.91 | 0.10 | 0.07 | 0.13 |
| Total | 100.85 | 100.83 | 100.09 | 99.20 | 99.67 | 99.26 | 99.06 | 98.49 | 100.21 | 100.53 | 100.07 | 100.74 | 100.36 | 100.65 | 101.29 | 100.93 | 99.97 | 99.69 |
| | | | | | | | | | | | | | | | | | | |
| Si | 3.05 | 3.05 | 3.04 | 3.04 | 3.05 | 3.02 | 3.04 | 3.04 | 3.05 | 3.05 | 3.05 | 3.04 | 3.04 | 3.04 | 3.04 | 3.05 | 3.03 | 3.04 | 3.03 |
| Al | 1.02 | 1.01 | 1.03 | 1.03 | 1.03 | 1.04 | 1.03 | 1.03 | 1.03 | 1.03 | 1.02 | 1.03 | 1.01 | 1.02 | 1.01 | 0.99 | 0.99 | 0.99 |
| S T-site | **4.07** | **4.06** | **4.07** | **4.07** | **4.08** | **4.06** | **4.07** | **4.06** | **4.08** | **4.08** | **4.07** | **4.07** | **4.05** | **4.06** | **4.06** | **4.01** | **4.03** | **4.02** |
| | | | | | | | | | | | | | | | | | | |
| Ca | 0.00 | 0.00 | 0.00 | 0.00 | 0.00 | 0.00 | 0.00 | 0.00 | 0.00 | 0.01 | 0.00 | 0.00 | 0.00 | 0.00 | 0.00 | 0.02 | 0.03 | 0.02 |
| Na | 0.91 | 0.92 | 0.91 | 0.91 | 0.91 | 0.06 | 0.02 | 0.02 | 0.90 | 0.90 | 0.91 | 0.92 | 0.10 | 0.04 | 0.05 | 0.95 | 0.94 | 0.95 |
| K | 0.01 | 0.01 | 0.01 | 0.01 | 0.01 | 0.89 | 0.91 | 0.91 | 0.01 | 0.01 | 0.01 | 0.00 | 0.84 | 0.91 | 0.87 | 0.01 | 0.00 | 0.01 |
| S A-site | **0.92** | **0.93** | **0.92** | **0.92** | **0.92** | **0.94** | **0.93** | **0.94** | **0.91** | **0.92** | **0.92** | **0.92** | **0.94** | **0.94** | **0.92** | **0.98** | **0.97** | **0.98** |
| | | | | | | | | | | | | | | | | | | |
| Endmember c | | | | | | | | | | | | | | | | | | |
| An (Ca) | 0.00 | 0.00 | 0.00 | 0.00 | 0.00 | 0.00 | 0.00 | 0.00 | 0.00 | 0.01 | 0.00 | 0.00 | 0.00 | 0.00 | 0.00 | 0.02 | 0.03 | 0.02 |
| Ab (Na) | 0.99 | 0.99 | 0.99 | 0.99 | 0.99 | 0.06 | 0.03 | 0.03 | 0.98 | 0.98 | 0.98 | 0.99 | 0.11 | 0.04 | 0.06 | 0.97 | 0.97 | 0.97 |
| Or (K) | **0.01** | **0.01** | **0.01** | **0.01** | **0.01** | **0.94** | **0.97** | **0.97** | **0.01** | **0.01** | **0.01** | **0.01** | **0.89** | **0.96** | **0.94** | **0.01** | **0.00** | **0.01** |

Appendix 1.3: Mineral Chemistry analysis for feldspars
Recalculated to 8O

| Thin Section | MC7037 | MC7037 | MC7037 | MC7037 | MC7037 | MC7037 | MC7037 | MC7037 | MC7037 | MC7037 | MC7037 | MC7037 | MC7037 | MC7037 | MC7037 | MC7037 | MC7037 | MC7037 |
|---|---|---|---|---|---|---|---|---|---|---|---|---|---|---|---|---|---|---|
| Circle No | C1 | C1 | C1 | C1 | C1 | C1 | C1 | C1 | C1 | C2 | C2 | C2 | C2 | C2 | C2 | C3 | C3 | C3 |
| Location |  |  |  | rim | rim | rim | rim |  |  | rim | rim | core | core | core | core | core | core | core |
| **wt%** |  |  |  |  |  |  |  |  |  |  |  |  |  |  |  |  |  |  |
| SiO2 | 69.24 | 68.58 | 68.20 | 68.62 | 68.52 | 69.19 | 68.33 | 67.72 | 66.27 | 67.45 | 69.28 | 68.94 | 69.03 | 69.61 | 68.30 | 68.33 | 68.69 | 68.46 |
| Al2O3 | 18.85 | 18.84 | 18.83 | 18.91 | 19.05 | 19.23 | 19.04 | 16.85 | 18.01 | 19.38 | 19.43 | 19.10 | 19.05 | 19.01 | 19.00 | 18.76 | 19.58 | 19.12 |
| Fe2O3 | 0.05 | 0.00 | 0.08 | 0.00 | 0.00 | 0.05 | 0.06 | 0.06 | 0.11 | 0.11 | 0.03 | 0.15 | 0.24 | 0.00 | 0.00 | 0.04 | 0.12 | 0.01 |
| MgO | 0.08 | 0.00 | 0.06 | 0.03 | 0.00 | 0.07 | 0.06 | 0.00 | 0.04 | 0.00 | 0.03 | 0.02 | 0.02 | 0.08 | 0.00 | 0.09 | 0.00 | 0.07 |
| CaO | 0.17 | 0.35 | 0.37 | 0.39 | 0.53 | 0.46 | 0.62 | 0.22 | 0.02 | 0.65 | 0.64 | 0.59 | 0.47 | 0.35 | 0.43 | 0.48 | 0.35 | 0.50 |
| Na2O | 11.52 | 11.38 | 10.97 | 11.23 | 11.34 | 11.50 | 11.11 | 2.66 | 1.41 | 10.87 | 11.42 | 11.28 | 11.24 | 11.64 | 11.37 | 11.27 | 11.27 | 11.18 |
| K2O | 0.07 | 0.04 | 0.06 | 0.06 | 0.07 | 0.08 | 0.06 | 11.11 | 14.18 | 0.11 | 0.14 | 0.07 | 0.10 | 0.01 | 0.00 | 0.05 | 0.28 | 0.14 |
| **Total** | **99.99** | **99.19** | **98.55** | **99.24** | **99.51** | **100.59** | **99.28** | **98.61** | **100.03** | **98.56** | **100.97** | **100.15** | **100.15** | **100.70** | **99.10** | **99.01** | **100.29** | **99.49** |
|  |  |  |  |  |  |  |  |  |  |  |  |  |  |  |  |  |  |  |
| Si | 3.03 | 3.03 | 3.04 | 3.03 | 3.02 | 3.01 | 3.02 | 3.16 | 3.05 | 3.00 | 3.01 | 3.02 | 3.02 | 3.02 | 3.02 | 3.02 | 3.00 | 3.02 |
| Al | 0.97 | 0.98 | 0.99 | 0.98 | 0.99 | 0.99 | 0.99 | 0.93 | 0.98 | 1.02 | 0.99 | 0.99 | 0.98 | 0.97 | 0.99 | 0.98 | 1.01 | 0.99 |
| **S T-site** | **4.00** | **4.01** | **4.03** | **4.01** | **4.00** | **4.00** | **4.01** | **4.09** | **4.03** | **4.02** | **4.00** | **4.00** | **4.01** | **4.00** | **4.01** | **4.00** | **4.01** | **4.01** |
|  |  |  |  |  |  |  |  |  |  |  |  |  |  |  |  |  |  |  |
| Ca | 0.01 | 0.02 | 0.02 | 0.02 | 0.03 | 0.02 | 0.03 | 0.01 | 0.00 | 0.03 | 0.03 | 0.03 | 0.02 | 0.02 | 0.02 | 0.02 | 0.02 | 0.02 |
| Na | 0.98 | 0.97 | 0.95 | 0.96 | 0.97 | 0.97 | 0.95 | 0.24 | 0.13 | 0.94 | 0.96 | 0.96 | 0.95 | 0.98 | 0.97 | 0.97 | 0.95 | 0.96 |
| K | 0.00 | 0.00 | 0.00 | 0.00 | 0.00 | 0.00 | 0.00 | 0.66 | 0.83 | 0.01 | 0.01 | 0.00 | 0.01 | 0.00 | 0.00 | 0.00 | 0.02 | 0.01 |
| **S A-site** | **0.99** | **0.99** | **0.97** | **0.98** | **1.00** | **1.00** | **0.98** | **0.91** | **0.96** | **0.98** | **1.00** | **0.99** | **0.98** | **1.00** | **0.99** | **0.99** | **0.99** | **0.99** |
|  |  |  |  |  |  |  |  |  |  |  |  |  |  |  |  |  |  |  |
| **Endmember c** |  |  |  |  |  |  |  |  |  |  |  |  |  |  |  |  |  |  |
| An (Ca) | 0.01 | 0.02 | 0.02 | 0.02 | 0.03 | 0.02 | 0.03 | 0.01 | 0.00 | 0.03 | 0.03 | 0.03 | 0.02 | 0.02 | 0.02 | 0.02 | 0.02 | 0.02 |
| Ab (Na) | 0.99 | 0.98 | 0.98 | 0.98 | 0.97 | 0.97 | 0.97 | 0.26 | 0.13 | 0.96 | 0.96 | 0.97 | 0.97 | 0.98 | 0.98 | 0.97 | 0.97 | 0.97 |
| **Or (K)** | **0.00** | **0.00** | **0.00** | **0.00** | **0.00** | **0.00** | **0.00** | **0.72** | **0.87** | **0.01** | **0.01** | **0.00** | **0.01** | **0.00** | **0.00** | **0.00** | **0.02** | **0.01** |

Appendix 1.3: Mineral Chemistry analysis for feldspars
Recalculated to 8O

| Thin Section | MC7037 | MC7037 | MC7037 | MC7037 | MC7039 | MC7039 | MC7039 | MC7039 | MC7039 | MC7039 | MC7039 | MC7039 | MC7039 | MC7039 | MC7039 | MC7039 | MC7039 | MC7039 |
|---|---|---|---|---|---|---|---|---|---|---|---|---|---|---|---|---|---|---|
| Circle No | C4 | C4 | C4 | C4 | C1 | C1 | C1 | C1 | C1 | C1 | C1 | C2 | C2 | C2 | C2 | C2 | C2 | C2 |
| Location | core | core | core | core | | | | | rim | rim | rim | | | | | | | |
| | | | | | | | | | | | | | | | | | | |
| wt% | | | | | | | | | | | | | | | | | | |
| SiO2 | 68.75 | 68.64 | 68.86 | 68.04 | 69.13 | 68.01 | 67.94 | 67.93 | 67.75 | 68.09 | 67.76 | 70.80 | 70.86 | 70.26 | 71.80 | 70.60 | 68.34 | 68.57 |
| Al2O3 | 19.01 | 18.93 | 18.81 | 18.95 | 14.97 | 15.02 | 14.90 | 14.76 | 14.75 | 14.85 | 14.90 | 17.67 | 16.70 | 17.51 | 16.69 | 17.46 | 15.07 | 15.06 |
| Fe2O3 | 0.08 | 0.18 | 0.03 | 0.00 | 0.07 | 0.09 | 0.03 | 0.10 | 0.23 | 0.22 | 0.29 | 0.19 | 0.17 | 0.17 | 0.17 | 0.15 | 0.28 | 0.31 |
| MgO | 0.13 | 0.01 | 0.04 | 0.00 | 0.00 | 0.00 | 0.03 | 0.05 | 0.00 | 0.00 | 0.00 | 0.08 | 0.08 | 0.07 | 0.05 | 0.10 | 0.00 | 0.02 |
| CaO | 0.51 | 0.40 | 0.40 | 0.43 | 0.00 | 0.00 | 0.00 | 0.00 | 0.00 | 0.00 | 0.00 | 1.82 | 1.12 | 1.62 | 0.72 | 1.53 | 0.00 | 0.00 |
| Na2O | 11.27 | 11.36 | 11.31 | 11.13 | 0.68 | 0.53 | 0.38 | 0.60 | 0.72 | 0.68 | 0.77 | 7.81 | 9.50 | 9.93 | 10.69 | 10.19 | 1.22 | 1.15 |
| K2O | 0.01 | 1.12 | 0.14 | 0.00 | 16.03 | 15.79 | 16.18 | 15.95 | 15.69 | 16.08 | 15.71 | 0.60 | 0.58 | 0.66 | 0.60 | 0.52 | 14.89 | 15.36 |
| Total | 99.76 | 100.64 | 99.60 | 98.55 | 100.88 | 99.43 | 99.46 | 99.38 | 99.15 | 99.92 | 99.43 | 98.97 | 99.02 | 100.20 | 100.73 | 100.55 | 99.79 | 100.46 |
| | | | | | | | | | | | | | | | | | | |
| Si | 3.02 | 2.98 | 3.03 | 3.03 | 3.18 | 3.18 | 3.18 | 3.17 | 3.17 | 3.16 | 3.16 | 3.23 | 3.19 | 3.11 | 3.15 | 3.11 | 3.17 | 3.16 |
| Al | 0.98 | 0.97 | 0.98 | 0.99 | 0.81 | 0.83 | 0.82 | 0.81 | 0.81 | 0.81 | 0.82 | 0.95 | 0.89 | 0.91 | 0.86 | 0.91 | 0.82 | 0.82 |
| S T-site | 4.00 | 3.96 | 4.00 | 4.02 | 4.00 | 4.01 | 4.00 | 3.99 | 3.99 | 3.98 | 3.98 | 4.17 | 4.07 | 4.02 | 4.01 | 4.02 | 4.00 | 3.98 |
| | | | | | | | | | | | | | | | | | | |
| Ca | 0.02 | 0.02 | 0.02 | 0.02 | 0.00 | 0.00 | 0.00 | 0.00 | 0.00 | 0.00 | 0.00 | 0.09 | 0.05 | 0.08 | 0.03 | 0.07 | 0.00 | 0.00 |
| Na | 0.96 | 0.96 | 0.96 | 0.96 | 0.06 | 0.05 | 0.03 | 0.05 | 0.07 | 0.06 | 0.07 | 0.69 | 0.83 | 0.85 | 0.91 | 0.87 | 0.11 | 0.10 |
| K | 0.00 | 0.06 | 0.01 | 0.00 | 0.94 | 0.94 | 0.97 | 0.95 | 0.94 | 0.95 | 0.94 | 0.03 | 0.03 | 0.04 | 0.03 | 0.03 | 0.88 | 0.90 |
| S A-site | 0.98 | 1.04 | 0.99 | 0.98 | 1.00 | 0.99 | 1.00 | 1.01 | 1.00 | 1.01 | 1.01 | 0.81 | 0.92 | 0.97 | 0.98 | 0.97 | 0.99 | 1.01 |
| | | | | | | | | | | | | | | | | | | |
| Endmember c | | | | | | | | | | | | | | | | | | |
| An (Ca) | 0.02 | 0.02 | 0.02 | 0.02 | 0.00 | 0.00 | 0.00 | 0.00 | 0.00 | 0.00 | 0.00 | 0.11 | 0.06 | 0.08 | 0.03 | 0.07 | 0.00 | 0.00 |
| Ab (Na) | 0.98 | 0.92 | 0.97 | 0.98 | 0.06 | 0.05 | 0.03 | 0.05 | 0.07 | 0.06 | 0.07 | 0.85 | 0.90 | 0.88 | 0.93 | 0.90 | 0.11 | 0.10 |
| Or (K) | 0.00 | 0.06 | 0.01 | 0.00 | 0.94 | 0.95 | 0.97 | 0.95 | 0.93 | 0.94 | 0.93 | 0.04 | 0.04 | 0.04 | 0.03 | 0.03 | 0.89 | 0.90 |

Appendix 1.3: Mineral Chemistry analysis for feldspars
Recalculated to 8O

| Thin Section | MC7039 | MC7039 | MC7039 | MC7039 | MC7039 | MC7039 | MC7046 | MC7046 | MC7046 | MC7046 | MC7046 | MC7046 | MC7046 | MC7046 | MC7046 | MC7046 | MC7046 | MC7046 |
|---|---|---|---|---|---|---|---|---|---|---|---|---|---|---|---|---|---|---|
| Circle No | C2 | C2 | C2 | C2 | C2 | C2 | C1 | C1 | C1 | C1 | C1 | C1 | C1 | C1 | C1 | C1 | C1 | C1 |
| Location |  |  |  |  |  |  | core | core | core | core | core |  |  |  |  |  |  |  |
| wt% |  |  |  |  |  |  |  |  |  |  |  |  |  |  |  |  |  |  |
| SiO2 | 68.50 | 68.35 | 67.28 | 68.12 | 67.96 | 68.07 | 65.78 | 65.30 | 64.39 | 65.34 | 65.79 | 65.13 | 64.97 | 64.98 | 64.58 | 65.31 | 71.25 | 72.67 |
| Al2O3 | 14.93 | 14.97 | 14.42 | 14.90 | 14.87 | 14.81 | 17.56 | 17.34 | 17.10 | 17.40 | 17.28 | 16.67 | 16.97 | 17.52 | 17.17 | 17.48 | 14.82 | 15.08 |
| Fe2O3 | 0.27 | 0.30 | 0.09 | 0.15 | 0.12 | 0.00 | 0.22 | 0.30 | 0.19 | 0.10 | 0.33 | 0.76 | 0.35 | 0.09 | 0.27 | 0.07 | 0.76 | 0.79 |
| MgO | 0.09 | 0.00 | 0.10 | 0.14 | 0.03 | 0.15 | 0.02 | 0.00 | 0.04 | 0.14 | 0.00 | 0.01 | 0.07 | 0.06 | 0.05 | 0.05 | 0.00 | 0.00 |
| CaO | 0.00 | 0.00 | 0.00 | 0.00 | 0.00 | 0.00 | 0.00 | 0.00 | 0.00 | 0.00 | 0.00 | 0.00 | 0.00 | 0.00 | 0.00 | 0.00 | 0.00 | 0.00 |
| Na2O | 1.19 | 0.91 | 1.09 | 1.12 | 1.06 | 1.35 | 0.47 | 0.36 | 0.47 | 0.25 | 0.42 | 0.48 | 0.40 | 0.44 | 0.35 | 0.41 | 11.38 | 11.45 |
| K2O | 15.03 | 15.50 | 15.20 | 15.18 | 15.31 | 15.01 | 15.69 | 16.07 | 15.97 | 16.32 | 16.15 | 15.93 | 15.84 | 16.15 | 16.02 | 16.09 | 0.10 | 0.07 |
| Total | 100.01 | 100.03 | 98.17 | 99.61 | 99.36 | 99.38 | 99.74 | 99.36 | 98.15 | 99.56 | 99.96 | 98.97 | 98.59 | 99.24 | 98.44 | 99.42 | 98.30 | 100.06 |
| Si | 3.17 | 3.17 | 3.17 | 3.17 | 3.17 | 3.17 | 3.06 | 3.05 | 3.04 | 3.04 | 3.05 | 3.05 | 3.06 | 3.03 | 3.04 | 3.04 | 3.20 | 3.21 |
| Al | 0.82 | 0.82 | 0.80 | 0.82 | 0.82 | 0.81 | 0.96 | 0.95 | 0.95 | 0.95 | 0.94 | 0.92 | 0.94 | 0.96 | 0.95 | 0.96 | 0.78 | 0.78 |
| S T-site | 3.99 | 3.99 | 3.98 | 3.98 | 3.99 | 3.98 | 4.02 | 4.00 | 3.99 | 3.99 | 3.99 | 3.98 | 4.00 | 3.99 | 3.99 | 4.00 | 3.98 | 3.99 |
| Ca | 0.00 | 0.00 | 0.00 | 0.00 | 0.00 | 0.00 | 0.00 | 0.00 | 0.00 | 0.00 | 0.00 | 0.00 | 0.00 | 0.00 | 0.00 | 0.00 | 0.00 | 0.00 |
| Na | 0.11 | 0.08 | 0.10 | 0.10 | 0.10 | 0.12 | 0.04 | 0.03 | 0.04 | 0.02 | 0.04 | 0.04 | 0.04 | 0.04 | 0.03 | 0.04 | 0.99 | 0.98 |
| K | 0.89 | 0.92 | 0.91 | 0.90 | 0.91 | 0.89 | 0.93 | 0.96 | 0.96 | 0.97 | 0.96 | 0.95 | 0.95 | 0.96 | 0.96 | 0.96 | 0.01 | 0.00 |
| S A-site | 1.00 | 1.00 | 1.01 | 1.00 | 1.01 | 1.01 | 0.97 | 0.99 | 1.00 | 0.99 | 0.99 | 1.00 | 0.99 | 1.00 | 0.99 | 0.99 | 1.00 | 0.98 |
| Endmember c |  |  |  |  |  |  |  |  |  |  |  |  |  |  |  |  |  |  |
| An (Ca) | 0.00 | 0.00 | 0.00 | 0.00 | 0.00 | 0.00 | 0.00 | 0.00 | 0.00 | 0.00 | 0.00 | 0.00 | 0.00 | 0.00 | 0.00 | 0.00 | 0.00 | 0.00 |
| Ab (Na) | 0.11 | 0.08 | 0.10 | 0.10 | 0.10 | 0.12 | 0.04 | 0.03 | 0.04 | 0.02 | 0.04 | 0.04 | 0.04 | 0.04 | 0.03 | 0.04 | 0.99 | 1.00 |
| Or (K) | 0.89 | 0.92 | 0.90 | 0.90 | 0.90 | 0.88 | 0.96 | 0.97 | 0.96 | 0.98 | 0.96 | 0.96 | 0.96 | 0.96 | 0.97 | 0.96 | 0.01 | 0.00 |

Appendix 1.3: Mineral Chemistry analysis for feldspars
Recalculated to 8O

| Thin Section | MC7046 | MC7046 | MC7046 | MC7046 | MC7046 | MC7046 | MC7046 | MC7046 | MC7046 | MC7046 | MC7046 |
|---|---|---|---|---|---|---|---|---|---|---|---|
| Circle No | C1 | C1 | C1 | C1 | C1 | C1 | C1 | C1 | C1 | C1 | C1 |
| Location | | | | | | | | | | | |
| | | | | | | | | | | | |
| wt% | | | | | | | | | | | |
| SiO2 | 72.79 | 72.89 | 72.42 | 73.17 | 72.20 | 71.23 | 71.49 | 70.76 | 72.28 | 71.29 | 72.69 |
| Al2O3 | 15.07 | 15.04 | 14.85 | 15.04 | 14.94 | 14.74 | 14.72 | 14.49 | 14.82 | 14.60 | 14.84 |
| Fe2O3 | 0.79 | 0.77 | 0.90 | 1.23 | 1.16 | 0.91 | 0.84 | 1.12 | 1.15 | 1.14 | 1.20 |
| MgO | 0.00 | 0.00 | 0.00 | 0.07 | 0.21 | 0.00 | 0.00 | 0.00 | 0.00 | 0.00 | 0.00 |
| CaO | 0.00 | 0.00 | 0.00 | 0.00 | 0.00 | 0.00 | 0.00 | 0.00 | 0.00 | 0.00 | 0.00 |
| Na2O | 11.71 | 11.56 | 11.61 | 11.52 | 11.41 | 11.40 | 11.47 | 11.49 | 11.50 | 11.45 | 11.54 |
| K2O | 0.07 | 0.06 | 0.10 | 0.78 | 0.79 | 0.06 | 0.10 | 0.12 | 0.12 | 0.13 | 0.11 |
| Total | 100.43 | 100.31 | 99.87 | 101.81 | 100.70 | 98.34 | 98.62 | 97.97 | 99.86 | 98.61 | 100.38 |
| | | | | | | | | | | | |
| Si | 3.19 | 3.21 | 3.20 | 3.17 | 3.16 | 3.20 | 3.20 | 3.18 | 3.20 | 3.19 | 3.20 |
| Al | 0.78 | 0.78 | 0.77 | 0.77 | 0.77 | 0.78 | 0.78 | 0.77 | 0.77 | 0.77 | 0.77 |
| S T-site | 3.97 | 3.99 | 3.97 | 3.94 | 3.93 | 3.97 | 3.97 | 3.95 | 3.97 | 3.96 | 3.97 |
| | | | | | | | | | | | |
| Ca | 0.00 | 0.00 | 0.00 | 0.00 | 0.00 | 0.00 | 0.00 | 0.00 | 0.00 | 0.00 | 0.00 |
| Na | 1.00 | 0.99 | 0.99 | 0.97 | 0.97 | 0.99 | 0.99 | 1.00 | 0.99 | 0.99 | 0.98 |
| K | 0.00 | 0.00 | 0.01 | 0.04 | 0.04 | 0.00 | 0.01 | 0.01 | 0.01 | 0.01 | 0.01 |
| S A-site | 1.00 | 0.99 | 1.00 | 1.01 | 1.01 | 1.00 | 1.00 | 1.01 | 0.99 | 1.00 | 0.99 |
| | | | | | | | | | | | |
| Endmember c | | | | | | | | | | | |
| An (Ca) | 0.00 | 0.00 | 0.00 | 0.00 | 0.00 | 0.00 | 0.00 | 0.00 | 0.00 | 0.00 | 0.00 |
| Ab (Na) | 1.00 | 1.00 | 0.99 | 0.96 | 0.96 | 1.00 | 0.99 | 0.99 | 0.99 | 0.99 | 0.99 |
| Or (K) | 0.00 | 0.00 | 0.01 | 0.04 | 0.04 | 0.00 | 0.01 | 0.01 | 0.01 | 0.01 | 0.01 |

Appendix 1.4 Major and trace element data

| Rock Type | Orthogneiss | Mafic dyke | Micro-granite | Xenoltih | Micro-granite | Granite | Monzonite | Felsic dyke | Granite | Felsic dyke | Granite | Xenoltih | Felsic dyke | Granite | Granite | Felsic dyke | Felsic dyke | Felsic dyke | Micro-granite |
|---|---|---|---|---|---|---|---|---|---|---|---|---|---|---|---|---|---|---|---|
| Sample Name | MC7-001 | MC7-002 | MC7-004 | MC7-005 | MC7-006 | MC7-007 | MC7-008 | MC7-009 | MC7-010 | MC7-012 | MC7-013 | MC7-015 | MC7-016 | MC7-017 | MC7-018 | MC7-019 | MC7-020 | MC7-023 | MC7-024A |
| **XRF major elements wt% oxide** | | | | | | | | | | | | | | | | | | | |
| $SiO_2$ | 62,4 | 48,0 | 67,3 | 45,6 | 73,9 | 73,9 | 58,1 | 74,9 | 73,5 | 74,2 | 73,5 | 71,7 | 73,7 | 74,1 | 73,6 | 73,8 | 74,3 | 73,9 | 74,6 |
| $TiO_2$ | 1,12 | 2,07 | 1,00 | 3,42 | 0,30 | 0,41 | 1,85 | 0,18 | 0,32 | 0,29 | 0,41 | 0,36 | 0,36 | 0,34 | 0,44 | 0,34 | 0,30 | 0,32 | 0,24 |
| $Al_2O_3$ | 15,0 | 15,3 | 12,7 | 12,7 | 10,6 | 9,17 | 14,1 | 9,04 | 9,47 | 9,36 | 9,70 | 9,10 | 9,16 | 10,4 | 9,96 | 9,52 | 9,19 | 12,6 | 9,64 |
| Fe2O3 | 9,01 | 14,0 | 6,37 | 15,3 | 5,04 | 6,77 | 9,71 | 5,76 | 6,39 | 6,00 | 6,33 | 7,65 | 6,72 | 4,83 | 5,92 | 6,00 | 6,19 | 2,92 | 5,24 |
| MnO | 0,14 | 0,20 | 0,16 | 0,22 | 0,15 | 0,17 | 0,17 | 0,11 | 0,17 | 0,14 | 0,20 | 0,19 | 0,19 | 0,09 | 0,14 | 0,15 | 0,15 | 0,07 | 0,11 |
| MgO | 3,03 | 5,83 | 1,13 | 5,63 | 0,24 | 0,25 | 2,45 | 0,21 | 0,28 | 0,23 | 0,42 | 0,37 | 0,24 | 0,32 | 0,33 | 0,21 | 0,22 | 0,36 | 0,25 |
| CaO | 0,75 | 8,30 | 2,35 | 10,2 | 0,32 | 0,16 | 5,52 | 0,14 | 0,15 | 0,18 | 0,19 | 0,22 | 0,14 | 0,27 | 0,34 | 0,22 | 0,11 | 0,30 | 0,12 |
| $Na_2O$ | 1,21 | 3,17 | 4,51 | 3,12 | 4,20 | 4,13 | 4,94 | 4,49 | 4,20 | 3,98 | 3,61 | 4,58 | 4,34 | 4,30 | 4,27 | 4,17 | 4,23 | 4,31 | 4,20 |
| $K_2O$ | 4,92 | 0,69 | 3,36 | 0,82 | 3,72 | 4,25 | 2,04 | 3,87 | 4,15 | 4,28 | 3,83 | 3,93 | 4,45 | 4,20 | 4,26 | 4,34 | 4,25 | 4,32 | 4,18 |
| $P_2O_5$ | 0,29 | 0,22 | 0,12 | 0,27 | 0,01 | 0,01 | 0,13 | 0,01 | 0,01 | 0,00 | 0,03 | 0,02 | 0,01 | 0,02 | 0,02 | 0,01 | 0,01 | 0,02 | 0,01 |
| $SO_3$ | 0,01 | 0,23 | 0,01 | 0,05 | 0,03 | 0,02 | 0,04 | 0,02 | 0,01 | 0,01 | 0,01 | 0,07 | 0,01 | 0,01 | 0,01 | 0,01 | 0,01 | 0,00 | 0,01 |
| $Cr_2O_3$ | 0,06 | 0,03 | 0,01 | 0,03 | 0,01 | 0,01 | 0,01 | 0,01 | 0,04 | 0,04 | 0,03 | 0,05 | 0,01 | 0,04 | 0,04 | 0,01 | 0,04 | 0,05 | 0,01 |
| NiO | 0,01 | 0,01 | 0,00 | 0,01 | 0,00 | 0,00 | 0,00 | 0,00 | 0,00 | 0,00 | 0,00 | 0,00 | 0,00 | 0,01 | 0,00 | 0,00 | 0,00 | 0,00 | 0,00 |
| $H_2O$- | 0,20 | 0,31 | 0,19 | 0,50 | 0,26 | 0,26 | 0,21 | 0,20 | 0,27 | 0,17 | 0,41 | 0,34 | 0,19 | 0,23 | 0,14 | 0,19 | 0,14 | 0,29 | 0,39 |
| LOI | 1,43 | 1,67 | 0,13 | 1,58 | 0,74 | 0,44 | 0,42 | 0,38 | 0,28 | 0,21 | 0,59 | 0,55 | 0,39 | 0,26 | 0,08 | 0,42 | 0,22 | 0,57 | 0,82 |
| Total | 99,5 | 100 | 99,4 | 99,5 | 99,5 | 100 | 99,7 | 99,3 | 99,3 | 99,1 | 99,2 | 99,1 | 99,9 | 99,5 | 99,6 | 99,4 | 99,4 | 100 | 100 |
| $SiO_2$ anh | 63,6 | 48,8 | 67,9 | 46,6 | 74,8 | 74,3 | 58,5 | 75,7 | 74,3 | 75,0 | 74,5 | 72,7 | 74,0 | 74,7 | 74,0 | 74,6 | 74,9 | 74,3 | 75,4 |
| **ICP-MS trace elements ppm** | | | | | | | | | | | | | | | | | | | |
| Sc | 29,0 | 30,6 | 9,96 | 42,9 | 3,43 | 3,30 | 18,4 | 4,12 | 3,82 | 3,23 | 3,63 | 3,95 | 3,59 | 3,15 | 3,78 | 3,42 | 3,61 | 4,54 | 4,98 |
| Ti | 9648 | 20634 | 10827 | 42073 | 1924 | 1560 | 11495 | 955 | 1708 | 1150 | 2125 | 1996 | 1997 | 1431 | 2467 | 1949 | 1875 | 1269 | 2329 |
| V | 155 | 316 | 41,9 | 464 | 4,42 | 6,08 | 213 | 3,09 | 22,4 | 23,8 | 19,7 | 26,5 | 3,11 | 22,9 | 24,9 | 5,71 | 19,7 | 4,48 | 29,1 |
| Cr | 352 | 99,3 | 10,3 | 97,1 | 21,9 | 6,98 | 6,33 | 4,55 | 213 | 266 | 175 | 273 | 6,8 | 215 | 208 | 52,0 | 221 | 8,39 | 225 |
| Co | 33,6 | 59,9 | 139 | 79,2 | 232 | 233 | 92,9 | 156 | 2,68 | 1,98 | 3,15 | 3,99 | 113 | 5,86 | 4,98 | 131 | 6,08 | 205 | 2,59 |
| Ni | 82,1 | 104 | 19,8 | 65,5 | 15,6 | 8,9 | 15,3 | 7,0 | 15,6 | 18,2 | 19,7 | 21,0 | 13,6 | 17,5 | 19,1 | 14,2 | 20,0 | 7,67 | 15,6 |
| Cu | 96,4 | 115 | 27,0 | 136 | 21,7 | 17,9 | 34,9 | 13,7 | 13,7 | 14,7 | 25,3 | 51,0 | 21,3 | 24,9 | 22,0 | 38,7 | 26,0 | 11,1 | 34,9 |
| Ga | 33,5 | 25,4 | 39,4 | 23,6 | 39,7 | 50,3 | 35,4 | 44,0 | 41,8 | 40,9 | 43,0 | 52,3 | 38,6 | 48,7 | 41,2 | 38,3 | 42,7 | 43,2 | 50,9 |
| Rb | 155 | 21,3 | 69,8 | 27,1 | 90,9 | 113 | 48,6 | 169 | 97,2 | 137 | 97,9 | 87,9 | 125 | 84,6 | 72,6 | 118 | 134 | 139 | 84,2 |
| Sr | 148 | 504 | 173 | 412 | 20,8 | 11,4 | 297 | 16,8 | 11,9 | 3,9 | 12,1 | 25,2 | 3,8 | 18,0 | 30,8 | 10,9 | 9,24 | 8,52 | 23,2 |
| Zr | 342 | 177 | 591 | 119 | 758 | 987 | 352 | 2680 | 455 | 1571 | 1032 | 531 | 1737 | 459 | 673 | 1648 | 1663 | 1699 | 706 |
| Nb | 16,8 | 9,59 | 38,1 | 8,11 | 44,0 | 66,7 | 23,4 | 149 | 58,8 | 93,5 | 78,4 | 36,3 | 105 | 31,1 | 51,4 | 95,3 | 96,4 | 97,8 | 53,5 |
| Y | 38,9 | 32,6 | 90,0 | 27,7 | 98,7 | 106 | 52,3 | 531 | 59,0 | 219 | 154 | 69,4 | 287 | 52,9 | 318 | 237 | 162 | 216 | 98,9 |
| Cs | 4,62 | 0,54 | 0,65 | 0,52 | 0,34 | 0,47 | 0,90 | 0,33 | 0,30 | 0,27 | 0,32 | 0,50 | 0,30 | 0,39 | 0,35 | 0,42 | 0,43 | 0,37 | 0,38 |
| Ba | 1135 | 311 | 650 | 125 | 393 | 628 | 413 | 174 | 226 | 113 | 416 | 1609 | 104 | 373 | 376 | 131 | 171 | 78,2 | 683 |
| Hf | 9,02 | 4,65 | 15,4 | 3,20 | 18,7 | 27,3 | 9,10 | 65,7 | 12,8 | 38,9 | 25,6 | 15,1 | 42,1 | 12,2 | 17,4 | 39,5 | 39,5 | 43,04 | 19,2 |
| Ta | 1,20 | 0,66 | 2,64 | 0,60 | 2,96 | 4,64 | 1,58 | 9,91 | 2,54 | 6,11 | 5,35 | 1,98 | 6,63 | 2,15 | 3,22 | 6,17 | 6,11 | 6,21 | 3,41 |
| Pb | 26,4 | 15,6 | 16,2 | 9,88 | 24,0 | 17,5 | 8,4 | 51,6 | 18,1 | 32,4 | 15,9 | 12,4 | 35,1 | 11,4 | 13,2 | 39,4 | 28,8 | 26,6 | 12,8 |
| Th | 14,4 | 0,97 | 6,09 | 0,61 | 7,09 | 7,35 | 2,90 | 16,4 | 8,01 | 9,97 | 8,33 | 6,70 | 9,25 | 4,07 | 5,84 | 9,06 | 9,33 | 10,4 | 6,32 |
| U | 3,47 | 0,20 | 1,15 | 0,13 | 0,82 | 1,11 | 0,59 | 3,68 | 0,91 | 1,91 | 1,44 | 1,16 | 1,45 | 0,67 | 1,10 | 1,42 | 1,68 | 1,40 | 1,12 |

Appendix 1.4 Major and trace element data

| Rock Type | Orthogneiss | Mafic dyke | Micro-granite | Xenoltih | Micro-granite | Granite | Monzonite | Felsic dyke | Granite | Felsic dyke | Granite | Xenoltih | Felsic dyke | Granite | Granite | Felsic dyke | Felsic dyke | Felsic dyke | Micro-granite |
|---|---|---|---|---|---|---|---|---|---|---|---|---|---|---|---|---|---|---|---|
| Sample Name | MC7-001 | MC7-002 | MC7-004 | MC7-005 | MC7-006 | MC7-007 | MC7-008 | MC7-009 | MC7-010 | MC7-012 | MC7-013 | MC7-015 | MC7-016 | MC7-017 | MC7-018 | MC7-019 | MC7-020 | MC7-023 | MC7-024A |
| *ICP-MS REE ppm* | | | | | | | | | | | | | | | | | | | |
| La | 51,3 | 18,8 | 48,6 | 12,5 | 53,9 | 33,0 | 27,4 | 250 | 43,5 | 233 | 53,9 | 59,3 | 242 | 25,0 | 171 | 313 | 383 | 138 | 50,4 |
| Ce | 86,9 | 31,3 | 92,1 | 20,9 | 107 | 66,7 | 50,2 | 494 | 74,0 | 401 | 113 | 97,4 | 387 | 42,9 | 179 | 534 | 445 | 218 | 74,5 |
| Pr | 10,6 | 4,5 | 12,3 | 3,21 | 14,4 | 7,65 | 6,99 | 64,6 | 11,3 | 57,4 | 12,8 | 12,0 | 64,7 | 5,68 | 43,9 | 74,7 | 77,3 | 32,3 | 10,2 |
| Nd | 44,8 | 22,4 | 58,7 | 17,3 | 65,7 | 35,2 | 33,0 | 293 | 49,1 | 256 | 56,7 | 51,2 | 293 | 26,4 | 218 | 326 | 296 | 139 | 44,2 |
| Sm | 9,39 | 5,88 | 15,2 | 5,2 | 16,6 | 9,49 | 9,17 | 74,6 | 12,0 | 59,7 | 15,3 | 10,6 | 74,9 | 6,43 | 58,9 | 69,7 | 53,0 | 30,5 | 10,7 |
| Eu | 1,80 | 1,95 | 3,56 | 1,92 | 3,51 | 2,65 | 2,51 | 12,2 | 2,91 | 7,70 | 4,07 | 2,41 | 12,5 | 1,76 | 14,9 | 9,17 | 6,18 | 4,88 | 2,76 |
| Gd | 8,57 | 6,40 | 16,9 | 6,24 | 17,4 | 11,9 | 9,6 | 86,7 | 10,9 | 52,7 | 19,6 | 10,0 | 80,7 | 7,17 | 70,4 | 58,4 | 36,8 | 33,1 | 12,8 |
| Tb | 1,27 | 1,06 | 2,67 | 0,93 | 3,16 | 2,57 | 1,60 | 14,7 | 1,88 | 7,76 | 4,01 | 1,69 | 12,1 | 1,27 | 10,1 | 7,94 | 5,18 | 5,6 | 2,28 |
| Dy | 8,19 | 6,49 | 17,8 | 5,71 | 20,0 | 18,7 | 10,2 | 90,6 | 12,0 | 46,3 | 29,1 | 12,0 | 69,9 | 9,77 | 62,5 | 45,3 | 32,7 | 39,4 | 17,0 |
| Ho | 1,59 | 1,30 | 3,39 | 1,05 | 3,72 | 4,10 | 1,95 | 17,6 | 2,15 | 8,43 | 5,92 | 2,41 | 12,2 | 1,99 | 11,7 | 8,50 | 6,26 | 8,0 | 3,43 |
| Er | 4,34 | 3,64 | 9,80 | 2,90 | 10,5 | 12,2 | 5,3 | 46,4 | 6,4 | 22,2 | 17,0 | 7,59 | 31,3 | 6,3 | 30,5 | 23,0 | 19,0 | 22,7 | 10,4 |
| Tm | 0,62 | 0,52 | 1,39 | 0,39 | 1,57 | 1,78 | 0,78 | 6,3 | 0,99 | 3,02 | 2,48 | 1,12 | 4,34 | 0,90 | 4,07 | 3,25 | 2,98 | 3,3 | 1,47 |
| Yb | 4,04 | 2,98 | 8,78 | 2,20 | 9,87 | 11,87 | 4,80 | 37,6 | 7,00 | 18,9 | 15,6 | 7,99 | 26,1 | 5,9 | 23,4 | 21,8 | 20,4 | 21,2 | 9,70 |
| Lu | 0,53 | 0,45 | 1,26 | 0,34 | 1,46 | 1,82 | 0,67 | 5,01 | 1,12 | 2,67 | 2,28 | 1,47 | 3,67 | 0,97 | 3,52 | 3,16 | 3,03 | 3,2 | 1,51 |

Appendix 1.4 Major and trace element data

| Rock Type | Micro-granite | Micro-granite | Syenite | Syenite | Mafic dyke | Felsic dyke | Orthogneiss | Felsic dyke | Felsic dyke | Micro-granite | Felsic dyke | Felsic dyke | Mafic dyke | Felsic dyke | Monzonite | Monzonite | Monzonite | Gabbroic | Mafic dyke |
|---|---|---|---|---|---|---|---|---|---|---|---|---|---|---|---|---|---|---|---|
| Sample Name | MC7-024B | MC7-025 | MC7-026 | MC7-027 | MC7-028 | MC7-029 | MC7-030 | MC7-031 | MC7-032 | MC7-033 | MC7-034 | MC7-035 | MC7-036 | MC7-038 | MC7-039 | MC7-040 | MC7-041 | MC7-042 | MC7-043 |
| *XRF major elements* | | | | | | | | | | | | | | | | | | | |
| $SiO_2$ | 73,6 | 73,7 | 74,0 | 66,3 | 60,2 | 72,6 | 60,6 | 74,5 | 75,7 | 73,4 | 72,7 | 76,7 | 48,5 | 72,4 | 59,5 | 58,2 | 57,5 | 45,0 | 45,2 |
| $TiO_2$ | 0,43 | 0,40 | 0,34 | 0,65 | 1,74 | 0,53 | 0,71 | 0,43 | 0,41 | 0,22 | 0,39 | 0,17 | 2,89 | 0,45 | 1,89 | 2,69 | 2,51 | 2,19 | 2,52 |
| $Al_2O_3$ | 10,5 | 10,8 | 10,9 | 14,4 | 13,9 | 11,2 | 17,5 | 9,58 | 9,42 | 7,50 | 13,9 | 12,4 | 13,5 | 12,5 | 13,5 | 12,9 | 11,1 | 15,3 | 14,5 |
| Fe2O3 | 5,68 | 5,34 | 4,61 | 6,41 | 8,78 | 5,85 | 6,14 | 6,12 | 5,95 | 8,55 | 3,15 | 0,57 | 15,1 | 5,09 | 10,2 | 11,2 | 13,3 | 12,6 | 14,3 |
| MnO | 0,18 | 0,12 | 0,18 | 0,31 | 0,28 | 0,11 | 0,13 | 0,22 | 0,17 | 0,11 | 0,03 | 0,02 | 0,22 | 0,03 | 0,26 | 0,23 | 0,26 | 0,17 | 0,20 |
| MgO | 0,26 | 0,30 | 0,37 | 0,44 | 1,91 | 0,39 | 1,95 | 0,22 | 0,22 | 0,26 | 0,25 | 0,22 | 5,46 | 0,23 | 1,90 | 2,42 | 2,70 | 7,87 | 7,10 |
| CaO | 0,21 | 0,19 | 0,26 | 1,53 | 3,74 | 0,45 | 4,28 | 0,18 | 0,42 | 0,10 | 0,14 | 0,21 | 8,77 | 0,08 | 5,03 | 5,31 | 4,98 | 11,0 | 9,87 |
| $Na_2O$ | 3,91 | 4,05 | 4,49 | 6,07 | 5,35 | 4,13 | 4,36 | 3,11 | 2,87 | 4,14 | 4,18 | 3,48 | 3,09 | 4,88 | 4,37 | 4,29 | 4,15 | 2,42 | 2,31 |
| $K_2O$ | 4,11 | 4,22 | 3,97 | 2,59 | 2,11 | 3,51 | 3,03 | 3,67 | 3,88 | 4,26 | 4,06 | 4,93 | 1,47 | 2,99 | 2,03 | 2,09 | 2,14 | 0,27 | 0,77 |
| $P_2O_5$ | 0,03 | 0,03 | 0,04 | 0,09 | 0,63 | 0,05 | 0,30 | 0,02 | 0,01 | 0,05 | 0,03 | 0,00 | 0,19 | 0,03 | 0,65 | 0,28 | 0,35 | 0,15 | 0,18 |
| $SO_3$ | 0,00 | 0,01 | 0,01 | 0,00 | 0,07 | 0,00 | 0,01 | 0,06 | 0,00 | 0,01 | 0,00 | 0,00 | 0,02 | 0,01 | 0,01 | 0,00 | 0,00 | 0,23 | 0,12 |
| $Cr_2O_3$ | 0,04 | 0,05 | 0,04 | 0,01 | 0,01 | 0,05 | 0,03 | 0,06 | 0,05 | 0,05 | 0,01 | 0,03 | 0,02 | 0,03 | 0,02 | 0,03 | 0,03 | 0,04 | 0,02 |
| NiO | 0,01 | 0,00 | 0,00 | 0,00 | 0,00 | 0,00 | 0,00 | 0,00 | 0,00 | 0,00 | 0,00 | 0,00 | 0,00 | 0,00 | 0,00 | 0,00 | 0,00 | 0,02 | 0,01 |
| $H_2O$- | 0,34 | 0,26 | 0,34 | 0,40 | 0,52 | 0,35 | 0,14 | 0,15 | 0,10 | 0,20 | 0,44 | 0,14 | 0,40 | 0,13 | 0,29 | 0,19 | 0,28 | 0,23 | 0,38 |
| LOI | 0,69 | 0,37 | 0,31 | 0,28 | 0,45 | 0,15 | 0,40 | 1,11 | 0,00 | 0,39 | 0,45 | 0,38 | 0,47 | 0,32 | 0,22 | 0,18 | 0,31 | 1,68 | 1,72 |
| Total | 100 | 99,8 | 99,9 | 99,4 | 99,7 | 99,4 | 99,6 | 99,4 | 99,2 | 99,2 | 99,8 | 99,3 | 100 | 99,2 | 99,9 | 100,1 | 99,6 | 99,2 | 99,2 |
| $SiO_2$ anh | 74,1 | 74,1 | 74,3 | 66,8 | 60,6 | 73,2 | 61,1 | 75,8 | 76,3 | 74,2 | 73,2 | 77,6 | 48,7 | 73,2 | 59,7 | 58,3 | 57,9 | 46,2 | 46,4 |
| *ICP-MS trace elements* | | | | | | | | | | | | | | | | | | | |
| Sc | 4,89 | 4,40 | 12,8 | 8,08 | 15,2 | 5,19 | 17,9 | 4,76 | 4,84 | 5,68 | 12,8 | 6,24 | 45,0 | 5,81 | 15,1 | 20,0 | 21,1 | 36,3 | 38,6 |
| Ti | 2184 | 1925 | 7089 | 3778 | 10707 | 3315 | 4430 | 2654 | 2550 | 935 | 1935 | 729 | 16091 | 2500 | 10114 | 15131 | 13647 | 12826 | 14163 |
| V | 29,9 | 22,7 | 6,34 | 3,83 | 67,9 | 43,9 | 98,3 | 35,0 | 27,6 | 26,8 | 1,90 | 15,6 | 493 | 16,3 | 94,2 | 179 | 224 | 333 | 419 |
| Cr | 259 | 179 | 10,3 | 7,69 | 11,4 | 260 | 136 | 353 | 284 | 260 | 3,97 | 166 | 70,0 | 171 | 124 | 115 | 110 | 205 | 86,9 |
| Co | 3,36 | 2,04 | 75,8 | 79,4 | 105 | 3,28 | 12,6 | 1,90 | 2,20 | 1,60 | 68,4 | 1,75 | 74,9 | 1,21 | 15,6 | 18,9 | 22,8 | 53,8 | 94,8 |
| Ni | 35,8 | 22,3 | 11,5 | 6,21 | 10,2 | 19,7 | 17,1 | 19,5 | 21,5 | 20,9 | 6,80 | 16,2 | 71,4 | 13,4 | 14,9 | 11,6 | 19,0 | 138 | 105 |
| Cu | 16,6 | 11,3 | 13,8 | 10,3 | 20,3 | 11,4 | 24,2 | 136 | 25,4 | 12,7 | 10,4 | 14,2 | 146 | 13,8 | 18,6 | 11,6 | 15,0 | 86,3 | 77,7 |
| Ga | 45,8 | 47,3 | 47,9 | 43,8 | 37,7 | 45,3 | 36,5 | 38,9 | 42,1 | 42,2 | 55,8 | 37,0 | 34,0 | 52,3 | 37,6 | 37,3 | 36,6 | 20,4 | 23,7 |
| Rb | 75,3 | 83,6 | 49,7 | 47,1 | 34,8 | 66,0 | 109 | 64,8 | 73,1 | 122 | 112 | 136 | 114 | 54,2 | 70,4 | 45,9 | 126 | 11,5 | 64,4 |
| Sr | 17,4 | 20,7 | 356 | 154 | 332 | 61,0 | 731 | 40,5 | 47,5 | 10,4 | 16,3 | 4,18 | 348 | 37,5 | 367 | 362 | 216 | 430 | 380 |
| Zr | 666 | 937 | 587 | 527 | 515 | 244 | 347 | 704 | 603 | 1928 | 857 | 309 | 125 | 751 | 320 | 662 | 398 | 64,4 | 90,5 |
| Nb | 48,8 | 62,6 | 47,0 | 44,4 | 45,5 | 22,9 | 11,4 | 46,4 | 40,9 | 128 | 46,9 | 42,8 | 10,6 | 55,0 | 28,7 | 50,1 | 28,2 | 4,60 | 5,95 |
| Y | 95,3 | 118 | 120 | 128 | 95,1 | 42,2 | 39,4 | 100 | 90,1 | 365 | 74,0 | 43,5 | 49,9 | 105 | 82,3 | 85,0 | 81,8 | 16,0 | 23,8 |
| Cs | 0,42 | 0,25 | 0,27 | 0,71 | 0,28 | 0,43 | 1,33 | 0,29 | 0,26 | 0,25 | 0,39 | 0,28 | 1,65 | 0,21 | 0,79 | 0,95 | 1,75 | 0,41 | 2,23 |
| Ba | 588 | 611 | 772 | 959 | 686 | 839 | 1543 | 812 | 1259 | 287 | 1925 | 526 | 575 | 1429 | 511 | 585 | 564 | 90,7 | 195 |
| Hf | 17,2 | 23,6 | 15,1 | 13,6 | 12,8 | 7,15 | 8,00 | 17,7 | 15,8 | 49,4 | 20,7 | 10,9 | 3,74 | 19,3 | 8,66 | 15,1 | 10,6 | 1,87 | 2,73 |
| Ta | 3,26 | 4,50 | 2,85 | 2,62 | 2,75 | 1,47 | 0,49 | 2,96 | 2,70 | 7,75 | 2,86 | 2,85 | 0,73 | 3,39 | 2,02 | 2,87 | 2,02 | 0,30 | 0,45 |
| Pb | 9,00 | 14,1 | 7,69 | 7,83 | 8,50 | 5,88 | 17,4 | 6,97 | 9,31 | 24,1 | 27,1 | 36,6 | 11,2 | 12,8 | 123 | 16,9 | 14,7 | 9,85 | 15,0 |
| Th | 6,06 | 8,24 | 3,95 | 3,62 | 2,93 | 2,66 | 5,50 | 8,60 | 7,26 | 12,0 | 7,70 | 9,10 | 1,45 | 7,53 | 3,10 | 2,86 | 3,31 | 0,29 | 0,49 |
| U | 1,14 | 1,49 | 0,74 | 0,73 | 0,68 | 0,53 | 0,41 | 1,28 | 1,15 | 2,11 | 1,47 | 1,86 | 0,23 | 1,53 | 0,52 | 0,66 | 0,61 | 0,07 | 0,11 |

Appendix 1.4 Major and trace element data

| Rock Type | Micro-granite | Micro-granite | Syenite | Syenite | Mafic dyke | Felsic dyke | Orthogneiss | Felsic dyke | Felsic dyke | Micro-granite | Felsic dyke | Felsic dyke | Mafic dyke | Felsic dyke | Monzonite | Monzonite | Monzonite | Gabbroic | Mafic dyke |
|---|---|---|---|---|---|---|---|---|---|---|---|---|---|---|---|---|---|---|---|
| Sample Name | MC7-024B | MC7-025 | MC7-026 | MC7-027 | MC7-028 | MC7-029 | MC7-030 | MC7-031 | MC7-032 | MC7-033 | MC7-034 | MC7-035 | MC7-036 | MC7-038 | MC7-039 | MC7-040 | MC7-041 | MC7-042 | MC7-043 |
| *ICP-MS REE ppm* | | | | | | | | | | | | | | | | | | | |
| La | 58,2 | 90,7 | 57,5 | 94,2 | 51,6 | 30,7 | 65,5 | 70,4 | 63,0 | 64,3 | 45,8 | 11,7 | 47,4 | 61,5 | 43,3 | 39,6 | 39,9 | 8,59 | 12,7 |
| Ce | 85,1 | 125 | 96,9 | 113 | 102 | 55,8 | 116 | 134 | 120 | 141 | 80,4 | 19,1 | 31,9 | 110 | 82,4 | 76,7 | 78,6 | 11,7 | 16,4 |
| Pr | 15,4 | 12,4 | 15,5 | 21,2 | 14,3 | 7,56 | 14,1 | 17,5 | 15,4 | 21,1 | 10,9 | 2,26 | 10,7 | 16,6 | 11,7 | 10,8 | 11,2 | 1,84 | 2,63 |
| Nd | 65,3 | 54,7 | 74,7 | 105 | 70,1 | 36,5 | 57,6 | 79,8 | 70,3 | 109 | 47,1 | 9,10 | 50,7 | 77,8 | 60,3 | 54,7 | 56,5 | 9,73 | 13,6 |
| Sm | 15,8 | 15,2 | 20,2 | 24,7 | 18,1 | 8,6 | 11,0 | 18,9 | 17,1 | 38,4 | 12,1 | 2,43 | 13,3 | 20,3 | 16,1 | 15,1 | 15,3 | 2,91 | 3,93 |
| Eu | 3,86 | 3,81 | 6,83 | 8,40 | 5,55 | 2,21 | 2,24 | 5,23 | 4,63 | 10,5 | 2,30 | 0,23 | 3,15 | 5,16 | 4,20 | 4,78 | 3,79 | 1,18 | 1,43 |
| Gd | 15,2 | 15,8 | 22,4 | 29,8 | 19,5 | 8,9 | 8,5 | 20,1 | 17,5 | 55,7 | 12,4 | 3,02 | 13,5 | 20,4 | 17,8 | 17,1 | 16,7 | 3,67 | 4,87 |
| Tb | 2,66 | 3,08 | 3,48 | 4,46 | 3,06 | 1,31 | 1,23 | 3,04 | 2,62 | 10,3 | 2,1 | 0,75 | 1,93 | 3,22 | 2,73 | 2,68 | 2,51 | 0,52 | 0,72 |
| Dy | 17,4 | 21,9 | 23,1 | 28,4 | 19,8 | 8,3 | 7,4 | 20,5 | 17,4 | 71,2 | 14,4 | 6,44 | 11,2 | 20,9 | 17,0 | 16,8 | 17,4 | 3,36 | 4,89 |
| Ho | 3,59 | 4,31 | 4,43 | 5,36 | 3,78 | 1,60 | 1,49 | 3,85 | 3,43 | 13,3 | 2,7 | 1,56 | 1,98 | 4,08 | 3,23 | 3,41 | 3,25 | 0,66 | 0,94 |
| Er | 10,0 | 12,2 | 12,1 | 14,9 | 10,2 | 4,50 | 4,03 | 11,0 | 9,6 | 36,3 | 8,1 | 5,31 | 4,98 | 11,6 | 8,69 | 9,28 | 8,74 | 1,57 | 2,48 |
| Tm | 1,46 | 1,78 | 1,64 | 2,15 | 1,46 | 0,65 | 0,56 | 1,44 | 1,32 | 4,79 | 1,20 | 0,84 | 0,63 | 1,61 | 1,21 | 1,31 | 1,19 | 0,23 | 0,33 |
| Yb | 9,46 | 11,0 | 9,61 | 14,1 | 8,41 | 4,14 | 3,43 | 9,84 | 8,72 | 27,6 | 7,93 | 5,91 | 3,69 | 10,5 | 7,12 | 8,06 | 7,35 | 1,35 | 1,85 |
| Lu | 1,27 | 1,37 | 1,38 | 2,27 | 1,13 | 0,62 | 0,50 | 1,38 | 1,30 | 3,89 | 1,15 | 0,90 | 0,48 | 1,60 | 0,97 | 1,19 | 1,10 | 0,19 | 0,28 |

# Appendix 1.4 Major and trace element data

| Rock Type | Felsic dyke | Gabbroic | Felsic dyke | Gabbroic | Gabbroic | Micro-granite | Gabbroic | Felsic dyke | Felsic dyke | Micro-granite | Monzonite | Granite | Monzonite | Gabbroic | Syenite | Micro-granite | Gabbroic | Gabbroic | Mafic dyke |
|---|---|---|---|---|---|---|---|---|---|---|---|---|---|---|---|---|---|---|---|
| Sample Name | MC7-044 | MC7-045 | MC7-047R | MC7-048 | MC7-050 | MC7-051 | MC7-052 | MC7-053 | MC7-054 | MC7-055 | MC7-056 | MC7-057 | MC7-058 | MC7-059 | MC7-060 | MC7-061 | MC7-062 | MC7-063 | MC7-064 |
| ***XRF major element*** | | | | | | | | | | | | | | | | | | | |
| $SiO_2$ | 74,5 | 46,0 | 73,6 | 47,3 | 49,7 | 71,1 | 46,2 | 74,4 | 75,7 | 70,6 | 59,2 | 67,9 | 60,3 | 47,4 | 63,9 | 73,5 | 44,7 | 51,0 | 49,2 |
| $TiO_2$ | 0,30 | 2,24 | 0,32 | 2,02 | 3,40 | 0,75 | 2,56 | 0,36 | 0,23 | 0,35 | 1,51 | 0,40 | 1,14 | 1,59 | 0,70 | 0,21 | 4,45 | 2,46 | 2,84 |
| $Al_2O_3$ | 9,28 | 14,4 | 11,9 | 18,1 | 12,8 | 11,5 | 13,2 | 8,94 | 9,83 | 12,9 | 13,9 | 15,1 | 17,2 | 19,8 | 14,9 | 12,2 | 17,7 | 15,0 | 13,6 |
| Fe2O3 | 6,14 | 12,5 | 3,52 | 10,8 | 16,0 | 5,86 | 13,2 | 6,42 | 4,86 | 4,77 | 9,97 | 3,00 | 7,09 | 8,44 | 6,79 | 2,86 | 12,8 | 11,4 | 15,6 |
| MnO | 0,16 | 0,19 | 0,11 | 0,16 | 0,23 | 0,15 | 0,20 | 0,09 | 0,10 | 0,27 | 0,31 | 0,07 | 0,28 | 0,12 | 0,30 | 0,06 | 0,16 | 0,19 | 0,27 |
| MgO | 0,23 | 7,89 | 0,32 | 4,67 | 4,54 | 0,71 | 7,25 | 0,21 | 0,24 | 0,30 | 1,74 | 0,76 | 0,98 | 4,68 | 0,55 | 0,29 | 4,42 | 4,39 | 4,41 |
| CaO | 0,12 | 11,8 | 0,41 | 12,8 | 8,50 | 1,38 | 12,4 | 0,08 | 0,07 | 0,27 | 4,26 | 2,36 | 3,24 | 13,6 | 1,49 | 0,21 | 12,6 | 8,93 | 8,03 |
| $Na_2O$ | 4,15 | 2,46 | 4,70 | 2,45 | 3,00 | 4,48 | 2,41 | 4,39 | 4,17 | 5,29 | 5,70 | 3,17 | 7,43 | 2,57 | 6,04 | 4,43 | 2,56 | 2,94 | 4,01 |
| $K_2O$ | 4,48 | 0,28 | 4,02 | 0,42 | 0,96 | 3,77 | 0,25 | 4,45 | 4,15 | 3,46 | 1,81 | 5,94 | 0,86 | 0,21 | 3,79 | 4,60 | 0,21 | 1,25 | 0,97 |
| $P_2O_5$ | 0,02 | 0,15 | 0,03 | 0,11 | 0,14 | 0,07 | 0,16 | 0,02 | 0,01 | 0,03 | 0,56 | 0,15 | 0,33 | 0,07 | 0,14 | 0,02 | 0,06 | 0,18 | 0,58 |
| $SO_3$ | 0,00 | 0,25 | 0,01 | 0,07 | 0,01 | 0,01 | 0,21 | 0,00 | 0,01 | 0,01 | 0,02 | 0,01 | 0,06 | 0,03 | 0,02 | 0,01 | 0,06 | 0,01 | 0,01 |
| $Cr_2O_3$ | 0,04 | 0,06 | 0,01 | 0,03 | 0,01 | 0,04 | 0,06 | 0,01 | 0,01 | 0,01 | 0,01 | 0,04 | 0,02 | 0,05 | 0,04 | 0,01 | 0,01 | 0,02 | 0,01 |
| NiO | 0,00 | 0,02 | 0,00 | 0,01 | 0,00 | 0,00 | 0,02 | 0,00 | 0,01 | 0,00 | 0,00 | 0,00 | 0,00 | 0,02 | 0,02 | 0,00 | 0,00 | 0,01 | 0,00 |
| $H_2O$- | 0,08 | 0,17 | 0,13 | 0,15 | 0,16 | 0,10 | 0,20 | 0,17 | 0,11 | 0,31 | 0,31 | 0,22 | 0,24 | 0,15 | 0,25 | 0,22 | 0,09 | 0,11 | 0,21 |
| LOI | 0,14 | 1,11 | 0,50 | 0,97 | 0,42 | 0,14 | 1,31 | 0,30 | 0,31 | 1,19 | 0,70 | 0,42 | 0,45 | 0,67 | 0,33 | 0,61 | 0,07 | 1,50 | 0,28 |
| Total | 99,7 | 99,5 | 99,6 | 100 | 99,9 | 100 | 99,6 | 99,9 | 99,8 | 99,8 | 100 | 99,6 | 99,5 | 99,3 | 99,2 | 99,2 | 99,9 | 99,5 | 100 |
| $SiO_2$ anh | 74,9 | 46,8 | 74,3 | 47,7 | 50,0 | 71,2 | 47,0 | 74,7 | 76,1 | 71,6 | 59,6 | 68,5 | 60,8 | 48,1 | 64,6 | 74,5 | 44,7 | 52,1 | 49,3 |
| ***ICP-MS trace eleme*** | | | | | | | | | | | | | | | | | | | |
| Sc | 3,95 | 45,3 | 4,00 | 34,1 | 34,9 | 5,24 | 51,49 | 3,34 | 3,66 | 4,44 | 19,5 | | 20,7 | 31,5 | 11,0 | 3,49 | 33,0 | 30,2 | 33,9 |
| Ti | 1542 | 11763 | 1481 | 11365 | 16832 | 3453 | 13545 | 2094 | 1389 | 2242 | 10093 | | 6136 | 10967 | 4862 | 1256 | 27995 | 15702 | 18650 |
| V | 18,3 | 360 | 11,4 | 373 | 474 | 48,3 | 395 | 2,13 | 3,65 | 5,40 | 52,8 | | 10,7 | 307 | 16,0 | 3,79 | 416 | 335 | 350 |
| Cr | 165 | 285 | 9,82 | 146 | 7,95 | 187 | 314 | 5,93 | 5,44 | 15,3 | 15,4 | | 99,0 | 249 | 112 | 6,90 | 6,84 | 106 | 6,71 |
| Co | 1,77 | 82,7 | 206 | 82,8 | 99,8 | 6,27 | 88,3 | 187 | 202 | 187 | 85,3 | | 3,86 | 76,5 | 2,75 | 180 | 93,3 | 90,9 | 91,7 |
| Ni | 18,1 | 141 | 9,8 | 71,2 | 17,9 | 17,8 | 119 | 10,4 | 12,5 | 17,1 | 18,6 | | 10,6 | 93,8 | 28,6 | 11,2 | 24,0 | 61,6 | 11,2 |
| Cu | 9,7 | 94,6 | 10,5 | 129 | 29,2 | 16,0 | 137 | 16,1 | 23,9 | 31,1 | 33,0 | | 14,9 | 78,7 | 13,7 | 9,2 | 19,3 | 83,7 | 18,4 |
| Ga | 46,9 | 21,4 | 43,7 | 24,5 | 28,4 | 43,2 | 20,8 | 41,3 | 42,4 | 51,6 | 45,0 | | 59,9 | 23,2 | 62,2 | 48,4 | 21,4 | 25,6 | 26,4 |
| Rb | 114 | 5,3 | 95,9 | 19,6 | 27,7 | 80,9 | 11,3 | 137 | 194 | 68,1 | 42,6 | | 10,7 | 4,4 | 45,3 | 97,0 | 5,9 | 41,9 | 34,5 |
| Sr | 7,0 | 430 | 44,2 | 471 | 330 | 90,3 | 389 | 9,46 | 27,5 | 56,6 | 356 | | 284 | 591 | 68,1 | 7,92 | 533 | 366 | 355 |
| Zr | 1062 | 73,7 | 1118 | 76,8 | 193 | 567 | 76,8 | 1830 | 1718 | 649 | 352 | | 93,3 | 29,9 | 304 | 486 | 37,5 | 190 | 116 |
| Nb | 68,1 | 5,17 | 73,2 | 5,55 | 16,0 | 51,3 | 5,21 | 107 | 91,1 | 41,7 | 35,0 | | 6,35 | 2,20 | 25,4 | 27,8 | 4,03 | 13,6 | 7,78 |
| Y | 109 | 19,1 | 147 | 17,5 | 52,6 | 95,4 | 22,4 | 209 | 80,7 | 123 | 92,0 | | 21,4 | 9,53 | 44,0 | 203 | 10,7 | 32,0 | 28,9 |
| Cs | 0,48 | 0,17 | 0,27 | 0,54 | 0,57 | 0,48 | 0,25 | 0,36 | 0,95 | 0,26 | 0,52 | | 0,12 | 0,09 | 0,62 | 0,21 | 0,19 | 1,04 | 1,22 |
| Ba | 264 | 83,4 | 554 | 84,7 | 289 | 720 | 128 | 96,7 | 36,1 | 721 | 911 | | 2545 | 90,1 | 2012 | 244 | 63,6 | 163 | 386 |
| Hf | 28,2 | 2,33 | 28,7 | 2,24 | 5,25 | 16,0 | 2,18 | 44,3 | 44,9 | 16,6 | 9,25 | | 2,25 | 0,90 | 7,30 | 12,1 | 1,22 | 5,30 | 2,99 |
| Ta | 4,73 | 0,36 | 5,27 | 0,36 | 1,21 | 3,43 | 0,37 | 7,10 | 6,67 | 2,68 | 2,22 | | 0,43 | 0,16 | 1,39 | 1,93 | 0,31 | 0,98 | 0,49 |
| Pb | 23,8 | 21,9 | 92,5 | 7,37 | 9,58 | 41,7 | 48,1 | 73,4 | 64,1 | 41,2 | 17,9 | | 3,97 | 2,45 | 7,98 | 12,7 | 4,57 | 9,21 | 8,41 |
| Th | 7,96 | 0,40 | 11,0 | 0,43 | 1,49 | 5,59 | 0,40 | 10,8 | 16,1 | 4,1 | 3,1 | | 0,84 | 0,17 | 1,89 | 3,99 | 0,25 | 2,20 | 0,68 |
| U | 1,63 | 0,13 | 1,51 | 0,17 | 0,28 | 0,99 | 0,08 | 2,01 | 3,15 | 1,69 | 0,58 | | 0,26 | 0,08 | 0,36 | 0,86 | 0,08 | 0,37 | 0,11 |

Appendix 1.4 Major and trace element data

| Rock Type | Felsic dyke | Gabbroic | Felsic dyke | Gabbroic | Gabbroic | Micro-granite | Gabbroic | Felsic dyke | Felsic dyke | Micro-granite | Monzonite | Granite | Monzonite | Gabbroic | Syenite | Micro-granite | Gabbroic | Gabbroic | Mafic dyke |
|---|---|---|---|---|---|---|---|---|---|---|---|---|---|---|---|---|---|---|---|
| Sample Name | MC7-044 | MC7-045 | MC7-047R | MC7-048 | MC7-050 | MC7-051 | MC7-052 | MC7-053 | MC7-054 | MC7-055 | MC7-056 | MC7-057 | MC7-058 | MC7-059 | MC7-060 | MC7-061 | MC7-062 | MC7-063 | MC7-064 |
| *ICP-MS REE ppm* | | | | | | | | | | | | | | | | | | | |
| La | 53,3 | 9,99 | 71,0 | 9,23 | 19,9 | 48,1 | 10,0 | 171 | 113 | 109 | 46,0 | | 17,8 | 7,05 | 37,9 | 263 | 6,53 | 19,0 | 18,7 |
| Ce | 127 | 12,9 | 154 | 12,8 | 32,1 | 99,2 | 14,4 | 299 | 184 | 209 | 88,6 | | 32,0 | 7,45 | 68,8 | 393 | 7,47 | 33,7 | 32,7 |
| Pr | 15,3 | 2,21 | 19,9 | 1,94 | 5,07 | 13,1 | 2,27 | 41,8 | 17,3 | 27,4 | 13,0 | | 4,5 | 1,08 | 9,08 | 83,5 | 1,19 | 4,49 | 4,60 |
| Nd | 72,5 | 11,7 | 88,5 | 10,2 | 26,0 | 60,6 | 12,2 | 182 | 55,0 | 128 | 67,4 | | 23,5 | 6,01 | 40,6 | 391 | 6,12 | 21,6 | 23,1 |
| Sm | 20,1 | 3,47 | 24,7 | 3,14 | 7,71 | 16,3 | 4,02 | 38,7 | 7,55 | 29,8 | 18,0 | | 6,27 | 1,71 | 9,84 | 97,8 | 2,03 | 5,88 | 6,34 |
| Eu | 4,55 | 1,43 | 5,45 | 1,20 | 2,34 | 4,25 | 1,38 | 5,46 | 0,57 | 5,49 | 5,89 | | 6,02 | 0,94 | 3,55 | 16,6 | 0,90 | 1,84 | 2,20 |
| Gd | 20,6 | 4,47 | 26,5 | 3,99 | 9,86 | 17,9 | 4,86 | 33,6 | 8,07 | 32,1 | 19,4 | | 5,97 | 2,07 | 9,44 | 84,1 | 2,38 | 6,56 | 6,82 |
| Tb | 3,48 | 0,66 | 4,25 | 0,58 | 1,48 | 2,78 | 0,71 | 5,78 | 1,72 | 4,36 | 2,77 | | 0,77 | 0,35 | 1,54 | 11,0 | 0,34 | 0,97 | 0,93 |
| Dy | 24,0 | 4,12 | 28,6 | 3,69 | 9,85 | 19,0 | 4,27 | 41,0 | 15,3 | 25,5 | 17,6 | | 4,97 | 2,02 | 9,39 | 58,6 | 2,21 | 6,41 | 5,98 |
| Ho | 4,78 | 0,82 | 5,54 | 0,74 | 1,87 | 3,66 | 0,87 | 8,24 | 3,46 | 4,58 | 3,37 | | 0,89 | 0,40 | 1,81 | 8,65 | 0,45 | 1,24 | 1,14 |
| Er | 13,9 | 1,95 | 16,2 | 1,84 | 4,84 | 10,2 | 2,35 | 24,9 | 13,5 | 12,3 | 9,24 | | 2,12 | 1,01 | 4,93 | 20,0 | 1,11 | 3,37 | 3,00 |
| Tm | 2,14 | 0,27 | 2,19 | 0,26 | 0,67 | 1,37 | 0,31 | 3,54 | 2,29 | 1,75 | 1,19 | | 0,27 | 0,14 | 0,74 | 2,38 | 0,14 | 0,48 | 0,42 |
| Yb | 14,3 | 1,62 | 13,7 | 1,40 | 3,95 | 9,21 | 1,69 | 22,9 | 17,0 | 11,7 | 7,56 | | 1,76 | 0,73 | 4,68 | 14,4 | 0,83 | 2,93 | 2,50 |
| Lu | 2,1 | 0,22 | 1,93 | 0,21 | 0,62 | 1,37 | 0,25 | 3,24 | 2,32 | 1,76 | 1,08 | | 0,24 | 0,12 | 0,74 | 1,93 | 0,11 | 0,42 | 0,34 |

Appendix 1.4 Major and trace element data

| Rock Type | Micro-granite | Gabbroic | Mafic dyke | Orthogneiss | Mafic dyke | Gabbroic | Gabbroic | Micro-granite | Felsic dyke | Granite | Granite |
|---|---|---|---|---|---|---|---|---|---|---|---|
| Sample Name | MC7-065 | MC7-066 | PD06-001 | PD06-002 | PD06-003 | PD06-004 | PD06-005 | PD06-006 | PD06-007 | PD06-008 | PD06-009 |

*XRF major element*

| | | | | | | | | | | | |
|---|---|---|---|---|---|---|---|---|---|---|---|
| $SiO_2$ | 72,8 | 47,4 | 50,2 | 69,2 | 50,5 | 45,7 | 51,1 | 69,5 | 74,8 | 73,7 | 73,7 |
| $TiO_2$ | 0,41 | 2,33 | 3,50 | 0,76 | 1,59 | 3,44 | 2,92 | 0,37 | 0,31 | 0,41 | 0,39 |
| $Al_2O_3$ | 11,8 | 13,8 | 13,3 | 13,2 | 17,7 | 13,3 | 13,1 | 13,5 | 9,87 | 10,34 | 9,78 |
| Fe2O3 | 4,64 | 13,1 | 14,4 | 4,2 | 11,2 | 15,6 | 13,3 | 4,91 | 5,32 | 5,47 | 6,18 |
| MnO | 0,08 | 0,19 | 0,27 | 0,07 | 0,19 | 0,22 | 0,19 | 0,14 | 0,15 | 0,13 | 0,15 |
| MgO | 0,26 | 6,47 | 4,02 | 0,94 | 3,00 | 5,57 | 4,85 | 0,27 | 0,23 | 0,32 | 0,30 |
| CaO | 0,21 | 11,6 | 6,76 | 2,02 | 7,62 | 10,55 | 9,20 | 0,26 | 0,13 | 0,29 | 0,16 |
| $Na_2O$ | 4,93 | 2,50 | 3,29 | 3,03 | 4,17 | 2,98 | 3,43 | 5,43 | 4,16 | 4,27 | 4,20 |
| $K_2O$ | 3,48 | 0,53 | 1,87 | 5,39 | 1,47 | 0,79 | 1,07 | 3,60 | 4,03 | 4,35 | 4,30 |
| $P_2O_5$ | 0,01 | 0,11 | 0,39 | 0,31 | 0,31 | 0,26 | 0,09 | 0,03 | 0,01 | 0,01 | 0,02 |
| $SO_3$ | 0,02 | 0,06 | 0,04 | 0,02 | 0,02 | 0,02 | 0,03 | 0,01 | 0,02 | 0,01 | 0,02 |
| $Cr_2O_3$ | 0,05 | 0,03 | 0,02 | 0,02 | 0,01 | 0,02 | 0,03 | 0,02 | 0,06 | 0,05 | 0,05 |
| NiO | 0,00 | 0,01 | 0,01 | 0,00 | 0,01 | 0,01 | 0,01 | 0,00 | 0,00 | 0,00 | 0,00 |
| $H_2O$- | 0,17 | 0,29 | 0,25 | 0,05 | 0,20 | 0,11 | 0,10 | 0,34 | 0,13 | 0,13 | 0,12 |
| LOI | 0,39 | 1,04 | 0,92 | 0,32 | 1,56 | 1,47 | 0,48 | 0,97 | 0,86 | 0,40 | 0,48 |
| Total | 99,2 | 99,5 | 99,2 | 99,4 | 99,5 | 100 | 99,8 | 99,4 | 100 | 99,8 | 99,9 |
| $SiO_2$ anh | 73,6 | 48,1 | 51,1 | 69,8 | 51,5 | 46,4 | 51,4 | 70,6 | 75,4 | 74,1 | 74,2 |

*ICP-MS trace eleme*

| | | | | | | | | | | | |
|---|---|---|---|---|---|---|---|---|---|---|---|
| Sc | 2,82 | 43,9 | 33,0 | 10,2 | 23,4 | 41,4 | 37,4 | 4,82 | 3,58 | 3,10 | 3,24 |
| Ti | 2392 | 15822 | 23960 | 4932 | 10483 | 21601 | 17730 | 2197 | 939 | 1338 | 1366 |
| V | 23,0 | 410 | 394 | 46,9 | 279 | 486 | 413 | 5,0 | 5,14 | 11,5 | 9,5 |
| Cr | 230 | 123 | 42,4 | 95,5 | 19,4 | 100 | 149 | 111 | 399 | 255 | 233 |
| Co | 5,0 | 93,7 | 85,5 | 127 | 69,4 | 66,2 | 86,6 | 98,2 | 218 | 114 | 133 |
| Ni | 39,3 | 97,1 | 69,0 | 12,7 | 35,6 | 77,9 | 68,9 | 22,8 | 14,1 | 14,1 | 29,0 |
| Cu | 24,7 | 136 | 37,4 | 14,2 | 47,1 | 99,1 | 99,3 | 23,8 | 14,0 | 12,8 | 15,9 |
| Ga | 49,3 | 22,8 | 37,7 | 33,9 | 28,4 | 24,2 | 31,3 | 49,3 | 40,8 | 48,0 | 45,5 |
| Rb | 61,5 | 19,3 | 62,1 | 293 | 83,3 | 43,3 | 21,0 | 82,5 | 108 | 76,6 | 96,6 |
| Sr | 21,7 | 373 | 345 | 300 | 637 | 404 | 308 | 23,9 | 4,070 | 15,0 | 9,58 |
| Zr | 311 | 107 | 290 | 472 | 130 | 114 | 203 | 1362 | 1221 | 359 | 800 |
| Nb | 22,3 | 7,14 | 20,1 | 33,8 | 6,95 | 7,9 | 15,7 | 90,1 | 76,4 | 24,4 | 56,7 |
| Y | 67,2 | 23,7 | 50,2 | 43,2 | 21,9 | 77,2 | 37,9 | 123 | 253 | 48,4 | 107 |
| Cs | 0,35 | 0,71 | 1,03 | 1,60 | 1,43 | 2,63 | 0,20 | 0,54 | 0,07 | 0,30 | 0,26 |
| Ba | 930 | 122 | 892 | 1146 | 475 | 142 | 294 | 573 | 255 | 448 | 338 |
| Hf | 8,14 | 3,20 | 7,86 | 11,8 | 3,35 | 3,16 | 5,55 | 33,0 | 31,2 | 10,0 | 22,4 |
| Ta | 1,46 | 0,45 | 1,37 | 2,16 | 0,40 | 0,56 | 1,06 | 6,17 | 4,92 | 1,69 | 3,80 |
| Pb | 7,08 | 6,52 | 27,8 | 47,4 | 16,3 | 11,6 | 6,12 | 19,8 | 42,9 | 7,10 | 17,5 |
| Th | 3,26 | 0,74 | 2,81 | 31,4 | 0,98 | 0,60 | 1,37 | 9,15 | 9,35 | 3,01 | 6,78 |
| U | 0,66 | 0,19 | 0,51 | 3,07 | 0,23 | 0,44 | 0,32 | 2,14 | 1,97 | 0,58 | 1,26 |

Appendix 1.4 Major and trace element data

| Rock Type | Micro-granite | Gabbroic | Mafic dyke | Orthogneiss | Mafic dyke | Gabbroic | Gabbroic | Micro-granite | Felsic dyke | Granite | Granite |
|---|---|---|---|---|---|---|---|---|---|---|---|
| Sample Name | MC7-065 | MC7-066 | PD06-001 | PD06-002 | PD06-003 | PD06-004 | PD06-005 | PD06-006 | PD06-007 | PD06-008 | PD06-009 |
| *ICP-MS REE ppm* | | | | | | | | | | | |
| La | 63,3 | 11,0 | 29,6 | 126 | 20,2 | 34,9 | 19,7 | 58,2 | 484 | 22,8 | 36,7 |
| Ce | 41,2 | 17,0 | 54,8 | 238 | 34,2 | 20,7 | 33,9 | 135 | 557 | 48,1 | 71,5 |
| Pr | 17,9 | 2,55 | 7,44 | 26,5 | 4,56 | 10,5 | 4,84 | 11,8 | 104 | 5,72 | 8,50 |
| Nd | 70,9 | 13,3 | 37,9 | 96,2 | 21,5 | 50,6 | 24,1 | 49,5 | 429 | 27,4 | 41,1 |
| Sm | 15,4 | 4,23 | 9,72 | 15,4 | 4,84 | 13,4 | 6,69 | 12,5 | 89,1 | 6,87 | 12,2 |
| Eu | 3,16 | 1,38 | 3,22 | 2,37 | 1,66 | 3,89 | 2,10 | 2,24 | 13,4 | 1,75 | 3,06 |
| Gd | 13,6 | 4,80 | 10,2 | 10,8 | 4,72 | 16,5 | 7,29 | 14,1 | 66,0 | 7,14 | 15,0 |
| Tb | 2,14 | 0,75 | 1,65 | 1,38 | 0,68 | 2,68 | 1,21 | 2,81 | 8,08 | 1,24 | 2,84 |
| Dy | 13,6 | 5,05 | 9,83 | 7,97 | 4,45 | 16,9 | 7,54 | 21,7 | 43,2 | 8,74 | 19,5 |
| Ho | 2,50 | 0,99 | 1,92 | 1,60 | 0,86 | 3,22 | 1,43 | 4,78 | 7,05 | 1,79 | 3,92 |
| Er | 6,96 | 2,65 | 5,29 | 4,23 | 2,36 | 8,49 | 3,92 | 14,6 | 18,1 | 5,16 | 11,4 |
| Tm | 1,07 | 0,34 | 0,72 | 0,65 | 0,31 | 1,09 | 0,54 | 2,31 | 2,53 | 0,80 | 1,74 |
| Yb | 6,92 | 1,82 | 4,53 | 3,86 | 2,10 | 6,66 | 3,40 | 14,5 | 16,4 | 5,30 | 11,3 |
| Lu | 1,04 | 0,26 | 0,64 | 0,58 | 0,29 | 0,94 | 0,47 | 2,07 | 2,34 | 0,80 | 1,64 |

Appendix 1.5 : Radiogenic isotope data
For Rb-Sr and Sm- Nd

| Rock Type | Sample Number | Rb | Sr | $^{87}Rb/^{86}Sr$ | $^{87}Sr/^{86}Sr_{(m)}$ | ± 2s | $^{87}Sr/^{86}Sr_{(i)}$ (88Ma) | E Sr (88Ma) | Sm ppm | Nd ppm | $^{147}Sm/^{144}Nd$ | $^{143}Nd/^{144}Nd_{(m)}$ | ± 2s | $^{143}Nd/^{144}Nd_{(i)}$ (120Ma) | E Nd (88Ma) | $T_{(DM)}$ |
|---|---|---|---|---|---|---|---|---|---|---|---|---|---|---|---|---|
| Coarse grained Gabbro | mc7050 | 25,6 | 304 | 0,244 | 0,70388 | 13 | 0,70358 | -11,61 | 6,41 | 22,5 | 0,172600 | 0,512871 | 7 | 0,512772 | 4,82 | 786 |
| Coarse grained Gabbro | mc7063 | 40,0 | 357 | 0,325 | 0,70469 | 12 | 0,70428 | -1,67 | 5,35 | 20,3 | 0,159150 | 0,512788 | 8 | 0,512696 | 3,34 | 824 |
| Gabbro | mc7045 | 4,67 | 365 | 0,037 | 0,70371 | 12 | 0,70367 | -10,35 | 2,76 | 9,10 | 0,183178 | 0,512890 | 9 | 0,512785 | 5,07 | 947 |
| Gabbro | mc7066 | 17,5 | 345 | 0,147 | 0,70403 | 14 | 0,70385 | -7,85 | 3,41 | 11,5 | 0,178939 | 0,512894 | 7 | 0,512791 | 5,19 | 827 |
| Gabbro | mc7052 | 9,83 | 348 | 0,082 | 0,70378 | 16 | 0,70368 | -10,21 | 3,14 | 10,2 | 0,186575 | 0,512898 | 7 | 0,512790 | 5,18 | 1013 |
| Micro-granite | mc7024a | 67,5 | 12,5 | 15,708 | 0,72442 | 18 | 0,71123 | 96,93 | 12,3 | 54,3 | 0,137135 | 0,512765 | 4 | 0,512686 | 3,15 | 640 |
| Micro-granite | mc7025 | 77,0 | 18,1 | 12,388 | 0,71893 | 19 | 0,70425 | -2,15 | 13,4 | 52,7 | 0,153999 | 0,512780 | 6 | 0,512691 | 3,25 | 775 |
| Monzonite | mc7041 | 120 | 196 | 1,771 | 0,70482 | 17 | 0,70271 | -23,91 | 12,6 | 47,5 | 0,160032 | 0,512796 | 8 | 0,512704 | 3,49 | 814 |
| Monzonite | mc7040 | 41,2 | 320 | 0,373 | 0,70448 | 12 | 0,70402 | -5,43 | 11,9 | 44,2 | 0,162864 | 0,512797 | 8 | 0,512704 | 3,49 | 853 |
| Monzonite | mc7008 | 43,8 | 246 | 0,515 | 0,70419 | 20 | 0,70360 | -11,39 | 7,13 | 27,0 | 0,159936 | 0,512809 | 7 | 0,512717 | 3,75 | 778 |
| Micro-granite | mc7006 | 85,7 | 14,3 | 17,451 | 0,72676 | 14 | 0,71085 | 91,61 | 14,3 | 57,0 | 0,151462 | 0,512743 | 7 | 0,512656 | 2,55 | 831 |
| Micro-granite | mc7024b | 66,0 | 13,9 | 13,792 | 0,72203 | 19 | 0,70631 | 27,17 | 7,95 | 34,5 | 0,139321 | 0,512766 | 7 | 0,512686 | 3,15 | 655 |
| Granite | mc7013 | 97,1 | 8,75 | 32,291 | 0,74476 | 28 | 0,71525 | 154,00 | 12,9 | 50,1 | 0,155097 | 0,512767 | 5 | 0,512678 | 2,99 | 820 |
| Granite | mc7018 | 71,3 | 25,0 | 8,290 | 0,71403 | 15 | 0,70547 | 15,29 | 50,2 | 195,5 | 0,155374 | 0,512756 | 5 | 0,512667 | 2,77 | 851 |
| Granite | mc7021 | 84,6 | 13,4 | 18,377 | 0,72652 | 19 | 0,71425 | 139,86 | 10,0 | 39,3 | 0,154246 | 0,512743 | 7 | 0,512655 | 2,53 | 866 |
| Mafic dyke | mc7002 | 18,2 | 418 | 0,126 | 0,70642 | 19 | 0,70626 | 26,50 | 4,51 | 17,2 | 0,158449 | 0,512596 | 8 | 0,512504 | -0,40 | 1312 |
| Mafic dyke | mc7043 | 59,1 | 336 | 0,511 | 0,71233 | 12 | 0,71172 | 103,93 | 3,22 | 11,1 | 0,175116 | 0,512782 | 8 | 0,512681 | 3,05 | 1157 |
| Felsic dyke | mc7019 | 114 | 3,65 | 0,431 | 0,81775 | 27 | 0,81650 | 1591,44 | 60,1 | 286 | 0,127304 | 0,512547 | 4 | 0,512474 | -1,00 | 940 |
| Felsic dyke | mc7032 | 70,4 | 42,4 | 4,822 | 0,71804 | 17 | 0,71244 | 114,22 | 14,4 | 62,3 | 0,139648 | 0,512411 | 6 | 0,512330 | -3,80 | 1357 |
| Alkali syenite | mc7027 | 45,5 | 131 | 1,008 | 0,70489 | 14 | 0,70378 | -8,75 | 20,0 | 85,9 | 0,140765 | 0,512824 | 8 | 0,512743 | 4,26 | 552 |
| Alkali syenite | mc7060 | 41,2 | 64,3 | 1,860 | 0,70741 | 17 | 0,70500 | 8,52 | 8,77 | 37,6 | 0,141269 | 0,512604 | 8 | 0,512522 | -0,05 | 999 |